Aston University

Some parts of this thesis may have been removed for copyright restrictions.

If you have discovered material in AURA which is unlawful e.g. breaches copyright, (either yours or that of a third party) or any other law, including but not limited to those relating to patent, trademark, confidentiality, data protection, obscenity, defamation, libel, then please read our Takedown Policy and contact the service immediately

CATALYTIC PYROLYSIS OF AGRICULTURAL RESIDUES FOR BIO-OIL PRODUCTION

Adisak Pattiya

Doctor of Philosophy

Aston University

November 2007

This copy of the thesis has been supplied on condition that anyone who consults it is understood to recognise that its copyright rests with its author and that no quotation from the thesis and no information derived from it may be published without proper acknowledgement.

CATALYTIC PYROLYSIS OF AGRICULTURAL RESIDUES FOR BIO-OIL PRODUCTION

Adisak Pattiya

Doctor of Philosophy, 2007

THESIS SUMMARY

Agricultural residues from Thailand, namely stalk and rhizome of cassava plants, were employed as raw materials for bio-oil production via fast pyrolysis technology. There were two main objectives of this project. The first one was to determine the optimum pyrolysis temperature for maximising the organics yield and to investigate the properties of the bio-oils produced. To achieve this objective, pyrolysis experiments were conducted using a bench-scale (150 g/h) reactor system, followed by bio-oil analysis. It was found that the reactor bed temperature that could give the highest organics yield for both materials was 490±15°C. At all temperatures studied, the rhizome gave about 2-4% higher organics yields than the stalk. It was found that the bio-oil derived from the rhizome had lower oxygen content, higher calorific value and better stability, thus indicating better quality than that produced from the stalk.

The second objective was to improve the bio-oil properties in terms of heating value, viscosity and storage stability. This was achieved by the incorporation of catalyst into the pyrolysis process to induce deoxygenation, cracking and reforming reactions of the pyrolysis vapour. Catalytic pyrolysis was initially performed in a micro-scale reactor to screen a large number of catalysts. Subsequently, seven catalysts were selected for experiments with larger-scale (150 g/h) pyrolysis unit. The catalysts were zeolite and related materials (ZSM-5, Al-MCM-41 and Al-MSU-F), commercial catalysts (Criterion-534 and MI-575), copper chromite and ash. Additionally, the combination of two catalysts in series was investigated. These were Criterion-534/ZSM-5 and Al-MSU-F/ZSM-5. The results showed that all catalysts could improve the bio-oils properties as they enhanced cracking and deoxygenation reactions and in some cases such as ZSM-5, Criterion-534 and Criterion-534/ZSM-5, valuable chemicals like hydrocarbons and light phenols were produced. The highest concentration of these compounds was obtained with Criterion-534/ZSM-5.

Key words: Biomass, catalysis, Thailand, vapour-phase upgrading, catalytic fast pyrolysis

TO

MY FAMILY

AND MY GIRLFRIEND

ACKNOWLEDGEMENTS

I would like to acknowledge my supervisor Dr James Titiloye and my associate supervisor Professor Tony Bridgwater for their advice given throughout the project.

I would also like to thank the past and present members of the Bio-Energy Research Group (BERG). Special thanks to Dr Heiko Gerhauser, Dr Cordner Peacocke, Dr Elma Gyftopoulou, Dr Islam Hussain, Mark Coulson and Jurgen Sitzman for sharing their theoretical and practical knowledge. Thanks also to Romani Fahmi and Stamos Dacey for their support in laboratory.

Special thanks also to Patchara Punyamoonwongsa for sharing her chemistry knowledge.

Financial support from the Royal Thai Government is gratefully acknowledged.

LIST OF CONTENTS

LIST OF TABLES

LIST OF FIGURES

1 INTRODUCTION

1.1 BACKGROUND

Due to environmental concern and possible future crisis in energy production and sustainability, the use and the development of renewable and sustainable energy sources are of paramount importance. Biomass is an accepted form of renewable energy and is seen as a means of helping to reduce global warming, by displacing the use of fossil fuels [1]. Energy stored in biomass is derived from sunlight and can be either directly utilised by combustion or transformed into different forms of energy via conversion technologies such as gasification, pyrolysis, fermentation, anaerobic digestion and mechanical extraction. Factors that influence the choice of conversion process are: the type and quantity of biomass feedstock; the desired form of required energy; environmental standards; economic conditions; and project specific factors [2]. For lignocellulosic biomass such as agricultural residues which globally exists in large quantities, fast pyrolysis can be one of the promising routes for converting biomass into liquid fuel (also known as bio-oil) with solid char and gases as valuable by-products.

Fast pyrolysis is generally defined as a moderate temperature (400-600°C) process in which biomass is rapidly heated in the absence of oxygen. Fast pyrolysis has gained growing interest due to the relative simplicity of the process coupled with the main product being in the form of liquid which can be readily stored and transported. Pyrolysis liquid is a complex mixture of water, acids, alcohols, aldehydes, esters, ketones, sugars, phenols, guaiacols, syringols, furans, and multifunctional compounds, such as hydroxyacetic acid, hydroxyacetaldehyde, hydroxyacetone, and 3-hydroxy-3-methoxy benzaldehyde [3]. It can be used either as a fuel or as a source of chemicals.

Since bio-oil is a mixture of thermal degradation products of biomass (with main building blocks, comprising of cellulose, hemicellulose and lignin), its elemental composition resembles that of biomass rather than that of petroleum oils [4].

Therefore, the bio-oil contains significant amount of oxygenated compounds derived from cellulose, hemicellulose and lignin. It is the majority of these oxygenated compounds in bio-oil that result in bio-oil instability and contribute to the lower heating values than compared to that of conventional fuel oils [4]. In addition to the oxygen content that limits the use of bio-oil as a fuel, the lignin-derived compounds are also expected to affect the bio-oil quality [5]. The lignin derivatives present in bio-oil are known collectively as pyrolytic lignin, which has an average molecular weight between 650 and 1300 g/mol and may be composed of tri- and tetramers of lignin sub-units (hydroxyphenyl, guaiacyl and syringyl units) [6]. These heavy molecules are found to be related to the high viscosity and low storage stability of bio-oil [5]. If these large molecules could be further cracked down into lower molecular weight compounds, it is expected that the initial viscosity of bio-oil would be reduced accordingly. Therefore, in order to improve the quality of the bio-oils in terms of heating values, viscosity and storage stability, the oxygen and the large molecules derived from lignin need to be removed or transformed into more useful products. This can be achieved by the introduction of catalysts into the pyrolysis process.

Since this project is funded by the Royal Thai Government, the biomass materials studied were selected based on the availability of the biomass resources in Thailand, which is described in the next section.

1.2 AGRICULTURAL RESIDUES IN THAILAND

Deemed as an agricultural country, Thailand has various biomass sources available for utilisation. The energy potential, availability and current utilisation of biomass in Thailand have been reviewed extensively with Table 1-1 summarising the key agricultural residues potential in Thailand [7-14]. It is evident from the table that nearly 560 PJ of biomass energy from agricultural residues exists for exploitation. Some of these residues are already being used by direct combustion as shown by the example of sugarcane bagasse which has been used in sugar mills boilers to generate energy for their own use.

Table 1-1 Estimation of agricultural residues potential in Thailand [7-14]

Type	Production (2006) (Mt) [9]	Residues	Amount of residue generated (Mt)	Amount of residue used for energy (Mt)	Residues available for energy purpose (Mt)	Calorific value* (MJ kg^{-1}) [12]	Energy potential	
							(PJ)	(Mtoe)
Sugarcane	47.66	Bagasse	13.87	10.998	2.87	6.43	18.46	0.441
		Tops/leaves	14.39	0.000	14.19	6.82	96.78	2.312
Rice	29.27	Husk	6.73	3.413	3.32	12.85	42.65	1.019
		Straw	13.08	0.000	8.95	8.83	79.02	1.887
Oil palm	6.24	Empty Bunches	2.67	0.080	1.56	16.44	25.65	0.613
		Fibre	0.92	0.787	0.12	16.19	1.99	0.048
		Shell	0.31	0.180	0.01	17.00	0.19	0.005
		Fronds	16.25	0.000	16.25	7.97	129.52	3.094
		Male bunches	1.45	0.000	1.45	14.86	21.61	0.516
Cassava	22.58	Stalk	1.99	0.000	1.39	13.38 [10]	18.61	0.445
		Rhizome	11.07	0.000	10.84	10.61 [10]	115.06	2.748
Maize	3.70	Corn cob	0.92	0.178	0.62	16.63	10.30	0.246
Total							**559.84**	**13.372**

*Lower heating value (LHV) on as-received basis

In Table 1-1, the amounts of residues used for energy show that parts of sugarcane bagasse, rice husk and empty bunches, fibre and shell of oil palm have already been exploited, while sugarcane tops/leaves, rice straw, oil palm fronds and male bunches as well as stalk and rhizome of cassava have hardly been used for energy purposes. However, not all of the residues can be used for energy production as some are needed to be set aside for other purposes, such as re-plantation as is the case for cassava stalk.

The figures in Table 1-1 suggest that sugarcane tops/leaves, oil palm fronds and cassava rhizome are the three agricultural wastes having highest exploitable energy contents. Among these, cassava residues are the easiest to be collected from the field, while sugarcane tops/leaves and palm fronds are scattered throughout the fields for agronomic reasons.

With the aim of reducing dependence on crude oil imports, the Thai government has granted licences to 18 new factories, in addition to the existing 6 currently in

operation, to produce bio-ethanol. The main raw materials for bio-ethanol plants are sugarcane, molasses and cassava. This shows that the demand for cassava tubers as feedstock to bio-ethanol plants will increase, thus causing the increase in the residues.

Another critical issue that makes the agricultural residues from cassava in Thailand more interesting is the low price of its product (roots or tubers). Farmers who grow cassava have faced this problem for a long time. Therefore, a lot of research has been done in order to improve the quality of cassava roots and make them more valuable. Another way of increasing the value of cassava plants is to employ their agricultural residues. Hence, research on agricultural wastes from Thai cassava plantations is of great interest since the residues contain high exploitable energy, are abundant in supply and have relatively low market price incentive for cassava roots.

1.3 CASSAVA PLANTS (*Manihot esculenta* Crantz)

Cassava is also known as manioc, manihot, yuca, mandioca, aipin, castelinha, macaxeira and tapioca. It is an important source of food in tropical countries where it is grown for its starchy, tuberous roots. Its scientific names are as follows [15]:

Order	:	Geraniales or Euphorbiales
Class	:	Dicotyledloneae
Sub-class	:	Archichlamydeae
Sub-division	:	Angiospermae
Family	:	Euphorbiaceae
Tribe	:	Manihoteae
Genus	:	Manihot
Species	:	*Manihot esculenta* Crantz, *M. ultissima* Phol or *M. aipi* Phol

Cassava is a shrubby perennial crop and is harvested approximately 12 months after planting. At harvest, the top parts of the plants are cut before being uprooted. Some parts of the stalk are cut into one-foot-long pieces and retained for re-plantation, while some are discarded or left in the field for soil conditioning purpose. Some cassava rhizome is burnt, while some is left in the field. The use of each part of cassava is

summarised by Figure 1-1. In addition, Figure 1-2 depicts the main parts of a cassava plant.

Figure 1-1 The use of cassava in Thailand [15]

Figure 1-2 Parts of a cassava plant (adapted from [16])

The major varieties of cassava in Thailand are Kasetsart 50, Rayong 90, Rayong 5 and Rayong 72. The main characteristics of these varieties are summarised in Table 1-2. It can be seen that there is no significant difference among these variety in terms of their production and percentage of starch. The period of stalk kept for re-plantation is the maximum time that the stalk can be retained before re-plantation; beyond this point, the stalk will be dried and cannot be used to grow a new plant, thereby becoming agricultural residues. According to a farmer, cassava variety Kasetsart 50 gives relatively big tubers, and the tubers have high starch content in comparison to other varieties. Additionally, the Kasetsart 50 is the most common variety in Thailand. Therefore, the focus of this project is to study only the cassava variety Kasetsart 50 because it is readily available. Cassava variety Kasetsart 50 is one of the genetically modified products from Kasetsart University, Thailand. Figure 1-3 depicts this variety.

Table 1-2 Characteristics of the main cassava varieties in Thailand [15]

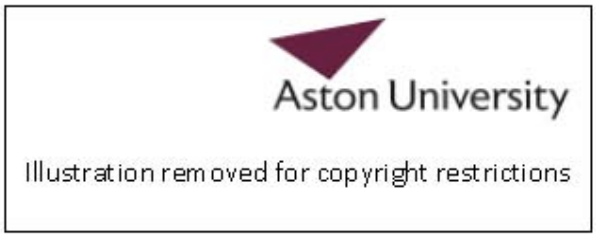

Since cassava root has its own value already and one of the main purposes of this project is to find an alternative way of increasing the value of cassava cultivation by utilising its agricultural residues, the stalk and rhizome of cassava plants are proposed and used as raw materials for bio-oil production.

Figure 1-3 Cassava variety Kasetsart 50 [15]

1.4 OBJECTIVES

There are two key objectives to this project. The first objective focuses on the application of fast pyrolysis technology to agricultural residues from cassava plantations in order to produce liquid fuel. This study is to determine the optimum pyrolysis condition, in particular the reaction temperature, at which the highest organics yield can be obtained. Also in the scope of this objective, the properties of the bio-oils produced from stalk and rhizome of cassava plants are investigated.

The second objective of this work is to explore the introduction of catalysts into the pyrolysis process. This is to improve the bio-oil properties in terms of heating values, viscosity and storage stability, thus making it more amenable to utilisation. The use of

catalysts is also expected to yield liquid products rich in high-value chemicals and fuel additives.

1.5 ORGANISATION OF THE THESIS

The thesis contains nine chapters including this chapter. An overview of fast pyrolysis of biomass is presented in **chapter 2** where the definition and basic components of biomass are given together with a brief discussion of fast pyrolysis principles and products. Based on the discussion, it is suggested that the bio-oil product should be upgraded. Consequently, the bio-oil upgrading options are outlined. One of the promising options for bio-oil upgrading is catalytic vapour cracking and reforming, which is the main focus of this project. Therefore **chapter 3** reviews previous related work on catalytic pyrolysis as well as the catalyst selection criteria, which leads to a number of promising catalysts chosen for the current work.

Since the biomass materials investigated (cassava stalk and rhizome) are relatively new to the bio-energy field and are not fully characterised in the past according to the open literature, **chapter 4** presents a wide range of the biomass characterisation methods applied as well as the results and discussion for both feedstocks. According to the biomass characterisation results, both feedstocks are rather similar, but the cassava rhizome has slightly higher heating value and better (lower) ash content. Therefore, only cassava rhizome is selected for catalytic pyrolysis studies. Because of the large number of catalysts considered as promising and suggested for catalytic pyrolysis work according to chapter 3, catalyst screening study is of great importance for reducing the number of pyrolysis experimental runs in a bench-scale pyrolysis unit. Consequently, catalyst screening tests have been performed using a micro-scale batch reactor. This technique is also known as analytical pyrolysis-gas chromatography/mass spectrometry (Py-GC/MS). The catalyst screening experiments are described in detail in **chapter 5**.

Unlike the micro-scale reactor where the pyrolysis vapours go directly through the GC/MS without condensation, the bench-scale (150g/h) fast pyrolysis unit is used for bio-oil production. A description of the bench-scale pyrolysis experimental set-up for

both non-catalytic and catalytic pyrolysis runs is provided in **chapter 6**. Also included in this chapter is the calculation of mass balance and the analytical techniques used for characterisation of all pyrolysis products (bio-oil, char and non-condensable gases).

In **chapters 7** and **8**, the results of the bench-scale fast pyrolysis experiments (non-catalytic and catalytic) in terms of mass balances and bio-oils properties are reported and discussed. Finally, the overall conclusions of the present work and the recommendations for future work are provided in **chapter 9**.

2 FAST PYROLYSIS OF BIOMASS

2.1 INTRODUCTION

This chapter begins with a description of biomass definition and its basic constituents followed by principles of fast pyrolysis for biomass processing. Subsequently, details of fast pyrolysis products in terms of their characteristics and applications are provided. Then, selected key factors that are known to affect the yields and properties of fast pyrolysis products are discussed. Based on the information given, it is suggested that the properties of bio-oil should be modified to make it more amenable to utilisation. Consequently, options for upgrading bio-oil are reviewed in the last section.

2.2 BIOMASS

Biomass can be defined as organic matter that stores solar energy in chemical bonds via photosynthesis process. Biomass includes wood and wood wastes, agricultural crops and residues, animal wastes, and municipal and industrial wastes. The typical elements of biomass are carbon, hydrogen, oxygen and nitrogen with small amounts of other atoms such as alkali and alkaline earth metals. These elements are basic to the major components of biomass, namely water, cellulose, hemicellulose, lignin, organic extractives and inorganic matter. The following sub-sections describe each biomass component in more detail.

2.2.1 Water

The amount of water present in biomass varies considerably depending on its freshness and species. For fresh biomass, the moisture content can be more than 50 wt%. There are two forms of water content in biomass, namely intrinsic and extrinsic [1]. While the former is the moisture content of the material without the influence of weather effects, the latter is influenced by prevailing weather conditions during

harvesting. Since biomass is generally hygroscopic in nature, its overall moisture content can vary during storage if it is exposed to the air, depending on the air humidity and temperature. If the biomass is stored in a dry and warm environment like in the north eastern part of Thailand, the moisture content can be decreased. The amount of water in the biomass is important from fast pyrolysis aspects as it will ultimately end up in the liquid product. As a rule of thumb, the moisture content of biomass used as feedstock for fast pyrolysis should be below 10 wt%. This moisture content can be measured as part of proximate analysis. This analysis will be discussed in chapter 4.

2.2.2 Cellulose

Cellulose is a natural polymer containing 5000-10000 glucose units with the formula $(C_6H_{10}O_5)_n$. It has an average molecular weight of 10^6 or more [17]. The basic repeating unit of the cellulose polymer consists of two glucose anhydride units called a cellobiose unit [17]. The chemical structure of cellulose is shown in Figure 2-1. Cellulose generally represents about 40-50 wt% of biomass [1]. When biomass is pyrolysed at a heating rate of 50°C/min, the main decomposition temperature zone of cellulose is postulated to be in the range of 350-500°C, which is higher than that of hemicellulose [18].

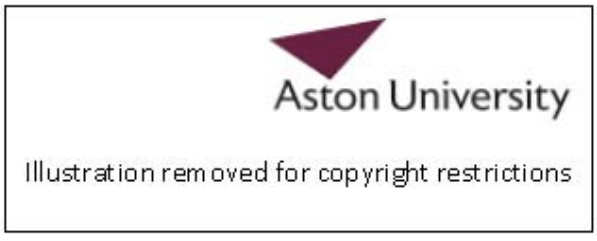

Figure 2-1 Chemical structure of cellulose [17]

2.2.3 Hemicellulose

In contrast to cellulose, which is a polymer of only glucose, hemicellulose (also known as polyose) is a polymer of five different sugars. It contains five-carbon sugars

(usually xylose and arabinose) and six-carbon sugars (galactose, glucose, and mannose), all of which are highly substituted with acetic acid [19, 20]. Many of them have the general formula $(C_5H_8O_4)_n$ [21]. Hemicellulose consists of around 200 sugar units and has an average molecular weight of <30,000 [1]. Hemicellulose is amorphous because of its branched nature and is relatively easy to hydrolyse to its monomer sugars compared to cellulose [19]. It can also be thermally degraded more easily than cellulose as it was observed from the lower decomposition temperature range (250-350°C) when biomass is pyrolysed at 50°C /min [18]. This is probably due to the shorter and less uniform chains of hemicellulose.

2.2.4 Lignin

Another major component of biomass is lignin whose content varies greatly depending on the types of biomass. For instance, it accounts for 27-30 wt% of softwood, 20-25 wt% of hardwood and 5-20 wt% of switchgrass [1]. In addition, some biomass species can contain very high lignin content such as walnut shell whose lignin content was reported to be 52.3 wt% [22]. Lignin is a type of polymeric material and is composed substantially of aromatic ring-containing units; it is described as a three-dimensional, cross-linked, alkylated phenolic polymer [23]. Unlike the polysaccharides (cellulose and hemicellulose), the chemical structure of lignin is complex as the degree of polymerisation of lignin in biomass cannot be universally quoted because it is difficult to be extracted without changing its chemical structure. In addition, no simple structural formula of lignin can be reported because it consists of various types of substructures which appear to repeat haphazardly. Nevertheless, the lignin of almost all biomass plants consists of different proportions of three types of phenyl-propane units, namely *p*-hydroxyphenyl, guaiacyl and syringyl units, which originate from *p*-coumaryl, coniferyl and sinapyl alcohols, respectively. The chemical structures of these alcohol precursors are illustrated by Figure 2-2. In lignin, the monomer units are linked by ether (C-O-C) and carbon-to-carbon (C-C) bonds as can be seen from Figure 2-3 which shows an example of possible partial structure of lignin molecule. When thermally decomposed, lignin gives a wide range of phenolic compounds substituted with hydroxyl and methoxy groups. It was suggested that the main range of lignin decomposition temperature

when pyrolysing biomass at a heating rate of 50°C/min is between 350°C and 500°C and the lignin continues to decompose at temperature higher than 500°C with a slower rate [18].

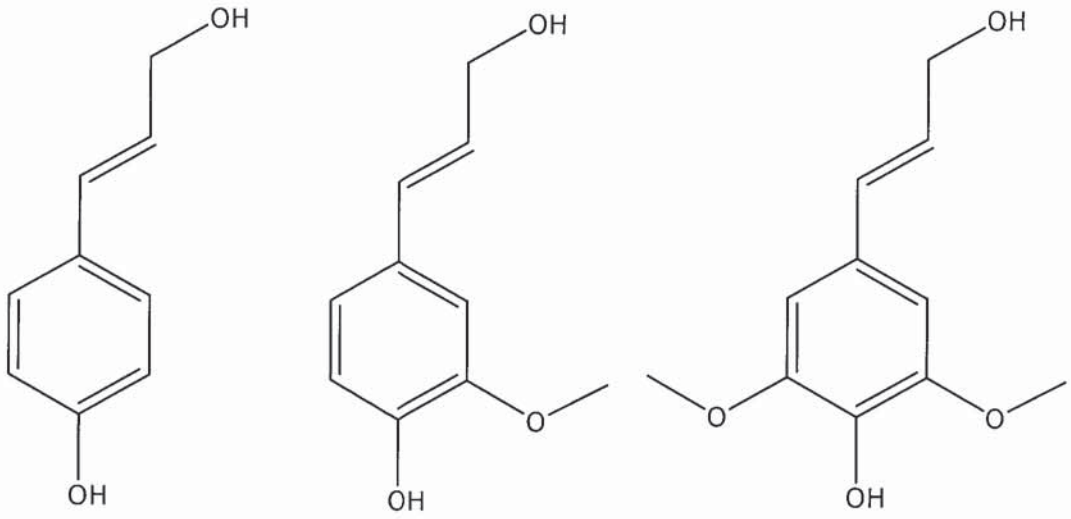

***p*-Coumaryl alcohol** **Coniferyl alcohol** **Sinapyl alcohol**

Figure 2-2 *p*-Coumaryl, coniferyl and sinapyl structures

2.2.5 Organic extractives

Another important component of biomass is composed of low molecular weight organic extractives. Examples of biomass extractives are fats, waxes, proteins, terpenes, gums, resins, simple sugars, starches, phenolics, essential oils, pectins, mucilages, glycosides and saponins [17]. These can be extracted from biomass with various solvents such as ethanol, toluene, water, acetone, dichloromethane or hexane. Since using different solvents lead to different extractives content, it is important to specify the solvents when reporting the extractives content. The determination of extractives content of biomass samples was performed during structural analysis and will be discussed in chapter 4 (section 4.2.2.4). It is important to note that the extractives content measured in chapter 4 includes not only organic materials, but also includes part of the inorganic matter whose details are described below.

Figure 2-3 Partial structure of lignin molecule [24]

2.2.6 Inorganic minerals

Besides water and organic materials, inorganic minerals are present in biomass. Generally the main elemental constituents of biomass minerals are silicon (Si), calcium (Ca), potassium (K), sodium (Na), and magnesium (Mg) with smaller amounts of sulphur (S), phosphorous (P), iron (Fe), manganese (Mn) and aluminium (Al). These constituents occur as oxides (O^{2-}), carbonates (CO_3^{2-}), sulfates (SO_4^{2-}), chlorides (Cl^-) and phosphates (PO_4^{3-}) [25] and are known collectively as ash. The concentrations of ash range from less than 1% in softwoods to 15% in herbaceous

biomass and agricultural residues [26]. The ash content is measured as the residue after burning at 575°C to constant weight. The determination of ash content of biomass samples will be discussed in more detail in chapter 4 as part of the proximate analysis (section 4.2.2.1).

2.3 FAST PYROLYSIS PRINCIPLES

Fast pyrolysis is a moderate temperature (400-600°C) process in which biomass is rapidly heated in the absence of any oxidising agent. Under these conditions, biomass decomposes producing pyrolysis vapour and solid residue, which is called char or bio-char. Part of the pyrolysis vapour is condensed to a dark brown mobile liquid which has a heating value of about half that of conventional fuel oil [27], whereas the rest is non-condensable gaseous product.

The essential features of a fast pyrolysis process are: (i) very high heating and heat transfer rates that require a finely ground biomass feed, (ii) carefully controlled temperature of around 500°C and vapour phase temperature of 400-450°C, (iii) short vapour residence time of typically less than 2 seconds, and (iv) rapid cooling of the pyrolysis vapours to give the bio-oil product [28].

Fast pyrolysis can be carried out in a wide range of reactor types such as fluid bed, ablative, circulating fluid bed, entrained flow, rotating cone, transported bed and vacuum moving bed. It is not the intention to review the reactor configurations here, since an extensive and excellent review already exists [27]. Nevertheless, a fluidised-bed type reactor is described below because this configuration was used in this project.

A conceptual fluidised bed fast pyrolysis system is shown in Figure 2-4. The system starts with drying unit to obtain biomass with moisture content below 10 wt% in order to control the water content of bio-oil product because water in the biomass feedstock would inevitably end up in the bio-oil. Drying is not always necessary, especially if the biomass is already naturally dried. Since drying also consumes energy or heat, the heating source can be obtained by combustion of char and/or gaseous products. After drying, the biomass feedstock is ground to particle size of less than 2 mm in order to

achieve high heating and heat transfer rate. In the fluidised bed pyrolysis reactor, sand, a typical fluidising medium, is pre-heated to a temperature of around 500°C. It is important that the initial bed temperature prior to biomass feeding should be slightly higher than expected reaction temperature since it is known that the heat of reaction for the fast pyrolysis process is marginally endothermic [17]. The heat for pyrolysis reactor can be derived from char burning. Nitrogen is used as a typical fluidising gas to start up the process. Then, the recycle gas stream is used. The dried and ground biomass particles are conveyed to the reactor by, for example, a screw feeder. Once a particle is heated, primary pyrolysis vapour is evolved. This vapour includes water, aerosols, condensable vapour and non-condensable gases, all of which are derived from the degradation by fragmentation and depolymerisation of the original biomass components. The pyrolysis vapour together with solid residues is entrained out of the reactor passing a cyclone where most of the solid char is separated and the vapour is cooled and collected by a bio-oil recovery unit. This unit can be composed of a quench column and an electrostatic precipitator (ESP). The use of ESP is possible due to the polar character of the pyrolysis vapour [29].

Figure 2-4 Fast pyrolysis process principles [27]

The advantages of fast pyrolysis for bio-oil production are simplicity of the process, atmospheric pressure operation, main product being in the form of liquid that can be readily stored and transported, estimated low production cost, high thermal efficiency, and low fossil fuel inputs leading to CO_2 neutral fuel [30]. The overall energy balance

of biomass fast pyrolysis can give 60-70% efficiency to liquids with low environmental emissions due to low sulphur and nitrogen contents of the original biomass [31]. Bio-oil fuels generate more than 50% lower NO_x emissions than diesel oil in a gas turbine and no SO_x emissions are generated [17]. Although bio-oil is regarded as the main product from fast pyrolysis, solid char and non-condensable gases can also be considered as valuable by-products.

2.4 FAST PYROLYSIS PRODUCTS

2.4.1 Liquid bio-oil

Bio-oil is a dynamic mixture of water, char fines and compounds (monomers, oligomers, polymers or fragments) derived from cellulose, hemicellulose and lignin macropolymers of biomass, which include sugars, acids, alcohols, aldehydes, ketones, furans, esters, phenols, guaiacols, syringols and multifunctional compounds, such as hydroxyacetic acids, hydroxyaldehydes and hydroxyketones. These organic materials present in bio-oil are constantly reacting to move toward chemical equilibrium [32]. The actual composition of a bio-oil is a complex function of feedstock, pyrolysis technique, char removal system, condensation system, and storage conditions [3]. Bio-oil has nearly the same elemental composition as the biomass feedstock [33], thus having a high oxygen content, which makes it different from petroleum oils. Since bio-oil contains large proportion of organic acids such as acetic and formic acids, it has low pH value (typically 2-4).

Bio-oil can be separated into water soluble and insoluble fractions. The former contains light organic compounds, while the latter contains mainly large molecules derived from lignin, which are known as pyrolytic lignin. The content of water-insoluble fraction of bio-oil varies from about 20 to 40 wt% [34]. Pyrolytic lignin is composed mainly of tri- and tetramers of lignin sub-units (hydroxyphenyl, guaiacyl and syringyl units), has an average molecular weight between 650 and 1300 g/mol [6] and represents almost 80% of the original content of biomass lignin [29]. According to the thermal ejection theory postulated by Piskorz et al [35], lignin oligomers found

in pyrolytic lignin are formed by direct mechanical expulsion from biomass particles as a result of a partial cracking of lignin molecules. This theory is supported by a study of bio-oil nature by using small-angle neutron scattering (SANS) technique [36] by which bio-oils were found to be nanostructured fluids constituted by a complex continuous phase and nanoparticles mainly formed by the association of units of pyrolytic lignins. It was also found that the aggregation or polymerisation of these units during storage produces branched structures, which are responsible for bio-oil aging. The polymerisation continues until the heaviest lignin-rich fraction separates out of the matrix as a viscous sludge [36]. The consequence of polymerisation reactions can be noticed from the increase in the average molecular weight and the viscosity of bio-oil over time as it is known that the bio-oil viscosity is directly correlated with the average molecular weight (Mw) and the water insoluble fraction of bio-oil [5, 32]. The increase of bio-oil Mw during storage can also occur by condensation or dehydration reactions of carbohydrate-derived constituents such as aldehydes, and ketones [17], which produce water as a by-product. Therefore, an increase in water content of bio-oil during storage is apparent. This could ultimately lead to the phase separation of the bio-oil with heavy sludge at the bottom and light aqueous top phase.

Due to significant amounts of the oxygenated compounds including the lignin derivatives, bio-oils have relatively low heating values, are relatively unstable, have high viscosity, have low volatility and are corrosive and incompatible with the less polar petroleum oils [37]. Therefore, it is suggested that bio-oil should be upgraded in order to improve its properties prior to utilisation. Possible bio-oil upgrading options are discussed in section 2.6.

The bio-oils can be used either as whole bio-oil, fractionated bio-oil or extracted specific chemicals. The potential applications of the bio-oil include fuel for heat and power generation, slow release fertilizer, preservatives, liquid smoke, resin precursors and for production of chemicals such as acetic acid, hydroxyacetaldehyde, levoglucosan, levoglucosenone and maltol [38, 39].

2.4.2 Solid bio-char

Char obtained from fast pyrolysis of biomass is also called bio-char. It is the solid residue of pyrolysed biomass particles. Char is normally removed from the vapour stream by cyclone separation. It contains high proportion of carbon with small quantities of oxygen and hydrogen. It also contains most of the inorganics present in the original biomass. Therefore, it may be used for soil amendment. Since the char product has heating value (HHV) of around 23 MJ/kg, it can be used as an energy source for process heat. The char may also be used for production of hydrogen or syn-gas by steam reforming or thermal cracking processes [20, 38]. In addition, the char could be used as a solid fuel in boilers or could be co-fired with conventional fossil fuels. Consequently, char can be regarded as a valuable by-product.

2.4.3 Non-condensable gases

Non-condensable gases are composed mainly of carbon dioxide (CO_2), carbon monoxide (CO), hydrogen (H_2), methane (CH_4), ethene or ethylene (C_2H_4), ethane (C_2H_6), propene or propylene (C_3H_6) and propane (C_3H_8). Additionally, if the liquid collection unit is not 100% effective, some light volatile could be in the gaseous stream such as pentane, benzene, toluene, xylenes, acetaldehyde, etc.

Since pyrolysis gas contains significant amount of carbon dioxide along with methane and some other combustible gases, it might be used as a fuel for industrial combustion purposes [38]. It is suggested by Bridgwater [41] that the most effective utilisation method for the pyrolysis gaseous by-product is as the fluidising medium if a fluid bed is used and use in-plant for some of the process energy requirement, although its specific energy content is rather low.

2.5 KEY FACTORS AFFECTING FAST PYROLYSIS PRODUCTS

There are many factors that can affect fast pyrolysis products. It is not the intention of this section to review them all. Nevertheless, certain key factors are discussed in this

section including feedstock composition, pyrolysis temperature and residence time as well as char separation system.

2.5.1 Effect of feedstock composition

Components of biomass feedstock that are known to significantly affect yields and properties of pyrolysis products are mainly water, ash and lignin. High moisture content of biomass would lead to high water content of bio-oil, which affects the heating value, viscosity, pH and density of the bio-oil. Although the viscosity is lowered and the pH is increased by the increased water content of bio-oil, the heating value and the density (especially the energy density) are decreased.

The influence of mineral matter present in biomass during pyrolysis has previously been studied [25, 40, 42-45] and found that the inorganic species catalyse biomass decomposition and char-forming reactions, resulting in the reduction of liquid yields and the formation of char and non-condensable gases. It is also known that the alkali metals influence the thermal decomposition mechanism during fast pyrolysis by enhancing the fragmentation (ring scission) of the monomers making up the macro-polymer chains [45, 46]. These suggest that the content and composition of ash are important parameters which affect the yield and chemical composition of the pyrolysis products.

Amongst the macro-polymer components of biomass, lignin seems to significantly affect bio-oils properties. A clear, positive, dependence between lignin content in the feedstock and water insoluble fraction (pyrolytic lignin) of the bio-oil has been reported [47]. As discussed earlier in section 2.4.1, pyrolytic lignin is speculated to be responsible for the high viscosity, high average molecular weight and low stability of bio-oil. Moreover, Ghetti et al [48] studied the effect of biomass lignin content on burning characteristics of bio-oil products using thermogravimetric analysis (TGA) technique and concluded that biomass of low lignin content produces a lighter pyrolysis liquid product, which may be considered a better bio-oil for use as a fuel. It is therefore logical to state that the content of lignin in biomass can affect the bio-oil quality in terms of viscosity, molecular weight, stability and combustion behaviour,

and a lower lignin content of biomass appears to be beneficial to the bio-oil properties.

2.5.2 Effect of pyrolysis temperature

In fast pyrolysis processing, temperature can be either temperature of reaction or reactor temperature. The former is the temperature at which biomass particles pyrolyse and is difficult to measure. The reactor temperature is higher than the reaction temperature due to the heat loss or temperature gradient from the reactor wall to heat transfer medium and to biomass particles. Increasing the reactor temperature would increase the temperature of reaction. It is therefore important to define where the temperature is measured. In this project, fast pyrolysis for bio-oil production is carried out in a fluidised-bed reactor. Therefore, pyrolysis temperature is measured as an average temperature of the fluidised bed.

Generally, increasing temperature would lead to higher gas yield and lower char yield. Although the overall gas yield is increased with temperature, the yields of individual gases are not increased uniformly as it is known that increasing temperatures can enhance secondary cracking of pyrolysis vapour which ultimately produces CO and CH_4 rather than CO_2 [49]. The effect of temperature on bio-oil yield is more complex as bio-oil yield is the sum of organics and water yields. Therefore, it is easier to consider the yields of organics and water separately. In pyrolysis temperature range of 400-600°C, organics yields tend to reach a maximum at a specific temperature depending on feedstocks (500°C is a typical maximum temperature for wood feedstock). Temperatures below or above this would give lower organics yield. The effect of temperature on water yield is relatively small, but the yield appears to increase marginally with increasing temperature.

The effect of temperature on bio-oil chemical properties has been reported by Elliott in 1988 [50]. He concluded that for short-residence-time processing there is a direct correlation between chemical composition and operating temperature. As the temperature increases, the oxygen content decreases and the hydrogen to carbon ratio decreases. In addition, he also reported that the biological activity of pyrolysis oils, as

measured by mutagenic and tumor-initiating activity, correlates with pyrolysis temperature. The activity appears only in the high temperature (750°C or more) tars which contain high levels of polycyclic aromatic hydrocarbons (PAH). Similar finding has also been found by Horne and Williams in 1996 [51] that increasing pyrolysis temperature (from 400 to 550°C) led to an increase in PAH concentration of bio-oils produced from fast pyrolysis of mixed wood waste, but the overall PAH concentration in all bio-oils was low (< 120 ppm).

2.5.3 Effect of vapour residence time

Vapour residence time is measured as how long the pyrolysis vapour spends in the hot environment prior to condensation. It is mentioned earlier that an essential features of fast pyrolysis is the short vapour residence time of typically less than 2 seconds. This is to reduce secondary reactions such as thermal cracking, re-condensation, re-polymerisation and char formation, which can cause a reduction of organics yields as well as an increase in the yields of permanent gases and char. It has been shown by Piskorz et al [52] when pyrolysing whole sweet sorghum and sweet sorghum bagasse that increasing vapour residence time from ~0.2 to ~1.0 second led to a reduction of organics yields and an increase in the yields of char and gas.

2.5.4 Effect of char separation

In a fast pyrolysis process, solid char is normally separated by a cyclone or a series of cyclones. Separation of char out of the reactor zone as soon as possible is recommended as the char formed during pyrolysis serves as a vapour-cracking catalyst, which can decrease bio-oil yield and increase the yield of non-condensable gases. Generally, the efficiency of the char separation by cyclones is not 100%. As a consequence, some char is inevitably carried over from cyclones and ends up in the bio-oil as suspended submicron particles, thus increasing the bio-oil solids content and viscosity. The presence of high concentrations of submicron char particles in bio-oils will make them problematic for combustion in steam boilers, diesel engines, and turbine operations because of the potential release of the ash and alkali metals during

combustion [26]. In addition, agglomeration of the alkali metal-laden submicron char particles in the bio-oil taking place during cold room storage may cause problems for its long-term storage, transportation, and use [26]. The presence of char can also worsen the stability of bio-oil by catalysing reactions that lead to the increase in bio-oil viscosity [3]. Since the inefficient char separation during pyrolysis can deteriorate the pyrolysis liquid product, improving the char removal system would be useful. This can be achieved by, for example, applying hot vapour filtration technique whose detail is provided in section 2.6.1.

2.6 BIO-OIL UPGRADING OPTIONS

Depending upon the desired application, bio-oils can be used without modification or they may be chemically changed to meet the requirements of a specific application, e.g., storable boiler fuels or high-octane gasoline [33]. In this section, a selection of upgrading methods, namely hot vapour filtration, solvent addition and hydrotreating are outlined, whereas catalytic vapour cracking, which is the only upgrading technique experimentally investigated in this project, will be discussed in detail in chapter 3.

2.6.1 Hot vapour filtration

As discussed earlier in section 2.5.4 that char fines that are entrained out of cyclones and collect in bio-oil can affect the viscosity, stability and applications of bio-oil. Therefore, hot vapour filtration has been proposed as a more effective technique for capturing these fine particles. Depending on the feedstock particle size and ash content as well as the design of the hot filter, the efficiency of hot vapour filtration varies considerably.

Diebold [3] suggested that although cyclonic separation is the easiest way to remove char, even the best cyclones begin to lose their efficiency with char particles smaller than about 10 μm in diameter. This statement was supported by Lee et al [40] as they found when pyrolysing rice straw samples in a fluidised-bed reactor that by using a

cyclone char particle size 10-170μm was captured, whereas a hot vapour filter could remove solids of particle size around 0.3μm, leading to the bio-oil alkali metals (Na + K) content of 25 ppm and alkaline earth metals (Mg + Ca) content of 63 ppm. It has been reported by Diebold [3] that the best job of hot-gas filtration to date at the National Renewable Energy Laboratory (NREL) resulted in less than 2 ppm alkali and 2 ppm alkaline earth metals in bio-oil. The main difference between the NREL and Lee et al [40] works could be due to the biomass raw materials used and the design of the filtration units.

Although the main purpose of a hot vapour filtration unit is to capture fine particles in order to improve the char removal efficiency which leads to a reduction of bio-oil solids content, there are some side effects due to the existence of the unit in the pyrolysis system. When the char accumulates in the filter unit as a filter cake, it can function as a vapour-cracking catalyst which can cause a reduction of bio-oil yield. This problem is projected to be more severe in large scale operations because of the cracking of the reactive molecules or polymerisation of some of the bio-oil components to form char. A solution to this problem could be the use of very compact filters which can remove the char particles and maintain a very low residence time of 1 second or less in the hot vapour filter unit [26]. Moreover, the char cake may crack heavy molecules in pyrolysis vapour, particularly those derived from lignin. This would lead to the production of bio-oil of better quality in terms of solids content, viscosity and stability.

2.6.2 Solvent addition

Addition of solvents even with small quantities can dramatically improve bio-oil properties. Various solvents have been tested including alcohols (ethanol, methanol and isopropanol), acetone, ethyl acetate, tetralin and mixtures of two different solvents (methyl isobutyl kenone + methanol and acetone + methanol) [32, 53-57]. General beneficial effects of solvent addition on bio-oil properties are reduction of viscosity, improvement of stability measured by the rates of increase in viscosity and in average molecular weight during storage or ageing, decrease of density which would allow the bio-oil to be filtered more easily, increase in heating value or added

heating value, improved homogeneity and burning characteristics as well as delay of the bio-oil phase separation process. However, a disadvantage of the addition of solvents, especially alcohols, is the decrease of bio-oil flash point. To overcome this drawback, Oasmaa et al [58] proposed a simple technique called concentration method by which most of the water and part of the light reactive volatiles of fast pyrolysis liquid are replaced by alcohol. The water and light volatiles are removed from the main bio-oil collection container by increasing the condensation temperature to 50±4°C. This method results in an improvement of bio-oil quality in terms of homogeneity, viscosity, stability, odor and acidity without significantly decreasing the flash point of the bio-oil product.

The function of alcohol, an organic solvent, in bio-oil/alcohol blend appears to involve molecular dilution to slow the bio-oil ageing reactions and the formation of intermediate products by the reactions of alcohol with compounds present in bio-oil [32]. It is also believed that the addition of alcohols can enhance the solubility of the hydrophobic compounds such as high molecular mass lignin derivatives and extractives, leading to an improvement of bio-oil homogeneity [57]. Since an analysis of the mixture of bio-oil and ethanol shows the presence of acetals, hemiacetals and ester, the reactions probably include esterification of carboxylic acid groups, and acetalisation and hemiacetal formation of aldehyde groups [54]. These chemical reactions are summarised in Figure 2-5.

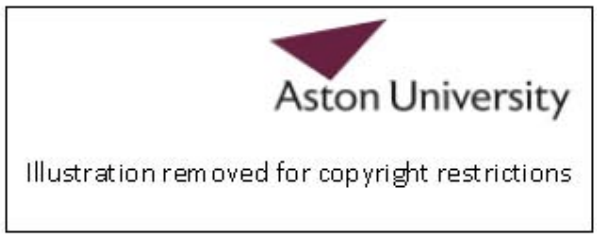

Figure 2-5 Reactions probable to occur in bio-oil with the addition of alcohol (reaction equations obtained from reference [3])

2.6.3 Hydrotreating

Hydrotreating is another upgrading option for improving bio-oil properties. The purpose of hydrotreating is to reject the oxygen in the form of water. Depending on the severity of the hydrotreating, more than 95% of oxygen in bio-oil can be removed, thus producing nearly pure hydrocarbons including aromatics and naphthenes (cycloalkanes). Hydrotreating can be conceptually characterised as follows [41, 59]:

$$\mathbf{C_6H_8O_4}\ \text{(Bio-oil)} + \mathbf{6H_2} \rightarrow \mathbf{6CH_2}\ \text{(Hydrocarbon equivalent to naptha)} + \mathbf{4H_2O}$$

To achieve hydrotreating, high pressures of 70 to 200 bars to provide a high hydrogen partial pressure and a two-stage process operating at about 250-400°C are normally required [41]. The first stage of hydrotreating is an initial stabilisation where a temperature of 250-275°C is applied. The second stage is a more conventional hydrotreating process operating at 350-400°C. The initial step consumes little hydrogen, but is essential to avoid polymerisation of the bio-oil at the higher temperature of the second stage. Another factor that is important for hydrotreating is the presence of solid catalysts. Typical hydrotreating catalysts include sulphided CoMo and NiMo based catalysts. During hydrotreating at high hydrogen pressure in the presence of catalyst, bio-oil reacts with H_2 to form water and saturate carbon-carbon bonds. To minimise the hydrogen consumption without decreasing the octane number of the liquid product, it is suggested that hydrogenation of aromatics in bio-oil should be avoided [20].

In addition to the benefit of hydrotreating in terms of bio-oil properties improvement, a useful side-effect of full hydrotreating (less than 2wt% oxygen in the final product) is that the product water readily separates from the hydrocarbon product and is relatively clean, and the water may also strip out the alkali metal derived from the wood ash and resolve one of the potential problems in using biomass-derived fuels in turbines [41]. Although hydrotreating is a promising upgrading option, the requirements of high pressure and the high hydrogen consumption may reduce the process feasibility, especially in economic aspects.

Another promising approach to upgrading bio-oil is the direct catalytic conversion in the vapor phase at low pressure and without hydrogen by catalytic vapour cracking and reforming. This can avoid the problem of re-evaporation of liquid bio-oil and allows pyrolysis and catalytic upgrading to occur in one thermal cycle. This method is therefore called "catalytic pyrolysis". Since this approach is the main aim of this project, a review of catalytic pyrolysis will be provided in the next chapter instead.

3 LITERATURE REVIEW ON CATALYTIC PYROLYSIS OF BIOMASS

3.1 INTRODUCTION

Bio-oil can be upgraded by the application of catalysts. An example of this already given in section 2.6.3 is hydrotreating where a catalyst such as sulphided Co-Mo or Ni-Mo is utilised in conjunction with high hydrogen pressure in order to remove oxygen from liquid bio-oil, thus producing hydrocarbon-rich liquid fuel. Another example is the application of zeolite catalysts such as ZSM-5 to liquid bio-oil at atmospheric pressure without hydrogen input in order to induce cracking and aromatic hydrocarbon formation reactions. This technique does not seem to be an attractive route because the liquid bio-oil needs to be re-vapourised prior to reactions over the catalyst. Condensation of pyrolysis vapour to obtain bio-oil and evaporation of bio-oil for upgrading purposes is not thermally efficient. Consequently, the introduction of catalysts into a pyrolysis process before condensation of pyrolysis vapour so as to induce vapour-phase catalytic reactions is a more promising route and is one of the main focuses of this project. Since the catalytic vapour-phase upgrading is carried out immediately after or at the same time as pyrolysis in one thermal cycle, the combination of the upgrading and the pyrolysis process is referred to as "catalytic pyrolysis of biomass".

As previously mentioned (chapter 2), bio-oils contain significant amount of oxygenated compounds including lignin derivatives which results in the relatively low heating values, low stability, high viscosity, low volatility and low pH. To overcome these problems, a catalyst can be incorporated into a pyrolysis unit and the catalyst is expected to enhance deoxygenation, cracking and reforming reactions. The deoxygenation of pyrolysis vapours generally includes decarboxylation, decarbonylation and dehydration that remove oxygen in the form of carbon dioxide, carbon monoxide and water, respectively. Regarding the cracking reactions, a desired catalyst would selectively crack the heavy molecules present in pyrolysis vapour, particularly lignin oligomers expelled from the lignin macropolymer of the original

biomass during pyrolysis [35] to produce lower molecular weight compounds, while minimising the cracking of low molecular weight molecules to permanent gases. In cracking lignin derivatives, deoxygenation can also occur; for example, when ether bonds (C-O-C), both ether bridge joining subunits and diaryl ether, are cleaved and carbon monoxide is generated [60]. Moreover, during cracking of pyrolysis vapours, some olefinic gases such as ethylene and propylene may occur as intermediates which can undergo further reforming reactions such as oligomerisation, cyclisation, isomerisation or aromatisation to produce high value liquid hydrocarbons. The severity of the cracking, deoxygenation and reforming reactions influences the liquid product distribution and depends largely on types of catalyst as well as process parameters such as temperature, residence time and weight hourly space velocity, WHSV (h^{-1}) (defined as the ratio of the biomass feed rate (g/h) to the amount of catalyst used (g)). The effects of catalyst types and process parameters are reviewed in the next sections.

There are four possible configurations that can be used to incorporate catalyst into a fluidised-bed pyrolysis system: (i) co-feeding biomass and catalyst, (ii) use catalyst as the whole or part of the fluidising medium, (iii) close-coupled in-bed catalysis, and (iv) close-coupled catalyst in a secondary reactor [61]. In co-feeding biomass and catalyst, the catalyst is added to the biomass before experiments. Depending on the nature of the catalyst, the addition can be either by wet impregnation or dry mixing. Possible drawbacks of this mode of catalyst addition include a difficulty in recovering the catalyst and a high chance of catalyst particles entraining out of the cyclone and ending up in the liquid product. The use of catalyst as the whole or part of the fluidising medium is the easiest way to add catalyst into the pyrolysis process. In this mode, the pyrolysis and catalytic reactions take place under the same operating temperature. It also allows an immediate contact of pyrolysis vapour with the catalyst. However, the catalyst may be rapidly deactivated by coking or deposition of the char fines and condensed pyrolysis vapour. The third mode of catalyst addition is the close-coupled in-bed catalysis where catalyst is placed as fixed or fluidised bed at the reactor freeboard. In this configuration, pyrolysis vapour together with char particles passes over the catalyst bed, leading to accumulation of the char which could ultimately increase the pressure drop across the bed. Therefore, the char particles should be separated from the pyrolysis vapour stream by a cyclone prior to being

passed over a catalyst bed. This idea leads to an occurrence of the fourth incorporation mode, which is close-coupled catalyst in a secondary reactor. This mode also allows the catalyst to be operated under a different operating temperature from the primary pyrolysis reactor. It can eliminate the problem of char accumulation, thus preventing the premature catalyst deactivation. As a consequence, this catalytic pyrolysis arrangement is the only one investigated in this project. Details of the equipment setup for the current study can be found in section 6.2.

Various catalysts can be applied for catalytic pyrolysis of biomass. The most widely investigated catalysts for this purpose include zeolites, especially ZSM-5 type, and zeolite-like mesoporous catalytic materials. In addition, metal oxides and certain natural catalysts have also been studied in the field of catalytic pyrolysis. The literature review of catalytic pyrolysis of biomass with these different types of catalyst is given below.

3.2 ZEOLITE CATALYSIS

3.2.1 General description of zeolites

Zeolites are microporous crystalline solids with well-defined channels or pores of uniform diameter. They consist of SiO_4 and AlO_4^- tetrahedra, which are interlinked by the sharing of oxygen atoms to give a three-dimensional network through which long channels run [62]. Different types of zeolites have different structures or frameworks, which result in their different properties and applications.

Zeolites can be used as catalysts in many applications such as cracking of heavy oil in petroleum refinery industries. The catalytic activities of zeolites are related to their shape selectivity and acidity. There are three types of shape selectivity, namely reactant selectivity, product selectivity and restricted transition state selectivity [62].

Reactant selectivity means that only starting materials of a certain size and shape can enter the interior of the zeolite pores and undergo reactions at the catalytically active

sites. If the molecular size of a reactant is larger than the pore apertures, it cannot react. Therefore, zeolites are also called molecular sieves. In spite of the considerable molecular sieve effect, 100 % selectivity is often not attained because the reactants can also react to a certain degree on the outer surface of the zeolite crystals [62].

Product selectivity occurs when only products of a certain size and shape that can leave the pore system are formed. This type of shape selectivity can also have drawbacks. Large molecules that are unable to exit the pores can be converted to undesired by-products or undergo coking, thus leading to catalyst deactivation.

The third form of shape selectivity depends on the fact that chemical reactions often proceed via intermediates. Owing to the pore system, only those intermediates that geometrically fit to the zeolite cavities can be formed during catalysis. Therefore, only products produced through intermediates that are suitable for a specific type of zeolites can be formed.

Apart from the size and shape selectivity functionality of zeolites, acidity is an important property in catalysis application. There are two types of acid sites, namely Brönsted (proton donor) and Lewis (electron pair acceptor) sites that exist in zeolites. Although both sites are involved in catalytic activities, the former appear to be stronger. The strength of zeolite acidity relates not only to the number of the acid sites, but also to the natures of the acid sites (Brönsted or Lewis). The zeolite acidity can be measured experimentally by for example temperature programmed desorption (TPD) of ammonia, FT-IR measurements of pyridine adsorption and ^{1}H MAS solid state NMR for the determination of the total acidity, nature of acid sites and number of hydroxyl groups present on zeolite catalysts, respectively. Moreover, zeolite acidity can be estimated from the Si/Al ratio; the high value of this ratio (>10) indicates the low concentration of acid sites of high strength, whereas the low Si/Al ratio (1-1.5) results in the high concentration of acid sites of medium strength [62].

3.2.2 Conceptual catalytic upgrading with zeolite ZSM-5

ZSM-5 is a zeolite that possesses the three-dimensional system of intersecting channels which is made up of elliptical straight channels (0.51 × 0.55 nm) and near

circular zig-zag channels (0.54 × 0.5 nm) [63]. It is initially developed by Mobil and is used in methanol-to-gasoline (MTG) process. The use of a monofunctional zeolite ZSM-5 catalyst in converting biomass pyrolysis liquid into gasoline-range hydrocarbons was suggested by Bridgwater and Cottam [59] to conceptually follow the equation:

$$C_6H_8O_4 \rightarrow 4.6CH_{1.2} + 1.4CO_2 + 1.2H_2O$$

where $C_6H_8O_4$ and $CH_{1.2}$ represent pyrolysis liquid and hydrocarbon products (mainly aromatics), respectively. This gives a maximum stoichiometric yield of 42 wt% on liquid, or a maximum energetic yield of about 50 wt%. If a bifunctional or multifunctional catalyst that can generate in situ hydrogen through shifting the carbon monoxide in the product gas is used, the process would be expected to operate more in a carbon limited environment rather than hydrogen limited, as depicted in the following equation with a maximum stoichiometric yield of 55 wt% on liquid [59]:

$$C_6H_8O_4 + 3.6H_2 \rightarrow 6CH_{1.2} + 4H_2O$$

The processing conditions for the upgrading are atmospheric pressure, temperature from 350°C to 600°C and hourly space velocities of around 2 [41]. There are a number of beneficial process parameters including low-pressure (atmospheric) processing; no hydrogen addition, temperature similar to those preferred for optimum yields of bio-oil; and a close coupled process, which offer significant processing and economic advantages over hydrotreating [41]. In addition, a higher grade of gasoline (high octane gasoline) is produced than from hydrotreating as the high yields of aromatics (BTX) are produced from the zeolite [59]. The mechanism for the formation of aromatic hydrocarbons is discussed in section 3.2.3.

3.2.3 Mechanism for aromatic formation by ZSM-5 catalysts

The mechanisms of cracking and reforming of biomass pyrolysis vapours on ZSM-5 catalysts are not well understood. However, Bridgwater [41] suggested a global mechanism, which is a combination of cracking on the catalyst surface followed by synthesis of aromatics in the catalyst pores.

By comparing the results of catalytic upgrading experiments using ZSM-5 and silicalite (a molecular sieve catalyst consisting of all silica and very low alumina possessing a uniform pore diameter with structure similar to ZSM-5, the only exception being the absence of acid sites [63, 64]), the functions of pore structure and acid sites could be elucidated. This work was carried out by Katikaneni et al [65] who suggested that it was the combination of shape selectivity and acidity that is responsible for alkylation, isomerisation, cyclisation and aromatisation reactions which ultimately resulted in the formation of aromatic hydrocarbons.

In addition, Williams and Horne [66, 67] suggested that the formation of aromatic and polycyclic aromatic compounds during the zeolite ZSM-5 catalytic upgrading of biomass pyrolysis oils occurs by a dual mechanistic route. First, low-molecular-weight hydrocarbons such as alkene gases are formed on the catalyst, which then undergo aromatisation reactions (possibly Diels-Alder reactions) to produce aromatic and polycyclic aromatic hydrocarbons. Additionally, deoxygenation of oxygenated compounds found in the non-phenolic fraction of the pyrolysis oils may directly form aromatic compounds without going through the alkene route.

3.2.4 Biomass pyrolysis vapours upgrading studies

Catalytic pyrolysis of biomass in a bench-scale reactor using ZSM-5 catalysts has been carried out extensively at the University of Leeds [66-74] . The experimental system used was a combined fluidised bed pyrolysis reactor unit with the freeboard of the reactor packed with the zeolite to form a fixed catalyst bed. The reactor was 10 cm diameter × 100 cm high, constructed of stainless steel with full gas flow and temperature control. The reactor was heated externally and the fluidised bed and freeboard could be separately temperature controlled. Biomass feedstocks tested included pine wood [68], mixed wood waste [66, 67, 69-72, 74, 75] and rice husk [73]. The primary pyrolysis and catalyst bed temperatures investigated ranged from 400°C to 600°C and the weight hourly space velocity (WHSV) was around 1 h^{-1}. It was found from these studies that ZSM-5 catalysts affected not only the products yields, but also the bio-oil composition. Generally, the catalysts decreased the yield of

liquid bio-oils along with increasing the yields of permanent gases, which included carbon dioxide (CO_2), carbon monoxide (CO), hydrogen (H_2), methane (CH_4), ethylene (C_2H_4) and propylene (C_3H_6) with minor concentrations of other hydrocarbon gases. The gas yields also increased with increasing catalytic bed temperature. The liquid bio-oil before catalysis was homogeneous and single phase. However, after the pyrolysis vapours were passed over the catalyst bed, the bio-oil products became two phases (aqueous and oil phases), which can be easily separated. This is because the oil phase contained significant amounts of hydrocarbons, mainly aromatics in gasoline boiling range such as benzene, toluene and alkylated benzenes. By raising the catalyst bed temperature, the concentration of these single ring aromatic hydrocarbons was also increased. Apart from the increase of the aromatics, which are regarded as valuable chemicals and fuel additives, phenol and methyl phenol were also reported to increase in concentration after the zeolite catalysis. This increase could be due to the larger substituted phenols such as dimethoxyphenol (derived from biomass lignin) being partially converted to phenol, which then undergoes alkylation to form methylated phenols [69]. The ZSM-5 catalyst was also found to be effective in deoxygenation reactions as could be seen from the significantly lowered oxygen content of bio-oils. The oxygen was removed in the form of water at low catalytic temperature and carbon oxides (CO and CO_2) at high catalytic temperatures [71, 73]. When analysing bio-oils by size exclusion chromatography (SEC) (also known as gel permeation chromatography (GPC)) technique, it was found that the molecular weight distribution of the catalytic bio-oils was shifted to lower range and with increasing catalyst bed temperatures, the molecular weights were further decreased [67, 71, 73].

In addition, Williams and Horne [67] investigated the influence of different zeolite catalysts (H-ZSM-5, Na-ZSM-5 and Y-zeolite) and activated alumina in comparison to an inert material (stainless steel ball-bearings). The results showed that there were only small differences in the product yields and compositions from the catalysis of biomass derived pyrolysis oils for the Na-ZSM-5 and H-ZSM-5 catalysts. The bio-oil produced with stainless steel in place of the catalysts was similar in composition to the non-catalytic bio-oil, showing that thermal reactions in the presence of stainless steel had a minor influence on the composition of the upgraded bio-oils. The ZSM-5

catalysts gave the highest yields of hydrocarbon products when compared to the Y-zeolite and activated alumina catalysts.

In general, the catalytic bio-oils produced at the University of Leeds appeared to be better for usage than the non-catalytic ones due to the lower concentrations of oxygenated compounds, the higher concentrations of hydrocarbons and the lower molecular weight range. However, the higher concentrations of polycyclic aromatic hydrocarbon (PAH), such as naphthalene, fluorene and phenanthrene and their alkylated derivatives, in the catalytic bio-oils are their drawbacks since some of these PAH are known to be carcinogenic and /or mutagenic. The PAH species were also increased with increasing catalyst bed temperatures. To overcome this problem, the PAH may need to be further processed by for example hydrocracking in a typical refinery; this could give gasoline range hydrocarbons as products.

Another notable drawback of the catalytic pyrolysis process reported was the formation of coke on the catalyst, which was in the range of 11-13 wt% on biomass fed basis for the ZSM-5 catalyst [67, 71], but the coke yield increased to 19.1 wt% for the Y-zeolite and 18.4 wt% for the activated alumina [67]. This was believed to be due to the larger pore size of Y-Zeolite (7.4 Å) and activated alumina (20 Å), which allows larger coke precursors to enter the pore structure of the catalyst, initiating and contributing to the increased formation of coke [67]. The deactivation of zeolite ZSM-5 is discussed in more details in section 3.2.5.

Similar findings were also reported when ZSM-5 or ZSM-5 based materials were applied by other research organizations [76-78] during catalytic pyrolysis of biomass using a conical spouted-bed reactor [76, 77] or a circulating fluid bed (CFB) reactor [78]. The catalysts led to the increase in liquid yield and the decrease in gas yield. The catalytic bio-oils were less oxygenated, lower in molecular weight range and higher in hydrocarbons concentration when compared to non-catalytic bio-oils.

In the attempt to enhance the catalytic pyrolysis, the effects of catalyst dilution [70], co-feeding methanol [79] and co-feeding steam [74] were investigated by researchers at the University of Leeds using the reactor configurations as mentioned earlier and the details are summarised below.

3.2.4.1 Effect of catalyst dilution [70]

Biomass in the form of waste wood chips was pyrolysed in a fluidised-bed reactor at 550°C to maximise the formation of pyrolytic vapours. The pyrolysis vapours were then passed over a fixed bed of ZSM-5 zeolite catalyst located at the reactor freeboard at 500°C. The catalyst bed was diluted with stainless steel ball bearings to increase the residence time of the pyrolysis vapours in the bed and to provide additional hot surface for thermal cracking of the vapours. Bio-oils produced without the secondary bed appeared to contain low quantities of aromatic hydrocarbons. The presence of the steel alone did not increase the amount of aromatic hydrocarbons significantly. The presence of the undiluted catalyst did increase the formation of aromatic hydrocarbons, and the combination of the catalyst and the steel together gave a further increase. From the analysis of the aromatic hydrocarbon fractions, the 1:2 catalyst:steel experiment gave three times the yield of monocyclic aromatic hydrocarbons observed in the undiluted catalyst experiment. Therefore the presence of steel in the catalyst bed appears to be very beneficial for the formation of monocyclic aromatic hydrocarbons since these compounds are considered as target chemicals for the upgrading of biomass pyrolysis vapours for use as either premium grade fuel or high-value chemicals. In addition the presence of steel in the catalyst bed also increased the formation of polycyclic aromatic hydrocarbons.

3.2.4.2 Effect of co-feeding methanol [79]

Methanol was injected into the top section of fluidised-bed reactor to mix with the pyrolysis vapour. The mixture was then passed over a fixed bed of zeolite HZSM-5 catalyst at 500°C. The results showed that the key effects of co-feeding methanol were the increase in the amount of oxygen removed from the pyrolysis vapours as water at the expense of CO and CO_2 formation and the significant increase in the formation of alkylated phenolic and aromatic hydrocarbon products. Additionally, the formation of the PAH was also observed to be suppressed by the presence of methanol.

The significant increase in the yields of hydrocarbons was also found by other researchers [75, 80] when pyrolysis liquids or vapours were co-processed with

methanol over ZSM-5 catalyst, thus indicating that the co-feeding of methanol appears to provide synergistic benefits in terms of the valuable aromatic hydrocarbons production.

3.2.4.3 Effect of co-feeding steam [74]

Biomass was pyrolysed in a fluidised bed reactor at 550°C and the pyrolysis vapours in the presence of steam were passed over a zeolite catalyst bed maintained at either 500°C or 550°C. The bio-oils were analysed using coupled gas chromatography/mass spectrometry to determine the concentration of PAH. The presence of steam was found to significantly increase the formation of PAH. It was concluded that when steam is used to improve the formation of hydrocarbons, the concentrations of PAH are also increased.

3.2.5 Catalyst deactivation

According to previous studies [66, 69, 81-83] on catalytic upgrading of pyrolysis liquids, vapours or model compounds using zeolite ZSM-5, deactivation of the catalyst can be either reversible or irreversible. The reversible deactivation occurred by coking. Gayubo et al [83] suggested that the coke deposits can be divided into two fractions based on the two peaks of DTG curves obtained from the spent catalyst. The first fraction, which burns at lower temperature, is the thermal coke, which is probably the residue deposited on the matrix of the catalyst particles. The second fraction corresponds to the internal catalytic coke (possibly has a graphitic carbon structure similar to that generated in the transformation of methanol and ethanol) located in the ZSM-5 zeolite, which burns at higher temperature. Since the thermal coke deposits contain significant quantities of oxygen [66, 69], it is believed that these deposits which condensed on the catalyst surface are derived from the oxygenated components of pyrolysis vapours such as high molecular weight lignin derivatives (phenolic-based compounds), high molecular weight carbohydrate-derived compounds and small, but reactive molecules such as aldehydes (especially acetaldehyde) and furfural [69, 83].

The irreversible deactivation of the catalyst was suggested to take place via the dealuminating effect of steam at high temperature (≥450°C), which result in a sharp decrease of the catalyst acidity when it is used in successive reaction-regeneration cycles [81]. This deactivation may involve the formation of polycyclic aromatic hydrocarbons that are too large to leave the pores, thus blocking the active acid sites as mentioned earlier in section 3.2.4.3 that the presence of steam enhanced the formation of PAH [74]. It is therefore suggested that to avoid irreversible loss of catalyst activity the operation should be performed at temperature below 450°C and without addition of steam, although it is known that the presence of steam can have beneficial effects such as the increase in the formation of monocyclic aromatic hydrocarbons [74] and the attenuation of the overall coke content [82].

The catalyst deactivation also influences the pyrolysis products. It is known from section 3.2.4 that ZSM-5 catalysts can increase the concentrations of hydrocarbons (both monocyclic and polycyclic aromatic hydrocarbons), reduce oxygenated compounds and decrease molecular weight range of bio-oils. These changes are reported to reduce in their severity when the catalyst deactivated as observed from either increasing the catalysis run time [69] or increasing the number of regeneration cycles [66]. The former occurred by the combination of reversible and irreversible deactivation, whereas the latter indicates merely irreversible deactivation.

3.3 ZEOLITE-LIKE CATALYSIS

According to Baerlocher et al [84], zeolites and zeolite-like materials do not comprise an easily definable family of crystalline solids; a simple criterion for distinguishing zeolites and zeolite-like materials from denser tectosilicates is based on the framework density (FD), the number of tetrahedrally coordinated atoms (T-atoms) per 1000 $Å^3$. Basically, zeolite-like catalysts are crystalline micro or mesoporous materials having zeolite-like structure or layer structure.

Zeolite-like catalysts that have been previously tested in catalytic pyrolysis of biomass include MCM-41 [85-89], SBA-15 [86, 90] and MSU-S [91] mesoporous materials using either a micro-scale batch reactor [85, 90] or a bench-scale fixed-bed

reactor [86-89, 91]. MCM-41 (Mobile Crystalline Material) is an ordered mesoporous silicate molecular sieve of the M41S type, which possesses a porous system consisting of hexagonally arranged channels with diameters varying from 15 to 100 Å and has a high surface area of about 1000 m^2/g [92]. SBA-15 is also an ordered mesoporous silicate material, which possesses hexagonal structure and has long-range order, large monodispersed mesopores (up to 500 Å) and thick walls (typically between 3 and 9 nm) which make them more thermally and hydrothermally stable than MCM-41 type materials [86]. Another mesoporous molecular sieve tested in catalytic pyrolysis of biomass is MSU-S type, which exhibits high hydrothermal stability and increased acidity compared to Al-MCM-41 catalysts [91]. The great interest in attempting these mesoporous catalytic materials during catalytic pyrolysis of biomass arises from the fact that the main targeted compounds that need to undergo reactions (cracking, deoxygenating and reforming to produce a liquid product with lighter and less oxygenated compounds and rich in high-value products) are bulky molecules, particularly those derived from lignin. This therefore requires catalysts structures with channel diameters at mesopore scale.

Pyrolysis of bark-free spruce wood was conducted at 500°C in a micro-scale batch reactor in order to test Al-MCM-41 [85] and SBA-15 [90] catalysts. In the reactor system, also known as pyrolysis-gas chromatography/mass spectrometry (Py-GC/MS), approximately 1.5-2.0 mg of biomass samples were pyrolysed generating pyrolysis vapours, which were then passed over catalyst beds where the catalytic reactions took place. The catalysed pyrolysis vapours were subsequently entrained to the GC/MS equipment connected online to the pyrolysis unit in order to analyse the pyrolysis products. It is important to note that in Py-GC/MS system the pyrolysis vapours are not condensed to liquid bio-oil. Therefore, the pyrolysis products produced from the micro-reactor may not be exactly the same as those generated by any larger scale pyrolysis units involving liquid bio-oil condensation as pyrolysis vapour may undergo changes upon condensation [33]. However, the Py-GC/MS is a rapid method and is extremely useful for catalyst screening as various catalytic materials can be comparatively evaluated with different process parameters such as biomass/catalyst ratio, pyrolysis temperature and heating rate. The Al-MCM-41 catalysts tested by Adam et al [85] included an unmodified, a transition metal (Cu) modified, a pore enlarged with a spacer and a pore enlarged by altering the template

chain length. The biomass/catalyst ratio applied was 1:1. The purpose of the work was to find out whether aluminosilicate mesopore catalysis can improve the bio-oils quality, which was monitored by aldehyde yield (for stability indicator), organic acid yield (for pH or corrosiveness indicator) and phenol yield (because phenol is one of the high value chemicals). Results showed that the presence of the catalysts led to a complete elimination of levoglucosan, a decrease in aldehyde yields, an increase in acetic acid yields, an increase in the yield of phenol and a slight increase in hydrocarbon yield [85]. In addition, the catalysts were found to promote the scission of the aliphatic side chain of phenol derivatives, leading to a decrease in the yield of high molecular mass ($\geq$138) phenols. When SBA-15 and Al-SBA-15 were tested in comparison to a commercial fluid cracking catalyst (FCC) by the same group of researchers [90], similar results were found; the presence of catalysts led to an increase in light phonols, a decrease in heavy phenolics compounds and an increase in organic acids. The amounts of the furan and furan derivatives were also increased, whereas the aldehydes (hydroxyacetaldehyde, propanal and 5-hydroxymethyl furfural) yields were decreased. Char and water formation was enhanced by the use of catalysts. Among the three catalysts, FCC was found to be the most effective catalyst for the changes of the pyrolysis products. Moreover, aluminum incorporation into SBA-15 structure enhanced the effectiveness of the compounds in the upgrading of pyrolysis vapours.

As mentioned earlier, the zeolite-like mesoporous catalysts (MCM-41, SBA-15 and MSU-S types) were tested in a bench-scale fixed-bed reactor [86-89, 91]. In all experiments, the reactor was filled with 0.7 g of catalyst, or glassbeads for the non-catalytic tests and the piston was filled with 1.5 g of biomass. As soon as the reactor reached the desired reaction temperature (500°C), the biomass was transferred into the pyrolysis zone by means of a specially designed piston system and the pyrolysis products were in contact with the catalyst for 15 min. During the run, a constant stream of N_2 (100 cm^3/min) was fed from the top of the reactor for the continuous withdrawal of the products and the maintenance of the inert atmosphere. By using this experimental setup, Adam et al [86] investigated the catalytic activities of Al-MCM-41 materials with a Si/Al ratio of 20 and with three different mean pore sizes (24 Å, 28 Å and 30 Å) in comparison to Cu-Al-MCM-41, SBA-15 and Al-SBA-15. They found that after catalysis, gas yields increased, coke/char yields remained the same or

slightly decreased and aqueous part in the liquid phase increased. The organic yields increased with increasing the pore size of Al-MCM-41 catalysts. The analysis of the organic liquid showed that the hydrocarbon and phenol yields increased, while the carbonyls and acids yields decreased due to the catalytic activities. All the catalysts studied reduced the amounts of the undesirable compounds (defined as carbonyls, acids and PAHs) in the bio-oil, while more desirable compounds (hydrocarbons, phenols and alcohols) were obtained. However, one of the catalysts drawbacks is the PAH formation. The pore enhancement of the Al-MCM-41 appears to worsen the bio-oil quality because by increasing pore size, the yield of undesirable products increased at a higher rate than the desirable products. The incorporation of Cu into the Al-MCM-41 was found to increase the amounts of desirable products more than undesirable ones. In addition, the incorporation of Al into SBA-15 framework led to very high content of desirable products in the bio-oils; however the undesirable products also increase. This confirms the Py-GC/MS results as mentioned above that aluminum incorporation into SBA-15 structure enhanced the effectiveness of the compounds in upgrading pyrolysis vapours.

Apart from the effect of pore sizes of Al-MCM-41 materials that have been studied using the bench-scale fixed-bed reactor, the effect of Si/Al ratios [87, 88], the effect of metal incorporation [87, 89] and the effect of different species of biomass raw materials [86, 87] on pyrolysis products were recently investigated. The results can be summarised as follows.

The lowest Si/Al ratio (20) enhanced the production of phenols, while the intermediate Si/Al ratios (34 or 51) promoted the reduction of undesirable fractions (carbonyls, acids and heavy compounds) [87]. High Si/Al ratios (50 or 51) of the Al-MCM-41 samples enhanced the production of the organic phase of the bio-oil, while low Si/Al ratios (20, 30 or 34) favoured the production of non-condensable gases [87, 88].

The metals that were incorporated into Al-MCM-41 and tested for catalytic pyrolysis of biomass included copper (Cu), iron (Fe) and zinc (Zn). Without the metal incorporation, Al-MCM-41 enhanced the production of hydrocarbons; however in the presence of the metals, the amounts of hydrocarbons were not increased [87].

Incorporation of Cu led to a significant increase of the concentration of hydrogen in the gas stream [87]. Furthermore, the quality of the bio-oil based on the yield of phenols is increased for Cu and Fe incorporated Al-MCM-41 catalysts. However, for Zn–Al-MCM-41, the yield of phenols was lower than the unmodified Al-MCM-41 material, indicating that zinc is a less favorable metal for conversion of biomass to phenols than iron and copper [89].

Comparison of different biomass feedstocks during the catalytic pyrolysis was carried out by Adam et al [86] and Antonakou et al [87]. The former studied miscanthus and spruce, whereas the latter investigated miscanthus and Lignocel beech wood. The results form both works provide a general conclusion that the effect of catalysts on pyrolysis products was influenced by the type of biomass feedstocks and in some cases the Al-MCM-41 performed no better than the conventional zeolites. In other words, a catalyst that can be used to give desired pyrolysis products for a specific type of biomass may not provide the same results when other types of biomass are catalytically pyrolysed. Therefore, this needs to be taken into consideration when studying catalytic pyrolysis of biomass.

Hydrothermally stable mesoporous aluminosilicates (MSU-S) assembled from zeolite Beta (BEA) seeds were tested by Triantafyllidis et al [91] in catalytic pyrolysis of biomass using the same bench-scale fixed-bed reactor and pyrolysis conditions as described above. Two MSU-S materials were investigated. The first one (MSU-S/H_{BEA}) had a hexagonal mesopore structure with 30 Å mean pore size, whereas the second one (MSU-S/W_{BEA}) possessed a wormhole-like mesopore structure (HMS-type) with high textural porosity and 35 Å mean pore size. The use of the mesoporous aluminosilicates MSU-S led to significantly lower organic yields and also to higher coke and char yields, compared to non-catalytic pyrolysis. With regard to the quality of the organic phase of the bio-oil, the MSU-S catalytic materials were found to increase the formation of polycyclic aromatic hydrocarbons (PAHs) and heavy fractions, while they dramatically decreased the yields of acids, alcohols and carbonyls, and phenols. These effects were more pronounced in the wormhole-like MSU-S/W_{BEA} sample with the high textural porosity possibly because diffusion of large reactants and products was facilitated compared to the hexagonal pore structure of MSU-S/H_{BEA}. Since the bio-oils produced with the two MSU-S catalysts contained

mainly hydrocarbons, PAH and heavy compounds together with a relatively low content of oxygenated compounds (phenols, acids, carbonyls and alcohols), it is suggested that the bio-oils may be of high value for refinery upgrading processes such as fluid catalytic cracking (FCC) units for "green gasoline" production or hydrotreating/hydrocracking processes for "green diesel" production [91].

3.4 METAL OXIDES CATALYSIS

Catalysts containing metal oxides that have been investigated in the field of catalytic pyrolysis of biomass include zinc oxide (ZnO) [93], Criterion-534 (Co-Mo/Al_2O_3) [94, 95], DHC-32 (Ni-W/Al_2O_3) [96] and HC-K 1.3Q (Ni-Mo/Al_2O_3) [96]. Pyrolysis studies with these catalysts are summarised below.

A zinc oxide catalyst from Haldor Topsoe containing 99% ZnO and 0.5% Mg was applied by Nokkosmaki et al [93] in a bench-scaled fluidised-bed pyrolysis reactor close-coupled with a secondary catalyst bed reactor in order to investigate the effect of the catalyst on yields and properties of bio-oils. Pine sawdust was pyrolysed at 525°C and nitrogen was used as carrier gas. After the pyrolysis reactor, the pyrolysis vapours were passed through a hot gas filter kept at 475°C to remove char particles. Subsequently, the vapours were led through a bed of catalyst maintained at 400°C, followed by a condensation unit to obtain bio-oil products. The results showed that the ZnO was a mild catalyst as the liquid yield did not reduce substantially. According to the bio-oil analysis, the catalyst had no effect on water-insoluble fraction (lignin-derived compounds), but it decomposed the diethyl ether-insoluble fraction (water-soluble anhydrosugars and polysaccharides). The presence of the catalyst lowered the initial viscosity of bio-oil (measured at 50°C) from 9.5 cSt (without catalyst) to 5.7 cSt (with the ZnO catalyst). According to an accelerated ageing test of bio-oil which was performed at 80°C for 24 hours, the increase in viscosity was significantly lower for the ZnO-treated bio-oil (55%) than for the reference bio-oil without any catalyst (129%), thus indicating an improvement in the stability.

Ates et al [94, 95] studied the catalytic pyrolysis of *Euphobia rigida* using a commercial Co-Mo catalyst (Criterion-534) in a bench-scale fixed-bed reactor in

order to investigate the effects of catalyst ratios (0%, 5%, 10% and 25% by weight) and water vapour velocities (0.0, 0.6, 1.3 and 2.7 cm/s) on bio-oil yields. Ten grams of the biomass sample having average particle size of 0.55 mm was mixed with the catalyst and placed in the reactor. The pyrolysis experiments were conducted at a slow heating rate of 7°C/min to a final temperature of 550°C. The results showed that by using 20 wt% of the Criterion-534 catalyst in static atmosphere, bio-oil yield on dry, ash-free basis was increased from 21.65% (without any catalyst) to 30.98% [94]. The yield was increased further when applying water vapor and reached the maximum of 42.56% with 1.3 cm/s water vapour velocity [95]. In addition, the bio-oil analysis results suggested that the presence of steam enhanced the formation of aromatic compounds [95].

The same group of researchers, Ates and co-workers, also tested two commercial catalysts from petrochemical industry, namely DHC-32 (Ni-W/Al_2O_3) and HC-K 1.3Q (Ni-Mo/Al_2O_3), in catalytic pyrolysis of biomass so as to explore the influence of catalysts on bio-oil yields and properties [96]. The former contains mainly (wt%); aluminium oxide (40.0–60.0%), nickel oxide (1.0–6.0%), silicon oxide (10.0–30.0%), tungsten oxide (15.0–25.0%), while the latter is composed mainly of (wt%); aluminium oxide (35.0–65.0%), molybdenum trioxide (0.1–28.0%), silica (amorphous) (0.1–20.0%), molybdenum metal/powder (1.0–15.0%), nickel oxide (0.1–6.0%), aluminium phosphate (0.1–3.0%). Two biomass samples (*Euphobia rigida* and sesame stalk) were pyrolysed at a slow heating rate of 7°C/min using a bench-scale fixed-bed reactor The results showed that at a final pyrolysis temperature of 500°C, the use of catalysts led to the increase of bio-oil yields and the decrease of gas yields for both biomass samples. The increases in the yields of bio-oils were more pronounced when using HC-K 1.3Q catalyst. With regards to the bio-oil composition, different catalysts have generally been used with an aim to decrease the amount of oxygenated compounds in the bio-oils. However, it was found that the oxygenated compounds increased in the catalytic *Euphobia rigida* bio-oils compared with the non-catalytic one. It is thought that this phenomenon is a result of the terpenoid structure of the *Euphobia rigida* biomass. Nevertheless, for the sesame stalk, this situation is vice versa as adding a catalyst could decrease the amount of these compounds. These results are consistent with the works carried out by Adam et al

[86] and Antonakou et al [87] as mentioned earlier that the biomass types and/or composition also play an important role during the catalytic pyrolysis.

3.5 UPGRADING WITH NATURAL CATALYSTS

Natural catalysts that may be promising for catalytic pyrolysis of biomass include alkali and alkaline earth metal-based catalysts and slate. As mentioned in section 2.5.1 that inorganic compounds (containing alkali and alkaline earth metals) present in biomass have catalytic effects on pyrolysis reactions such as cracking and char forming, thus increasing gas yields and decreasing liquid yields. Since cracking reactions are involved, the bio-oil produced would expect to have lower molecular weight and possibly lower initial viscosity. It was found from a study by Nik-Azar et al [42] that alkali metals could decrease the molecular weight of bio-oil from 300 amu when raw beech wood was used as feedstock to about 190 amu when the wood samples were impregnated with potassium (K) or sodium (Na) cations, although the use of these metals also decreased the bio-oil yield. The alkali and alkaline earth metal-based catalysts are readily available in the forms of ash and char. Therefore these two materials may be used for catalytic pyrolysis of biomass with an aim of cracking heavy molecules in pyrolysis vapours to produce bio-oils of lower molecular weight and viscosity. Another type of natural catalysts that could be used for bio-oil upgrading is slate since it was found to improve the bio-oil quality in terms of stability, initial viscosity and heating value with no significant loss in the liquid yield [61, 97].

3.6 SELECTION OF CATALYSTS FOR SCREENING TESTS

As discussed earlier (section 3.1), promising catalysts are expected to perform cracking, deoxygenation and reforming reactions during the upgrading process. As a consequence, the selection of catalysts for this project is based not only on the suggestions from the previous studies, but also on these catalysts functionalities. The investigation of catalytic pyrolysis of biomass in the present work begins with catalyst screening using a micro-scale batch reactor (Py-GC/MS) system (chapter 5). This is

followed by bench-scale experimentation (chapter 8). For catalyst screening tests, the following catalysts are chosen according to their known and anticipated functions.

1. **ZSM-5** is chosen because it is known to be an effective catalyst for cracking, deoxygenation and synthesis of aromatic hydrocarbons. The study of this catalyst would be useful for comparison with literature data as the majority of previous work was done on this type of catalyst, although the biomass raw material utilised in the present work (cassava rhizome) is different from others.

2. **Al-MCM-41** is chosen because it is expected to perform selective cracking and deoxygenation reactions of the large molecules (such as those derived from lignin) in pyrolysis vapours as it has active acid sites in a uniform structure with about 30 Å pores (compared to about 5.5 Å for ZSM-5).

3. **Al-MSU-F** is a zeolite-like catalyst possessing a cellular foam framework of 150 Å pores. It is selected and used alongside ZSM-5 and Al-MCM-41 due to its very large pores and its acidity, which expected to induce selective cracking of lignin oligomers exploded from the original biomass. In addition, no previous attempt has been found on testing this very large pore size catalyst. The use of Al-MSU-F catalyst is therefore beneficial for extending the knowledge in the field of biomass catalytic pyrolysis.

4. **ZnO** was reported by Nokkosmaki et al [93] to be a promising catalyst for improving initial viscosity and stability of pine sawdust bio-oil. The mechanism occurred was not well-understood, but it seems from the bio-oil analysis that the reduction of water-soluble anhydrosugars and polysaccharides is related to the improvement. A ZnO catalyst is chosen in the current project with an intention of expanding the knowledge of applying this catalyst to the pyrolysis process, especially with different biomass feedstock.

5. **Co-Mo/Al_2O_3 (Criterion-534)** is generally known to promote deoxygenation reactions when operating at high pressure in the presence of hydrogen (hydrotreating process). Co-Mo/Al_2O_3 was previously used as a fluidising

medium in a bench-scale unit of WFPP (waterloo fast pyrolysis process) to pyrolyse cellulose and poplar wood utilising hydrogen at atmospheric pressure as carrier gas and fluidising gas [98]. The results showed that over the Co-Mo catalyst there was a greatly increased yield of C_{2+} hydrocarbons (that is C_2, C_3, and C_4 hydrocarbon gases and the portion of the C_5 and higher hydrocarbons), while the production of methane is minimised. This indicates that Co-Mo/Al_2O_3 has a potential for cracking and producing hydrocarbon from biomass even at atmospheric pressure. This type of catalyst was further studied in catalytic pyrolysis of biomass at atmospheric pressure and without hydrogen input by Ates et al [94, 95] as discussed earlier. However, the heating rate applied during the pyrolysis process of Ates et al work was at 7°C/min, which is regarded to be slow. Consequently, the Co-Mo/Al_2O_3 is chosen in the current project in order to investigate its catalytic behaviour during fast pyrolysis of a selected biomass (cassava rhizome) at atmospheric pressure and in the absence of additional hydrogen and this catalyst is expected to enhance cracking reactions, to increase light hydrocarbon yields and to deoxygenate the bio-oil product.

6. **Slate** is chosen to extend the work carried out by Salter [61] and Scholze [97] as they suggested that slate is a promising catalyst for improving bio-oil stability, viscosity and heating value without significant reduction of liquid yield.

7. **Ash** is a natural catalyst that contains catalytically active minerals such as alkali and alkaline earth metals. These metals are known to be effective for cracking reactions. Therefore ash is selected because it is expected to crack the heavy molecules present in pyrolysis vapours to produce lighter and less viscous bio-oil.

8. **Char** is a solid residue obtained from pyrolysis of biomass. It contains a high proportion of ash originating from the biomass. Char is chosen with reasons similar to those given for the ash and it is used alongside the ash for comparison and for differentiating the effects of char itself (char pore structure

and morphology) and the ash present in the char during the catalytic upgrading.

9. **MI-575** is a commercial catalyst containing zirconium oxide (ZrO_2) and cerium oxide (CeO_2). Recently, zirconia was found to be a selective catalyst for tar and ammonia oxidation in gasification gas cleaning and was found to be active at 550°C [99]. This implies that the catalysts may be useful for pyrolysis processes as they may selectively crack the lignin derivatives present in biomass pyrolysis vapours, thus giving lighter pyrolysis products. Since pyrolysis is a reducing environment, it is important to use a modified zirconia catalyst instead to ensure that the catalyst is still active under the pyrolysis conditions. Consequently, a mixture of zirconia, alumina and ceria in the form of alumina-stabilised ceria (MI-575) is selected for the present study with an expectation that this catalyst would perform cracking reactions of large pyrolysis vapour molecules and would ultimately improve the bio-oil quality in terms of viscosity.

10. **ZrO_2** is selected to be used alongside the MI-575 in order to monitor the influence of this chemical in MI-575 catalyst on pyrolysis product distribution.

11. **CeO_2** is selected because of the same reason given for ZrO_2.

12. **Copper chromite** is selected because it is a proven catalyst for hydrogenation of carbonyl group while leaving other functional groups untouched [100]. This is very important as the carbonyl compounds are believed to have an adverse effect on bio-oil storage stability. However, during hydrogenation process, hydrogen pressure is normally required. The effect of this catalyst during biomass pyrolysis at atmospheric pressure without hydrogen input is not well understood. This is therefore worth being investigated.

4 CHARACTERISATION OF BIOMASS FEEDSTOCKS

4.1 INTRODUCTION

In this project, stalk and rhizome parts of cassava plants are used as biomass feedstocks for fast pyrolysis study. Before commencing pyrolysis experimentation, the feedstocks are characterised to obtain basic data used for calculation in chapters 7 and 8. This chapter presents the detailed characterization of the biomass samples using a combination of analytical methods, which include proximate, ultimate, structural, inorganic elemental, heating values and thermogravimetric (TGA) and derivative thermogravimetric (DTG) analyses.

4.2 MATERIALS AND METHODS

4.2.1 Biomass materials

Biomass samples of agricultural wastes from cassava plantations (stalk and rhizome) were shipped from Thailand. The biomass materials were ground using a Fritsh blade grinder with 1-mm sieve. The samples were then sieved and their particle size distributions are listed in Table 4-1. It is known that biomass with different particle sizes exhibits different properties such as ash and moisture contents, heating value and pyrolysis behaviour [101]. It has also been established that only biomass of particle size range 355-500 μm can be continuously fed into the 150 g/h pyrolysis unit with minimised blockage problems. As a consequence, only the stalk and rhizome samples of this particle size range were applied unless otherwise stated.

Table 4-1 Particle-size distribution of cassava stalk and rhizome samples

Particle size (μm)	Content (wt %, as-received basis)	
	Cassava Stalk	**Cassava Rhizome**
<75	6.15	12.97
75-250	15.46	24.97
250-355	10.33	11.78
355-500	17.13	18.57
500-600	12.90	12.32
600-850	33.23	18.59
850-1000	4.81	0.82
Total	**100.00**	**100.00**

4.2.2 Characterisation methods

4.2.2.1 Proximate analysis

The proximate analysis is used for the determination of moisture, volatile matter, ash, and fixed carbon contents of biomass samples. The analysis was performed according to the ASTM standard test methods for measuring moisture, volatile and ash contents, which are ASTM E1756-01, E872-82 and E1755-01, respectively. Briefly, the moisture was determined as loss in weight in a drying oven at 105°C. The volatile matter was determined as loss in weight at 950°C for 7 minutes. The ash content was measured as the residue after burning to constant weight at 575°C. The fixed carbon content was determined by difference.

4.2.2.2 Ultimate analysis

Ultimate analysis was performed in order to determine the basic elemental composition of the biomass samples. Carbon, hydrogen, nitrogen and sulphur contents were measured, while oxygen contents were calculated by difference. The instruments used were CE-440 and Carlo-Erba elemental analysers, which are based on combustion methods. The analysis was carried out by an external company (MEDAC Ltd., Surrey, UK).

4.2.2.3 Inorganic elements

The contents of inorganic elements present in biomass, namely potassium (K), calcium (Ca), phosphorous (P), magnesium (Mg), sodium (Na), chlorine (Cl) and copper (Cu), were determined by calculation based on the ash content and composition. The ash content was obtained from the proximate analysis as mentioned above, whereas the ash composition analysis was performed by MEDAC Ltd (Surrey, UK) company using ICP-OES (inductively coupled plasma-optical emission spectrometer) technique.

4.2.2.4 Structural analysis

Structural analysis was conducted for the determination of extractives, cellulose, hemicellulose and lignin contents. There are several methods in existence for this analysis. The current analysis was carried out according to a standard method described by Ona et al. [102]. In this method, biomass samples were extracted with a mixture of 95% ethanol and toluene (1:2 by volume) for 6 hours followed by 95% ethanol for 4 hours and distilled water for 4 hours by a Soxhlet extractor. The extractives contents were then calculated from the weight loss. Lignin contents were determined as Klason lignin or acid-insoluble lignin, which is the residue after hydrolysis with 72% sulphuric acid. Holocellulose samples were prepared by delignification using acid chlorite method where sodium chlorite ($NaClO_2$) was used for the reaction in acetate buffer (pH 3.5). Hemicellulose was removed by alkali extraction method in which 17.5% NaOH solution was applied.

4.2.2.5 Heating values

The heating values of the samples were determined by bomb calorific experiments and by calculation based on ultimate analysis results. A bomb calorimeter was used to measure higher heating values (HHV) according to the ASTM D2015 standard test method. Basically, the bomb calorimeter is used for measuring heats of combustion in oxygen. A known weight of material was burnt completely in an excess oxygen

environment in a steel vessel, which is called a bomb. Therefore, the reaction took place at constant volume. The temperatures were measured and plotted in order to find the temperature change (ΔT). By using a known heat of combustion substance such as benzoic acid (26.43 kJ/g at 25°C) as a calibrant, heat capacity of the calorimeter (C) can be calculated from the following equation.

$$Q = C\Delta T$$

Equation 4-1

Q is the heat liberated by the combustion of the weighed quantity of the calibrant. Once the heat capacity of the calorimeter (C) is known, unknown materials can be made to burn in the bomb and the temperature rise is simultaneously recorded. After that the Q can be calculated from Equation 4-1. Then, the heating value can be calculated from the known amount of the sample.

The heat of combustion obtained from bomb calorimetry method is in fact the same as higher heating value (HHV) since the enthalpy change for the reaction assumes a common temperature (25°C) of the compounds before and after combustion, and at this temperature the water produced is in the liquid form. However, the biomass samples were not dried before testing. Therefore, the heat of combustion was HHV on as-received basis and was calculated into dry basis by the following relationship [103].

$$HHV_{ar} = HHV_{dry}\left(1 - \frac{H_2O}{100}\right)$$

Equation 4-2

The HHV_{ar} and HHV_{dry} are higher heating values on as-received basis and on dry basis, respectively. The H_2O refers to the biomass moisture content in wt %.

With regard to the calculation method, a plethora of formulae have been proposed for estimating HHV of fuels [22, 104-107]. The correlations are typically based on basic analysis data such as proximate, ultimate and structural analyses. Most recently,

Sheng and Azevedo [106] proposed new formulae to estimate HHV of biomass fuels using proximate and ultimate analyses. Among the formulae, the one based on the composition of main elements (C, H and O) as shown in Equation 4-3 was suggested to be most accurate for biomass fuels. Consequently, this correlation was used in the present study.

$$HHV_{dry}\,(MJ/kg) = -1.3675+0.3137C+0.7009H+0.0318O^{*}$$

Equation 4-3

The C and H are weight percentages of carbon and hydrogen on dry basis, respectively. O^{*} is the sum of the contents of oxygen and other elements (including S, N, Cl, etc.) in the organic matter, i.e.

$$O^{*}(\%) = 100-C-H-Ash$$

Equation 4-4

Therefore, Equation 4-3 has been adopted for estimating the heating values of cassava stalk and rhizome. In addition, the lower heating values (LHV) of biomass samples were also calculated according to Equation 4-5 [103] since LHVs are more realistic data for energy balances of thermochemical conversion process systems.

$$LHV_{dry}\ (MJ/kg) = HHV_{dry} - 2.442\cdot 8.936H/100$$

Equation 4-5

where H is weight percentage of hydrogen on dry basis.

4.2.2.6 Thermogravimetric analysis (TGA)

Two samples of cassava residues were analysed using TGA and DTG techniques. A computerised Perkin-Elmer Pyris 1 TGA thermogravimetric analyser was employed with a nitrogen gas flow of 100 mL/min at 10°C/min heating rate.

4.3 RESULTS AND DISCUSSION

Table 4-2 summarises the results of proximate and ultimate analyses, calculated molecular formulae, inorganic matter contents, structural compositions and heating values of cassava stalk and rhizome in comparison with the available literature data [108, 109].

Table 4-2 Results of the analysis of agricultural wastes from cassava plantation

Analysis	Cassava stalk		Cassava rhizome	
	This work	**Literature [108]**	**This work**	**Literature [109]**
Proximate (wt %, dry basis)				
Volatile matter	79.90%	89.47%	77.75%	81.13%
Fixed carbon	14.09%	6.89%	18.20%	10.39%
Ash	6.01%	3.63%	4.05%	8.49%
Moisture	15.54%	12.21%	8.31%	10.94%
Ultimate (wt %, dry-ash free basis)				
Carbon	51.12%	46.56%	51.59%	
Hydrogen	6.87%	8.16%	6.69%	
Nitrogen	0.67%	0.39%	1.27%	No data
Oxygen	41.34%	44.73%	40.45%	
Sulphur	< 0.1	0.17%	<0.1	
Molecular formula	$CH_{1.6}O_{0.61}$	$CH_{2.09}O_{0.72}$	$CH_{1.54}O_{0.59}$	-
Inorganic matter (ppbw, dry biomass basis)				
K	977.39		368.96	
Ca	950.92		391.23	
P	559.97		217.08	
Mg	276.68	No data	291.60	No data
Na	7.82		9.32	
Cl	130.52		51.84	
Cu	0.23		0.20	
Structural analysis (wt %, extractives-free basis)				
Cellulose	35.71%		31.19%	
Hemicellulose	41.75%	No data	44.47%	No data
Lignin	22.54%		24.34%	
Extractives	13.21%		10.80%	
Heating values (MJ kg^{-1}, dry basis)				
Bomb calorimetry	17.58	17.56	23.67	20.10
Calculated HHV	19.49	19.63	19.93	-
Calculated LHV	17.99	17.85	18.47	-

From the proximate analysis, the measured moisture contents differ by 2-3 % from the available literature data. This is due to the extrinsic moisture content or the level of dryness, since the fresh stalk and rhizome can have a moisture content up to 50% or more. The cassava residues contain very high volatiles contents, approximately 80%. This is a good sign for pyrolysis liquid yield. The ash contents measured in the present work are much different from the literature value. This is probably due to sample variety and different biomass sources, which indicate the difference in soil contamination. When compared with other biomass feedstocks like wood chips (0.1 % ash), softwood (1.7% ash) or spruce wood (1.5% ash) [104], the ash contents of cassava stalk and rhizome are higher. Since higher ash content implies higher level of inorganic compounds, the thermal conversion processing like fast pyrolysis of cassava residues could be subjected to stronger catalytic effect, which could result in lower liquid yield and higher gas yields compared with when wood is used as feedstock. However, the ash contents of the cassava residues (4-6 wt%) are lower than some of other agricultural residues such as rice straw and rice husk whose ash contents are 12.08 [40] and 12.50 [110] wt% (moisture-free basis), respectively.

According to the ultimate analysis, the cassava wastes contain about 50 wt% carbon, 7 wt% hydrogen, 41 wt% oxygen, and small amounts of nitrogen and sulphur. These residues can be ideal waste sources for clean energy production due to the trace amounts of nitrogen and sulphur. The ultimate analysis results of cassava stalk are similar to those from the reported literature data [108]. For cassava rhizome, there is no published ultimate analysis data. This work presents for the first time ultimate analysis results for cassava rhizome.

The analysis of the biomass inorganic contents shows that the cassava stalk and rhizome samples contain mainly potassium (K), calcium (Ca), phosphorous (P), magnesium (Mg) and chlorine (Cl) with small quantities of sodium (Na) and copper (Cu). In addition, it is apparent that the amounts of the individual elements are mostly lower in the case of cassava rhizome. This also corresponds to its lower ash contents. Hence, one would expect that the cassava rhizome would be a better feedstock for bio-oil production from a fast pyrolysis process in terms of the potential for producing a higher liquid yield and a lower gas yield.

The heating values of the biomass measured by both bomb calorimetry and calculation are quite similar to those from the literature. The cassava rhizome has higher heating value than that of the stalk. The higher heating values (HHV) of cassava wastes are between 17-24 MJ/kg (dry basis). This implies that they are potential energy sources for bio-fuel production.

Structural analysis results of biomass may be useful data for modeling pyrolysis processes as indicated by several previous studies [18, 111-114]. From structural analysis, cassava wastes have 31-36% of cellulose and 42-44% of hemicellulose. Generally, lignin contents of biomass vary considerably. For example, corncob and walnut shell contain 15.0% and 52.3% of lignin, respectively [115]. Cassava residues stalk and rhizome as found in this work have lignin contents between 23-24%. These are considered to be low-lignin biomass species. Ghetti et al. [48] suggested that biomass of low lignin content produces a lighter pyrolysis product, which may be considered a better bio-oil for use as fuel. Therefore, residues from cassava plantations exhibit a high potential to be converted into bio-fuel via pyrolysis processes.

The thermal degradation behaviour of cassava stalk and rhizome was studied by TGA and DTG and the results are shown in Figure 4-1. The TGA curves show that approximately 70 % by weight of the samples were decomposed at the temperature below 500°C. Most of the weight lost occurred at the temperature between 250 and 350°C. This is an indication that cassava stalk and rhizome are easily decomposed via thermal processing and would be excellent feedstocks for pyrolysis reactions.

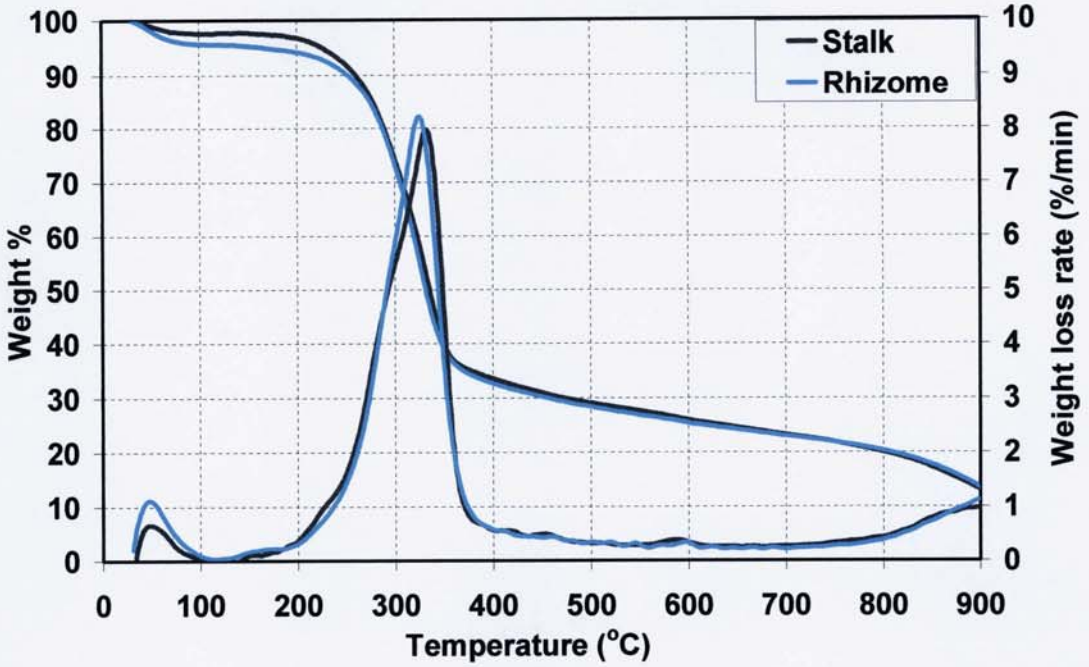

Figure 4-1 TGA and DTG curves of cassava stalk and rhizome

4.4 CONCLUDING REMARKS

Characterisation of biomass residues, stalk and rhizome of cassava plants, has been reported in this chapter. The results are generally useful to provide basic information for the design, modelling and exploitation of thermochemical conversion processes involving agricultural residues from cassava plantations. Proximate, ultimate, structural, inorganic matter and heating value analyses were conducted on the samples. The results show that the biomass samples have high volatile contents (78-80%, dry basis) and contain 51% carbon, 7% hydrogen, 41% oxygen, 0.7-1.3% nitrogen and < 0.1% sulphur. Structural analysis reveals that cassava residues are composed of about 36% cellulose, 44% hemicellulose and 24% lignin. The main inorganic elements found in both feedstocks are mainly potassium, calcium, phosphorous and magnesium. The lower heating values (LHV) of both samples are approximately 18 MJ/kg on dry basis. The overall results indicate that the cassava residues contain high volatile, very low nitrogen and sulphur, and rather low lignin with a medium heating value, suggesting that a high quality and environmentally benign bio-fuel could be produced via thermochemical conversion processing such as fast pyrolysis. In addition, the TGA and DTG curves for the two samples show

similarity in thermal decomposition behaviour and about 70% of the samples were decomposed at temperature below 500°C.

5 CATALYST SCREENING FOR FAST PYROLYSIS OF BIOMASS

5.1 INTRODUCTION

In order to upgrade the pyrolysis liquid product, the incorporation of catalyst into the pyrolysis process is utilised. The main pyrolysis equipment used to produce catalytic bio-oils is a fluidised-bed reactor with a scale of 150 g/h biomass throughput. The experimental setup is described in chapter 6 and the catalytic pyrolysis experimentation using this bench-scale reactor system is discussed in chapter 8. To minimise the number of these trials, catalysts have first been screened using a microscale reactor system. This is based on pyrolysis-gas chromatography/mass spectrometry (Py-GC/MS) technique. The catalyst screening is beneficial for investigating the relative effect of different catalysts on estimated or conjectural bio-oil properties.

In the screening tests, cassava rhizome is used as biomass raw material and the catalysts tested include zeolite and related materials (ZSM-5, Al-MCM-41 and Al-MSU-F type catalysts), metal oxides (Zinc oxide, Zirconium (IV) oxide, Cerium (IV) oxide and Copper Chromite catalysts), proprietary commercial catalysts (Criterion-534 and MI-575) and natural catalysts (slate, char and ashes).

Since a large number of catalysts are involved in the experiments and the results obtained are complex being in the form of multivariate data, a statistical tool is essential to fully exploit and extract the useful information from the large set of data. The statistical technique applied is principal components analysis (PCA). PCA can be defined as a technique to reduce the information dimensionality of a dataset containing a large number of intercorrelated variables by projection methods, in a way that minimises the loss of information. In reality, data, particularly multivariate data, consist of two main parts, information and noise of data. The information is what is subsequently developed to become knowledge. One of the main functions of the PCA is to decompose the data matrix into an information part and a noise part.

The PCA technique has previously been shown to be useful for analysis of multivariate Py-GC/MS data [116-119]. The purpose of PCA is to analyse large set of data in order to detect, and model, the "hidden phenomena" [120]. In this catalyst screening case, the hidden correlations between pyrolysis products and catalyst samples are explored and detected.

To assess the bio-oil quality, three properties are hypothetically observed based on the pyrolysis products identified from the GC/MS. These are viscosity, stability and acidity. The viscosity is evaluated by comparing the quantity of the heavy and oxygenated lignin derived compounds as it is expected that these compounds contribute to high viscosity of bio-oil. The stability was observed from the amount of carbonyl compounds since it is known that they are reactive and can cause instability [3]. Acidity of the bio-oil was considered according to the percentage yields of organic acids such as acetic, formic and lactic acids found in the products.

5.2 MATERIALS AND METHODS

5.2.1 Biomass feedstock

Cassava rhizome (CR) from Nakhon Ratchasima province in Thailand was used as feedstock in this study. The rhizome was ground to particle size less than 100 μm and its main characteristics are shown in Table 4-2.

5.2.2 Catalysts

Fifteen catalyst samples were used to investigate their impact on pyrolysis product distribution and subsequently to predict the change in bio-oil properties. Table 5-1 shows all the catalysts and their main properties.

Table 5-1 Characteristics of catalysts

Catalyst types	Name	Source	Composition[a]	Surface area (m^2/g)
Zeolite and related materials[b]	Zeolite ZSM-5 type	BDH (UK) Company	Si/Al ratio: 50	300
	Aluminosilicate mesostructured, hexagonal framework, Al-MCM-41 type	Sigma-Aldrich Company Ltd.	Si/Al ratio: 40	1120
	Aluminosilicate mesostructured, cellular foam framework, Al-MSU-F type	Sigma-Aldrich Company Ltd.	Si/Al ratio: 40	560
Metal oxides	Zinc oxide	Acros Organics	99.5% ZnO	ND[c]
	Zirconium (IV) oxide	Acros Organics	98.5% ZrO_2	ND[c]
	Cerium (IV) oxide	Acros Organics	99.9% CeO_2	ND[c]
	Copper chromite catalyst ($CuCr_2O_4$)	Acros Organics	51% CuO and 49% Cr_2O_3	ND[c]
Proprietary commercial catalysts	Criterion-534	Criterion Catalysts & Technologies	85-95% Al_2O_3, 1-3% CoO and 5-10% MoO_3	300
	Alumina Stabilised Ceria (MI-575)	GRACE Davison	71.0% CeO_2, 25.0% ZrO_2, 2.2% La_2O_3, 0.10% Al_2O_3 and 0.1% CaO	55
Natural catalysts	Char	Solid residue from pyrolysis of cassava rhizome	62.9% C, 2.4% H, 1.1% N and 25% Ash	ND[c]
	Uncalcined slate (SLT)	Thailand	ND[c]	ND[c]
	Slate calcined at 750 °C (SLT750)	Thailand	ND[c]	ND[c]
	Slate calcined at 850 °C (SLT850)	Thailand	ND[c]	ND[c]
	Ash from Char (Ash_C)	Residue after burning the char from cassava rhizome at 575 °C	12.8% K, 15.3% Ca, 10.2% P, 5.8% Mg, 0.83% Cl, 0.10% Na and 0.03% Cu	ND[c]
	Ash from Biomass (Ash_B)	Residue after burning cassava rhizome at 575 °C	9.1% K, 9.7% Ca, 5.4% P, 7.2% Mg, 1.3% Cl, 0.23% Na and 49 ppm Cu	ND[c]

[a]The composition of most catalysts are provided by the manufacturers except for char and ashes whose compositions were determined in this work according to the procedure described in section 6.4.2.
[b]The mean pore diameters of ZSM-5, Al- MCM-41 and Al-MSU-F are 5.5, 31 and 150 Å, respectively.
[c]ND denotes "not determined".

5.2.3 Pyrolysis GC/MS

Pyrolysis experiments were carried out using a pyrolysis autosampler CDS AS-2500 with pyroprobe CDS 2000. Approximately 0.5 mg of cassava rhizome was placed in a quartz tube along with a quartz filler rod designed for use with the autosampler. In catalytic pyrolysis experiments, the catalyst was placed above the biomass as a fixed bed and quartz wool was used to separate the biomass and catalyst layers, as shown in Figure 5-1. The amount of catalysts was 0.5 mg (to obtain 1:1 biomass: catalyst ratio) except for the two types of ash in which 0.125 mg of catalyst was applied. This is necessary in order to control the amount of alkali metals in the ash and char as it was noticed that the char contained approximately 25% of ash. The pyroprobe programme was set at the heating rate of 3000°C/second with a final temperature of 600°C and hold for 10 seconds. Although the pyroprobe temperature was set at 600°C, the actual temperature in the biomass sample cannot be measured directly but is typically 100°C less according to the unit's handbook. This is as a result of temperature difference between the heating source and the sample. Thus the sample temperature can be considered to be about 500°C. In addition, during the biomass pyrolysis experiment it is likely that the temperature difference will reduce as the experiment progresses.

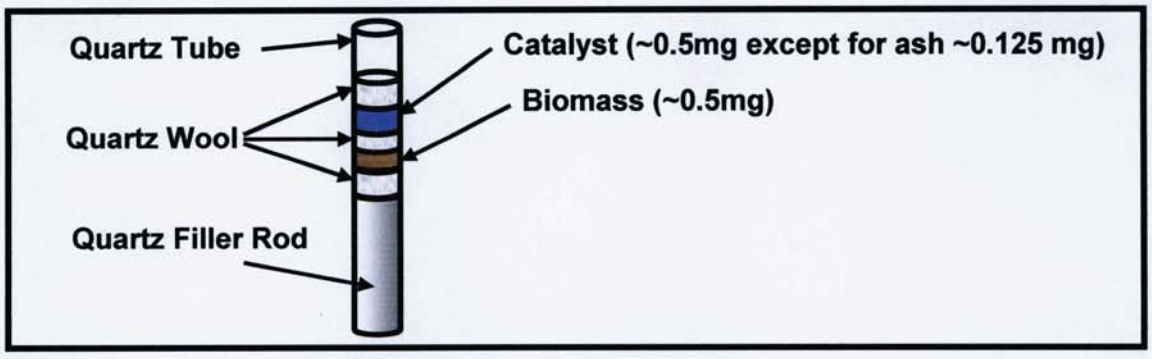

Figure 5-1 Micro-scale pyrolysis reactor

PerkinElmer AutoSystem XL Gas Chromatograph was used to separate the pyrolysis vapours. The column used was PP 1701, 60 m × 25 μm with a 0.25 μm film thickness. Helium at a velocity of 38 cm/s was used as a carrier gas and the split injection ratio was 1:125. The oven programme was started at 45°C for 4 minutes and

heated at heating rate of 4°C/min to 240°C. The injector and detector temperatures were set at 280°C.

The separated compounds were then analysed using a PerkinElmer Turbomass Gold Mass Spectrometer with Electron Impact (EI) mode. The mass spectra were obtained at the ionisation energy of 70 eV from *m/z* 28 to 600 with a speed of 1.0 s/decade.

Identification of chromatographic peaks from pyrolysis GC/MS experiments was carried out by comparing the mass ions (*m/z*) of each peak with NIST mass spectral database and literature data of pyrolysis products from lignocellulosic materials [93, 116, 121-130]. Four runs were performed per sample and the averaged values were used for analysis.

5.2.4 Principal component analysis (PCA)

The Unscrambler® software was used in this study for analysis and evaluation of the data. The software generates score and loading plots, which are the maps of samples and variables, respectively. Fifteen catalytic runs plus one non-catalytic reference run were set as samples, while all chromatographic peaks were set as variables. Full cross validation was selected for all models. In addition, the model size and the number of principal components were set at maximum. A full introduction and application of PCA to multivariate data can be found in reference [120]. Only a brief interpretation of the score and loading plots generated by the PCA technique is given here. To explain how to interpret these plots, Figure 5-2 adapted from [131] is used as an example. It shows the score and loading plots of a PCA model of semiconductor data. The samples of this model are 44 chemical compounds used as semiconductors. The variables are the properties of the compounds such as atomic number, melting point, radii, lattice const, VE and En. The properties data of the 44 semi-conductor materials were used for calculation in the PCA model and the score and loading plots were generated. The key point for the interpretation of these plots is that if the samples or variables are clustered or stay in the same location of the plots, they have similar behaviour. If the sample(s) in the score plot locate at the same position as variable(s) in the loading plot, the sample(s) have statistically high value of the variable(s).

Conversely, if the sample(s) lie in the opposite direction of the variable(s), the sample(s) have statistically low value of the variable(s). Examples of the interpretation can be seen from the plots in Figure 5-2.

Figure 5-2 Interpretation of score and loading plots of principal component analysis (PCA) (adapted from reference [131])

5.3 RESULTS AND DISCUSSION

Typical pyrograms obtained with and without zeolite and zeolite-like catalysts are presented in Figure 5-3. Table 5-2 lists a total of 102 peaks identified from the pyrograms in order of their retention times. The pyrograms in Figure 5-3 show that it is not feasible to visually observe the main relationships among catalysts, compounds and between catalysts and compounds. Therefore, the mean relative percentages of pyrolysis products calculated from the chromatographic peak areas (shown in Table 5-3) were subjected to principal components analysis (PCA). Various PCA models were created using the Unscrambler® software in order to investigate the relative effect of catalysts on pyrolysis products.

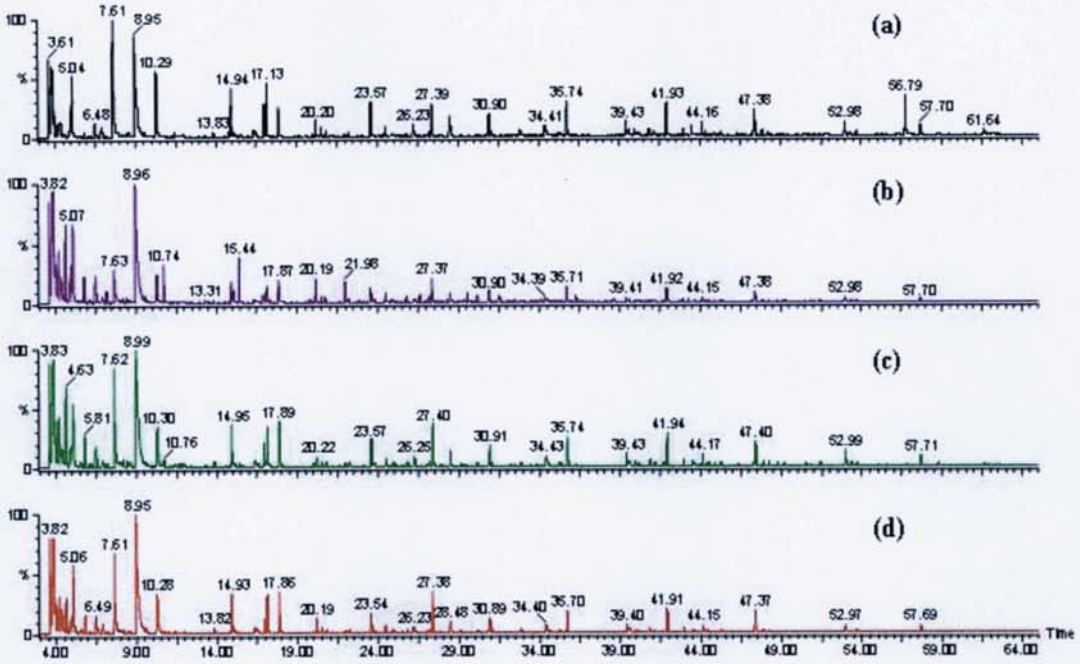

Figure 5-3 Pyrograms of cassava rhizome pyrolysis products (a) CR (without catalyst), (b) with ZSM-5, (c) with Al-MCM-41 and (d) with Al-MSU-F type

The first PCA model was created with all catalysts samples and all compounds in order to view the distribution of catalysts and compounds in the score and loading plots. Figure 5-4 (a) and (b) depict the score and the corresponding loading plots for the first and second principal components (PC1 and PC2) where they explained 47% and 15% of the total variance, respectively. These total variance values are analogous to the percentages of the information part that can be explained by the principal components.

From Figure 5-4 (a), it can be observed that SLT, SLT750, SLT850, ZnO, ZrO_2, CeO_2 and CR are grouped together, indicating the similar compounds distribution in the loading plot (Figure 5-4 (b)). This implies that there may not be significant changes in the bio-oil quality if these catalysts are applied. The same trend was observed even when plotting with the third and fourth principal components (PC3 and PC4), which explained 12% and 6% of the total variance (Figure 5-5 (a) and (b)). Therefore, based on the first four principal components which explained up to 80% of the total variance, slates, ZnO, ZrO_2 and CeO_2 should not be included in the next PCA models.

Table 5-2 Assignment of cassava rhizome pyrolysis products

Peak ID*	R/T (min)	Compound name/Synonyms	Fomula	MW	Origin**
4	4.17	Acetaldehyde/Acetic aldehyde/Ethanal	C_2H_4O	44.05	C
5	4.28	Methanol/Methyl alcohol	CH_4O	32.04	C
6	4.60	Furan/Furfuran/Furane/Oxacyclopentadiene	C_4H_4O	68.08	C
7	4.85	2-Propenal/Acrylic aldehyde/Aqualin/2-Propen-1-one	C_3H_4O	56.06	C
8	4.97	Acetone/2-Propanone/Propanone/Dimethyl ketone	C_3H_6O	58.08	C
9	5.03	Methylglyoxal/2-Oxopropanal/1,2-Propanedione	$C_3H_4O_2$	72.06	C
10	5.49	2-Methyl-propanal/Isobutanal	C_4H_8O	72.11	C
11	5.79	2-Methyl-furan/Methylfuran	C_5H_6O	82.10	C
12	6.46	2,3 Butanedione	$C_4H_6O_2$	86.09	C
13	6.86	3-Pentanone/Pentan-3-one/Diethyl ketone (DEK)	$C_5H_{10}O$	86.13	C
14	7.19	Benzene/Benzole/Coal naphtha/Phenyl hydride	C_6H_6	78.11	L
15	7.61	Hydroxyacetaldehyde/Glycolaldehyde	$C_2H_4O_2$	60.05	C
16	8.18	Formic acid	CH_2O_2	46.03	C
17	8.50	2-Butenal (cis or trans)/Crotonaldehyde/Crotonal	C_4H_6O	70.09	C
18	8.61	2-Hydroxy-propanoic acid/Lactic acid	$C_3H_6O_3$	90.08	C
19	8.90	Acetic acid	$C_2H_4O_2$	60.05	C
20	9.50	2,3-Pentanedione/2,3-Pentadione/Acetylpropionyl	$C_5H_8O_2$	100.12	C
21	10.29	1-Hydroxy-2-propanone/Hydroxypropanone/Acetone alcohol	$C_3H_6O_2$	74.08	C
22	10.74	Toluene/Methylbenzene	C_7H_8	92.14	L
23	11.40	1,2-Dihydroxyethene/(E)-Ethene-1,2-diol	$C_2H_4O_2$	60.05	C
24	13.81	2-Propenoic acid, methyl ester/Acrylic acid methyl ester	$C_4H_6O_2$	86.09	C
25	14.58	Cyclopentanone/Ketocyclopentane/Pyran-2,4(3H)-dione, 3-acetyl-6-methyl-	C_5H_8O	84.12	C
26	14.77	1-Hydroxy-2-butanone	$C_4H_8O_2$	88.11	C
27	14.94	3-Hydroxypropanal (Isomer of 1-Hydroxy-2-propanone)	$C_3H_6O_2$	74.08	C
29	15.21	3-Butenal-2-one/2-Oxobut-3-enal	$C_4H_4O_2$	84.07	C
30	15.53	2(3H)-Furanone/(3H)-Furan-2-one/α-Furanone/α-Crotonolactone	$C_4H_4O_2$	84.07	C
31	16.34	3(2H)-Furanone/(2H)-Furan-3-one	$C_4H_4O_2$	84.07	C
32	16.45	3-Furaldehyde/3-Furancarboxaldehyde	$C_5H_4O_2$	96.09	C
33	16.56	Propanoic acid, 2-methyl-, anhydride/Isobutyric anhydride	$C_8H_{14}O_3$	158.20	C
34	16.89	Xylenes/ Dimethylbenzenes/m-Xylols	C_8H_{10}	106.17	L
35	16.98	Butanedial/Succinaldehyde	$C_4H_6O_2$	86.09	C

Table 5-2 (Continued)

Peak ID*	R/T (min)	Compound name/Synonyms	Fomula	MW	Origin**
36	17.14	2-Hydroxy-3-oxobutanal	$C_4H_6O_3$	102.09	C
37	17.88	Furfural/2-Furaldehyde/2-Furanaldehyde/2-Furancarboxaldehyde	$C_5H_4O_2$	96.09	C
38	20.00	5-Methyl-2(3H)-furanone/α-Angelica lactone/2,3-Dihydro-5-methyl-2-furanone	$C_5H_6O_2$	98.10	C
39	20.21	2-Furanmethanol /2-Furfuryl alcohol	$C_5H_6O_2$	98.10	C
40	20.55	1-Acetyloxy-2-propanone/1-Acetoxypropane-2-one/2-Oxopropyl acetate	$C_5H_8O_3$	116.12	C
41	20.83	2-Ethyl-butanal (or Tetrahydro-4-methyl-3-furanone)	$C_6H_{12}O$	100.16	C
42	21.56	1-(2-Furanyl)ethanone/Acetylfuran/ 2-Acetylfuran/Furyl methyl ketone	$C_6H_6O_2$	110.11	C
43	22.22	4-Cyclopentene-1,3-dione	$C_5H_4O_2$	96.09	C
45	23.09	2-Hydroxy-butanedial/2-Hydroxysuccin aldehyde	$C_4H_6O_3$	102.09	C
46	23.60	2-Hydroxy-2-cyclopenten-1-one	$C_5H_6O_2$	98.10	C
47	24.48	Dihydro-methyl-furanone	$C_5H_6O_2$	98.10	C
49	24.93	5-Methyl-2-furancarboxaldehyde/5-Methylfurfural/2-Formyl-5-methylfuran/2-Methyl-5-formylfuran	$C_6H_6O_2$	110.11	C
50	25.24	1-Acetyloxy-2-butanone/1-Acetoxy-2-butanone/1-Hydroxy-2-butanone acetate/ 2-Oxobutyl acetate	$C_6H_{10}O_3$	130.14	C
51	25.51	3-Acetyldihydro-2(3H)-furanone/α-Acetylbutyrolactone	$C_6H_8O_3$	128.13	C
52	25.70	3-Methyl-2-cyclo-penten-1-one	C_6H_8O	96.13	C
53	25.83	Butyrolactone/Dihydro-2(3H)-furanone/Butyric acid lactone	$C_4H_6O_2$	86.09	C
54	26.26	2(5H)-Furanone/5H-Furan-2-one	$C_4H_4O_2$	84.07	C
55	26.62	p-Ethyl-styrene	$C_{10}H_{12}$	132.21	L
56	26.98	5-Methyl-2(5H)-furanone/β-Angelica lactone	$C_5H_6O_2$	98.10	C
59	27.42	4-Hydroxy-5,6-dihydro-(2H)-pyran-2-one	$C_5H_6O_3$	114.10	C
61	28.53	2-Hydroxy-3-methyl-2-cyclopenten-1-one/Maple lactone	$C_6H_8O_2$	112.13	C
63	29.59	1H-Indene, 2,3-dihydro-5-methyl-/5-Methylindan	$C_{10}H_{12}$	132.21	L
64	30.19	Phenol	C_6H_6O	94.11	L-H
65	30.92	2-Methoxyphenol/Guaiacol/Guaicol	$C_7H_8O_2$	124.14	L-G
66	31.12	2,5-Dimethyl-4-hydroxy-3(2H)-furanone/Alletone/Furaneol/Pineapple ketone	$C_6H_8O_3$	128.13	C
67	31.51	1H-Indene, 2,3-dihydro-4,7-dimethyl-/2,3-Dihydro-4,7-dimethyl-1H-indene/ 4,7-Dimethylindan	$C_{11}H_{14}$	146.23	L
68	32.22	3-Furancarboxylic acid, methyl ester/ /Methyl 3-furoate/3-Furoic acid, methyl ester	$C_6H_6O_3$	126.11	C
69	32.46	o-Cresol/2-Methyl phenol	C_7H_8O	108.14	L-H
70	32.78	3-Ethyl-2-hydroxy-2-cyclopenten-1-one	$C_7H_{10}O_2$	126.16	C

Table 5-2 (Continued)

Peak ID*	R/T (min)	Compound name/Synonyms	Fomula	MW	Origin**
71	32.90	Maltol/3-Hydroxy-2-methyl-4H-pyran-4-one	$C_6H_6O_3$	126.11	C
72	33.48	2-Methyl-1,3-cyclohexanedione	$C_7H_{10}O_2$	126.16	C
73	33.89	4-Methyl-5H-furan-2-one/4-Methyl-2(5H)-furanone	$C_5H_6O_2$	98.10	C
75	34.64	3,4-Dihydro-3-methyl-2,5-furandione/Methylsuccinic anhydride	$C_5H_6O_3$	114.10	C
76	35.29	3,5-Dihydroxy-6-methyl-2,3-dihydro-4H-pyran-4-one	$C_6H_8O_4$	144.13	
77	35.78	2-Methoxy-4-methyl phenol/Creosol/p-Methylguaiacol/4-Methylguaiacol	$C_8H_{10}O_2$	138.17	L-G
78	36.26	3,5-Dihydroxy-2-methyl-4H-pyran-4-one/5-Hydroxymaltol/3,5-Dihydroxy-2-methyl-4-pyrone	$C_6H_6O_4$	142.11	C
79	39.47	4-Ethyl-2-methoxyphenol/4-Ethyl guaiacol/4-Hydroxy-3-methoxy ethylbenzene/p-Ethylguaiacol	$C_9H_{12}O_2$	152.19	L-G
80	39.63	3-Methyl-2,4-furandione/3-Methyl-2,4(3H,5H)-furandione	$C_5H_6O_3$	114.10	C
82	40.23	2,3-Anhydro-d-mannosan	$C_6H_8O_4$	144.13	C
83	40.91	1,4:3,6-Dianhydro-a-d-glucopyranose	$C_6H_8O_4$	144.13	C
84	41.21	1,5-Anhydro-arabinofuranose	$C_5H_8O_4$	132.12	C
85	41.96	2-Methoxy-4-vinylphenol/4-Vinylguaiacol/p-Vinylguaiacol/4-Hydroxy-3-methoxystyrene	$C_9H_{10}O_2$	150.18	L-G
86	43.01	Eugenol/2-Methoxy-4-allylphenol/2-Methoxy-1-hydroxy-4-allylbenzene/Allylguaiacol	$C_{10}H_{12}O_2$	164.20	L-G
87	43.12	4-Propyl guaiacol/2-Methoxy-4-propyl phenol	$C_{10}H_{14}O_2$	166.22	L-G
88	43.30	Propanoic acid, 2-methyl-, 3-hydroxy-2,4,4-trimethylpentyl ester	$C_{12}H_{24}O_3$	216.32	C
89	43.54	5-(Hydroxymethyl)-2-furancarboxaldehyde/5-(Hydroxymethyl)-2-furfural/HMF/5-(Hydroxymethyl)-2-furaldehyde	$C_6H_6O_3$	126.11	C
90	44.19	2,6-Dimethoxy phenol/Syringol/1,3-Dimethoxy-2-hydroxybenzene/Pyrogallol dimethylether	$C_8H_{10}O_3$	154.17	L-S
91	44.19 /44.33	Indole/Ketole/Benzopyrrole/1-Azaindene	C_8H_7N	117.15	
92	44.92	4-Hydroxydihydro-2(3H)-furanone (or 2-Hydroxy-butanedial)	$C_4H_6O_3$	102.09	C
93	45.32	2-Methoxy-4-(1-propenyl)phenol/Isoeugenol,c&t/4-Propenylguaiacol/4-Hydroxy-3-methoxypropenylbenzene	$C_{10}H_{12}O_2$	164.20	L-G
94	47.29	1,5-Anhydro-β-D-xylofuranose	$C_5H_8O_4$	132.12	C
95	47.41	2-Methoxy-4-[(1E)-1-propenyl]phenol/trans-Isoeugenol/(E)-Isoeugenol/trans-p-Propenylquaiacol	$C_{10}H_{12}O_2$	164.20	L-G
96	47.92	4-Methyl syringol/2,6-Dimethoxy-4-methylphenol	$C_9H_{12}O_3$	168.19	L-S
97	48.26	Vanillin/2-Methoxy-4-formylphenol/4-Hydroxy-3-methoxybenzaldehyde	$C_8H_8O_3$	152.15	L-G
98	48.46	Hydroquinone/1,4-Benzenediol/4-Hydroxyphenol/Dihydroxybenzene	$C_6H_6O_2$	110.11	L-H
99	50.48	Propanoic acid, 2-methyl-, 1-(1,1-dimethylethyl)-2-methyl-1,3-propanediyl ester	$C_{16}H_{30}O_4$	286.41	
100	50.58	Homovanillin/Ethanal, 2-(4-hydroxy-3-methoxyphenyl)/2-(4-hydroxy-3-methoxyphenyl)acetaldehyde	$C_9H_{10}O_3$	166.18	L-G
101	50.63 /50.80	4-Ethyl syringol	$C_{10}H_{14}O_3$	182.22	L-S

Table 5-2 (Continued)

Peak ID*	R/T (min)	Compound name/Synonyms	Fomula	MW	Origin*
103	51.44	1-(4-Hydroxy-3-methoxyphenyl)ethanone/Acetoguaiacone	$C_9H_{10}O_3$	166.18	L-G
104	53.01	4-Vinyl-2,6-dimethoxyphenol/4-Vinyl syringol/2,6-Dimethoxy-4-vinylphenol	$C_{10}H_{12}O_3$	180.20	L-S
105	53.35	1-(4-hydroxy-3-methoxyphenyl)-2-Propanone/Guaiacylacetone/Vanillyl methyl ketone/ 4-Hydroxy-3-methoxyphenyl acetone	$C_{10}H_{12}O_3$	180.20	L-G
106	53.72	2,6-dimethoxy-4-(2-propenyl)-Phenol/4-Allyl syringol/4-Allyl-2,6-dimethoxyphenol/Methoxyeugenol	$C_{11}H_{14}O_3$	194.23	L-S
107	55.03	Coniferyl alcohol (cis)/(Z)-4-(3-hydroxyprop-1-enyl)-2-methoxyphenol	$C_{10}H_{12}O_3$	180.20	L-G
108	55.62	cis-4-Propenyl-2,6-dimethoxyphenol/4-Propenyl syringol (cis)	$C_{11}H_{14}O_3$	194.23	L-S
111	56.89	1,6-Anhydro-β-D-glucopyranose/Levoglucosan	$C_6H_{10}O_5$	162.14	C
112	57.73	trans-4-Propenyl-2,6-dimethoxyphenol/4-Propenyl syringol (trans)	$C_{11}H_{14}O_3$	194.23	L-S
113	58.77	4-Hydroxy-3,5-dimethoxybenzaldehyde/Syringaldehyde/Syringe aldehyde/Cedar aldehyde	$C_9H_{10}O_4$	182.18	L-S
114	61.13	1-(4-Hydroxy-3,5-dimethoxyphenyl)ethanone/Acetosyringone/3,5-Dimethoxy-4-hydroxyacetophenone/Acetosyringon	$C_{10}H_{12}O_4$	196.20	L-S
115	61.67	4-((1E)-3-Hydroxy-1-propenyl)-2-methoxyphenol/(E)-Coniferyl alcohol/trans-Coniferyl alcohol	$C_{10}H_{12}O_3$	180.20	L-G
117	62.16	1,6-Anhydro-β-D-glucofuranose	$C_6H_{10}O_5$	162.14	C
119	62.56	Syringyl acetone	$C_{11}H_{14}O_4$	210.23	L-S

*Peak IDs#1-3, 28, 44, 48, 57-58, 60, 62, 74, 81, 102, 109-110, 119 and 118 are unknown

**C, L-H, L-G and L-S represent carbohydrate, p-Hydroxyphenyl lignin, Guaiacyl lignin and Syringyl lignin, respectively.

Table 5-3 Mean percentages of chromatographic peak areas

Peak ID	CR	ZSM	MCM	MSU	ZnO	ZrO_2	CeO_2	$CuCr_2O_4$	Criterion	MI-575	Char	Ash_C	Ash_B	SLT	SLT750	SLT850
4	1.0	4.5	3.5	3.6	1.1	1.0	1.1	4.0	7.3	3.6	1.7	1.7	1.4	1.1	1.3	1.3
5	1.6	2.7	1.3	2.0	1.5	1.4	1.4	1.2	3.6	3.1	1.9	2.0	1.9	1.6	1.7	1.6
6	0.2	5.6	4.2	3.3	0.2	0.2	0.1	2.2	2.6	0.3	0.3	0.2	0.2	0.2	0.2	0.2
7	0.3	1.5	1.0	1.0	0.3	0.3	0.3	0.8	1.6	0.8	0.4	0.4	0.4	0.3	0.3	0.3
8	0.0	2.3	0.0	1.0	0.0	0.0	0.0	1.4	3.4	4.9	0.0	0.0	0.0	0.0	0.0	0.0
9	5.1	7.0	6.5	5.5	5.6	5.1	4.8	5.6	5.2	4.2	5.9	5.5	5.7	6.3	6.0	6.0
10	0.2	0.5	0.5	0.6	0.2	0.2	0.2	1.0	0.8	0.3	0.3	0.2	0.2	0.2	0.2	0.2
11	0.3	1.9	1.8	1.6	0.3	0.3	0.3	0.9	2.2	0.6	0.6	0.4	0.3	0.3	0.3	0.4
12	1.4	3.8	2.2	2.5	1.4	1.4	1.5	2.1	3.9	4.1	2.1	2.2	1.8	1.3	1.5	1.5
13	0.8	0.6	0.6	0.8	0.9	0.9	0.9	0.7	0.6	0.5	0.8	0.7	0.8	0.8	0.9	1.0
14	0.0	1.1	0.2	0.3	0.1	0.0	0.1	0.6	0.0	0.2	0.2	0.0	0.0	0.0	0.0	0.0
15	9.6	4.2	7.8	7.8	9.9	8.8	7.8	8.2	5.9	6.7	6.5	6.1	8.2	11.1	10.5	9.8
16	0.2	0.3	0.3	0.3	0.2	0.2	0.1	0.3	0.3	0.2	0.2	0.2	0.2	0.2	0.2	0.2
17	0.0	0.0	0.3	0.2	0.4	0.3	0.5	0.3	0.9	0.7	0.3	0.4	0.2	0.0	0.0	0.2
18	0.4	0.3	0.4	0.3	0.4	0.4	0.4	0.4	0.0	0.0	0.4	0.6	0.5	0.6	0.6	0.3
19	14.6	23.4	19.6	23.5	17.0	16.0	15.4	17.3	18.1	14.4	18.5	16.1	18.7	16.8	15.4	14.2
20	0.3	1.2	0.2	0.9	0.4	0.4	0.3	0.9	0.7	0.9	0.5	0.5	0.5	0.4	0.5	0.6
21	5.0	2.4	3.4	3.8	5.3	4.9	4.9	3.4	2.9	4.2	5.1	7.0	6.5	5.4	5.9	5.2
22	0.2	2.9	0.3	0.2	0.2	0.2	0.2	0.3	0.3	0.2	0.2	0.2	0.2	0.2	0.2	0.2
23	0.3	0.0	0.2	0.2	0.2	0.2	0.3	0.2	0.2	0.2	0.2	0.1	0.2	0.3	0.2	0.2
24	0.5	0.3	0.6	0.6	0.5	0.5	0.4	0.5	0.6	0.5	0.4	0.3	0.3	0.4	0.4	0.4
25	0.1	0.2	0.2	0.2	0.2	0.1	0.2	0.2	0.4	0.7	0.2	0.2	0.1	0.1	0.2	0.2
26	0.4	0.0	0.1	0.2	0.4	0.4	0.5	0.1	0.1	0.2	0.4	1.1	0.6	0.3	0.3	0.3
27	2.7	1.4	2.9	3.0	3.0	2.8	2.8	3.0	2.5	2.6	2.8	2.5	3.1	3.0	3.1	3.2
28	0.3	1.1	0.3	0.3	0.3	0.3	0.3	0.5	0.6	0.6	0.4	0.3	0.3	0.3	0.3	0.4
29	0.1	0.0	0.2	0.2	0.2	0.0	0.1	0.2	0.2	0.1	0.0	0.0	0.0	0.1	0.1	0.1
30	0.2	0.1	0.1	0.2	0.2	0.2	0.2	0.2	0.1	0.1	0.1	0.1	0.2	0.2	0.2	0.2
31	0.7	0.2	0.9	0.9	1.1	1.0	1.0	0.4	0.3	0.5	0.6	0.9	1.0	0.9	0.9	1.0
32	0.3	0.4	0.0	0.0	0.0	0.0	0.0	0.5	0.5	0.5	0.3	0.0	0.0	0.0	0.0	0.0
33	0.3	0.2	0.3	0.3	0.3	0.3	0.3	0.3	0.2	0.7	0.3	0.3	0.3	0.2	0.3	0.3
34	0.0	0.5	0.0	1.1	0.0	0.0	0.0	0.0	0.0	0.0	0.0	0.0	0.0	0.0	0.0	0.0

Table 5-3 (Continued)

Peak ID	CR	ZSM	MCM	MSU	ZnO	ZrO_2	CeO_2	$CuCr_2O_4$	Criterion	MI-575	Char	Ash_C	Ash_B	SLT	SLT750	SLT850
35	2.4	0.4	1.5	0.0	2.4	2.2	2.3	1.7	1.5	1.8	2.3	2.5	2.2	1.9	2.2	2.2
36	2.8	1.2	2.3	2.1	2.9	2.6	2.7	2.6	2.0	2.4	2.4	2.1	2.7	2.9	2.9	2.9
37	2.1	3.0	3.0	3.9	2.3	2.5	2.4	3.8	6.0	4.1	2.9	3.1	2.6	2.0	2.2	2.5
38	0.2	0.1	0.1	0.1	0.2	0.2	0.2	0.2	0.3	0.2	0.2	0.2	0.2	0.2	0.2	0.2
39	1.0	2.4	0.8	0.9	1.1	1.0	1.1	0.8	0.6	1.2	1.0	1.3	1.2	1.0	1.1	1.0
40	0.5	0.4	0.4	0.4	0.6	0.5	0.7	0.4	0.3	0.5	0.6	1.0	0.9	0.5	0.6	0.6
41	0.6	0.5	0.5	0.4	0.6	0.5	0.6	0.5	1.2	1.2	0.8	0.8	0.6	0.4	0.5	0.5
42	0.1	0.1	0.1	0.1	0.1	0.1	0.1	0.2	0.4	0.4	0.1	0.1	0.1	0.1	0.1	0.1
43	0.3	0.4	0.4	0.4	0.3	0.3	0.3	0.4	0.4	0.3	0.2	0.3	0.3	0.3	0.3	0.3
44	0.1	0.0	0.0	0.0	0.1	0.1	0.1	0.0	0.0	0.0	0.1	0.2	0.2	0.1	0.1	0.1
45	0.1	0.1	0.1	0.1	0.1	0.1	0.1	0.1	0.1	0.1	0.1	0.1	0.1	0.1	0.1	0.1
46	2.6	1.4	2.1	1.9	2.9	2.7	3.0	2.0	1.5	1.8	2.4	2.0	2.9	2.2	2.5	2.4
47	0.8	1.1	0.7	0.7	0.9	0.7	0.8	0.7	0.6	0.7	0.6	0.6	0.7	0.7	0.7	0.7
48	0.1	0.2	0.1	0.1	0.1	0.2	0.1	0.0	0.0	0.1	0.0	0.1	0.1	0.1	0.1	0.1
49	0.2	0.2	0.2	0.3	0.2	0.2	0.2	0.3	0.9	0.3	0.4	0.4	0.2	0.2	0.2	0.3
50	0.2	0.0	0.1	0.1	0.2	0.2	0.2	0.1	0.0	0.0	0.2	0.2	0.2	0.1	0.2	0.2
51	0.2	0.1	0.2	0.2	0.2	0.1	0.2	0.2	0.2	0.1	0.1	0.1	0.1	0.1	0.1	0.1
52	0.1	0.2	0.1	0.1	0.1	0.1	0.1	0.1	0.4	0.6	0.2	0.3	0.1	0.1	0.1	0.1
53	0.3	0.6	0.4	0.4	0.3	0.3	0.3	0.4	0.6	0.9	0.3	0.4	0.4	0.3	0.3	0.3
54	1.1	0.5	0.9	0.8	1.1	1.0	1.1	1.2	1.0	0.8	0.8	0.8	1.1	1.0	1.0	1.2
55	0.1	0.7	0.0	0.0	0.1	0.0	0.1	0.0	0.0	0.0	0.0	0.0	0.0	0.1	0.0	0.0
56	0.1	0.1	0.1	0.1	0.1	0.1	0.1	0.1	0.2	0.1	0.1	0.1	0.1	0.1	0.1	0.1
57	0.1	0.0	0.1	0.1	0.2	0.1	0.1	0.1	0.1	0.1	0.1	0.1	0.1	0.1	0.1	0.1
58	0.3	0.5	0.4	0.3	0.3	0.3	0.3	0.4	0.5	0.4	0.3	0.2	0.3	0.2	0.2	0.3
59	2.4	2.2	2.9	3.0	2.7	2.6	2.4	2.4	1.8	2.4	1.9	1.3	1.5	2.6	2.2	2.1
60	0.2	0.1	0.1	0.1	0.2	0.1	0.0	0.2	0.1	0.0	0.0	0.0	0.0	0.1	0.0	0.0
61	1.8	0.8	1.2	1.0	1.8	1.7	2.0	1.2	1.1	1.7	1.8	2.8	1.9	1.4	1.6	1.5
62	0.2	0.2	0.2	0.2	0.2	0.1	0.2	0.2	0.2	0.2	0.2	0.1	0.1	0.2	0.1	0.1
63	0.0	0.7	0.0	0.0	0.0	0.0	0.0	0.0	0.0	0.0	0.0	0.0	0.0	0.0	0.0	0.0
64	0.1	0.5	0.2	0.2	0.1	0.1	0.2	0.4	0.4	0.3	0.2	0.2	0.2	0.1	0.1	0.2
65	1.8	1.3	1.5	1.3	1.9	1.8	1.9	1.9	1.0	1.8	2.0	2.4	1.7	1.5	1.6	1.8

Table 5-3 (Continued)

Peak ID	CR	ZSM	MCM	MSU	ZnO	ZrO_2	CeO_2	$CuCr_2O_4$	Criterion	MI-575	Char	Ash_C	Ash_B	SLT	SLT750	SLT850
66	0.3	0.1	0.2	0.2	0.3	0.3	0.3	0.2	0.2	0.2	0.2	0.2	0.2	0.3	0.3	0.2
67	0.0	0.8	0.0	0.0	0.0	0.0	0.0	0.0	0.0	0.0	0.0	0.0	0.0	0.0	0.0	0.0
68	0.2	0.1	0.1	0.1	0.2	0.2	0.1	0.1	0.0	0.0	0.1	0.1	0.1	0.1	0.1	0.1
69	0.0	0.4	0.2	0.2	0.0	0.0	0.0	0.2	0.3	0.3	0.2	0.2	0.1	0.0	0.0	0.1
70	0.1	0.0	0.1	0.0	0.1	0.1	0.1	0.0	0.0	0.1	0.1	0.4	0.2	0.1	0.1	0.0
71	0.8	0.3	0.5	0.5	0.9	0.9	0.9	0.5	0.4	0.7	0.8	0.8	0.8	0.7	0.8	0.8
72	0.2	0.1	0.1	0.1	0.2	0.1	0.2	0.1	0.3	0.2	0.1	0.2	0.1	0.1	0.1	0.1
73	0.1	0.1	0.1	0.1	0.1	0.1	0.1	0.2	0.2	0.2	0.1	0.1	0.1	0.1	0.1	0.2
74	1.2	0.5	1.1	1.0	1.2	1.0	0.9	0.8	0.7	0.7	0.8	0.5	0.7	1.0	0.9	0.9
75	0.2	0.1	0.1	0.2	0.2	0.1	0.1	0.2	0.2	0.0	0.2	0.0	0.1	0.1	0.1	0.1
76	0.3	0.1	0.3	0.0	0.3	0.3	0.2	0.3	0.0	0.2	0.2	0.2	0.2	0.3	0.2	0.2
77	3.2	1.2	2.3	1.9	3.3	3.0	3.2	2.8	1.5	2.4	3.2	2.9	2.8	2.9	3.2	3.2
78	0.1	0.6	0.1	0.1	0.1	0.1	0.2	0.1	0.1	0.2	0.1	0.1	0.0	0.1	0.1	0.1
79	1.2	0.6	1.1	0.9	1.4	1.2	1.4	1.1	0.5	1.2	1.4	1.2	1.1	1.2	1.3	1.4
80	0.4	0.3	0.5	0.4	0.4	0.4	0.3	0.5	0.4	0.4	0.4	0.3	0.4	0.3	0.3	0.4
81	0.5	0.0	0.3	0.3	0.5	0.5	0.5	0.5	0.2	0.5	0.6	0.5	0.5	0.5	0.6	0.6
82	0.3	0.1	0.2	0.2	0.4	0.3	0.3	0.3	0.1	0.4	0.5	0.6	0.6	0.4	0.4	0.4
83	0.5	0.2	0.5	0.3	0.6	0.5	0.5	0.5	0.3	0.5	0.6	0.6	0.5	0.5	0.5	0.5
84	0.4	0.2	0.4	0.4	0.4	0.3	0.4	0.3	0.3	0.4	0.4	0.4	0.4	0.5	0.4	0.4
85	2.5	0.9	2.1	1.6	2.7	2.6	2.7	2.6	1.3	2.5	2.8	3.2	2.6	2.2	2.4	2.7
86	0.5	0.2	0.4	0.3	0.5	0.5	0.5	0.4	0.3	0.6	0.6	0.6	0.6	0.4	0.5	0.5
87	0.0	0.0	0.0	0.0	0.0	0.1	0.0	0.1	0.0	0.1	0.2	0.2	0.1	0.0	0.0	0.1
88	0.0	0.0	0.0	0.0	0.0	0.1	0.1	0.0	0.0	0.0	0.0	0.2	0.0	0.0	0.0	0.4
89	1.2	0.0	0.8	0.5	1.1	1.3	1.1	0.6	0.3	0.6	0.5	0.7	0.9	1.2	1.0	1.1
90	1.1	0.3	0.8	0.6	1.0	1.0	1.0	1.1	0.5	0.9	1.2	1.2	0.9	0.9	1.0	1.0
91	0.2	0.1	0.1	0.2	0.3	0.3	0.3	0.2	0.1	0.2	0.2	0.3	0.3	0.2	0.2	0.3
92	0.2	0.0	0.2	0.1	0.2	0.2	0.2	0.2	0.0	0.2	0.2	0.1	0.1	0.2	0.2	0.2
93	0.3	0.1	0.2	0.2	0.3	0.3	0.3	0.2	0.1	0.3	0.4	0.3	0.3	0.2	0.2	0.3
94	0.3	0.0	0.2	0.0	0.2	0.3	0.3	0.0	0.0	0.0	0.2	0.2	0.2	0.3	0.3	0.2
95	1.9	0.8	1.6	1.5	2.1	2.1	2.1	1.9	1.1	2.1	2.6	2.4	2.1	1.8	1.9	2.1
96	0.6	0.1	0.4	0.2	0.6	0.6	0.6	0.6	0.2	0.4	0.7	0.6	0.5	0.5	0.5	0.6

Table 5-3 (Continued)

Peak ID	CR	ZSM	MCM	MSU	ZnO	ZrO2	CeO2	CuCr2O4	Criterion	MI-575	Char	Ash_C	Ash_B	SLT	SLT750	SLT850
97	0.4	0.2	0.3	0.2	0.4	0.4	0.4	0.3	0.2	0.3	0.4	0.3	0.3	0.4	0.4	0.3
98	0.1	0.0	0.0	0.0	0.1	0.0	0.1	0.0	0.0	0.0	0.0	0.1	0.0	0.1	0.1	0.0
99	0.1	0.0	0.0	0.0	0.0	0.2	0.1	0.0	0.0	0.0	0.0	0.3	0.0	0.2	0.2	0.6
100	0.2	0.0	0.1	0.0	0.1	0.2	0.2	0.0	0.0	0.0	0.0	0.1	0.0	0.2	0.2	0.2
101	0.1	0.0	0.0	0.0	0.1	0.1	0.1	0.1	0.0	0.0	0.2	0.2	0.1	0.1	0.1	0.1
102	0.0	0.0	0.0	0.0	0.1	0.1	0.1	0.0	0.0	0.0	0.0	0.0	0.0	0.1	0.1	0.1
103	0.2	0.0	0.2	0.1	0.2	0.2	0.2	0.1	0.0	0.1	0.2	0.2	0.2	0.2	0.2	0.2
104	1.1	0.3	1.0	0.6	1.1	1.1	1.1	1.0	0.4	0.8	1.1	1.1	1.0	1.1	1.2	1.0
105	0.3	0.1	0.2	0.2	0.2	0.3	0.3	0.2	0.1	0.2	0.3	0.3	0.2	0.3	0.3	0.4
106	0.3	0.1	0.2	0.2	0.3	0.3	0.3	0.2	0.1	0.2	0.3	0.3	0.3	0.3	0.3	0.3
107	0.1	0.0	0.1	0.1	0.1	0.1	0.1	0.0	0.0	0.0	0.1	0.1	0.0	0.1	0.1	0.1
108	0.1	0.0	0.1	0.1	0.1	0.2	0.2	0.0	0.0	0.0	0.2	0.1	0.1	0.1	0.1	0.1
109	0.2	0.0	0.0	0.0	0.1	0.1	0.1	0.0	0.0	0.0	0.0	0.1	0.0	0.1	0.1	0.1
110	0.2	0.0	0.0	0.0	0.1	0.2	0.2	0.0	0.0	0.0	0.0	0.1	0.0	0.2	0.1	0.1
111	5.8	0.0	0.1	0.0	0.0	5.5	5.2	0.0	0.0	0.0	2.0	1.6	2.4	4.1	3.4	3.4
112	0.9	0.2	0.7	0.5	0.9	1.0	1.0	0.6	0.3	0.6	1.0	1.0	0.8	1.0	1.0	0.9
113	0.1	0.0	0.1	0.1	0.1	0.1	0.1	0.0	0.0	0.0	0.1	0.1	0.0	0.1	0.1	0.1
114	0.1	0.0	0.1	0.0	0.0	0.1	0.1	0.0	0.0	0.0	0.1	0.1	0.0	0.1	0.0	0.0
115	0.7	0.0	0.2	0.0	0.2	0.4	0.4	0.1	0.0	0.0	0.1	0.1	0.2	0.3	0.3	0.1
116	0.1	0.0	0.1	0.1	0.1	0.1	0.1	0.1	0.0	0.0	0.2	0.1	0.0	0.2	0.2	0.4
117	0.1	0.0	0.0	0.0	0.0	0.0	0.0	0.0	0.0	0.0	0.0	0.0	0.0	0.0	0.0	0.0
118	0.3	0.0	0.2	0.0	0.2	0.4	0.3	0.0	0.0	0.0	0.1	0.1	0.1	0.2	0.2	0.2
119	0.1	0.0	0.1	0.0	0.1	0.1	0.1	0.0	0.0	0.0	0.1	0.1	0.0	0.1	0.1	0.2
Total	100.0	100.0	100.0	100.0	100.0	100.0	100.0	100.0	100.0	100.0	100.0	100.0	100.0	100.0	100.0	100.0

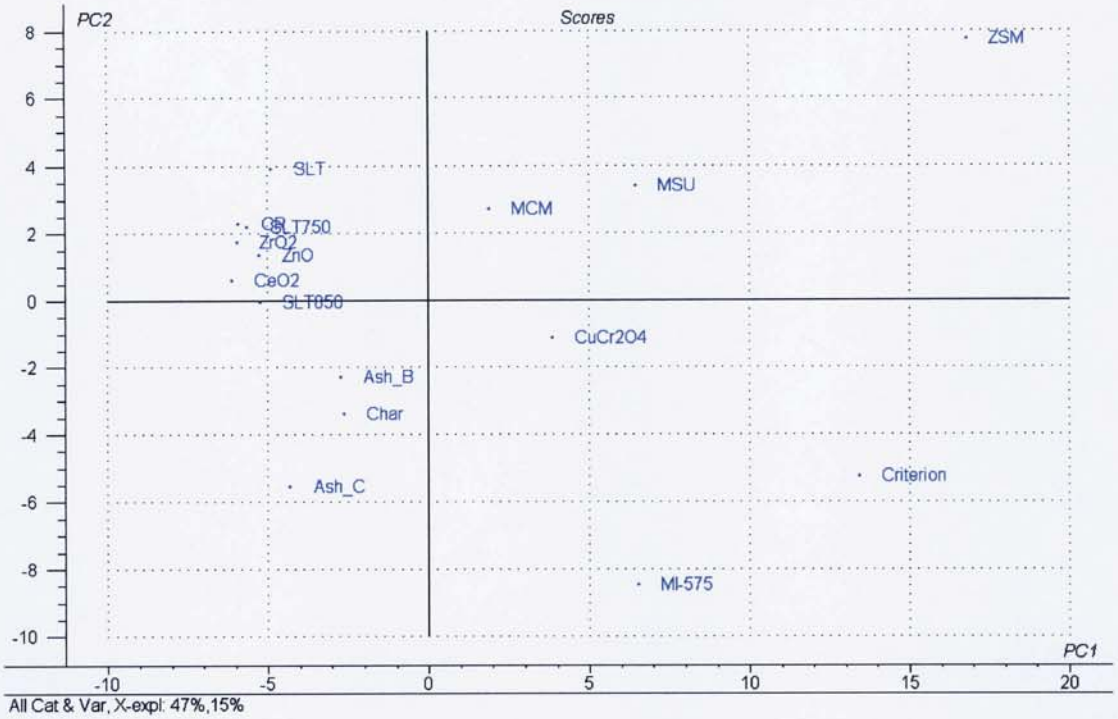

(a)

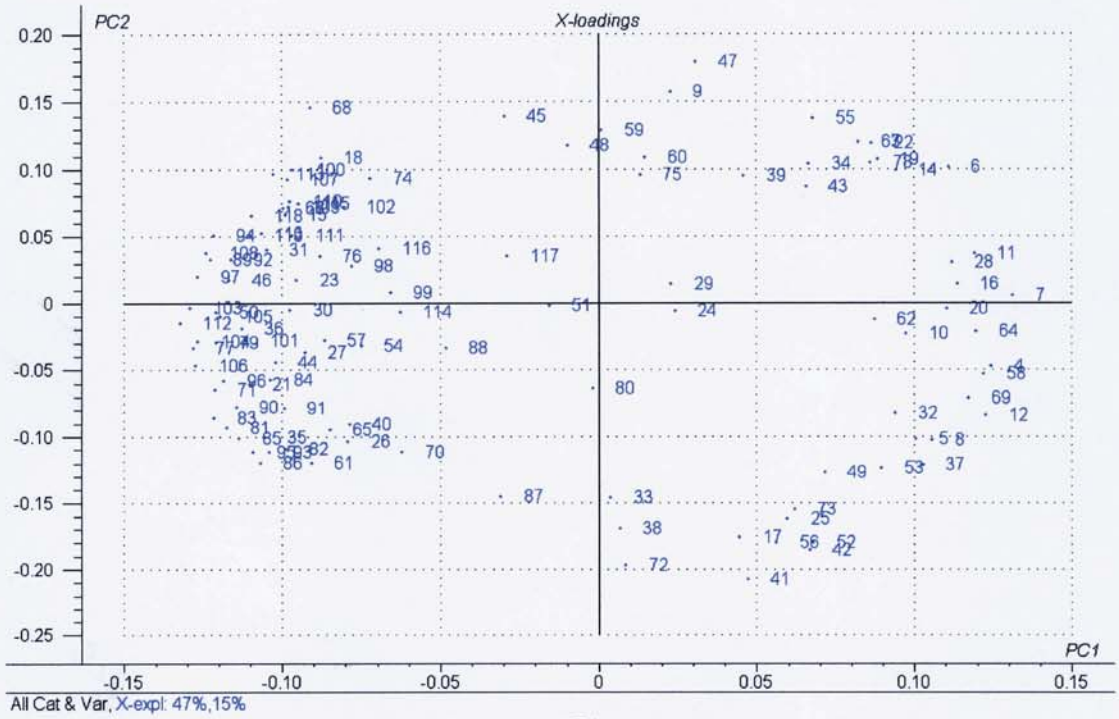

(b)

Figure 5-4 Score (a) and loading (b) plots of PC1 and PC2 for model with all catalysts and all compounds

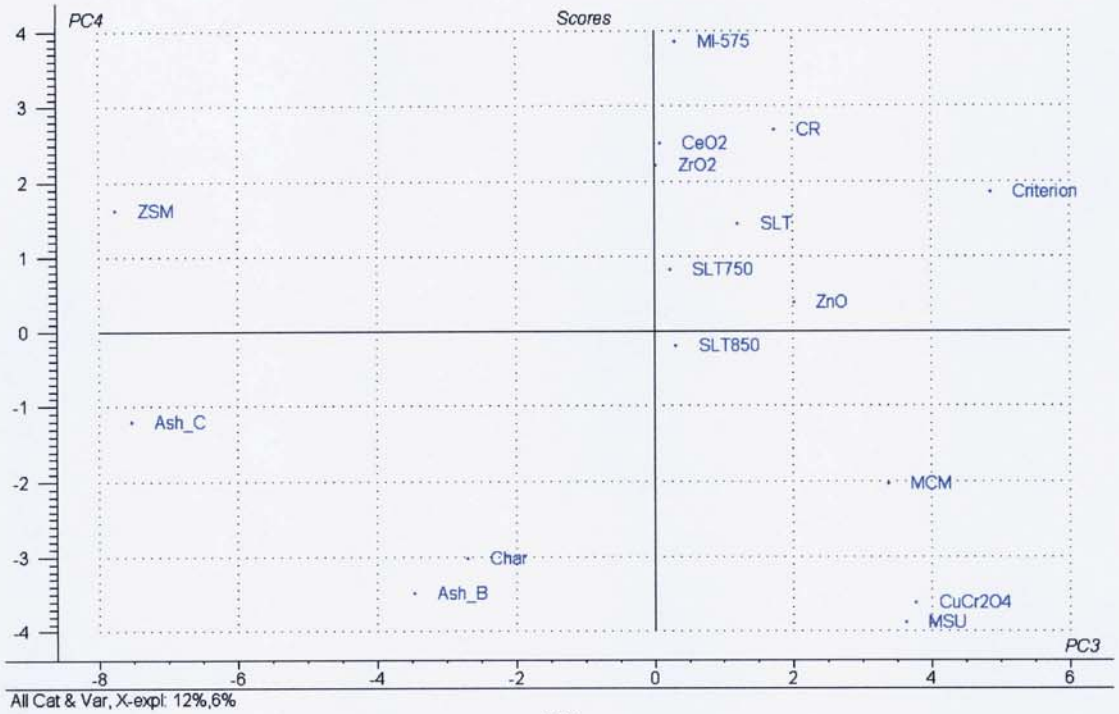

(a)

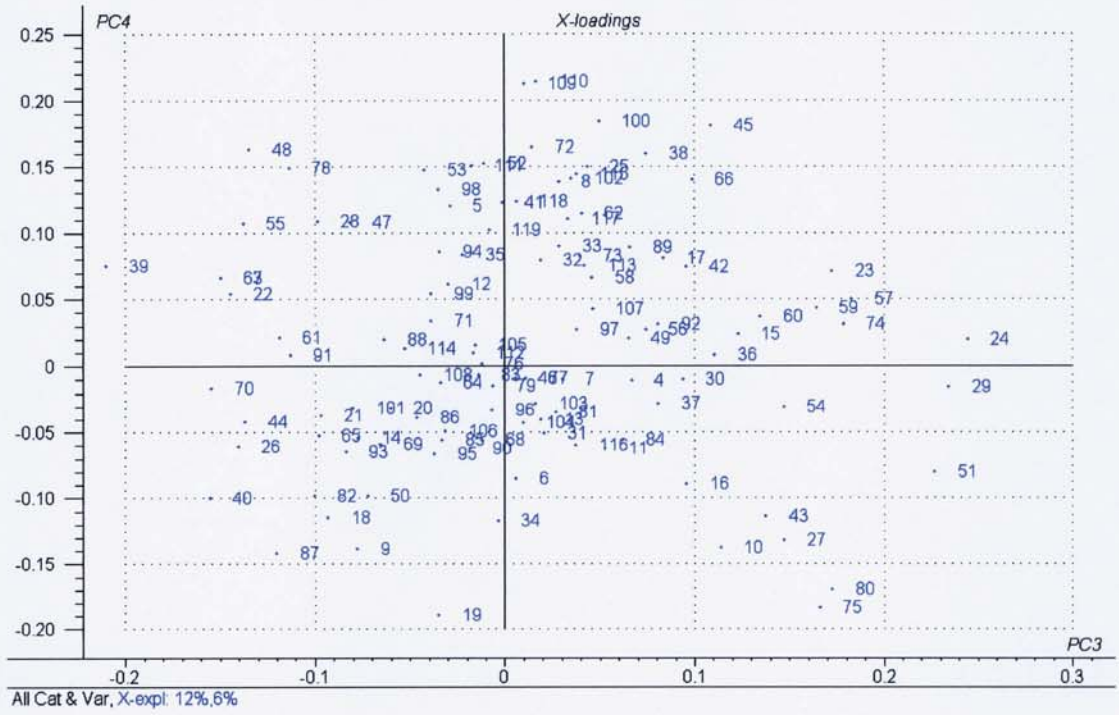

(b)

Figure 5-5 Score (a) and loading (b) plots of PC3 and PC4 for model with all catalysts and all compounds

Viscosity is one of the most important properties of bio-oil, especially if its application involves pumping and injecting. It is known that the viscosity of bio-oil has a positive correlation with its molecular weight [5] and most of the heavy pyrolysis products are derived from lignin. Thus, the second PCA model used includes all lignin derivatives and the selected catalysts. Its score and corresponding loading plots are presented in Figure 5-6 (a) and (b). It is expected from this model that catalysts that help to reduce the lignin derivatives would have a high potential for decreasing the bio-oil viscosity.

Figure 5-6 (b) reveals that there are two main groups of compounds separated by the first principal component which explains up to 64% of the total variance: one on the left side of the origin, which are mainly oxygenated lignin derivatives, and the other on the right side of the origin, which are aromatic hydrocarbons (p-Ethyl-styrene (ID#55), 5-Methylindan (ID#63), Toluene (ID#22), Xylenes (ID#34), Benzene (ID#14)) and phenols (Phenol (ID#64) and o-Cresol (ID#69)). When considering this together with the score plot, it is evident that ZSM-5 catalyst located on the positive PC1 direction shows a high potential not only for reducing the oxygenated lignin compounds, which is advantageous to bio-oil viscosity improvement, but also for producing aromatic hydrocarbons and phenols, which are valuable products.

In addition, Figure 5-6 demonstrated that Criterion-534 and Al-MSU-F have a similar behaviour to the ZSM-5, although less pronounced. However the main difference between Criterion-534 and Al-MSU-F is that Criterion-534 tends to produce more phenols than Al-MSU-F. Al-MCM-41 also exhibits a potential for selectively decreasing the amount of oxygenated lignin-derived compounds as it lies on the right side of the "CR" (sample without any catalyst) and far away from oxygenated lignin species group. Ash of biomass, copper chromite and MI-575 could reduce most, but not all, of the oxygenated lignin derivatives as they are explained by the negative second principal component (PC2). This suggests that these catalysts could enhance the production of some lignin components, which are also explained by negative PC2, such as 4-Propyl guaiacol (ID#87) and Eugenol (ID#86). However, because the PC1 explains 64% and PC2 explains 13%, the influence of PC1 is much stronger than that of PC2. It can therefore be deduced that ash of biomass, copper chromite and MI-575 are promising for lowering bio-oil viscosity.

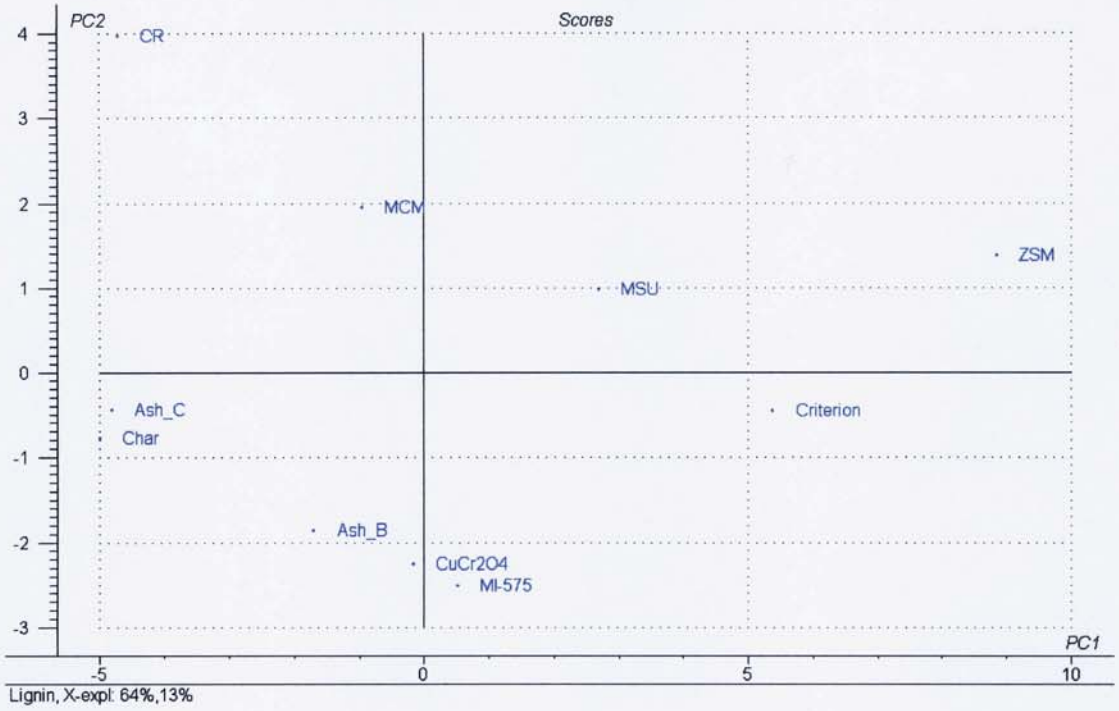

(a)

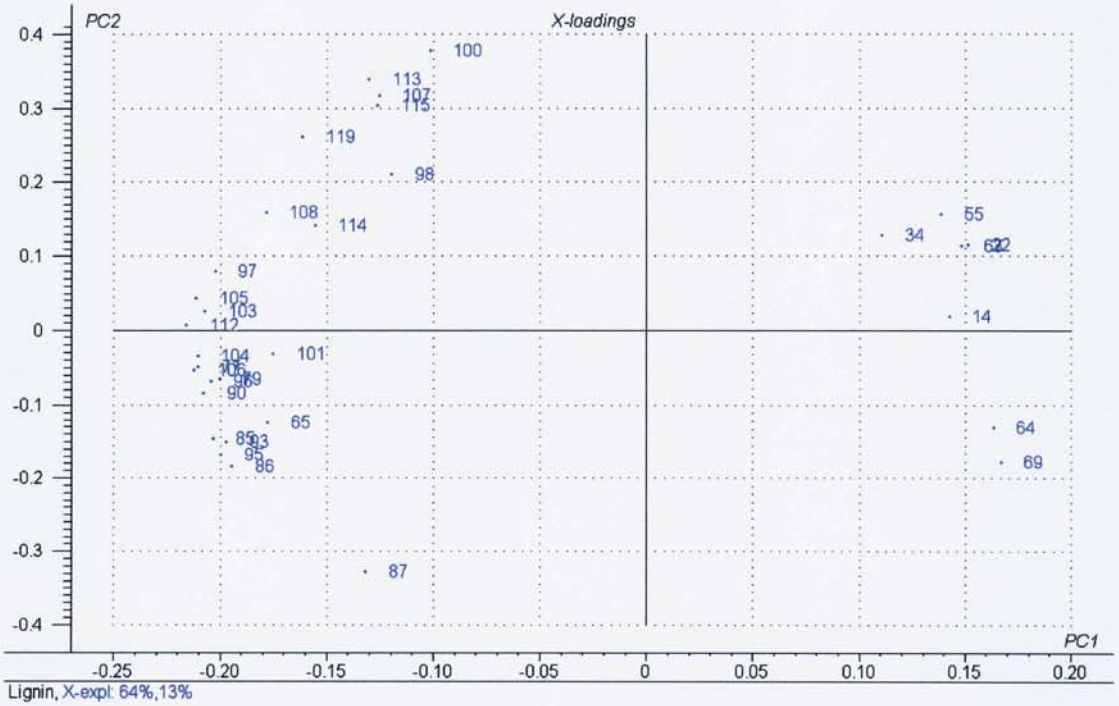

(b)

Figure 5-6 Score (a) and loading (b) plots of PC1 and PC2 for model with selected catalysts and lignin-derived products

Moreover, Char and its ash lie close to each other in the score plot (Figure 5-6 (a)). This indicates that their influence on lignin products is similar and is different from the other catalysts in that the char and its ash did not selectively reduce all or most of the oxygenated lignin derivatives, but they actually tend to increase the quantity of some lignin compounds lying in the third quadrant of the score plot.

Another PCA plots related to viscosity prediction was established, but the resultant plots are not shown here as they reach similar conclusions to the lignin derivatives model. The additional model includes all heavy compounds having molecular mass more than 150. It was found from this model that not only are the oxygenated lignin derivatives selectively reduced by ZSM-5, Criterion-534 and Al-MSU-F, but heavy carbohydrate derived products such as Levoglucosan and 1,6-Anhydro-β-D-glucofuranose (IDs#111 and 117, respectively) are also decreased in quantity.

It is widely believed that the presence of reactive aldehydes and ketones in bio-oils are responsible for various reactions in ageing processes, leading to instability. In order to assess or predict whether the bio-oil stability can be improved by the addition of catalysts or not, a PCA model was set up with the 9 selected catalyst samples and all carbonyl compounds identified. The score and loading plots for the first two principal components are presented in Figure 5-7 (a) and (b), respectively. Based on these plots, there is no single catalyst illustrating the selectivity towards the reduction of all carbonyl compounds. Instead, ZSM-5, Criterion-534 and MI-575 express a trend to decrease one group of carbonyls, which is on the positive PC1 of the loading plot, while simultaneously increasing another group of carbonyls, which is on the negative PC1 of the loading plot. The compounds clustered on the positive PC1 values are carbonyl compounds containing hydroxyl group (IDs#15, 21, 26, 36, 46, 61, 70, 76, 89, 92, 103, 105, 113 and 114), furanones (IDs#30, 31 and 54) and others (IDs#13, 35, 40, 50 and 119). It can be observed that most of the compounds in this group are hydroxyl-containing carbonyls, while most of the compounds on the negative PC1 are carbonyls without any other group except for compounds 45, 59 and 78 that have hydroxyl group. To judge which catalyst will ameliorate or deteriorate the stability of bio-oil, knowledge of which carbonyl compounds are more reactive is required. Since this is not well understood and is still an issue for further research, it is

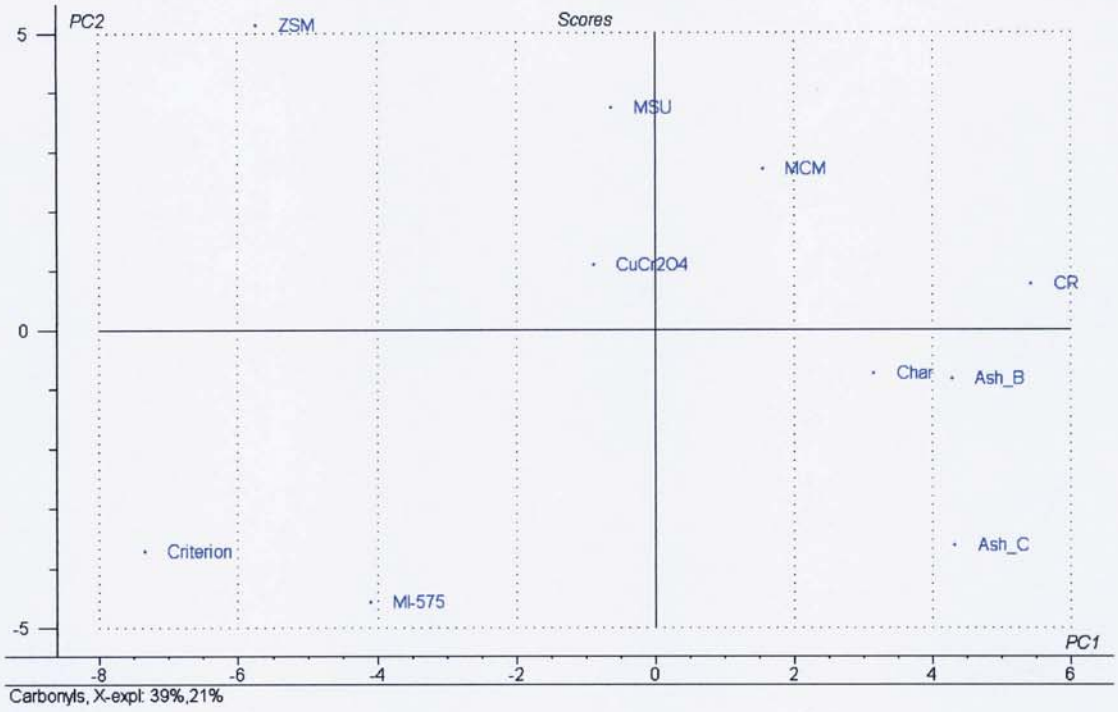

(a)

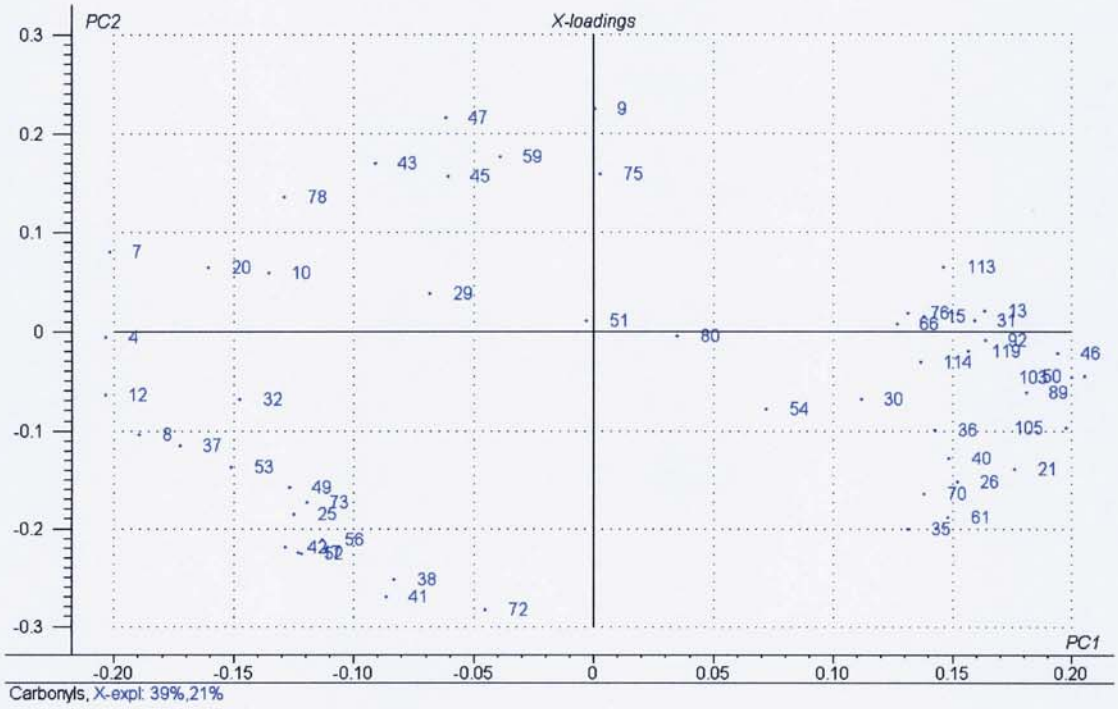

(b)

Figure 5-7 Score (a) and loading (b) plots of PC1 and PC2 for model with selected catalysts and all carbonyl compounds

not possible from the data obtained in this work to draw a decisive conclusion on bio-oil stability. Nevertheless, assuming that all carbonyls reactiveness does not differ significantly, the Al-MCM-41, Al-MSU-F and copper chromite would be the best catalysts in terms of bio-oil stability, since they partly reduce carbonyls compounds on the right side of PC1 in the loading plot (Figure 5-7 (b)) and simultaneously do not produce significant amounts of compounds on the negative PC1 as it is the case for ZSM-5, Criterion-534 and MI-575.

Apart from viscosity and stability, acidity is also one of the crucial properties of pyrolysis liquid, especially for fuel applications as it leads to the corrosiveness of bio-oil. The effect of catalysts on potential change in bio-oil acidity can be investigated by comparing the percentage amounts of acetic, formic and lactic acids produced. By implementing the nine selected catalysts plus one control sample and mean percentage peak areas of acetic acid (ID#19), formic acid (ID#16) and lactic acid (ID#18), another PCA model was established. Since only three compounds are involved, a bi-plot is used to evaluate the correlation between catalysts and pyrolysis products as shown by Figure 5-8. It can be seen from the first two principal components which explained up to 95% of the total variance that ZSM-5 and Al-MSU-F favour the production of both acetic and formic acids, while decreasing lactic acid. Although the natural catalysts (char and ashes) tend not to produce a significant amount of acetic and formic acids, they increased lactic acid percentage yield. From the bi-plot, Criterion-534 and MI-575 lie in the opposite side of compound ID#18 (lactic acid), suggesting that they considerably reduce lactic acid yield. From Table 5-3, these catalysts actually completely eliminated the formation of lactic acid. When compared with other catalysts, MI-575 lies far away from all acids, indicating that higher pH of bio-oil would be achieved by this catalyst. If acidity of the bio-oil is the main concern, especially in fuel application, MI-575 may be chosen as it could also improve the viscosity as mentioned earlier. However, if the zeolite and related materials are to be applied for hydrocarbon production or other purposes, a concentration method proposed by Oasmaa et al [58] may be useful since it can remove significant amounts of volatile carboxylic acids.

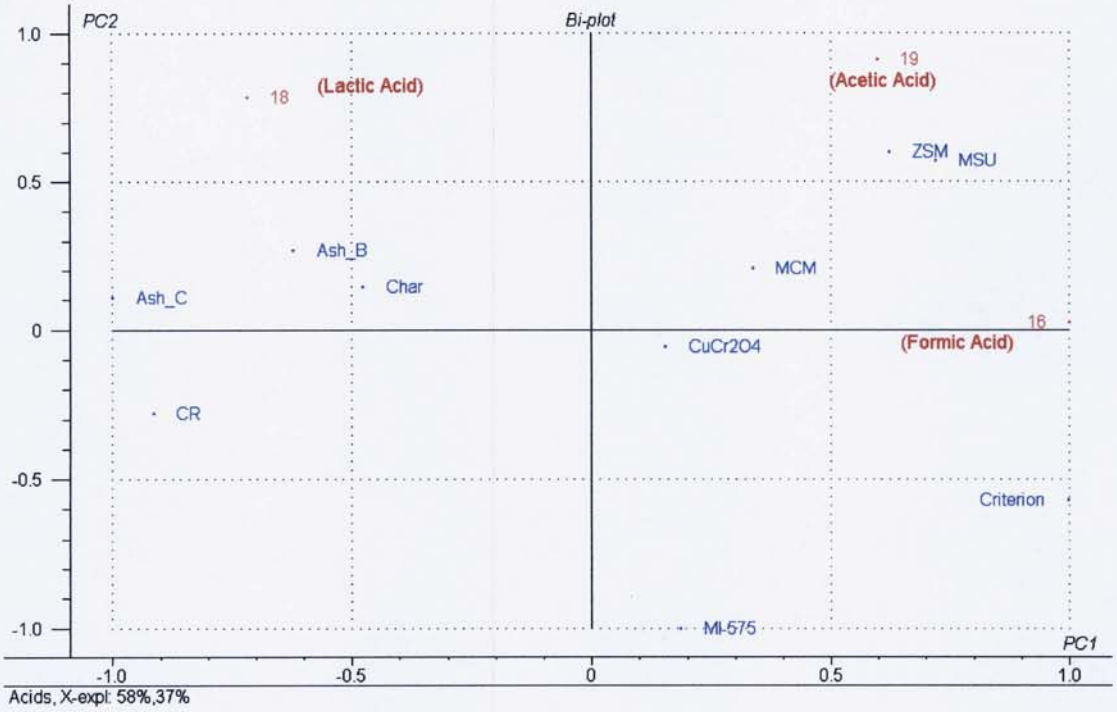

Figure 5-8 Bi-plot of PC1 and PC2 for model with selected catalysts and three organic acids

5.4 CONCLUDING REMARKS

Catalyst screening for fast pyrolysis of biomass was studied by pyrolysis-GC/MS coupled with multivariate data analysis. The principal components analysis was useful for screening catalysts as shown in this study. Catalysts with little influence on pyrolysis product distribution were eliminated prior to detailed study. More specifically, slates, ZnO, ZrO_2 and CeO_2 were found to be inactive catalysts for changing bio-oil quality under the conditions studied.

ZSM-5, Criterion-534 and Al-MSU-F showed a high potential for reducing bio-oil viscosity as they were selective to the reduction of all oxygenated lignin-derived compounds and concurrently enhanced the formation of aromatic hydrocarbons and phenols. Although less pronounced, Al-MCM-41, copper chromite, MI-575 and ash of biomass could also improve the viscosity of bio-oil, while char and its ash have an insignificant effect.

Predicting the bio-oil stability is difficult as no single catalyst was found to selectively reduce all carbonyl compounds. The bio-oils produced with most of the active catalysts except for MI-575 are predicted to be lower in pH compared to non-catalytic bio-oils, provided that water contents of the bio-oils are in the same range.

According to the results reported in this chapter, the catalysts recommended for the bench-scale fast pyrolysis experimentation are ZSM-5, Criterion-534, Al-MSU-F, Al-MCM-41, copper chromite, MI-575 and ash of biomass.

6 EXPERIMENTAL FAST PYROLYSIS

6.1 INTRODUCTION

This chapter describes the equipment and the procedures used for the production of bio-oils with and without catalysts as well as the mass balance calculation. Also included are methods for characterisation of the obtained pyrolysis products (bio-oil, char and non-condensable gases). The characterisation of bio-oils includes water content, solids content, pH value, elemental composition analysis, heating values, molecular weight distribution, stability and liquid GC/MS analysis. The properties of char examined are basic element, ash content and composition as well as heating values. Finally the non-condensable gases are analysed for their composition.

6.2 BENCH-SCALE FAST PYROLYSIS UNIT

In chapter 5, fast pyrolysis experiments were carried out using a micro-scale batch reactor in order to produce pyrolysis vapours, which were then analysed using GC/MS technique. It has been shown that the method is rapid and useful for catalyst screening. Therefore, further work has been performed based on a larger-scale pyrolysis unit for bio-oil production in order to investigate the effect of parameters such as biomass feedstocks, pyrolysis temperatures and catalysts on yields and properties of pyrolysis products. The experimental setups for both catalytic and non-catalytic pyrolysis are described in this section, while section 6.4 describes the characterisation techniques used for the analysis of pyrolysis products.

6.2.1 Non-catalytic pyrolysis experiments

Non-catalytic pyrolysis experiments were conducted in a bench-scale (150 g/h throughput) fluidised-bed reactor unit. This unit was adapted from Waterloo Fast Pyrolysis Process (WFPP) [52]. The biomass feeding tube and liquid collection

system of the unit were further modified in this project. Details of the modifications are given in section 6.2.1.1 and 6.2.1.2. This section explains the modified reactor system as depicted in Figure 6-1. The unit consists mainly of a feeder, a reactor and a product collection system. A schematic diagram of the feeder is shown in Figure 6-2. The feeder consists of a tubular storage hopper made of clear Perspex, a stirrer and an entrain tube. The reactor (Figure 6-3) was constructed from 316 stainless steel tube with 4 cm diameter and 26 cm length. It was filled with approximately 150 g of sand with particle size range of 355-500 μm. The sand was used as a fluidising and heat transfer medium. The product collection system was composed of a water condenser (Davies-type double surface heat exchanger), an electrostatic precipitator (ESP) and two dry ice/acetone condensers (cold-finger type).

Figure 6-1 Bench-scale non-catalytic fast pyrolysis unit (adapted from [132])

All experiments were initiated by flowing nitrogen at the flow rate of approximately 5-7 l/min to remove the air within the system, followed by preheating the reactor using a muffle electrical furnace until the temperatures of the fluidising medium reached a steady state. Five thermocouples were used to record the temperatures at different positions in the unit. These included (i) fluidised bed, (ii) biomass feeding tube end, (iii) reactor freeboard, (iv) transfer line and (v) gas exit after cotton wool filter. Once the thermocouples (i) and (ii) reached a steady value, which is typically about 20°C higher than the expected pyrolysis temperature, the run was ready to begin.

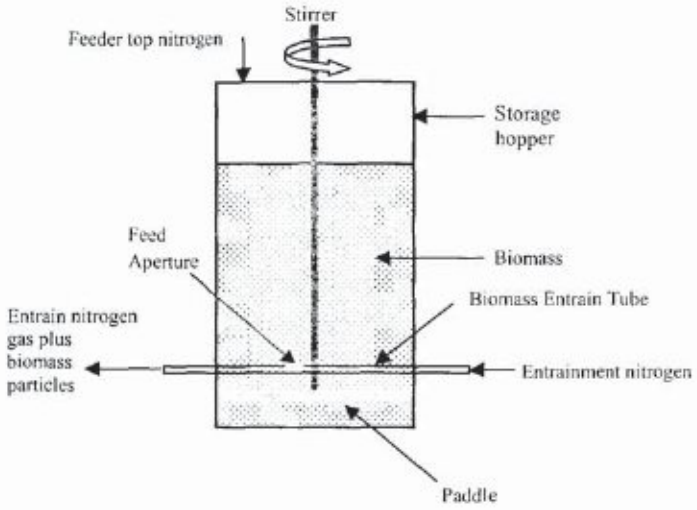

Figure 6-2 Biomass feeder

Aston University

Illustration removed for copyright restrictions

Figure 6-3 150 g/h fluidised bed reactor (adapted from [133])

The reason why the initial setting of the pyrolysis temperature needs to be slightly higher is because the overall pyrolysis reaction of lignocellulosic biomass is endothermic. Therefore, the temperature decreases slightly after biomass is fed. The degree of temperature reduction depends on the biomass feed rate and the amount of entrainment and fluidising nitrogen. Based on the experience with Aston's 150 g/h unit, a reduction of around 20-30°C normally occurs. Apart from the temperature recording, the pressure was also monitored during the run at three places, (i) fluidising nitrogen inlet, (ii) entraining nitrogen inlet and (iii) pyrolysis gas exit (between the cotton wool filter and gas meter). The first two pressure measurements were useful as indicators of blockage along the vapour entrainment pathway and in the biomass feeding tube, respectively. The last one was used for getting gas pressure data in order to calculate the non-condensable gas yields.

The biomass particles in the feeder were continuously carried into the reactor at the middle of the fluidised bed by nitrogen entrained flow via the air-cooled feeding tube. It is important to note that the feeding tube needs to be cooled in order to avoid pre-pyrolysis of biomass particles inside the feed tube, which can lead to a blockage. The biomass feed rate was controlled by the speed of the stirrer, the entrainment nitrogen flow rate and the feeder top nitrogen flow rate. Once the biomass particles reached the fluidised bed, heat was transferred from the hot fluidising medium to the biomass particles mainly by conduction and convection and the thermal degradation of the biomass occurred, producing vapours including aerosols, water and non-condensable gases, and generating the residue solid char. The product mixture was carried out of the reactor passing the cyclone where the solid was separated and collected in the char pot. The vapours together with some char fines that could not be removed by the cyclone were then passed through a liquid product collection system consisting of a water condenser, an electrostatic precipitator (ESP) and a series of two dry ice/acetone condensers. In the water condenser, part of the pyrolysis vapour was condensed and the liquid together with the uncondensed vapour flew into the ESP where most of the uncondensed vapour together with aerosols and char fines can be captured by the electrostatic charge supplied. The liquid mixture was then collected in a 100 ml round bottom flask called "Oil Pot 1" located under the ESP. Not all the liquid can be collected in the Oil Pot 1 since the pyrolysis vapour also contained some water and

light volatile compounds such as formaldehyde, acetaldehyde and some ketones with low boiling points. Most of these compounds were condensed by using a series of two dry ice/acetone condensers where the temperature inside the condensers is estimated to be around -30°C. The liquids condensed by these condensers were collected in two 50 ml round bottom flasks named "Oil Pot 2" and "Oil Pot 3". Although the dry ice/acetone condensers could maintain the pyrolysis vapour at a very low temperature, there were still some volatiles that could not be condensed and collected in the oil pots, but could be captured in the cotton wool filter instead. This is attributed to the low partial pressure of the volatiles in the condensers due to the dilution effect of the nitrogen carrier gas. This problem is widely known in large-scale pyrolysis plants and can be solved by minimising the nitrogen carrier gas flow rate and/or maximising the biomass feed rate. After the cotton wool filter, the nitrogen carrier gas together with the non-condensable pyrolysis gases passed through the gas meter where the volume of the exit gas was recorded. Then part of the gas mixture was pumped into an online gas chromatograph (GC) for gas composition analysis and the rest was vented.

6.2.1.1 Modification of biomass feeding tube

In the past three years or longer, the biomass feeding tube of the 150 g/h pyrolysis unit had been one of the big obstacles for running the rig continuously and successfully. The feedstock blockages in the feeding tube noticed from a sudden increase of the entraining nitrogen pressure had been known by researchers at Aston University, especially in the case of non-woody feedstocks, such as oil palm empty fruit bunches (EFB), straw, agricultural residues from cassava plantations, etc. These feedstocks appeared to contain some needle-like particles that blocked the feeding tube. In addition, the powder or dust present in the feedstock tended to accumulate and stick to the wall of the feeding tube and eventually blocked the tube due to its very small internal diameter (~2 mm). This problem had been solved by double or triple sieving of biomass to remove the needle-like particles and/or the biomass powder. Alternatively, slowing down the biomass feed rate to below 50 g/h was also found to be useful for preventing the blockage. However, the two or three times sieving was tedious and the use of low biomass feed rate could also cause a longer duration run and problems with undetectable GC peaks could arise because of the low

concentration of pyrolysis gases in the carrier nitrogen gas. Therefore, it was an intended purpose of this project to permanently solve this problem by constructing a new feeding tube with a larger inside diameter. The biomass feeding tube was built from three stainless steel tubes with different diameters as conceptually illustrated in Figure 6-4. The first tube from the inside is for transporting biomass feedstock, while the second and the third tubes are for cooling air in and out, respectively. The main difference between the new and old feeding tubes is the inside diameter of the inner tube where biomass travels through. It has been changed from 2 mm to 3.28 mm. It was expected that the larger diameter of the tube would facilitate the biomass entrainment with significantly reduced chances of blockage.

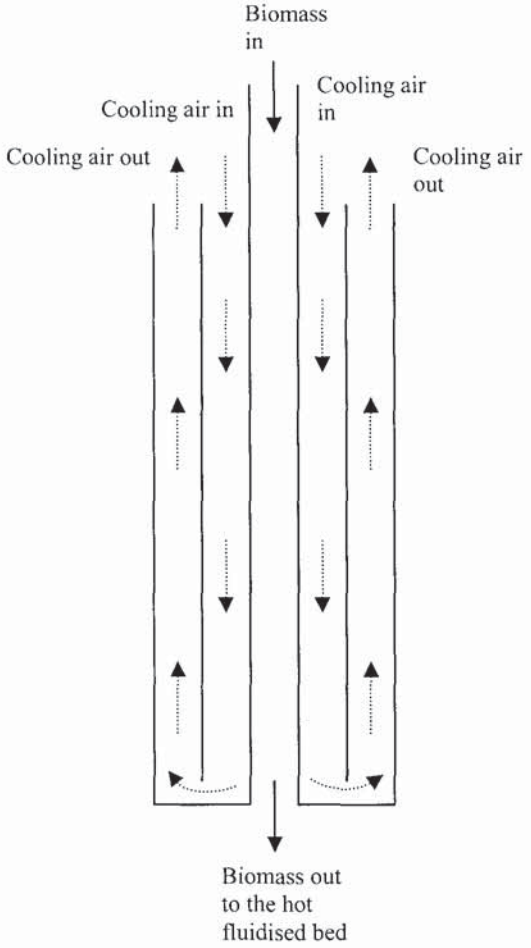

Figure 6-4 Feeding tube concept (not to scale)

The dimensions of the three tubes used for constructing the new feeding tube are given in Figure 6-5. The inner tube was made of welded hard drawn 304 type stainless steel (gauge no 8), whereas the middle and the outer tubes were constructed of 316 stainless steel.

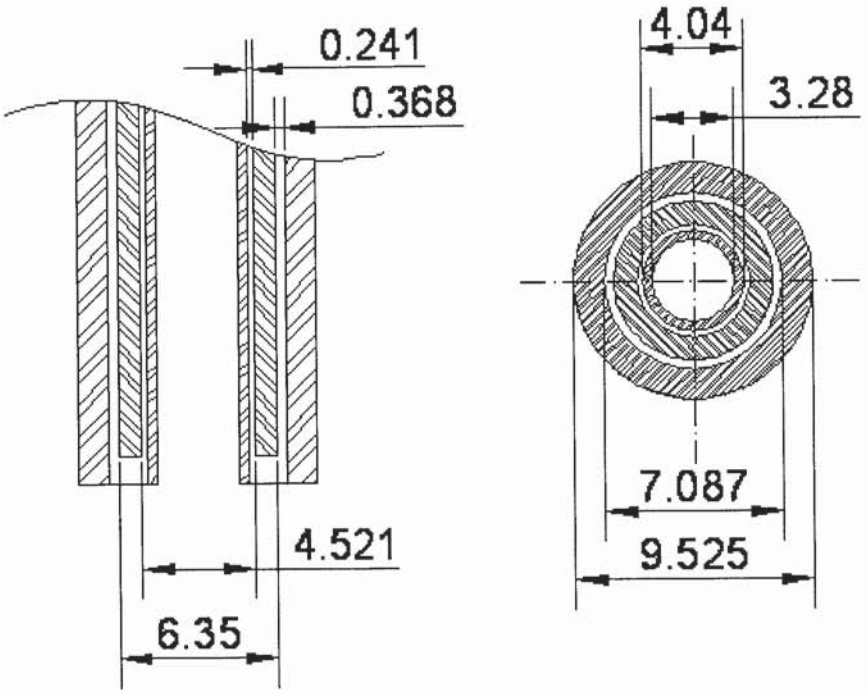

Figure 6-5 Dimensions (in mm) of the new feeding tube

After the construction, the new feeding tube was tested for its performance and compared with the old one. It was found when using cassava stalk as feedstock that the new feeding tube could cope with 150 g/h biomass feed rate without any blockage compared with only 40-45 g/h when the old feeding tube was applied. Therefore, this new feeding tube was used in this work for both catalytic and non-catalytic experiments.

6.2.1.2 Modification of liquid collection system

The liquid product collection system previously used (prior to the commencement of this project) in the 150 g/h pyrolysis unit was composed of a water condenser, an electrostatic precipitator and only one dry ice/acetone condenser. It was observed that approximately 3-8 g of liquid could not be condensed by the system and was captured by the cotton wool filter. It was also noticed that some of the light volatiles could pass the cotton wool filter to the gas meter and to the online GC vacuum pump, which was observed from the smell of volatiles at the gas meter and the pump. This caused not only the damages to both the gas meter and the pump, but also the poor mass balance

closure. Therefore, to prevent the damages to these devices and to improve the efficiency of the liquid product collection, a second dry ice/acetone condenser has been introduced to the pyrolysis unit. This secondary condenser was especially useful for catalytic pyrolysis experiments due to higher amounts of light volatiles produced during catalytic cracking.

6.2.2 Catalytic pyrolysis experiments

Catalytic pyrolysis experiments were carried out using a unit similar to the one used for non-catalytic pyrolysis experiments described in the previous section. The only difference between these two units is the addition of a secondary catalytic reactor. The secondary reactor was placed after the cyclone and before the water condenser as illustrated by Figure 6-6. The reactor constructed of 316 stainless steel was 4.27 cm inside diameter and 49 cm high. The reactor was equipped with three type-K thermocouples to record temperatures at the inlet and outlet of the reactor as well as at the middle of the catalyst bed. The catalyst was supported by a ring of metal mesh and approximately 10 g of glass wool. The glass wool serves two functions. Firstly, it can hold catalysts whose particle size is very small or smaller than the mesh size (<100 μm), thereby preventing them from falling down to the bottom of the reactor. Secondly, the glass wool functions as a hot vapour filter by capturing the char fines in the vapour that cannot be separated by the cyclone. This helps to prolong the catalyst activity as the char fines can otherwise cover the catalyst surface leading to catalyst deactivation. The use of glass wool can also reduce the solids content of the bio-oil, thus improving its quality. Glass wool was also placed at the top of the catalyst bed for preventing catalyst powder from blowing out of the reactor and for filtering the vapour after catalytic reaction. The glass wool plugs were also used to ensure that the catalyst was in the form of fixed bed. The catalyst bed temperature for all experiments was maintained at approximately 500°C. The amount of catalyst used was 100 g for most of the runs except when testing Al-MCM-41 and Al-MSU-F mesoporous materials only about 10 g was used due to their low densities and the limited supplies. All catalysts were calcined in a muffle oven at 500°C for 6 hours and kept in a desiccator prior to use.

Figure 6-6 Bench-scale catalytic fast pyrolysis unit (adapted from [132])

6.3 MASS BALANCE CALCULATION

All metal and glassware items used in the bench-scale pyrolysis unit were weighed before and after each run in order to calculate the yields of pyrolysis products. By weighing the feeder before and after the run, the amount of biomass fed can be calculated. The solid yield is a combination of the char collected in the char pot, reactor and transfer line, and the char fines or solids present in the liquid bio-oil. Determination of bio-oil solid content is described in section 6.4.1.2. The liquid product was fractionated into 5 fractions, which are (1) water condenser oil, (2) ESP oil, (3) Pot 1 oil, (4) Pot 2 oil and (5) Pot 3 oil. The water condenser and the ESP oils were sticky and difficult to remove. They were therefore washed with ethanol 3-5 times and these bio-oil/ethanol mixtures were kept for water and solid contents analysis (see section 6.4.1.1 and 6.4.1.2). In addition, the permanent gas yields were calculated based on the gas composition obtained from GC analysis (section 6.4.3), total gas volume and the exit gas temperature and pressure recorded. An example of mass balance report is shown in Table 6-1. The pyrolysis temperature was the averaged value of temperature data recorded from two thermocouples at the fluidised

bed every 5 minutes throughout the run. The vapour residence time was calculated as the time that pyrolysis vapours spent in the hot space of the reactor system prior to condensation. Details of the mass balance spreadsheet are provided in APPENDIX-B.

Table 6-1 A typical mass balance summary report of a bench-scale fast pyrolysis run

	Unit	
Test name		**AP17**
Fluidising medium		**Sand**
particle size	*μm*	**355-500**
Feedstock		**Cassava Rhizome**
particle size	*μm*	**355-500**
Moisture content	*wt%*	**8.18%**
Ash content	*wt%, dry basis*	**4.13%**
Pyrolysis temperature	*°C*	**477.38**
Vapour residence time	*seconds*	**0.74**
Feed rate	*g/h, dry basis*	**140.80**
Product yields	*wt%, dry basis*	
Char		**19.97%**
Liquids		**64.93%**
Organics		49.76%
Reaction water		15.17%
Gas		**10.10%**
H_2		0.06%
CH_4		0.32%
CO		2.72%
CO_2		6.80%
C_2H_4		0.05%
C_2H_6		0.07%
C_3H_6		0.05%
C_3H_8		0.02%
Closure	*wt%, dry basis*	**95.00%**

6.4 CHARACTERISATION OF PYROLYSIS PRODUCTS

Fast pyrolysis of biomass gives liquid bio-oil as main product with solid char and non-condensable gases as valuable by-products. All products were analysed in order to complete the mass balance and to gain insight into the products properties. This section explains the analytical methods applied for characterisation of bio-oil, char and non-condensable gases.

6.4.1 Bio-oil

The main product of biomass fast pyrolysis is liquid bio-oil. It contains water, char fines and organic compounds derived from fragmentation and depolymerisation of cellulose, hemicellulose and lignin polymers. In order to investigate the properties of bio-oils produced from catalytic and non-catalytic experiments, characterisation of bio-oils includes water content, solid content, pH value, elemental analysis, heating value, molecular weight distribution, gas chromatography/mass spectrometry (GC/MS) analysis and stability. Theses analyses are describe in the following sub-sections.

6.4.1.1 Water content

For solid biomass, water content was easily determined by drying in an oven at 105°C. This technique is not applicable for bio-oil samples since they also contain light organic volatiles that would be evaporated together with water upon heating at 105°C. Consequently, alternative technique known as Karl Fischer (KF) titration, which is widely used and recommended for bio-oil water content determination, was applied using a Metrohm 758 KFD Titrino instrument. Prior to the measurement, a calibration of the instrument with HPLC-grade water was performed. Four liquid samples from each pyrolysis experiment were subjected to water content analysis. These included two ethanol washing liquids from water condenser and ESP, a liquid from Oil Pot 1 and a liquid mixture of Pot 2 and Pot 3 oils (denoted as "Pot 2+3 oil"). Each sample was tested in triplicate. Because the amounts of ethanol in the washing liquids are known, the amounts of water present in these liquids can be calculated once obtaining their water and solid contents.

6.4.1.2 Solids content

Although most of the solid was separated from the pyrolysis vapour by the cyclone and collected in the char pot, there were still some char fines entrained to the liquid collection system and became parts of the liquid product. The quantity of the solid

was determined by vacuum filtration technique. Approximately 7-10 g of water condenser and ESP washing liquids or 1-2 g of Pot 1 liquid was filtered through a pre-dried and pre-weighed Whatman No.2 qualitative filter paper whose mean pore size was 8 μm. The liquid was then washed with excess amount of ethanol until the filtrate was clear to ensure that there was no organic liquid left on the filter paper. The filter paper with the residue was air-dried for approximately 15 minutes and in an oven at 105°C for around 30 minutes, cooled in a desiccator and weighed; this method is suggested by Oasmaa and Peacocke [134]. The solids content could then be calculated. It was observed earlier that the liquid mixture of Oil Pot 2 and Oil Pot 3 contained no char fines. Therefore, this liquid was not included in the analysis of solids content.

6.4.1.3 pH value

It is well known that bio-oil is acidic due to the presence of carboxylic compounds such as acetic and formic acids. In this study, the non-catalytic pyrolysis liquid collected from Oil Pot 1 and a liquid mixture of Pot 2 and Pot 3 oils were subjected to pH determination, while the pH of the washing liquids were not measured because they were already diluted with ethanol and the pH value would not be representative of the bio-oils. The instrument used was a Metrohm 713 pH meter at room temperature. Before the measurement, the instrument was calibrated with liquid calibration standards of pH 4, 7 and 9.

6.4.1.4 Elemental analysis

All liquid fractions (washing liquids and Pot 1-3 oils) were proportionately mixed to obtain a single liquid product named "Liq". The Liq contains approximately 20 wt% of organics and around 80 wt% of the rest (ethanol, water and solids). All Liq samples were subjected to CHN analysis using CE-440 and Carlo Erba elemental analysers with ±0.3% absolute accuracy. The analysis was done by MEDAC Ltd., Surrey, UK. After obtaining the carbon, hydrogen and nitrogen (CHN) contents of the Liq samples, the elemental analysis of the bio-oil was calculated by subtracting the

carbon, hydrogen and oxygen amounts of the known quantities of ethanol and water in order to obtain the carbon hydrogen and nitrogen contents of bio-oils on dry, solvent-free basis. In addition, the oxygen content of bio-oils was calculated by difference.

6.4.1.5 Heating value

The higher heating values (HHV) of bio-oils were calculated based on a correlation developed by Channiwala and Parikh [105] as shown by Equation 6-1. The lower heating values (LHV) were calculated from HHV and the hydrogen content by Equation 4-5.

$$HHV_{dry}\ (MJ/kg) = 0.3491C + 1.1783H + 0.1005S - 0.1034O - 0.015N - 0.0211A$$

Equation 6-1

Where C, H, S, O, N and A represent mass percentages on dry basis of carbon, hydrogen, sulphur, oxygen, nitrogen and ash contents of bio-oil, respectively. The C, H, N and O contents of bio-oil were obtained by the elemental analysis as mentioned in section 6.4.1.4. The sulphur content was not taken into account because it was lower than the detection limits of the instrument (<0.1 wt%). The ash content was estimated from the solids content of bio-oil by assuming that the solids present in bio-oil contains 5 wt% of ash.

The heating values calculated by Equation 6-1 is on dry basis. To calculate the values on as-produced or wet basis, Equation 4-2 and the following equation [103] were applied taking into account the water content of bio-oil (H_2O, wt%).

$$LHV_{wet} = LHV_{dry}(1 - H_2O/100) - 2.442 \cdot H_2O/100$$

Equation 6-2

6.4.1.6 Molecular weight distribution

Molecular weight distribution of pyrolysis liquids was determined using gel permeation chromatography (GPC) technique. The instrument used was an integrated GPC system, PL-GPC50 from Polymer Laboratories, UK, equipped with a PLgel 3 μm MIXED-E column, 300×7.5 mm, and a refractive index (RI) detector. The detector temperature was set at 40°C. Liquid samples were dissolved in HPLC-grade THF (tetrahydrofuran) solvent at a concentration of 0.01 g/ml and were filtered through a 0.2 μm Millipore Millex-GN nylon filter in order to avoid column plugging by solids or insoluble impurities. Approximately 100 μm of the prepared samples was injected using a PL-AS RT GPC autosampler. HPLC-grade THF was used as an eluent with a flow rate of 1 ml/min. Prior to the measurement, GPC calibration was made with a series of polystyrene calibration standards with molecular weight range of 162 to 19880 g/mol. Calculation of molecular weight averages was done by the Cirrus 3.0 software. The software offers two methods of data calculation, height based and area based. Height based calculation is analogous to the integrator packages of the late seventies and uses a simplified method of calculation, whereas area based calculation is the rigorous treatment of data and the method of choice for high accuracy work [135]. In this work, the area based method was chosen. The number average molecular weight (Mn), weight average molecular weight (Mw), molecular weight at highest peak (Mp) and polydispersity (PD = Mw/Mn) were calculated by the software based on the refractive index (RI) signal and the calibration curve obtained.

6.4.1.7 Stability

Normally, bio-oil stability is expressed as a change in viscosity after storage at a specific temperature for a specific time, e.g. at room temperature for 6 months. Nevertheless, in the current project it is not possible to measure the bio-oil viscosity due to the limited sample quantity obtained. Recently Oasmaa and Kuoppala [5] found that the bio-oil viscosity had a linear relationship with its average molecular weight. Therefore, a change in the average molecular weight over time was determined and the stability was calculated according to the equation below.

$$Stability = \frac{MW_{stored} - MW_{fresh}}{Storage\ days} \quad (g/mol \cdot day)$$

Equation 6-3

The MW_{stored} and MW_{fresh} are the average molecular weights of bio-oils after storing at room temperature for approximately 6 months and after a few hours of production, respectively. In the case of non-catalytic bio-oils, the MW_{stored} represents the average molecular weight after accelerated ageing test by storing bio-oils at 80°C for 24 hours.

6.4.1.8 Gas chromatography/mass spectrometry (GC/MS) analysis

In order to identify compounds present in the bio-oil, GC/MS liquid injection method was applied. In the case of non-catalytic pyrolysis experiments, liquid samples analysed were Pot 1 oil, Pot 2+3 oil and a mixture of condenser and ESP washing liquids, which is named "CondEP". It was found that different fractions contained different compounds. Therefore, in order to compare the bio-oils from different runs, especially the bio-oils obtained from catalytic pyrolysis, a representative liquid fraction is required. Consequently, a mixture of all liquid fractions (Liq) was tested and used for comparison between different pyrolysis runs. Since the samples were mixtures of organic compounds, water, char fines and ethanol solvent with different properties, each sample was further diluted in order to obtain a constant organics content (17.5 wt%) in the mixture. The samples were also filtered through a Millipore Millex-GN nylon filter with 0.2 μm pore size prior to the injection.

The gas chromatography/mass spectrometry (GC/MS) analysis of bio-oil representative liquid samples (Liq) was conducted using a PerkinElmer AutoSystem XL Gas Chromatograph. The separation was made on a 60 m × 0.25 mm id DB-1701 column with 0.25 μm film thickness. Its phase composition was 14%-cyanopropyl-phenyl-86%-dimethylpolysiloxane. In addition, a fused silica capillary column (5 m × 0.25 mm) was used as a guard column and placed before the main column. The GC oven temperature was held at 45°C for 4 min and then programmed to 240°C at 4°C/min. The oven was maintained at this final temperature for 20 min. The injector

temperature was 280°C with a split ratio of 1:25. Helium was the carrier gas with a velocity of 38 cm/s. At the end of the column, a PerkinElmer Turbomass Gold Mass Spectrometer with electron impact (EI) mode was connected and functioned as a detector. The mass spectrometer was operated at 280°C with ionisation energy of 70 eV. The mass range from *m/z* 35 to 600 was scanned with a speed of 1.0 s/decade. Data acquisition and processing was performed using PerkinElmer Turbomass 5.0 software. Identification of the compounds was achieved by comparing the mass spectrum (*m/z* distribution) with NIST mass spectral database and literature data [93, 116, 121-130].

6.4.2 Char

6.4.2.1 Elemental analysis

The elemental analysis of char samples was performed in order to determine the carbon, hydrogen, nitrogen and sulphur contents. Only one char sample, which was used as a catalyst in a micro-scale reactor (Table 5-1) was analysed. The technique applied is the same as described in section 6.4.1.4.

6.4.2.2 Ash content and composition

The ash content of the char sample was measured as the mass percent of residue after burning to constant weight at 575°C according to ASTM E1755-01 standard method. The ash obtained was then subjected to metals analysis for determination of potassium (K), calcium (Ca), phosphorous (P), sodium (Na) and copper (Cu) contents, using Varian Vista MPX ICP-OES (inductively coupled plasma-optical emission spectrometer) system. In addition, the chlorine (Cl) content of the ash was measured by Schöniger flask combustion followed by either titration or ion-chromatography. All of the ash composition analyses were performed by MEDAC Ltd., Surrey, UK

6.4.2.3 Heating value

Based on the data obtained from the elemental analysis and the ash content of the char sample, its heating value was calculated using Equation 6-1 as mentioned in section 6.4.1.5. The heating value was used for calculation of the energy distribution in section 8.3.3.

6.4.3 Non-condensable gases

During a pyrolysis run, the non-condensable gases were sampled every three minutes into a CP-4900 micro gas chromatograph with a thermal conductivity detector (TCD) from Varian Chromatography System Inc, The Netherlands. The instrument was equipped with a molecular-sieve coated capillary column (CP-Molsieve 5A) for separation of hydrogen (H_2), oxygen (O_2), nitrogen (N_2), methane (CH_4) and carbon monoxide (CO) and a CP-PoraPLOT column for elution of nitrogen (N_2), methane (CH_4), carbon dioxide (CO_2), ethylene (C_2H_4), ethane (C_2H_6), propylene (C_3H_6) and propane (C_3H_8). In addition, helium (He) was used as the carrier gas. For quantitative analysis, the columns were calibrated with known-composition standard gas mixtures. The software used for the analysis was Star Chromatography Workstation 6.0.

7 NON-CATALYTIC FAST PYROLYSIS RESULTS AND DISCUSSION

7.1 INTRODUCTION

Fast pyrolysis experiments of two selected biomass feedstocks, namely cassava stalk (CS) and cassava rhizome (CR), were conducted using the bench-scale continuous fluidised-bed reactor. The overall objective of these experiments was to investigate the yields and properties of pyrolysis products produced from both feedstocks as well as to identify the optimum pyrolysis temperature for obtaining the highest organic liquid yields. The optimum temperature of a chosen biomass feedstock will be adopted for the study of catalytic pyrolysis. A total of eight experimental runs were performed with the two feedstocks and at four different temperatures ranging from ~440°C to ~540°C. The results of mass balance analysis and the properties of the pyrolysis products from selected runs are discussed below.

7.2 MASS BALANCES

Table 7-1 summarises the mass balances of all the non-catalytic experiments. As can be seen from the table that the mass balance closures are above 95%, which is within the acceptable level. The 5% loss is thought to be mainly due to the unidentified and undetectable permanent gases. This was observed from the presence of certain extra peaks, which could not be identified in the gas chromatograms. Since the amounts of loss are in a small range of 3-5%, there is therefore no need for data normalisation.

There were two main intended variables among the eight pyrolysis runs, namely the feedstocks and the pyrolysis temperatures, although the vapour residence time and the biomass feed rate also vary slightly owing to uncontrollable or fluctuation situations. It can be seen from Table 7-1 that the rhizome gave higher liquid yields with lower char and gas yields than the stalk for all reaction temperatures studied. This effect can be linked to the lower ash content of the rhizome samples as it is known that during

Table 7-1 Summary of mass balances for non-catalytic pyrolysis experiments

	Unit								
Test name		**AP14**	**AP12**	**AP10**	**AP13**	**AP15**	**AP17**	**AP11**	**AP16**
Feedstock		**Cassava stalk**				**Cassava Rhizome**			
particle size	*μm*	**355-500**	**355-500**	**355-500**	**355-500**	**355-500**	**355-500**	**355-500**	**355-500**
Moisture content	*wt%*	**7.40%**	**7.40%**	**7.40%**	**7.40%**	**8.25%**	**8.18%**	**8.25%**	**8.18%**
Ash content	*wt%, dry basis*	**5.22%**	**5.22%**	**5.22%**	**5.22%**	**4.74%**	**4.13%**	**4.74%**	**4.13%**
Pyrolysis temperature	*°C*	**436.61**	**475.00**	**502.00**	**526.32**	**442.64**	**477.38**	**509.57**	**536.57**
Vapour residence time	*seconds*	**0.79**	**0.75**	**0.73**	**0.52**	**0.86**	**0.74**	**0.72**	**0.68**
Feed rate	*g/h, dry basis*	**97.54**	**89.03**	**88.10**	**83.14**	**117.65**	**140.80**	**108.90**	**118.16**
Product yields	*wt%, dry basis*								
Char		**23.44%**	**20.91%**	**20.70%**	**20.96%**	**21.96%**	**19.97%**	**19.57%**	**18.54%**
Liquids		**61.14%**	**61.71%**	**58.81%**	**59.38%**	**63.33%**	**64.93%**	**64.91%**	**62.51%**
Organics		45.31%	45.96%	45.87%	44.80%	47.30%	49.76%	49.78%	48.05%
Reaction water		15.84%	15.76%	12.94%	14.58%	16.03%	15.17%	15.13%	14.46%
Gas		**10.64%**	**14.29%**	**15.70%**	**15.94%**	**10.03%**	**10.10%**	**11.04%**	**13.95%**
H_2		0.02%	0.10%	0.05%	0.07%	0.02%	0.06%	0.04%	0.11%
CH_4		0.22%	0.39%	0.58%	0.62%	0.30%	0.32%	0.45%	0.61%
CO		2.82%	3.99%	4.84%	4.91%	2.04%	2.72%	3.37%	4.73%
CO_2		7.43%	9.57%	9.92%	9.98%	7.48%	6.80%	6.92%	8.10%
C_2H_4		0.03%	0.06%	0.09%	0.12%	0.04%	0.05%	0.09%	0.16%
C_2H_6		0.06%	0.09%	0.11%	0.10%	0.07%	0.07%	0.08%	0.10%
C_3H_6		0.03%	0.06%	0.09%	0.10%	0.04%	0.05%	0.07%	0.12%
C_3H_8		0.02%	0.03%	0.03%	0.03%	0.03%	0.02%	0.02%	0.03%
Closure	*wt%, dry basis*	**95.22%**	**96.91%**	**95.22%**	**96.28%**	**95.32%**	**95.00%**	**95.52%**	**95.00%**

pyrolysis the inorganic compounds present in biomass in the form of ash can catalyse biomass decomposition and char-forming reactions, resulting in the reduction of liquid yields and the formation of char and non-condensable gases [25, 40, 42-45].

In fast pyrolysis of biomass, liquid bio-oil is generally regarded as the main product, while solid char and permanent gases are valuable by-products. Typically, bio-oils derived from wood contain 15-30 wt% of water [4]. This water is derived from the moisture in the biomass feedstock and the water produced during pyrolysis reaction, which is called "reaction water". In Table 7-1, only the reaction water is reported and the non-water part of bio-oil is then referred to as "organics", which is the desirable product. It is obvious from the table that CR gave about 2-4% higher organics than CS for all pyrolysis temperatures, whereas the reaction water yields for both feedstocks are not significantly different.

When considering the effect of pyrolysis temperature on product yields, it can be observed for both feedstocks that increasing temperature led to lower char yields and higher gas yields. This result is in agreement with previous studies [40, 51, 110, 136-141], in spite of the different biomass types and pyrolysis reactor systems applied. The reduction of char yields with increasing temperature could be due to greater primary decomposition of the biomass at higher temperature and/or secondary thermal decomposition of the char formed before being entrained out of the reaction zone. The increase of gas yields with increasing temperature is possibly due to a combination of secondary thermal cracking of the evolved pyrolysis vapours and the char secondary decomposition.

With regards to the yields of organics, increasing temperature appeared to slightly increase the yields until reaching a maximum then the further increase led to decreasing the yields. For cassava stalk and rhizome, the temperatures that gave highest organics yields were 475°C and 510°C, respectively. However, the difference of the yields was rather small in the temperature ranges of 475-502°C and 477-510°C for CS and CR, respectively. Therefore, the optimum pyrolysis temperature suggested in order to obtain the highest organics yields from the agricultural residues is 490±15°C. In addition, the reaction water yields were found to marginally decrease

with increasing temperature, indicating that the dehydration reactions taking place during fast pyrolysis were enhanced at lower temperature.

According to Table 7-1, the gaseous products contain mainly of carbon dioxide and carbon monoxide with small quantities of hydrogen and C_1-C_3 hydrocarbon gases. Most of the gases identified except hydrogen and propane increased in their mass yields with increasing temperature. Moreover, Figure 7-1 and Figure 7-2 present the gas composition in volume %. It can be noticed from the graphs that increasing pyrolysis temperature led to a decrease in CO_2 proportion and an increase in CO proportion for both feedstocks. This is mainly because most of the CO_2 was already generated by carboxyl release at a relatively low temperature [141]. In addition, the secondary thermal cracking of pyrolysis vapours produced CO and hydrocarbon gases rather than CO_2 [49]. Hydrogen mass yields and proportions as noticed from Table 7-1, Figure 7-1 and Figure 7-2 appeared to fluctuate within the temperature range studied. This is owing to the limitation of the GC instrument when experiencing low H2 concentrations in the product gas.

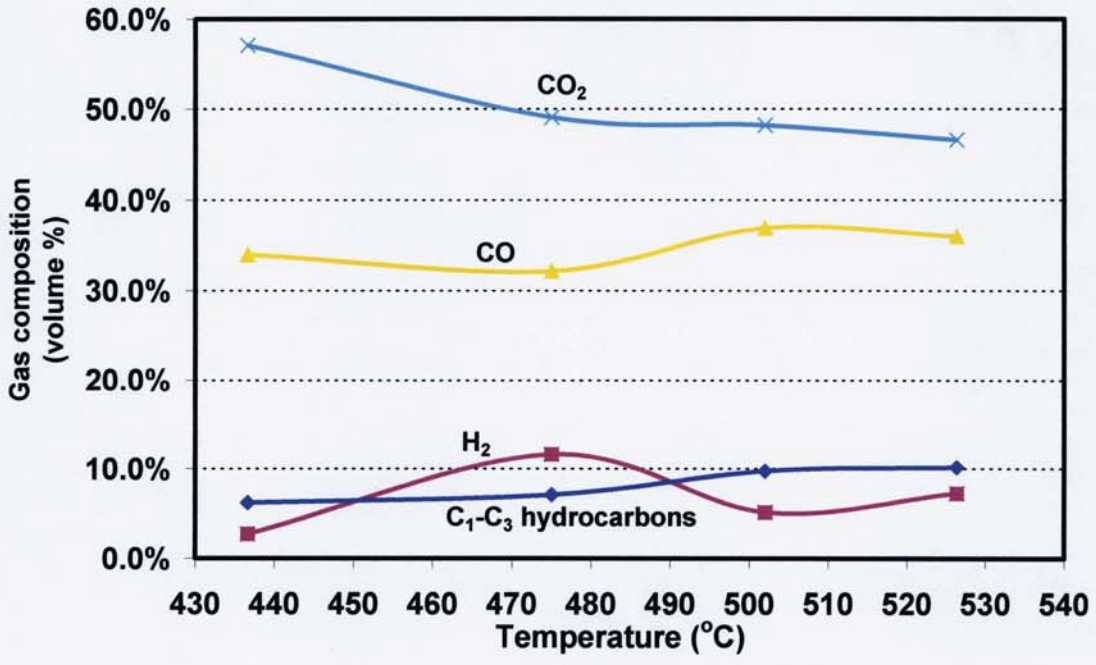

Figure 7-1 Composition of gaseous products obtained from fast pyrolysis of cassava stalk

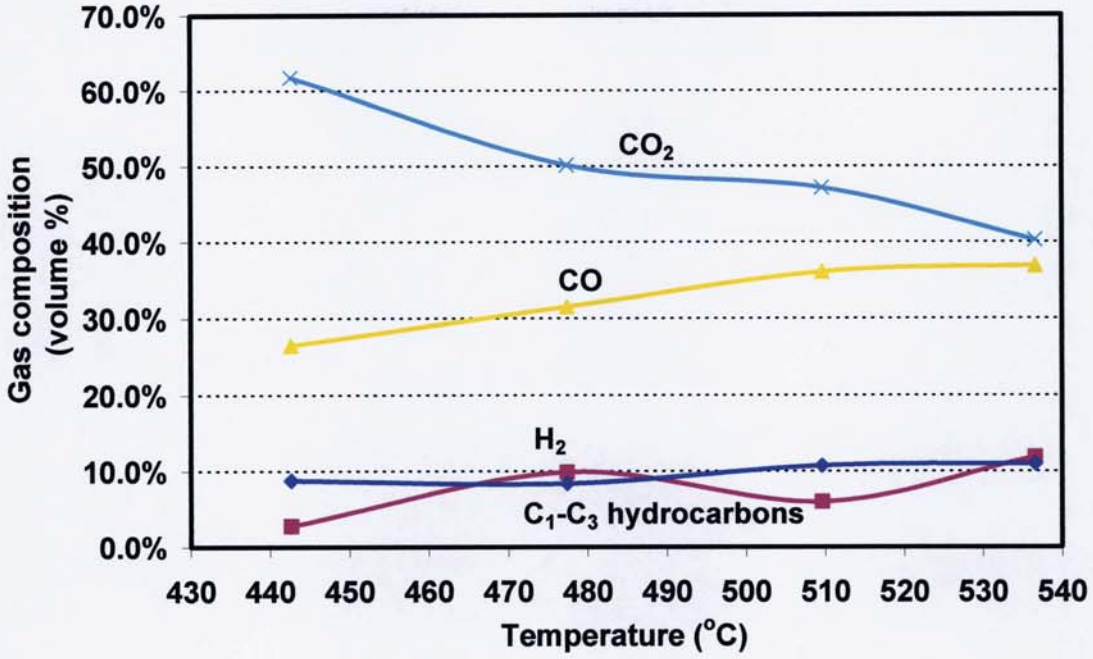

Figure 7-2 Composition of gaseous products obtained from fast pyrolysis of cassava rhizome

7.3 CHARACTERISATION OF BIO-OILS

Various properties of bio-oils produced from fast pyrolysis of cassava stalk and rhizome using the bench-scale (150 g/h) fluidised-bed reactor unit have been investigated and compared with literature data for bio-oils produced from wood and rice straw. These two feedstocks were selected as the former is a typical feedstock for bio-oil production from biomass fast pyrolysis, whereas the latter is a typical agricultural residue. The properties studied include water and solids contents, pH value, basic elemental composition, heating value, molecular weight distribution, stability and chemical composition by GC/MS analysis. Understanding the basic properties of bio-oils would be beneficial for identifying their appropriate applications and for upgrading them. It is important to emphasise that the bio-oils produced in this work were initially in five fractions as already mentioned in section 6.3 and 6.4.1.4. Therefore, the proportionate mixtures of all liquid fractions called "Liq" were used as representative bio-oil samples. It is also imperative to be aware that the mixtures were dissolved in a solvent, which was absolute ethanol, at a concentration of approximately 20 wt% organics. Consequently, properties such as water content, solids content, elemental composition and heating value have been calculated after

each analysis and reported on solvent-free basis. In the following subsections, all of the aforementioned properties of bio-oils produced from different feedstocks are reported and discussed.

7.3.1 Water content

In section 7.2, the yields of reaction water on dry biomass fed basis were discussed. Certainly the higher the reaction water yields, the higher the water content in the bio-oils. Water in bio-oils also comes from original moisture in the biomass feedstock. Water content of bio-oils is one of the factors affecting their quality and use. The presence of water in bio-oils can be disadvantageous and advantageous. It reduces the heating value, especially the LHV and flame temperature [4]. On the other hand, it improves bio-oil flow characteristics by reducing the viscosity. The water also leads to a more uniform temperature profile in the cylinder of a diesel engine as well as to lower NO_x emissions [4].

The water contents of bio-oils produced from cassava stalk and rhizome samples at different pyrolysis temperatures are summarised in Table 7-2. Also included in the table are water contents of wood and rice straw bio-oils. It can be seen from the table that the temperature had a small influence on bio-oils water contents. Yet, they seemed to be higher at lower temperature. This is in agreement with a study by Lee et al [40] where fast pyrolysis of rice straw at different temperatures was investigated. The water contents of CS and CR bio-oils were in the range of 31-33 wt%, which is marginally higher than those of typical wood bio-oils. When compared with a selected agricultural residue (rice straw), the water contents of CS and CR bio-oils appeared to be in the middle of the range 25-45 wt%. Nevertheless, the water contents of 31-33 wt% can be considered as high and may need to be reduced prior to use. One possible way to do this is the utilisation of a dehydrating agent such as 3A molecular sieve. This type of molecular sieve is mainly used to remove moisture in liquid or gaseous materials. Generally, this molecular sieve is used for the drying of highly polar compounds like methanol and ethanol. It has previously been used to remove water in the bio-oils after ethanol addition in order to enhance the esterification reaction [54, 142]. The use of this molecular sieve is technically possible, but may not be

economically feasible as it requires extra processes such as mixing and separation of the molecular sieve as well as the regeneration step that undoubtedly needs energy input to evaporate the adsorbed water.

Table 7-2 Water and solids contents of bio-oils produced from different feedstocks

Feedstock	Test name	Pyrolysis temperature, °C	Water content (wt %)	Solids content (wt%)
Cassava stalk	AP14	437	33.03	4.16
	AP12	475	33.04	3.01
	AP10	502	30.87	1.48
	AP13	526	31.62	5.60
Cassava rhizome	AP15	443	33.39	3.52
	AP17	477	31.60	3.13
	AP11	510	31.33	4.03
	AP16	537	31.43	3.98
Wood	Ref [4]	N/A	15-30	0.2-1
Rice straw	Ref [40]	412-598	25-45	0.1-3

A more promising route to lowering the amount of water in bio-oils has been proposed by Oasmaa et al [58]. The method was primarily developed for improving the storage stability of bio-oils without significantly decreasing their flash point. The technique includes the removal of water together with light reactive volatiles by increasing the condenser temperature to 50±4°C followed by the addition of alcohol to improve the viscosity and stability of the bio-oils. It was found that the water content of bio-oils from forestry residue feedstock could be decreased from 15-30 wt% to 4-5 wt% [58]. In fact, by using this method the water and low boiling point organic compounds were shifted from the primary bio-oil collection container to another one, just like the Oil Pot 2 and Pot 3 in this project. It is important to note that the water contents of CS and CR bio-oils displayed in Table 7-2 are the calculated values of all liquid fractions obtained. Since it was not possible to control the temperature and flow rate of the cooling water in the water condenser, the proportions of water in the primary liquid collector Oil Pot 1 varied among different pyrolysis runs. Therefore, to obtain the values of water contents that can be reasonably used to compare among different runs with different feedstocks and different pyrolysis conditions, the only calculated values of all fractions are reliable and have been used. However, in commercial-scale pyrolysis plants where temperature control of the

condenser is possible, the water collected by the Oil Pot 2 and Oil Pot 3 could be excluded from the main bio-oil product, which would result in the water contents of 18.29% and 17.61% for CS (AP12) and CR (AP17) bio-oils, respectively. Because the Pot 2+3 oils contain mostly water (~72 wt% water content) and very low organic liquid, when excluding these fractions from the main bio-oil fraction, the decrease of the organics yield would be only 0.5 wt%, which is negligible.

7.3.2 Solids content

Another component of bio-oil known to affect its properties is suspended solid particles. The solids present in bio-oil can cause erosion and blockages to equipment such as nozzles, valves and pumps, if bio-oil is to be utilised for generation of heat and power via boilers, engines or gas turbines [31]. Additionally, the inorganic compounds present in the solids are important to bio-oils ageing characteristics as they appear to catalyse polymerisation reactions during storage, leading to viscosity increases and growth in the apparent diameter of the suspended char [3]. Accordingly, bio-oil with lower solids content is generally preferred.

The solids contents of CS and CR bio-oils produced with different pyrolysis temperatures along with those of wood and rice straw oils from literature data are presented in Table 7-2. It can be seen that there is no relationship of the solids contents of CS and CR oils with pyrolysis temperature. They actually fluctuated in the range of 1.5-5.6 wt%. When compared with wood and rice straw feedstock, the agricultural residues from cassava plants gave rather high solids contents. One explanation for this is that the solids contents measured in this work included those of the sticky liquid on the wall surface of the water condenser and ESP after vigorous washing with ethanol solvent in order to get all organic fractions. It was also observed at the entrance of the water condenser that there was a significant amount of solid deposited. This solid did not look like normal char particles, but rather looked like sticky solid gum. If considering only the solids in Pot 1 oils, results showed that the solids contents were between 0.3 and 1.0 wt%, which is in the similar range of those of wood bio-oils.

Solids in bio-oils are composed of char fines entrained out of the cyclone and the secondary char formed by secondary reactions of pyrolysis vapours such as repolymerisation and recondensation. The reason why the char fines can escape the cyclone is because of their very small particles (less than about 10 μm in diameter) and the gas stream velocity in the cyclone is not high enough to separate these small solid particles. The problem cannot be efficiently solved by increasing the carrier gas velocity as doing this would require more energy to heat up the gas and would be more difficult to condense the pyrolysis vapours. Once the solids are in bio-oils, it is difficult to remove by liquid filtration because of the highly viscous nature of bio-oils. Nevertheless, by introducing a hot vapour filter prior to condensation units, the amounts of solids in bio-oils would be substantially reduced.

The solids content of bio-oil may not be an important issue, if the end product is a mixture of bio-oil and solid char in the form of slurry. This slurry which contains about 90% of energy from biomass could be used as a feedstock for gasification process to produce syngas or producer gas. In addition, the slurry is commercially known as BioOil Plus^{TM} from Dynamotive Energy Systems Corporation, which can be used as fuel in boilers.

7.3.3 Elemental composition, heating value and pH

The basic elemental compositions of selected CS and CR bio-oils are listed in Table 7-3 in comparison with literature data of different bio-oils. The percentages of carbon, hydrogen and oxygen of CR oils were similar to those of wood bio-oil, whereas CS bio-oils appeared to have lower carbon and hydrogen contents and higher oxygen content than CR bio-oils. With regards to nitrogen contents, both bio-oils produced from CS and CR had higher proportion than typical wood bio-oil. The higher nitrogen content in the CS and CR bio-oils may be due to the higher quantity of protein in the original biomass feedstock. The presence of nitrogen compounds can be a drawback when burning bio-oils because of the high potential for NO_x emissions. This problem may be prevented by pre-treatment of biomass prior to pyrolysis. The pre-treatment can be either washing with distilled water or with dilute acid solution. It was found by Lee et al [40] that nitrogen content of rice straw decreased from 1.60 wt% to 0.01

wt% after washing with distilled water. The pre-treatment also removed some alkali metals such as sodium and potassium that are known to have catalytic effect during pyrolysis.

Table 7-3 Elemental composition, heating value and pH of bio-oils produced from different feedstocks

Feedstock	**Cassava rhizome**	**Cassava stalk**	**Wood**	**Rice straw**
Test name/Reference	AP17	AP12	[4]	[40]
Elemental composition (wt%, dry basis)				
Carbon	53.09	51.54	54-58	-
Hydrogen	7.27	4.62	5.5-7.0	-
Nitrogen	0.81	0.69	0-0.2	-
Oxygen (by difference)	38.59	43.05	35-40	-
Ash	0.23	0.11	0-0.2	0.10
Heating value (MJ/kg)				
HHV, wet basis	15.80	12.70	16-19	17.3
HHV, dry basis	23.10	18.97	23 [41]	-
LHV, wet basis	13.94	11.22	-	-
LHV, dry basis	21.51	17.96	-	-
pH				
Pot 1 oil	3.26	3.04	2.5	4.2
Pot 2+3 oil	2.53	2.73	-	-

When comparing the elemental compositions of liquid bio-oils derived from cassava stalk and rhizome with their original biomass compositions (see chapter 4), it is evident that they are very similar. On elemental composition basis, the bio-oils differ significantly from petroleum oils, which contain mainly of hydrogen and carbon with very small quantity of oxygen. The oxygen in bio-oils exists in a variety of functional groups such as hydroxyl, carboxyl, carbonyl and oxy groups (see section 7.3.5 for details). It is the presence of oxygen that is responsible for certain unfavourable properties of bio-oils such as low heating value and instability. Therefore, bio-oils should be upgraded by catalytic deoxygenation in order to improve their heating values and stability.

The heating values of CS and CR bio-oils are shown in Table 7-3. It was found that the heating value of CR bio-oil was higher than that of CS oil. This is not surprising

as the oxygen content of CR pyrolysis liquid is lower than that of CS oil. This finding is consistent with the results obtained in chapter 4 where the heating value of CR biomass was discovered to be higher than that of CS biomass. In comparison with wood and rice straw bio-oils, CS and CR bio-oils had lower HHV (wet basis). This is due to the higher oxygen and water contents of CS and CR oils. Nevertheless, on dry basis the HHV of CR bio-oil was found to be comparable to that of wood, suggesting that the main difference is derived from the water content. According to the bio-oils heating values and their yields, the energy recovered in the form of liquid CS and CR bio-oils was calculated to be approximately 60% of the biomass energy input.

The pH values of fractions of pyrolysis liquids derived from cassava stalk and rhizome are displayed in Table 7-3. It was found that the Pot 2+3 oils were more acidic than the Pot 1 oils. Since the CR Pot 1 oil had higher pH than the CS Pot 1 oil and the CR Pot 2+3 oil had lower pH than the CS Pot 2+3 oil, it was not possible to come to a conclusion that which bio-oil is more acidic according to the available data. Nonetheless, it is logical to conclude that both CS and CR oils having pH around 2-3 were acidic. This is actually typical of fast pyrolysis liquids as can be seen that the pH values of wood and rice straw bio-oils are 2.5 and 4.2, respectively. The low pH values of bio-oils are caused by the presence of carboxylic compounds such as formic and acetic acids in large proportion. The pH value is one of the important bio-oils properties as it is an indicator of their corrosiveness. The acidic properties of bio-oils can cause corrosion of vessels and pipework. A solution suggested by Bridgwater et al [143] when dealing with the corrosive bio-oil is to carefully select appropriate materials. Examples of acceptable materials are stainless steel and some olefin polymers.

7.3.4 Molecular weight distribution and stability

The molecular weight distribution of samples was determined by the gel permeation chromatography (GPC) technique as described in section 6.4.1.6. In order to test the reproducibility of the GPC results, a selected Pot 1 oil sample was analysed three times and the distribution curves are illustrated by Figure 7-3. It is obvious from the

graphs that they are nearly identical with the average molecular weight (Mw) in the range of 348-352 g/mol.

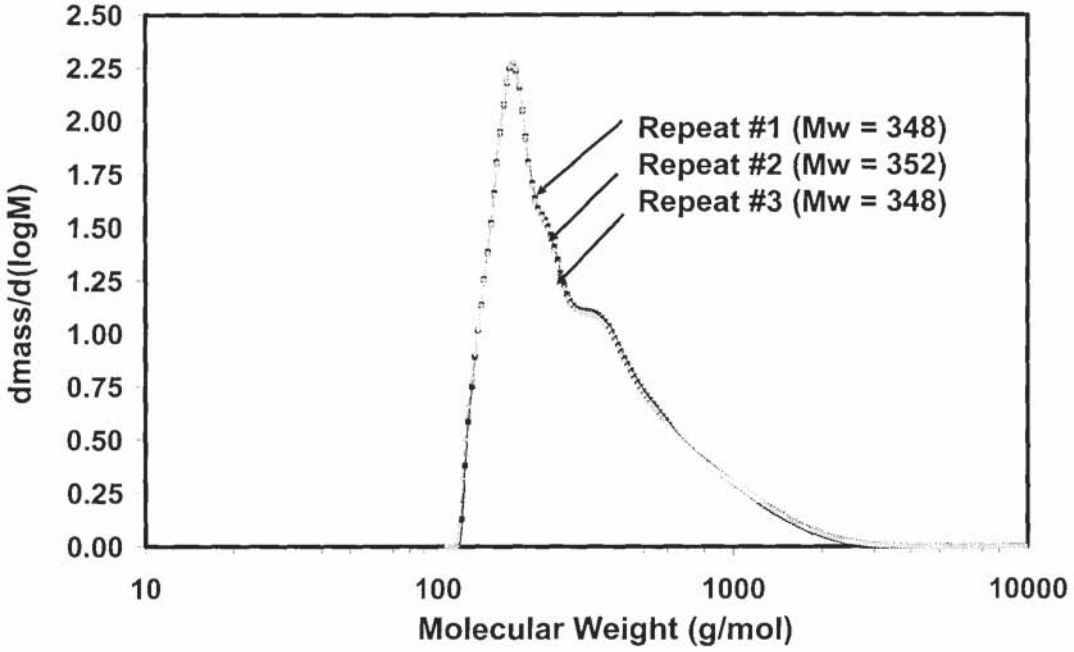

Figure 7-3 Reproducibility of GPC analysis

The different fractions of bio-oils derived from fast pyrolysis of cassava stalk and rhizome were analysed for their molecular weight distributions. The results for the weight average molecular weight (Mw), number average molecular weight (Mn), molecular weight at highest peak (Mp) and polydisperisty (PD) are summarised in Table 7-4. It is apparent from the table that the fresh pyrolysis liquid fractions derived from cassava rhizome had higher average molecular weights than the CS liquids. When combining these results with the water and solids contents of AP12 and AP17 bio-oils (Table 7-2), it is predicted that the CR bio-oil would have higher initial viscosity than the CS bio-oil as the former had higher molecular weight, lower water content and slightly higher solids content. The average molecular weights (Mw and Mn) of Pot 1 oils appeared to be higher than those of CondEP fractions (a proportionate mixture of washing liquids from the condenser and ESP) for both feedstocks. This is somewhat surprising as it was expected that the sticky liquids on the walls of condenser and electrostatic precipitator that were washed out by ethanol would have higher molecular weight than the Pot 1 oils. There are two possible explanations of the unexpected results. Firstly, the organic liquids left in water

condenser and ESP walls were mixed immediately with ethanol after the production and it is known that the addition of alcohol to bio-oils can slow down their ageing process [32] together with the fact that all liquid fractions were subjected to GPC analysis after about 4-5 hours of production. Consequently, the Mw increase during the 4-5 hours of the CondEP liquids was significantly lower than those of the Pot 1 oils, thus leading to the low average molecular weights. This explanation is based on an assumption that the difference between the molecular weights of the freshly produced CondEP liquids and Pot 1 oils is smaller than the molecular weight changes within 4-5 hours after production. Another possible explanation is that the Pot 1 oils contained larger proportion of heavy compounds that were in the form of aerosols than the mixture of liquids from the water condenser and the ESP. It was observed after starting pyrolysis runs for about 20-25 minutes that part of the liquid condensed by the water condenser could not flow down to the Oil Pot 1 due to the partial blockage by solid deposition. As a consequence, only the aerosols could pass through the small gap to the ESP, while leaving the condensed liquid of lower molecular weight remained in the condenser.

Table 7-4 Average molecular weight of pyrolysis liquid fractions produced from fast pyrolysis of cassava stalk and rhizome

Test name		**AP12**		**AP17**	
Feedstock		**Cassava stalk**		**Cassava rhizome**	
Molecular weight[a] (g/mol)		*Pot 1 oil*	*CondEP[b]*	*Pot 1 oil*	*CondEP[b]*
Fresh[c]	Mw	369	354	387	372
	Mn	247	248	260	251
	Mp	172	215	168	204
	PD	1.49	1.42	1.49	1.48
Aged[d]	Mw	778	ND	623	ND
	Mn	347		324	
	Mp	172		168	
	PD	2.24		1.92	
Stability (g/mol-day)		1.12	N/A	0.65	N/A

[a]Mw, Mn, Mp and PD refer to weight average molecular weight, number average molecular weight, molecular weight at highest peak and polydispersity, respectively.
[b]CondEP represents a proportionate mixture of ethanol washing liquid from the water condenser and electrostatic precipitator.
[c]Fresh samples were measured 4-5 hours after production.
[d]Aged samples were bio-oils stored at accelerated ageing conditions (at 80°C for 24 hours)

Because each fraction of pyrolysis liquid exhibited different molecular weight distributions, a proportionate mixture of all fractions (Liq) obtained from the AP17 test was then analysed in order to obtain a global average molecular weight. The result is compared with Pot 1 oil and CondEP in Figure 7-4. It can be seen that the molecular weight distribution curve of the Liq sample lies between those of Pot 1 oil and CondEP. Accordingly, the Mw of the Liq sample (385 g/mol) is in between those of Pot 1 oil (387 g/mol) and CondEP (372 g/mol). In order to compare the Mw of bio-oils from different runs, mixtures of all liquid fractions should be analysed. Since this was not realised during the analysis of AP12 samples, the data for AP12 Liq was then not available. Nonetheless, it is fortunate that both fresh Pot 1 oil and CondEP fractions from AP12 and AP17 runs showed the Mw and Mn in the same direction, thus making it possible to conclude that the initial molecular weight of the CR bio-oil was higher than that of the CS bio-oil.

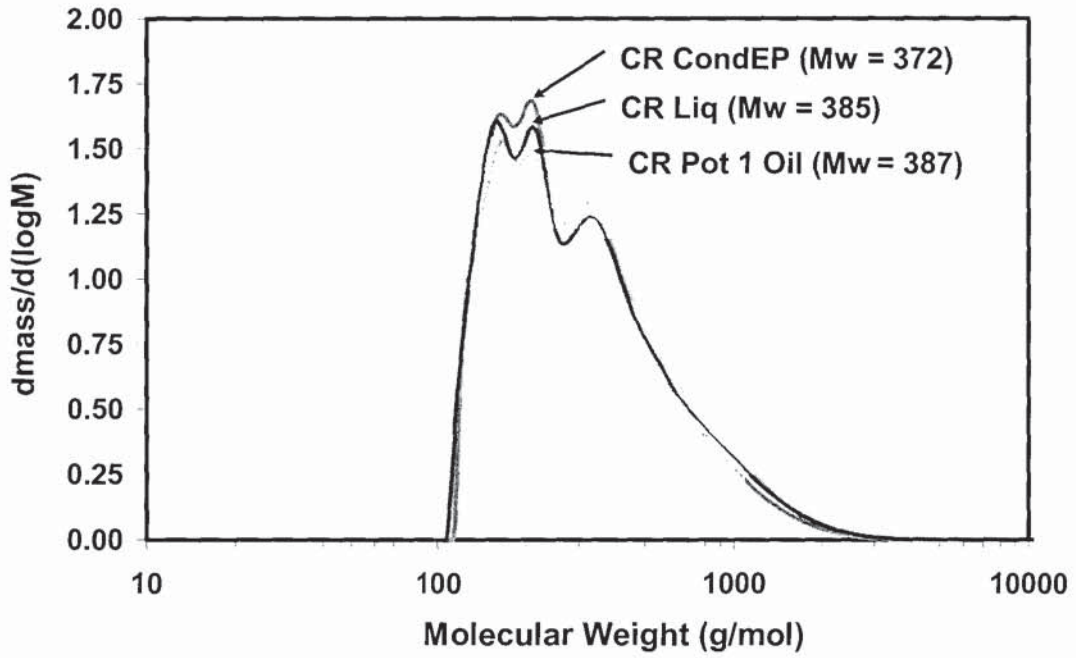

Figure 7-4 Molecular weight distributions of different pyrolysis liquid fractions derived from fast pyrolysis of cassava rhizome

As the Liq samples consisted of approximately 80 wt% of ethanol, the effect of ethanol addition on molecular weight distribution was then investigated. A randomly selected Pot 1 oil sample together with its mixture with 80 wt% of ethanol were analysed and the result is illustrated by Figure 7-5. It was found that immediately after mixing bio-oil with ethanol the average molecular weight was slightly increased. It is

believed that some reactions occurred within the mixture, causing the molecular weight increase. These reactions would be beneficial in a longer term for slowing down the bio-oil ageing process as it was shown by previous studies [3, 32, 54, 57, 58] that adding a small amount of alcohol (5-10%) could improve the bio-oil stability significantly.

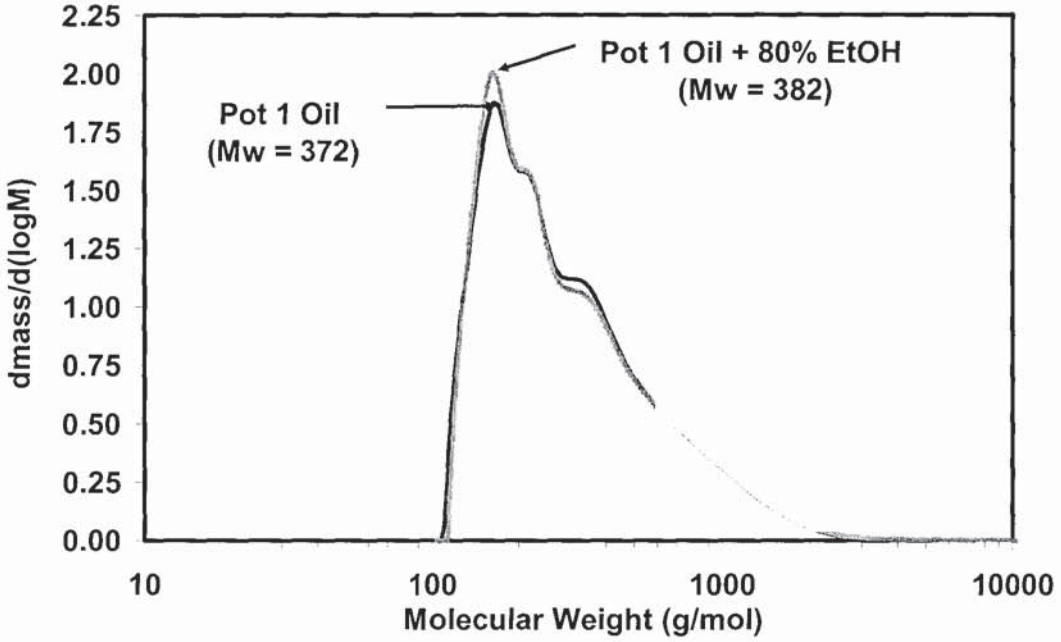

Figure 7-5 The effect of 80% ethanol addition on molecular weight of Pot 1 oil derived from cassava rhizome

Another parameter obtained from the GPC analysis and used for determining the molecular homogeneity of a liquid sample is referred to as polydispersity (PD). It is calculated as the ratio of weight average molecular weight to number average molecular weight (Mw/Mn). The PD is always equal to or more than 1. The high value of PD means the low molecular homogeneity. The PD values of CS and CR liquid fractions are presented in Table 7-4. It is evident that the polydispersity indices of all fresh liquids were similar and in the range of 1.42-1.49. Hence, the initial molecular homogeneity of bio-oils produced from the stalk and the rhizome is more or less the same.

In order to assess the stability of CS and CR bio-oils, two liquid samples, namely AP12 (CS) and AP17 (CR) Pot 1 oils, were subjected to accelerated ageing test at 80°C for 24 hours, which is roughly equivalent to storage at room temperature for 1 year [5]. The samples after ageing were then analysed for their molecular weight

distributions. The results in comparison with those of the fresh liquid samples are depicted by Figure 7-6, whereas their average molecular weights (Mw, Mn, Mp) and polydispersity indices are presented in Table 7-4. It can be seen that the average molecular weights (Mw and Mn) increased considerably after ageing for both bio-oil samples, while the molecular weights at highest peak (Mp) were exactly the same as before ageing. The Mw were increased from 369 to 778 g/mol for CS Pot 1 oil and from 387 to 623 g/mol for CR Pot 1 oil, whereas the Mn were increased from 247 to 347 g/mol for CS Pot 1 oil and from 260 to 324 g/mol for CR Pot 1 oil. The increases in the Mw and Mn of CS Pot 1 oil appeared to be greater than those of CR Pot 1 oil. In addition, the polydispersity indices were raised from 1.49 to 2.24 and from 1.49 to 1.92 for CS and CR Pot 1 oils, respectively. This means that after 1 year of storage the CS oil would have less molecular homogeneity than the CR oil. According to Figure 7-6, it can be observed that after ageing the portions of compounds with Mw lower than ~400 g/mol were reduced simultaneously with the increases in the portions of compounds having Mw higher than ~400 g/mol.

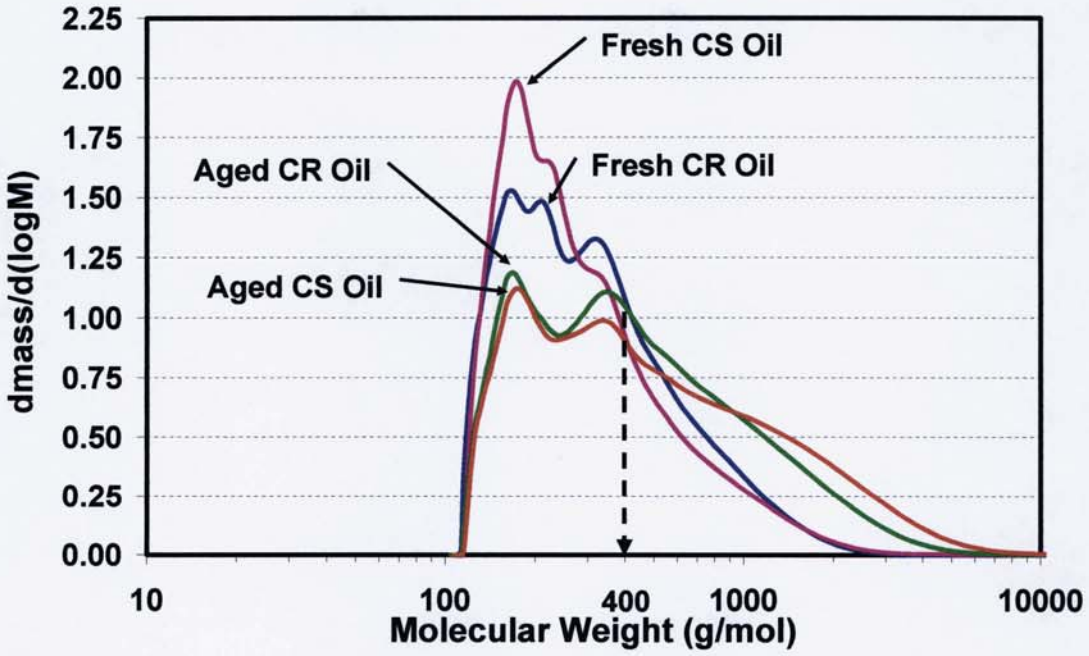

Figure 7-6 Molecular weight distribution of fresh and aged bio-oils derived from cassava stalk (CS) and cassava rhizome (CR) (Pot 1 oils from AP12 and AP17)

Based on the Mw data of the fresh and aged bio-oils produced from both feedstocks, stability indices were calculated and the results are shown in Table 7-4. It is clear that the CR oil was more stable that the CS oil. Although the initial molecular weight of

the CR oil was higher than that of the CS oil, after ageing the molecular weight of the CR oil was much lower than that of the CS oil.

To investigate the effect of pyrolysis temperature on the average molecular weight of bio-oil, Pot 1 oil and CondEP samples produced from pyrolysis of a selected feedstock, cassava rhizome, at different temperatures were subjected to GPC analysis. The resultant weight average molecular weights (Mw) were plotted against pyrolysis temperature as shown by Figure 7-7. It was found that as pyrolysis temperature was increased, the Mw of both fractions tended to increase. It is therefore logical to conclude that fast pyrolysis of cassava rhizome has a high tendency to give liquid products with higher Mw at higher pyrolysis temperature. There are three possible explanations for this phenomenon. First, part of the biomass components that is more difficult to degrade at low temperature such as lignin could be given off at higher temperature, which can contribute to the higher molecular weight compounds. Second, the high pyrolysis temperature led to the increase in the production of highly reactive radicals/compounds that could be involved in the polymerisation reactions upon condensation, resulting in the formation of high molecular weight compounds. Third, when increasing pyrolysis temperature from 443°C to 537°C, the vapour residence time was reduced from 0.86 to 0.68 seconds (see Table 7-1). Consequently, at higher temperature or lower vapour residence time, the chances of secondary vapour cracking are less than the runs with longer vapour residence time, leading to the higher Mw. An opposite trend of the current finding was observed for the liquid bio-oils from fast pyrolysis of rice husks at pyrolysis temperature range of 400-600°C [73], whereas the molecular weight of liquids derived from rapid pyrolysis of beech wood [42] and a mixture of waste wood shavings [51] appeared to be relatively constant with the temperature range studied (400-1100°C for the beech wood and 400-550°C for the wood mixture). It is therefore difficult to draw a general conclusion regarding the effect of pyrolysis temperature on Mw of bio-oils as there may be other factors that concurrently influence the Mw such as vapour residence time and biomass components, especially the lignin and ash content as well as the ash composition. An example of the effect of ash content, or specifically metal content, on Mw of pyrolysis liquid can be seen from a study by Nik-Azar et al [42]. The authors found that the tar (liquid) average molecular weight decreased with the addition of potassium, sodium and calcium cations onto wood samples.

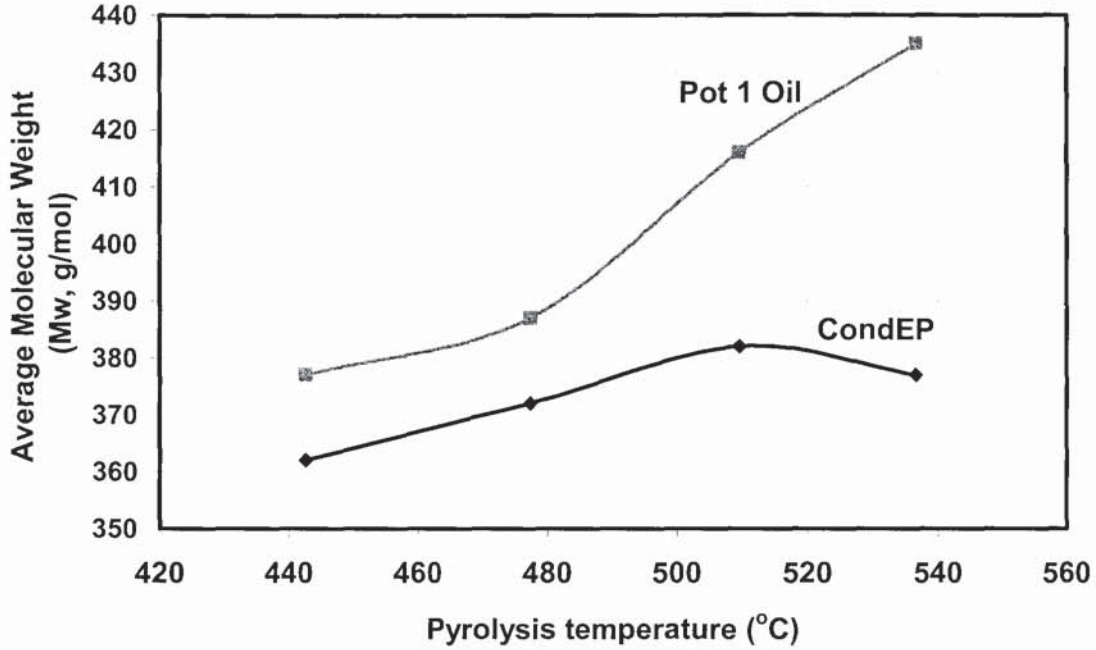

Figure 7-7 The effect of pyrolysis temperature on the average molecular weight of bio-oils derived from cassava rhizome

7.3.5 GC/MS analysis

Gas chromatography/mass spectrometry (GC/MS) technique was applied to the analysis of liquid products obtained from fast pyrolysis experiments. The purpose of GC/MS analysis was to identify and semi-quantify the chemical compounds present in different fractions of bio-oils produced from different biomass feedstocks. In addition, the changes in chemical composition of the CS and CR bio-oils during ageing were investigated.

The compounds identified including their retention times (R/T), molecular formulad, molecular weights (MW), origins and groups are provided in Table 7-5. Since bio-oil is a mixture of thermal degradation products of biomass that contains cellulose, hemicellulose and lignin building blocks, the compounds found in bio-oil are mostly oxygenated with small number of hydrocarbons. The large number of oxygenated species identified is consistent with the high oxygen content of the CS and CR bio-oils (39-43 wt%, dry basis), according to the elemental analysis (section 7.3.3).

Table 7-5 Identified chemical compounds present in bio-oils produced from fast pyrolysis of cassava stalk and rhizome

Peak ID	R/T (min)	Compound name/synomyms	Formula	MW	Origin	Group
1	4.46	Acetaldehyde/Acetic aldehyde/Ethanal	C_2H_4O	44.05	C	Aldehydes
2	4.87	Furan/Furfuran/Furane/Oxacyclopentadiene	C_4H_4O	68.08	C	Furans
3	6.48	Butanal/Butyraldehyde	C_4H_8O	72.11	C	Aldehydes
4	6.61	Ethyl Acetate/Acetic acid, ethyl ester	$C_4H_8O_2$	88.11	C	Ester
5	6.69	2,3 Butanedione/Butanedione/Diacetyl	$C_4H_6O_2$	86.09	C	Ketones
6	6.77	2-Butanone/Butanone/.Methyl ethyl ketone (MEK)	C_4H_8O	72.11	C	Ketones
7	7.13	3-Pentanone/Pentan-3-one/Diethyl ketone (DEK)	$C_5H_{10}O$	86.13	C	Ketones
8	7.30	Benzene/Benzole/Coal naphtha/Phenyl hydride	C_6H_6	78.11	L	Aromatics
9	7.80	Hydroxyacetaldehyde/Glycolaldehyde	$C_2H_4O_2$	60.05	C	Misc. Oxygenates
10	8.77	2-Butenal (cis or trans)/Crotonaldehyde/Crotonal	C_4H_6O	70.09	C	Aldehydes
11	8.80	Isopropyl Alcohol/2-Propanol	C_3H_8O	60.10	C	Alcohol
12	9.24	Acetic acid/Ethanoic acid	$C_2H_4O_2$	60.05	C	Acids
13	10.37	1-Hydroxy-2-propanone/Hydroxypropanone/Acetone alcohol	$C_3H_6O_2$	74.08	C	Misc. Oxygenates
14	10.81	Toluene/Methylbenzene	C_7H_8	92.14	L	Aromatics
15	11.04	Octane	C_8H_{18}	114.23	-	Alkane
16	12.05	3-Hydroxy-2-butanone/2-Hydroxy-3-butanone	$C_4H_8O_2$	88.11	C	Misc. Oxygenates
17	13.45	Propanoic acid/Propionic acid/Ethanecarboxylic acid	$C_3H_6O_2$	74.08	C	Acids
18	14.62	Cyclopentanone/Ketocyclopentane/Pyran-2,4(3H)-dione, 3-acetyl-6-methyl-	C_5H_8O	84.12	C	Ketones
19	14.80	1-Hydroxy-2-butanone	$C_4H_8O_2$	88.11	C	Misc. Oxygenates
20	14.92	3-Hydroxypropanal (Isomer of 1-Hydroxy-2-propanone)	$C_3H_6O_2$	74.08	C	Misc. Oxygenates
21	15.52	2-Propenal/Acrylic aldehyde/Aqualin/2-Propen-1-one	C_3H_4O	56.06	C	Aldehydes
22	16.48	Furfural/2-Furaldehyde/2-Furanaldehyde/2-Furancarboxaldehyde	$C_5H_4O_2$	96.09	C	Furans
23	16.94	Butanedial/Succinaldehyde	$C_4H_6O_2$	86.09	C	Aldehydes
24	16.95	Styrene/Vinylbenzene	C_8H_8	104.15	L	Aromatics
25	17.85	3-Methyl-furan	C_5H_6O	82.10	C	Furans
26	19.96	5-Methyl-2(3H)-furanone/a-Angelica lactone/2,3-Dihydro-5-methyl-2-furanone	$C_5H_6O_2$	98.10	C	Furans/Lactones
27	20.16	2-Furanmethanol /2-Furfuryl alcohol	$C_5H_6O_2$	98.10	C	Furans
28	20.49	1-Acetyloxy-2-propanone/1-Acetoxypropane-2-one/2-Oxopropyl acetate	$C_5H_8O_3$	116.12	C	Misc. Oxygenates
29	20.77	2-Methyl-2-cyclopenten-1-one/2-Methyl-2-cyclopentenone	C_6H_8O	96.13	C	Ketones
30	21.54	1-(2-Furanyl)ethanone/Acetylfuran/ 2-Acetylfuran/Furyl methyl ketone	$C_6H_6O_2$	110.11	C	Furans
31	22.12	2-Cyclopentene-1,4-dione	$C_5H_4O_2$	96.09	C	Ketones

Table 7-5 (Continued)

Peak ID	R/T (min)	Compound name/synomyms	Formula	MW	Origin	Group
32	23.03	3-Methyl-cyclopentanone & Cyclohexanone & Benzaldehyde	$C_6H_{10}O$ & $C_6H_{10}O$ & C_7H_6O	98.14 & 98.14 & 106.12	C	Ketones
33	24.87	5-Methyl-2-furancarboxaldehyde/5-Methylfurfural/2-Formyl-5-methylfuran/2-Methyl-5-formylfuran	$C_6H_6O_2$	110.11	C	Furans
34	25.64	3-Methyl-2-cyclo-penten-1-one	C_6H_8O	96.13	C	Ketones
35	25.73	Butyrolactone/Dihydro-2(3H)-furanone/Butyric acid lactone	$C_4H_6O_2$	86.09	C	Furans/Lactones
36	26.16	2(5H)-Furanone & 2(3H)-Furanone	$C_4H_4O_2$	84.07	C	Furans/Lactones
37	26.89	5-Methyl-2(5H)-furanone/β-Angelica lactone	$C_5H_6O_2$	98.10	C	Furans/Lactones
38	28.43	2-Hydroxy-3-methyl-2-Cyclopenten-1-one/Maple lactone & 2,5-Dimethylcyclopentanone	$C_6H_8O_2$ & $C_7H_{12}O$	112.00	C	Ketones
39	29.20	Acetophenone/Acetylbenzene	C_8H_8O	120.15	L	Misc. Oxygenates
40	30.08	Phenol	C_6H_6O	94.11	L	Phenols
41	30.83	2-Methoxyphenol/Guaiacol/Guaicol	$C_7H_8O_2$	124.14	L	Guaiacols
42	31.14	3-Methylindene/3-Methyl-1H-indene	$C_{10}H_{10}$	130.19	L	Aromatics
43	31.61	2-Methylfuran/Methylfuran/5-Methylfuran	C_5H_6O	82.10	C	Furans
44	32.10	Methyl 2-furoate/2-Furancarboxylic acid, methyl ester	$C_6H_6O_3$	126.11	C	Furans/Ester
45	32.38	o-Cresol/2-Methyl phenol	C_7H_8O	108.14	L	Phenols
46	32.80	Maltol/3-Hydroxy-2-methyl-4H-pyran-4-one	$C_6H_6O_3$	126.11	C	Misc. Oxygenates
47	33.40	Naphthalene/White tar	$C_{10}H_8$	128.17	L	Aromatics
48	33.78	4-Methyl-5H-furan-2-one/4-Methyl-2(5H)-furanone	$C_5H_6O_2$	98.10	C	Furans
49	34.03	p-Cresol/4-Methyl phenol	C_7H_8O	108.14	L	Phenols
50	34.12	m-Cresol/3-Methyl phenol	C_7H_8O	108.14	L	Phenols
51	34.21	2-Methoxy-3-methyl-phenol & 2-Methoxy-4-methyl-phenol/Creosol/4-Methylguaiacol/Homoguaiacol	$C_8H_{10}O_2$	138.17	L	Guaiacols
52	36.18	Dimethyl phenol (2,3-; 2,4- ; 2,5- & 2,6-)	$C_8H_{10}O$	122.17	L	Phenols
53	38.03	Ethylphenol (2-; 3- & 4-)	$C_8H_{10}O$	122.17	L	Phenols
54	39.43	4-Ethyl-2-methoxyphenol/4-Ethyl guaiacol/4-Hydroxy-3-methoxy ethylbenzene/p-Ethylguaiacol	$C_9H_{12}O_2$	152.19	L	Guaiacols
55	40.79	1,4:3,6-Dianhydro-α-d-glucopyranose	$C_6H_8O_4$	144.13	C	Sugars
56	41.87	2-Methoxy-4-vinylphenol/4-Vinylguaiacol/p-Vinylguaiacol/4-Hydroxy-3-methoxystyrene	$C_9H_{10}O_2$	150.18	L	Guaiacols

Table 7-5 (Continued)

Peak ID	R/T (min)	Compound name/synomyms	Formula	MW	Origin	Group
57	42.06	Biphenyl/Bibenzene	$C_{12}H_{10}$	154.21	L	Aromatics
58	42.93	Eugenol/2-Methoxy-4-allylphenol/2-Methoxy-1-hydroxy-4-allylbenzene/Allylguaiacol	$C_{10}H_{12}O_2$	164.20	L	Guaiacols
59	43.08	4-Propyl guaiacol/2-Methoxy-4-propyl phenol	$C_{10}H_{14}O_2$	166.22	L	Guaiacols
60	43.10	Dimethyl naphthalene (1,5-; 1,6-; 2,3-; 2,6- & 2,7-)	$C_{12}H_{12}$	156.23	L	Aromatics
61	43.44	5-(Hydroxymethyl)-2-furancarboxaldehyde/5-(Hydroxymethyl)-2-furfural/HMF/5-(Hydroxymethyl)-2-furaldehyde	$C_6H_6O_3$	126.11	C	Furans
62	44.10	2,6-Dimethoxy phenol/Syringol/1,3-Dimethoxy-2-hydroxybenzene/Pyrogallol dimethylether	$C_8H_{10}O_3$	154.17	L	Syringols
63	44.80	1,4-Dimethyl naphthalene	$C_{12}H_{12}$	156.23	L	Aromatics
64	45.26	2-Methoxy-4-(1-propenyl)phenol/Isoeugenol,c&t/4-Propenylguaiacol/4-Hydroxy-3-methoxypropenylbenzene	$C_{10}H_{12}O_2$	164.20	L	Guaiacols
65	47.34	2-Methoxy-4-(1-propenyl)phenol/Isoeugenol,c&t/4-Propenylguaiacol/4-Hydroxy-3-methoxypropenylbenzene	$C_{10}H_{12}O_2$	164.20	L	Guaiacols
66	47.84	1,2,3-Trimethoxybenzene/Methylsyringol	$C_9H_{12}O_3$	168.00	L	Syringols
67	48.18	Vanillin/2-Methoxy-4-formylphenol/4-Hydroxy-3-methoxybenzaldehyde	$C_8H_8O_3$	152.15	L	Guaiacols
68	48.36	Hydroquinone/1,4-Benzenediol/4-Hydroxyphenol/Dihydroxybenzene	$C_6H_6O_2$	110.11	L	Phenols
69	48.94	4-Hydroxybenzaldehyde/4-Formylphenol	$C_7H_6O_2$	122.12	L	Misc. Oxygenates
70	49.35	Resorcinol/1,3-Benzenediol	$C_6H_6O_2$	110.11	L	Phenols
71	49.90	4-Methyl-1,2-benzenediol/4-Methylcatechol/Homocatechol/Toluene-3,4-diol	$C_7H_8O_2$	124.14	L	Phenols
72	51.38	1-(4-Hydroxy-3-methoxyphenyl)ethanone/Acetoguaiacone	$C_9H_{10}O_3$	166.18	L	Guaiacols
73	53.28	1-(4-hydroxy-3-methoxyphenyl)-2-Propanone/Guaiacylacetone/Vanillyl methyl ketone/4-Hydroxy-3-methoxyphenyl acetone	$C_{10}H_{12}O_3$	180.20	L	Guaiacols
74	55.70	9-Methyl-9H-fluorene/9-Methylfluorene	$C_{14}H_{12}$	180.25	L	Aromatics
75	56.69	1,6-Anhydro-β-D-glucopyranose/Levoglucosan	$C_6H_{10}O_5$	162.14	C	Sugars
76	57.67	Methoxyeugenol/2,6-Dimethoxy-4-(2-propenyl)-phenol	$C_{11}H_{14}O_3$	194.23	L	Guaiacols
77	58.72	4-Hydroxy-3,5-dimethoxybenzaldehyde/Syringaldehyde/Syringe aldehyde/Cedar aldehyde	$C_9H_{10}O_4$	182.18	L	Syringols
78	61.07	1-(4-Hydroxy-3,5-dimethoxyphenyl)ethanone/Acetosyringone/3,5-Dimethoxy-4-hydroxyacetophenone/Acetosyringon	$C_{10}H_{12}O_4$	196.20	L	Syringols
79	62.00	1,6-Anhydro-β-D-glucofuranose	$C_6H_{10}O_5$	162.14	C	Sugars

These oxygenated compounds are in the group of aldehydes, ketones, furans, esters, alcohols, carboxylic acids, sugars and phenolics (phenols, guaiacols and syringols). The hydrocarbons identified from the CS or CR bio-oils are benzene (ID#8), toluene (ID#14), octane (ID#15), styrene (ID#24), 3-methylindene (ID#42), naphthalene and its methyl-substituted derivatives (IDs#47, 60 and 63), biphenyl (ID#57), 9-methylfluorene (ID#74). Nearly all of them are aromatic and they are believed to originate from the lignin macro-polymer. From Table 7-5, the heaviest molecule that could be identified from the GC/MS instrument was acetosyringone (ID#78) with molecular weight of 196.20 g/mol. In fact, the bio-oils also contain significant amount of molecules with molecular weight higher than that of acetosyringone as it has been found from the GPC analysis that the average molecular weight (Mw) of CS and CR bio-oils were in the range of 354-387 g/mol (section 7.3.4). Moreover, the Mw of certain molecules present in Pot 1 oils was found to be even higher than 2000 g/mol for fresh oils and higher than 6000 g/mol for aged oils (see Figure 7-6). This implies that not all molecules in the bio-oils could be identified by the GC/MS technique. Actually, the large molecules could not be eluted due to their low volatility. Oasmaa and Meier [144] mentioned that the GC-eluted part of pyrolysis liquid is typically 25-40 wt% of wet liquid and about 70-90 % of the eluted fraction can be identified. The non-eluted fraction could be the tri- and tetramer of lignin and some heavy non-volatile sugar molecules. When considering the minimum molecular weight of molecules that could be detected by the GPC technique, it can be seen that the compounds with Mw lower than 100 g/mol were not taken into account. This is due to the detection limit of the existing instrument. Therefore, the GC/MS analysis would be useful for fulfilling the gap, as it can detect the compounds of very low Mw such as acetaldehyde, furan, etc.

In order to investigate the difference in chemical composition of different fractions of bio-oils (Pot 1, Pot 2+3 and CondEP) and bio-oils produced from different feedstocks (cassava stalk and rhizome), a total of 12 liquid samples from four pyrolysis runs were subjected to the GC/MS analysis. The integrated area data of all identified peaks expressed as percentages of total peak areas are summarised in Table 7-6. The CS#1 and CS#2 samples were derived from fast pyrolysis of cassava stalk at 475°C and 502°C, respectively. The CR#1 and CR#2 samples were produced from fast pyrolysis of cassava rhizome at 476°C and 510°C, respectively. It can be seen from the table

Table 7-6 Peak area percentages of compounds identified from different fractions of CS and CR bio-oils

Peak ID	% Peak Area											
	CS#1[a]			CS#2[b]			CR#1[c]			CR#2[d]		
	Pot1	Pot2+3	CondEP	Pot1	Pot2+3	CondEP	Pot1	Pot2+3	CondEP	Pot1	Pot2+3	CondEP
1	0.23	9.83	0.19	0.19	8.87	0.16	0.13	7.79	0.00	0.51	15.50	0.20
2	0.55	0.05	0.87	0.48	0.00	0.77	1.00	0.42	2.21	0.00	0.00	2.26
3	0.00	1.12	0.00	0.00	1.63	0.00	0.00	1.03	0.00	0.00	1.25	0.00
4	0.00	0.00	0.00	0.00	0.00	0.31	0.00	0.00	0.32	0.00	0.00	0.25
5	0.41	23.97	0.29	0.45	19.57	0.25	0.62	21.92	0.37	0.92	25.36	0.00
6	0.08	0.00	0.89	1.17	0.00	0.00	0.00	0.00	0.00	0.00	0.00	0.00
7	0.49	2.01	0.00	0.26	1.09	0.00	0.00	0.96	0.00	0.00	0.00	0.00
8	0.00	0.20	0.00	0.00	0.32	0.00	0.00	0.00	0.00	0.00	0.23	0.00
9	4.65	0.00	1.67	2.85	0.88	0.85	4.78	1.59	1.75	8.61	0.00	1.93
10	0.00	5.44	0.00	0.00	5.29	0.00	0.00	5.70	0.00	0.00	6.52	0.00
11	0.28	0.00	0.11	0.00	0.00	0.10	0.39	0.00	0.00	0.00	0.00	0.00
12	13.15	9.54	9.74	11.39	5.25	7.89	26.72	16.25	13.07	21.62	4.84	10.99
13	13.40	24.95	6.62	10.77	24.08	4.43	15.64	22.57	6.42	9.81	19.04	6.31
14	0.00	1.07	0.00	0.00	0.55	0.00	0.00	0.00	0.31	0.00	0.92	0.00
15	0.00	0.27	0.00	0.00	0.00	0.00	0.00	0.00	0.00	0.00	0.29	0.00
16	0.34	1.67	0.00	0.27	1.11	0.00	0.33	0.00	0.00	0.00	1.19	0.00
17	0.08	0.00	0.00	0.00	0.00	0.12	0.29	0.00	0.00	0.00	0.00	0.00
18	0.04	0.85	0.00	0.00	0.63	0.00	0.07	0.61	0.00	0.00	0.55	0.00
19	0.53	0.64	0.27	0.43	0.67	0.23	0.53	0.00	0.00	0.00	0.00	0.00
20	10.53	5.71	4.85	5.99	4.33	3.16	11.20	4.85	5.46	15.73	5.06	6.21
21	0.55	0.00	0.00	0.00	0.00	0.00	0.00	0.00	0.00	0.00	0.00	0.33
22	2.01	0.83	2.91	0.00	11.76	2.69	0.00	1.45	2.25	2.03	11.66	0.00
23	4.30	2.52	1.16	2.71	2.08	0.93	1.87	1.65	0.65	2.50	0.97	0.85
24	0.00	0.00	0.00	0.00	0.00	0.00	3.09	0.00	0.00	0.00	0.00	0.00
25	0.00	0.00	0.00	2.62	0.38	0.00	0.00	0.00	0.00	0.00	0.00	0.00
26	0.19	0.07	0.29	0.00	0.00	0.23	0.00	0.00	0.20	0.00	0.00	0.23
27	0.61	0.00	0.73	0.66	0.00	0.62	0.46	0.00	1.03	0.00	0.00	0.80
28	1.14	1.44	0.90	1.42	1.57	0.75	1.91	1.49	0.77	1.63	1.54	0.91
29	1.16	2.62	0.00	0.00	1.64	0.59	1.03	2.04	0.49	0.00	1.80	0.32
30	0.11	0.37	0.20	0.00	0.38	0.20	0.15	0.48	0.14	0.00	0.00	0.00

Table 7-6 (Continued)

Peak ID	% Peak Area											
	CS#1[a]			CS#2[b]			CR#1[c]			CR#2[d]		
	Pot1	Pot2+3	CondEP	Pot1	Pot2+3	CondEP	Pot1	Pot2+3	CondEP	Pot1	Pot2+3	CondEP
31	0.78	0.47	0.42	0.25	0.39	0.00	0.30	0.68	1.27	0.00	0.69	1.38
32	3.60	0.00	5.20	2.45	0.00	2.55	1.51	0.00	3.11	2.60	0.00	3.39
33	0.15	0.38	0.24	0.00	0.82	0.23	0.27	0.35	0.16	0.00	0.23	0.23
34	0.24	0.00	0.42	0.32	0.23	0.43	0.28	0.00	0.26	0.00	0.00	0.29
35	0.50	0.00	0.66	0.50	0.00	0.61	0.64	0.00	0.72	0.00	0.00	0.78
36	1.60	1.19	2.19	1.50	0.65	2.06	2.09	1.33	2.30	1.68	0.89	2.65
37	0.29	1.14	0.49	0.72	4.28	0.34	1.04	0.00	0.39	0.00	0.00	0.38
38	2.40	0.00	4.00	2.03	0.00	4.12	2.14	0.00	3.64	1.57	0.00	3.90
39	0.09	0.00	0.00	0.00	0.00	0.00	0.59	0.00	0.00	0.00	0.00	0.00
40	0.55	0.12	1.14	0.72	0.33	2.79	2.95	0.00	0.86	0.80	0.19	1.06
41	2.08	0.93	3.86	2.32	1.23	3.45	0.00	0.94	3.92	1.64	0.73	3.93
42	0.00	0.00	0.00	0.00	0.00	0.20	0.00	0.00	0.00	0.00	0.00	0.00
43	0.43	0.00	0.23	0.00	0.00	0.00	0.00	0.00	0.00	0.00	0.32	0.00
44	0.37	0.00	0.06	0.00	0.00	0.00	0.10	0.00	0.12	0.00	0.00	0.18
45	0.98	0.00	0.58	1.86	0.00	0.61	0.00	0.00	0.63	0.00	0.00	0.74
46	1.92	0.00	0.00	0.00	0.00	0.53	0.00	0.00	0.00	0.00	0.00	0.00
47	1.25	0.00	0.00	0.00	0.00	0.00	0.00	0.00	0.00	0.00	0.00	0.00
48	1.36	0.00	0.51	4.88	0.00	0.68	0.42	0.00	0.52	1.34	0.00	1.55
49	0.60	0.00	0.27	3.84	0.00	0.39	0.23	0.00	0.40	0.73	0.00	0.51
50	1.11	0.00	0.45	0.00	0.00	0.00	0.34	0.00	0.00	0.00	0.00	0.00
51	2.27	0.30	5.21	2.03	0.00	4.73	2.49	0.65	5.64	7.37	0.24	0.17
52	0.25	0.00	0.45	0.00	0.00	0.18	0.24	0.00	0.42	0.00	0.00	0.85
53	0.08	0.00	0.18	0.00	0.00	0.66	0.00	0.00	0.21	0.00	0.00	0.17
54	0.68	0.00	1.98	0.00	0.00	1.37	0.44	0.00	3.51	0.00	0.00	2.21
55	6.40	0.00	0.90	0.41	0.00	1.02	0.45	0.00	0.94	0.00	0.00	1.20
56	5.83	0.00	10.31	5.85	0.00	7.19	0.61	5.28	0.00	0.00	0.00	0.00
57	0.00	0.00	0.00	0.69	0.00	0.00	0.00	0.00	0.00	0.00	0.00	0.00
58	0.47	0.00	1.33	0.00	0.00	1.53	0.56	0.00	1.40	0.00	0.00	1.87
59	0.19	0.00	0.41	0.00	0.00	0.61	0.28	0.00	0.57	0.00	0.00	0.81
60	0.22	0.00	0.00	0.00	0.00	0.00	0.00	0.00	0.00	0.00	0.00	0.00

Table 7-6 (Continued)

Peak ID	% Peak Area											
	CS#1[a]			CS#2[b]			CR#1[c]			CR#2[d]		
	Pot1	Pot2+3	CondEP	Pot1	Pot2+3	CondEP	Pot1	Pot2+3	CondEP	Pot1	Pot2+3	CondEP
61	0.50	0.00	0.91	0.34	0.00	1.02	0.66	0.00	1.14	0.00	0.00	1.55
62	1.17	0.00	2.72	1.04	0.00	3.21	0.82	0.00	2.51	0.96	0.00	3.31
63	0.06	0.00	0.00	0.00	0.00	0.00	0.00	0.00	0.00	0.00	0.00	0.00
64	1.51	0.28	5.37	0.31	0.00	0.87	1.38	0.00	0.80	1.97	0.00	0.00
65	0.00	0.00	0.00	1.84	0.00	5.63	0.00	0.00	4.80	0.00	0.00	6.65
66	0.42	0.00	1.10	9.64	0.00	1.29	0.42	0.00	1.24	0.00	0.00	1.63
67	0.00	0.00	0.92	9.89	0.00	1.65	0.84	0.00	1.22	11.55	0.00	1.86
68	0.00	0.00	1.77	0.00	0.00	2.09	1.59	0.00	0.63	0.00	0.00	0.79
69	0.09	0.00	0.16	0.00	0.00	0.18	0.05	0.00	0.12	0.00	0.00	0.16
70	0.10	0.00	0.00	0.00	0.00	0.49	0.00	0.00	0.00	0.00	0.00	0.00
71	0.12	0.00	0.05	0.00	0.00	0.47	0.00	0.00	0.36	0.00	0.00	0.00
72	0.23	0.00	0.58	0.00	0.00	0.82	0.29	0.00	0.77	0.00	0.00	1.11
73	0.20	0.00	0.49	0.00	0.00	0.72	0.18	0.00	0.62	0.00	0.00	0.67
74	0.00	0.00	0.00	0.00	0.00	3.73	0.00	0.00	0.00	0.00	0.00	0.00
75	2.83	0.00	9.35	2.68	0.00	13.24	4.62	0.00	16.16	3.62	0.00	18.70
76	1.04	0.00	2.71	0.95	0.00	2.84	0.59	0.00	2.26	0.80	0.00	2.47
77	0.14	0.00	0.49	1.31	0.00	0.65	0.28	0.00	0.64	0.00	0.00	0.87
78	0.09	0.00	0.22	0.00	0.00	0.35	0.07	0.00	0.31	0.00	0.00	0.40
79	0.00	0.00	0.00	0.00	0.00	0.21	0.00	0.00	0.00	0.00	0.00	0.00
Total	100.00	100.00	100.00	100.00	100.00	100.00	100.00	100.00	100.00	100.00	100.00	100.00

[a] CS#1 represents fresh liquid fractions produced from fast pyrolysis of cassava stalk at 475°C (Test name: AP12)
[b] CS#2 represents fresh liquid fractions produced from fast pyrolysis of cassava stalk at 502°C (Test name: AP10)
[c] CR#1 represents fresh liquid fractions produced from fast pyrolysis of cassava rhizome at 476°C (Test name: AP9)
[d] CR#2 represents fresh liquid fractions produced from fast pyrolysis of cassava rhizome at 510°C (Test name: AP11)

that not all compounds were present in all fractions. For example, butanal (ID#3) existed only in Pot 2+3 fractions. To see the presence and absence of individual compounds in each liquid fraction more clearly, a Venn diagram for the compound distribution is presented in Figure 7-8. It is obvious from the diagram that the majority of compounds are present in either all fractions (up to 25 compounds) or only Pot 1 and CondEP fraction (up to 37 compounds). There are 6 compounds found only in Pot 1 fraction, namely styrene (ID#24), acetophenone (ID#39), naphthalene (ID#47), biphenyl (ID#57) and dimethyld naphthalene (IDs#60 and 63). It can be observed that all of them are aromatic. The chemical species present only in Pot 2+3 fraction are butanal (ID#3), benzene (ID#8), 2-butenal (ID#10) and octane (ID#15). These chemicals could not be condensed by the water condenser or captured by the electrostatic precipitator, but they were condensed by the series of two dry-ice/acetone condensers. Nevertheless, it was believed that there were still some volatiles that could escape the dry-ice condensers and cotton wool filter to the gas stream, leading to the loss in mass balance closure. It was reported by Tsai et al [110] that a portion of light organic volatiles generated from biomass pyrolysis could escape a condensation train being kept at -10°C as the authors could identify BTX (benzene, toluene and xylenes), styrene and 2-methyl furan in the pyrolysis gas products. This indicates the importance of condensation efficiency because a loss of valuable chemicals such as BTX could occur. The compounds found only in CondEP fraction were ethyl acetate (ID#4) and 3-methylindene (ID#42). The existence of ethyl acetate was due to the esterification of ethanol (used as washing liquid) and acetic acid (a thermal degradation product of hemicellulose).

In general, the Venn diagram illustrates that all pyrolysis liquid fractions obtained from the 150 g/h fluidised-bed reactor unit are chemically different. Hence, it may not be logical to perform testing on physical or chemical properties of only one or two fractions of bio-oils.

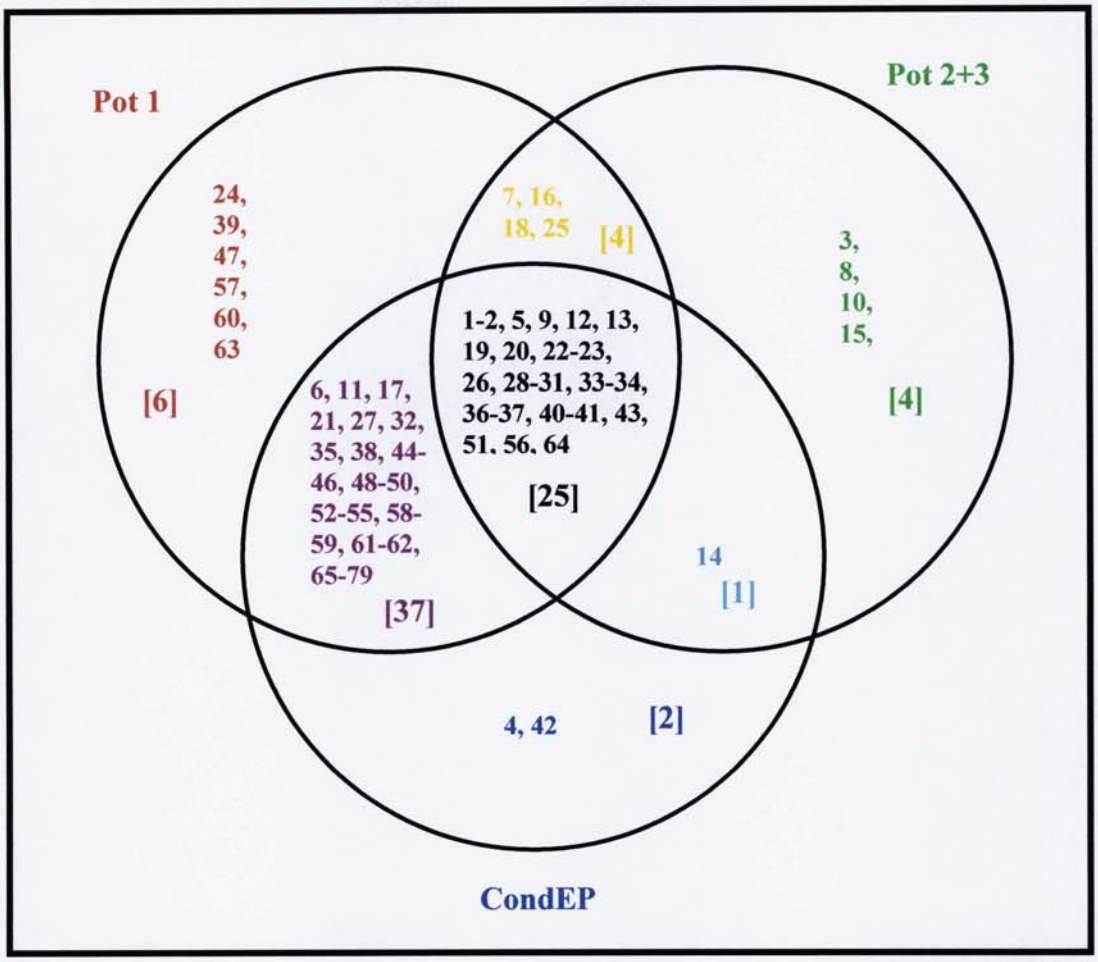

Figure 7-8 A Venn diagram showing the distribution of chemical compounds present in each fraction of CS and CR bio-oils (the figure in [ ] is the total number of compounds in each section)

The Venn diagram can only display the presence and absence of each compound, but cannot show that which compounds are predominantly present in which fraction. For instance, although acetaldehyde (ID#1) existed in all liquid fractions, according to Table 7-6 its concentration was predominantly high in Pot 2+3 fraction. As a consequence, the percentage data of all chromatographic peak areas from Table 7-6 were subjected to a statistical analysis. A principal component analysis (PCA) model was established based on all liquid fractions and all compounds. The resultant score and loading plots of PC1 and PC2 are presented in Figure 7-9. It can be seen from the score plot (Figure 7-9 (a)) that the first two principal components (PC1 and PC2), which explained 54 % of the total variance separate the samples into three groups according to their fractions. This indicates that the difference in chemical composition of the three fractions is much greater than that of the feedstocks (CS and CR).

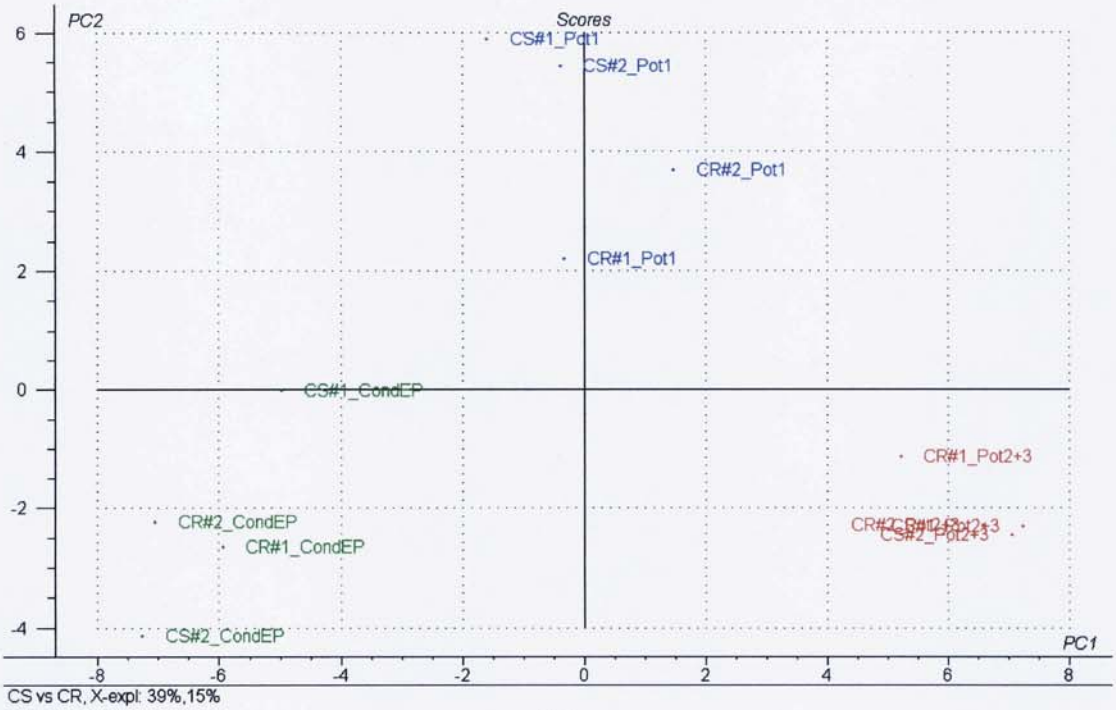

(a)

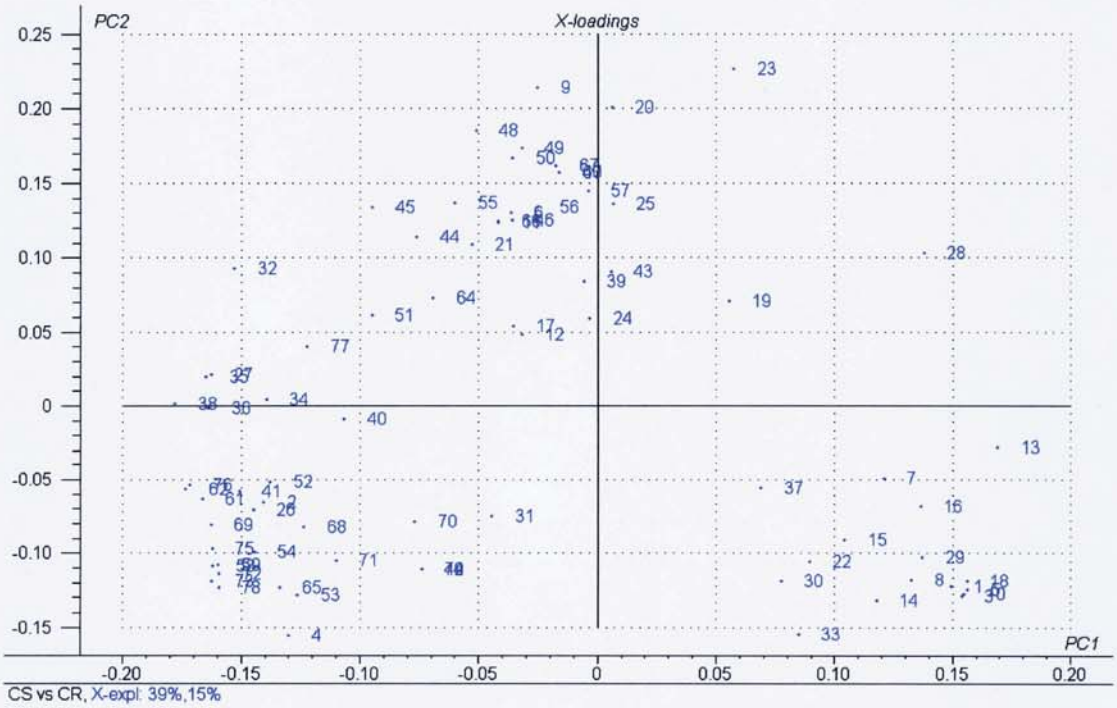

(b)

Figure 7-9 Score (a) and loading (b) plots of PC1 and PC2 for model with all liquid fractions and all compounds

When considering the score plot (Figure 7-9 (a)) together with its corresponding loading plot (Figure 7-9 (b)), it is apparent that the compounds predominantly existed in Pot 2+3 fractions were of IDs#1, 3, 5, 7, 8, 10, 13-16, 18, 22, 29-30, 33 and 37. These compounds are mainly low molecular weight aldehydes, ketones, furans and some low boiling point hydrocarbons such as benzene, toluene and octane. It can also be observed that most of them are derived from carbohydrate fraction of the original biomass. These compounds were difficult to condense at room temperature. The use of dry-ice/acetone condensers was therefore beneficial for their collection. The chemical species that are characteristic of the CondEP fraction (predominantly present in this fraction) include IDs#2, 4, 26-27, 32, 34-36, 38, 40-41, 52-54, 58-59, 61-62, 65, 68-69, 71-73 and 75-78. For Pot 1 fraction, the compounds present in statistically high proportion are IDs# 6, 9, 11, 20-21, 23, 25, 44-50, 55-57, 60, 63 and 66-67. It can be noticed that the CondEP and Pot 1 fractions contained the compounds that are derived from the fragmentation and depolymerisation of both carbohydrate (cellulose and hemicellulose) and lignin parts of the biomass feedstocks.

According to the first two principal components (Figure 7-9), it is not possible to distinguish the bio-oils produced from the two different feedstocks. Consequently, the third principal component was included in the analysis and the score and loading plots of PC1 and PC3 are depicted in Figure 7-10. It is obvious from Figure 7-10 (a) that there are two clusters of samples separated by the PC1. These clusters are CondEP and Pot 2+3 samples. According to the PC3 along the y-axis of Figure 7-10 (a), it was surprisingly found that the difference in chemical composition of the Pot 1 samples was not related to the difference in the biomass feedstocks, but rather the difference in the pyrolysis temperatures. The Pot 1 samples on the positive PC3, CS#1_Pot1 and CR#1_Pot1 were produced at pyrolysis temperatures of 475°C and 476°C, respectively, whereas the samples on the negative PC3, CS#2_Pot1 and CR#2_Pot1 were produced at higher pyrolysis temperature of 502°C and 510°C, respectively. Based on the statistical analysis of the first three principal components, which explained 66% of the total variance, it is logical to conclude that the bio-oils derived from cassava stalk and rhizome were chemically similar if they were produced at similar pyrolysis temperature, whereas the three fractions of the liquid products apparently differed in chemical composition. It is therefore suggested that if the bio-oils produced from different runs using the 150 g/h rig are to be comparatively

investigated, all liquid fractions or their proportionate mixtures must be carefully taken into account.

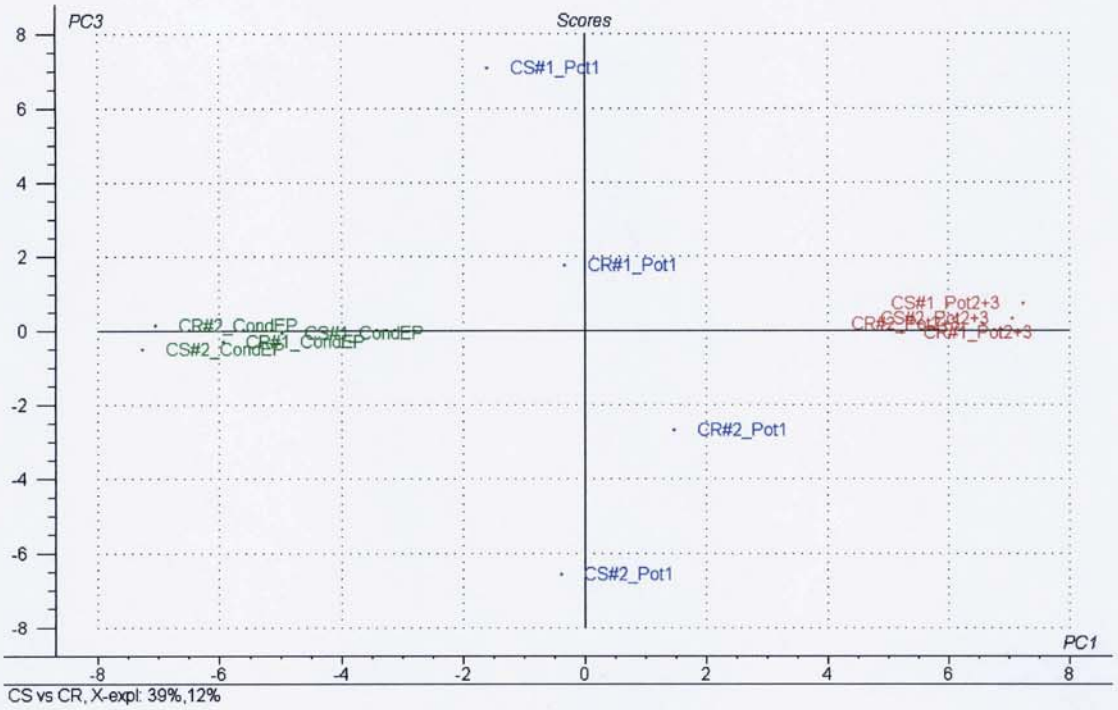

(a)

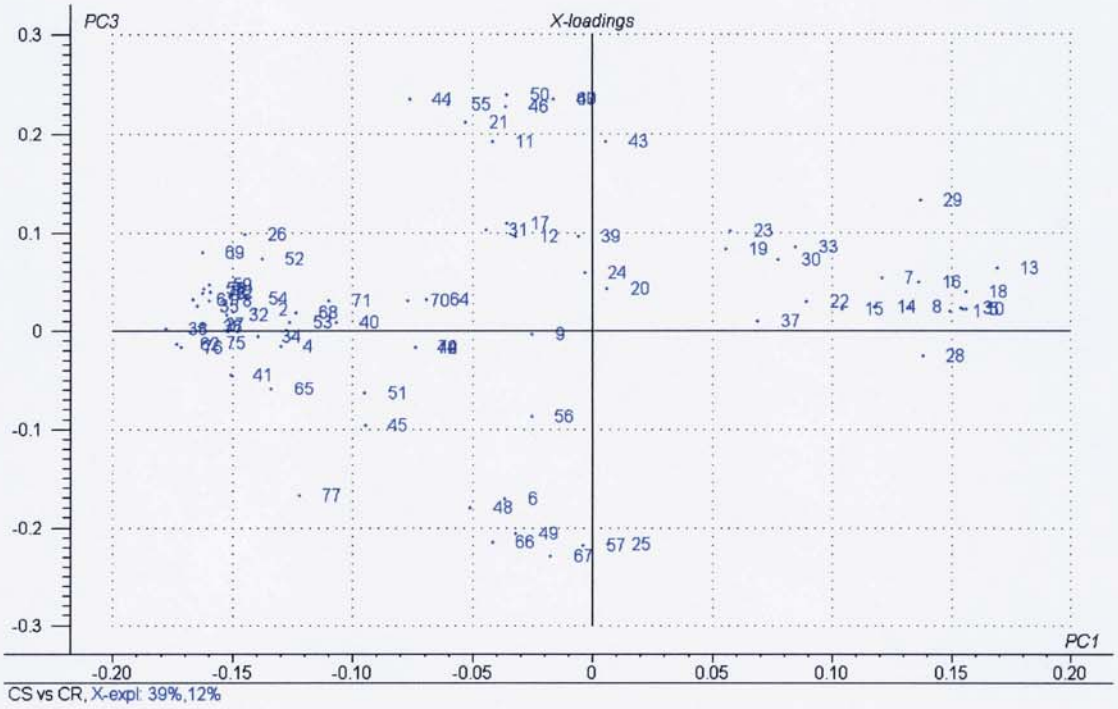

(b)

Figure 7-10 Score (a) and loading (b) plots of PC1 and PC3 for model with all liquid fractions and all compounds

To study the effect of ageing on chemical composition of bio-oils, three fresh Pot 1 samples (CS#1, CR#3 and CR#4) were aged by heating at 80°C for 24 hours. A total of six samples were then analysed by GC/MS method. The percentages of chromatographic peak areas for all samples are listed in Table 7-7. It can be observed from the table that a number of compounds disappeared after ageing. Theses compounds included 3-butanone (ID#6), 3-pentanone (ID#7), 2-cyclopentene-1,4-dione (ID#31), dimethyl naphthalene (ID#60), resorcinol (ID#70), 4-methyl-1,2-benzenediol (ID#71), 9-methyl fluorene (ID#74), acetosyringone (ID#78) and 1,6-anhydro-β-d-glucofuranose (ID#79). Among the compounds, only 2-cyclopentene-1,4-dione (ID#31) and acetosyringone (ID#78) existed in all fresh samples. The compounds disappeared after ageing are believed to be involved in the ageing reactions. Nevertheless, there are still a large number of compounds that may be involved in the reactions and decreased in their concentration rather than disappearing. To monitor compounds that decreased in their proportion at a statistically significant level, a PCA model was established with all fresh and aged samples and all identified compounds based on the data from Table 7-7. The obtained score and loading plots of PC1 and PC2 are presented in Figure 7-11. It can be seen from the score plot (Figure 7-11 (a)) that the first principal component is responsible for the difference in ageing, whereas the second principal component distinguishes the bio-oils according to their original biomass feedstocks. This implies that the difference in chemical composition of the fresh and aged samples is larger than that of the CS and CR bio-oils as the PC1 explained 38% of the total variance, while the PC2 described only 30% of the total variance.

Furthermore, the compounds that are characteristic of fresh oils no matter what biomass feedstock was used can be noticed from the IDs sitting on the negative position of the PC1 with small influence from the PC2 (group I in Figure 7-11 (b)). These compounds are hydroxyacetaldehyde (ID#9), 3-hydroxypropanal (ID#20), 2-cyclopentene-1,4-dione (ID#31), 3-methyl-cyclopentanone (ID#32), methyl 2-furoate (ID#44), 2-methyl phenol (ID#45), maltol (ID#46) and 4-vinylguaiacol (ID#56).

Moreover, the compounds in group II and III (Figure 7-11 (b)) decreased in their proportion upon ageing, although less statistically significant. It was also reported in

Table 7-7 Chromatographic peak area percentages of the compounds identified from fresh and aged Pot 1 oils

Peak ID	% Peak Area					
	CS#1[a]		CR#3[b]		CR#4[c]	
	Fresh	Aged	Fresh	Aged	Fresh	Aged
1	0.23	0.22	0.23	0.27	0.92	0.31
2	0.55	0.01	1.80	0.24	0.01	0.02
3	0.00	0.00	0.00	0.00	0.00	0.00
4	0.00	0.00	0.00	0.00	0.00	0.00
5	0.41	0.69	0.45	0.45	0.45	0.38
6	0.08	0.00	0.00	0.00	0.00	0.00
7	0.49	0.00	0.14	0.00	0.00	0.00
8	0.00	0.00	0.00	0.00	0.00	0.00
9	4.65	2.25	3.53	0.00	2.95	0.00
10	0.00	0.00	0.00	0.15	0.00	0.00
11	0.28	0.41	0.20	0.00	0.20	0.12
12	13.15	38.51	18.02	37.56	18.86	36.48
13	13.40	23.92	8.94	22.29	13.89	19.99
14	0.00	0.00	0.00	0.00	0.00	0.00
15	0.00	0.00	0.00	0.00	0.00	0.00
16	0.34	0.16	0.15	0.05	0.25	0.00
17	0.08	0.35	0.14	0.16	0.15	0.22
18	0.04	0.08	0.04	0.06	0.04	0.00
19	0.53	1.08	0.25	0.61	0.36	0.63
20	10.53	4.60	6.83	0.97	7.80	0.97
21	0.55	0.46	0.07	0.42	0.00	0.39
22	2.01	3.42	2.25	0.00	0.18	0.07
23	4.30	2.36	0.25	0.04	0.79	0.00
24	0.00	0.00	0.00	0.00	2.62	0.00
25	0.00	0.00	0.00	2.82	3.09	2.78
26	0.19	0.18	0.21	0.19	0.28	0.19
27	0.61	0.00	0.92	0.13	0.70	0.07
28	1.14	1.30	1.26	1.22	1.57	1.29
29	1.16	1.54	0.81	0.56	0.87	0.68
30	0.11	0.22	0.12	0.23	0.13	0.28
31	0.78	0.00	0.32	0.00	0.26	0.00
32	3.60	0.59	3.25	0.00	2.83	0.48
33	0.15	0.22	0.20	0.19	0.25	0.25
34	0.24	0.39	0.25	0.33	0.32	0.43
35	0.50	1.01	0.60	1.36	0.67	1.21
36	1.60	1.91	2.09	2.51	2.09	2.39
37	0.29	0.33	0.30	0.34	0.54	0.37
38	2.40	2.66	3.17	4.62	2.62	4.54
39	0.09	0.10	0.00	0.13	0.44	0.15
40	0.55	0.66	0.65	1.21	0.79	1.07
41	2.08	3.21	2.78	5.06	2.96	4.95
42	0.00	0.00	0.00	0.00	0.00	0.00
43	0.43	0.11	0.17	0.21	0.15	0.20
44	0.37	0.00	0.19	0.00	0.04	0.07
45	0.98	0.00	0.45	0.00	0.35	0.57
46	1.92	0.75	1.61	0.65	1.22	0.65
47	1.25	0.09	0.00	0.03	0.09	0.21
48	1.36	0.39	0.41	0.51	0.66	0.80
49	0.60	0.14	0.00	0.44	0.35	0.46
50	1.11	0.28	0.33	0.51	0.40	0.42
51	2.27	1.15	5.56	3.24	3.29	3.29
52	0.25	0.00	0.53	0.37	0.27	0.36
53	0.08	0.00	0.11	0.10	0.05	0.10

Table 7-7 (Continued)

Peak ID	% Peak Area					
	CS#1[a]		CR#3[b]		CR#4[c]	
	Fresh	Aged	Fresh	Aged	Fresh	Aged
54	0.68	0.26	1.29	0.84	0.97	0.96
55	6.40	0.26	0.80	0.04	0.65	0.63
56	5.83	0.17	4.18	0.03	3.17	0.16
57	0.00	0.00	0.00	0.00	0.00	0.00
58	0.47	0.46	0.76	1.01	0.99	1.21
59	0.19	0.00	0.27	0.37	0.43	0.34
60	0.22	0.00	0.00	0.00	0.04	0.00
61	0.50	0.11	1.02	0.13	0.73	0.24
62	1.17	1.00	1.71	1.73	1.50	1.95
63	0.06	0.00	0.27	0.08	0.06	0.08
64	1.51	0.15	0.53	0.50	0.18	1.71
65	0.00	0.15	3.30	1.25	4.03	0.00
66	0.42	0.28	0.78	0.68	0.82	0.91
67	0.00	0.22	0.77	0.44	0.92	0.66
68	0.00	0.23	0.79	0.34	0.95	0.39
69	0.09	0.00	0.12	0.00	0.04	0.05
70	0.10	0.00	0.00	0.00	0.00	0.00
71	0.12	0.00	0.23	0.00	0.00	0.00
72	0.23	0.13	0.46	0.29	0.40	0.44
73	0.20	0.13	0.40	0.25	0.33	0.30
74	0.00	0.00	1.53	0.00	0.00	0.00
75	2.83	0.54	8.86	1.46	5.51	1.66
76	1.04	0.13	1.69	0.29	1.20	0.44
77	0.14	0.00	0.34	0.03	0.20	0.04
78	0.09	0.00	0.17	0.00	0.11	0.00
79	0.00	0.00	0.13	0.00	0.00	0.00
Total	100.00	100.00	100.00	100.00	100.00	100.00

[a] CS#1 represents bio-oils produced from fast pyrolysis of cassava stalk at 475°C (Test AP12)
[b] CR#3 represents bio-oils produced from fast pyrolysis of cassava rhizome at 443°C (Test AP15)
[c] CR#4 represents bio-oils produced from fast pyrolysis of cassava rhizome at 477°C (Test AP17)

the literature [5, 32] that hydroxyacetaldehyde (ID#9) was one of the main compounds decreased in concentration during ageing. In addition, Oasmaa and Kuoppala [5] revealed the similar finding to the current results that the amounts of 4-vinylguaiacol (ID#56) and 5-(Hydroxymethyl)-2-furfural (ID#61, Group II) decreased during storage. According to the present results together with certain supports from literature data, it can be therefore deduced that the compounds present mainly in the fresh oils rather than the aged oils, especially in group I of Figure 7-11 (b), were highly reactive and could be involved in ageing reactions, leading to the unstable nature of bio-oils produced from cassava stalk and rhizome. Therefore, removing, reducing or transforming these compounds would be advantageous for improving bio-oils stability. This can be achieved by catalytic upgrading of either the liquid bio-oil or the pyrolysis vapour prior to condensation.

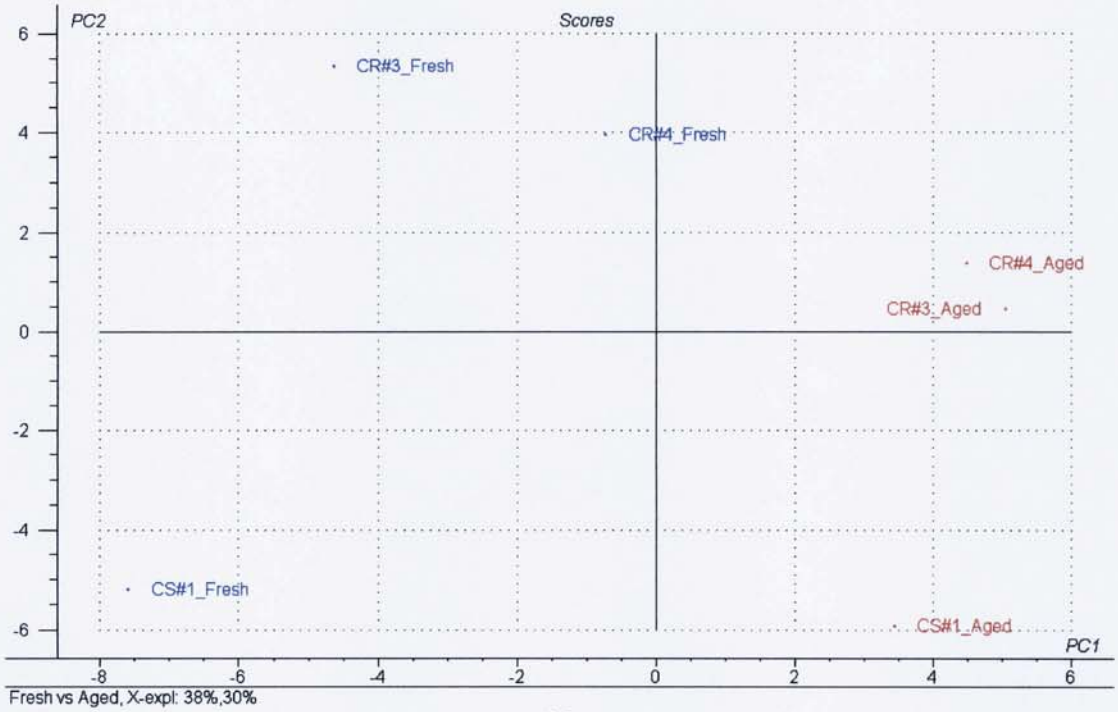

(a)

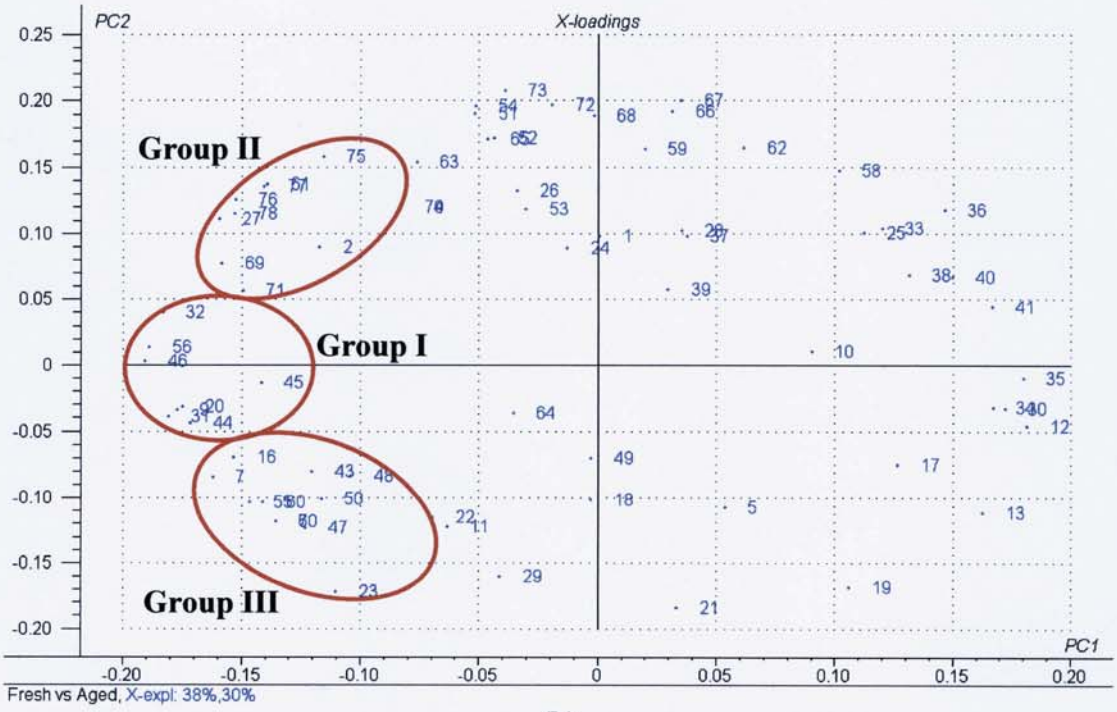

(b)

Figure 7-11 Score (a) and loading (b) plots of PC1 and PC2 for model with fresh and aged Pot 1 oils and all compounds

7.4 CONCLUDING REMARKS

The study of non-catalytic fast pyrolysis of stalk and rhizome of cassava plants was reported in this chapter. It was found that the organics yield of cassava rhizome was slightly higher (~2-4 wt%) than that of cassava stalk. The optimum pyrolysis temperature to obtain highest organics yield suggested for both feedstocks was 490±15°C. Based on the bio-oil analysis, the cassava rhizome was found to be a better feedstock for the production of bio-oil of better quality in terms of oxygen content, heating value and stability. When considering the organics yield together with the bio-oil properties for both feedstocks, it is suggested that the rhizome is a more promising feedstock. Therefore, the rhizome is chosen as feedstock for further study in the catalytic pyrolysis of biomass (chapter 8).

Another important conclusion that can be drawn from this chapter is that all liquid fractions produced from the 150 g/h rig were chemically different. Therefore, to comparatively study the bio-oil produced with different conditions, all fractions should be taken into consideration.

8 CATALYTIC FAST PYROLYSIS RESULTS AND DISCUSSION

8.1 INTRODUCTION

This chapter discusses the experimental results of the catalytic fast pyrolysis of a selected biomass feedstock (cassava rhizome). The biomass samples ground to particle size range of 355 – 500 μm were fed into the 150 g/h fluidised-bed reactor, which was heated to about 490°C. This temperature was established and reported in the previous chapter to be optimum for maximising the organics yield. The pyrolysis vapour including water, light volatile, heavy organics, radicals and non-condensable gases was passed over a fixed-bed of catalyst at around 500°C in order to upgrade the pyrolysis vapour prior to condensation (see section 6.2.2 for details of the experimental set-up). Seven different catalysts selected according to the recommendation following the catalyst screening tests (chapter 5) were used in this study. These include Criterion-534, biomass ash, copper chromite, ZSM-5, MI-575, Al-MCM-41 and Al-MSU-F. In addition, two catalytic pyrolysis runs were conducted using a two-stage process where either Criterion-534 or Al-MSU-F was used as a primary catalytic bed, and ZSM-5 was used as a secondary catalytic bed, which was placed on top of the primary one separated by a plug of glass wool. The catalyst sets are denoted as Criterion-534/ZSM-5 and Al-MSU-F/ZSM-5. The primary catalytic materials were intended to act as a guard bed for protecting the ZSM-5 catalyst from premature deactivation by the deposition of some compounds in the pyrolysis vapour that condense on the ZSM-5 surface. The guard bed was also expected to perform cracking reactions to a certain extent, thus leading to the formation of lower molecular weight compounds and some olefins. These compounds would then undergo further reactions on the active sites of the ZSM-5 catalyst, provided that they are small enough to enter the catalyst pores. Consequently, it was anticipated that more aromatic hydrocarbons could be produced by the two-stage process than the use of ZSM-5 alone. It is important to emphasise that ideal catalyst or set of catalysts would selectivity crack the large molecules (such as lignin derivatives), remove oxygen preferably in the form of CO_2 rather than H_2O and transform the low value

oxygenated compounds into higher value fuel additives or chemicals such as gasoline-range monocycle aromatic hydrocarbons, phenol and alkylated phenols.

Based on the experimental results obtained from the 9 runs of catalytic fast pyrolysis of cassava rhizome in the 150g/h pyrolysis unit, the mass balances and the analysis of the bio-oils are reported and discussed below.

8.2 MASS BALANCES

Since catalytic pyrolysis has been carried out with the secondary reactor (see section 6.2.2), it is essential to conduct a reference run with the 2nd reactor but without catalyst. As a consequence, a non-catalytic pyrolysis run was performed with the 2nd reactor containing only a plug of glass wool (~7 g). The photographs of the glass wool before and after use are shown in Figure 8-1. It was found that the glass wool was effective for capturing some char fines. Therefore, it may be used for hot vapour filtration to reduce the amount of solid particles and ash in bio-oils. Its effectiveness may be dependent on the density and the quantity of the glass wool bed.

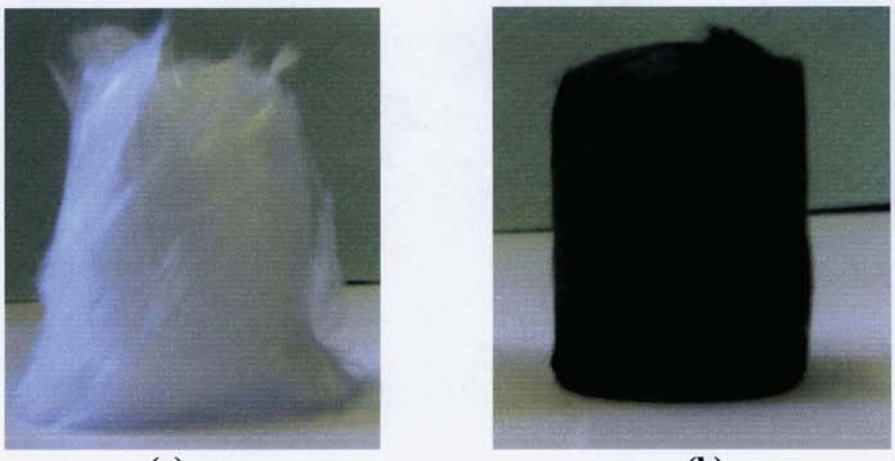

(a) **(b)**

Figure 8-1 Glass wool before (a) and after (b) the pyrolysis run

Table 8-1 summaries the mass balance analysis of the catalytic pyrolysis runs in comparison with the two non-catalytic runs. The mass balance closures of nearly all tests are 95% or higher except for Al-MSU-F/ZSM-5. The loss in mass balance is

believed to be mainly due to the unidentified compounds in the exit gas stream. When comparing the product yields of the two non-catalytic runs (with and without the secondary reactor), it is obvious that the main differences are the yields of organics and gas.

Table 8-1 Product yields (wt % on dry biomass basis) from catalytic pyrolysis of cassava rhizome

Catalyst	Liquid		Solid		Gas	Closure
	Organics	Reaction water	Primary[a]	Secondary[b]		
Non-catalytic without 2nd reactor	49.76	15.17	19.97	0.00	10.10	95.00
Non-catalytic with 2nd reactor	44.91	14.58	19.76	0.80	15.32	95.37
Criterion-534	26.90	19.81	17.32	9.07	22.22	95.32
Ash	41.82	17.63	18.21	1.20	16.37	95.23
Copper Chromite	48.62	16.08	17.47	0.23	14.76	97.15
ZSM-5	29.10	20.57	17.69	11.40	19.74	98.50
MI-575	48.13	15.63	15.32	0.00	16.34	95.42
Al-MCM-41	38.68	12.77	25.20	2.36	15.89	94.90
Al-MSU-F	45.32	13.70	20.15	2.54	12.89	94.60
Criterion-534/ZSM-5	23.21	19.92	18.10	8.75	26.18	96.16
Al-MSU-F/ZSM-5	39.69	16.19	20.80	1.09	15.08	92.85

[a]Primary solid represents particles collected in the char pot, deposited in the primary reactor body and transfer line, left in the condenser and ESP after ethanol washing and those present in the liquid product.
[b]Secondary solid represents all solid particles in the secondary reactor including char fines, compounds condensed on catalyst surface and coke formed by catalytic reaction.

It appears that the presence of the 2nd reactor with glass wool led to a reduction of approximately 5 wt% organics yield together with an increase of around 5 wt% gas yield. This is due to the thermal secondary reaction of the pyrolysis vapour when it was exposed to the heat at a longer residence time. Without the 2nd reactor, the apparent vapour residence time was about 0.7 seconds, whereas it was increased to about 2 seconds when the 2nd reactor was used. The thermal cracking may also take place when the vapour was in contact with the glass wool, thus producing more gases. When comparing the yields of individual gases (Table 8-2), it is apparent that all gaseous products except H_2 were increased by the thermal cracking reactions. Nevertheless, according to the volumetric gas composition (Figure 8-2), the concentrations of CO_2 and H_2 decreased with the increases in the proportion of CO

Table 8-2 Yields of individual gases (wt % on dry biomass basis) from catalytic pyrolysis of cassava rhizome

Catalyst	CO	CO_2	H_2	CH_4	C_2H_6	C_2H_4	C_3H_8	C_3H_6
Non-catalytic without 2nd reactor	2.72	6.80	0.06	0.32	0.07	0.05	0.02	0.05
Non-catalytic with 2nd reactor	5.14	9.04	0.02	0.65	0.12	0.17	0.04	0.14
Criterion-534	7.22	12.67	0.24	1.13	0.22	0.22	0.08	0.45
Ash	4.69	10.43	0.07	0.72	0.16	0.11	0.05	0.13
Copper Chromite	4.26	9.50	0.05	0.61	0.11	0.10	0.04	0.09
ZSM-5	7.22	9.63	0.04	0.59	0.12	0.89	0.11	1.13
MI-575	4.86	10.29	0.06	0.73	0.13	0.12	0.04	0.11
Al-MCM-41	4.72	9.95	0.26	0.54	0.12	0.12	0.04	0.15
Al-MSU-F	4.29	7.85	0.02	0.42	0.09	0.09	0.03	0.10
Criterion-534/ZSM-5	8.95	13.30	0.14	1.25	0.24	0.86	0.11	1.33
Al-MSU-F/ZSM-5	4.76	9.07	0.05	0.56	0.12	0.25	0.06	0.21

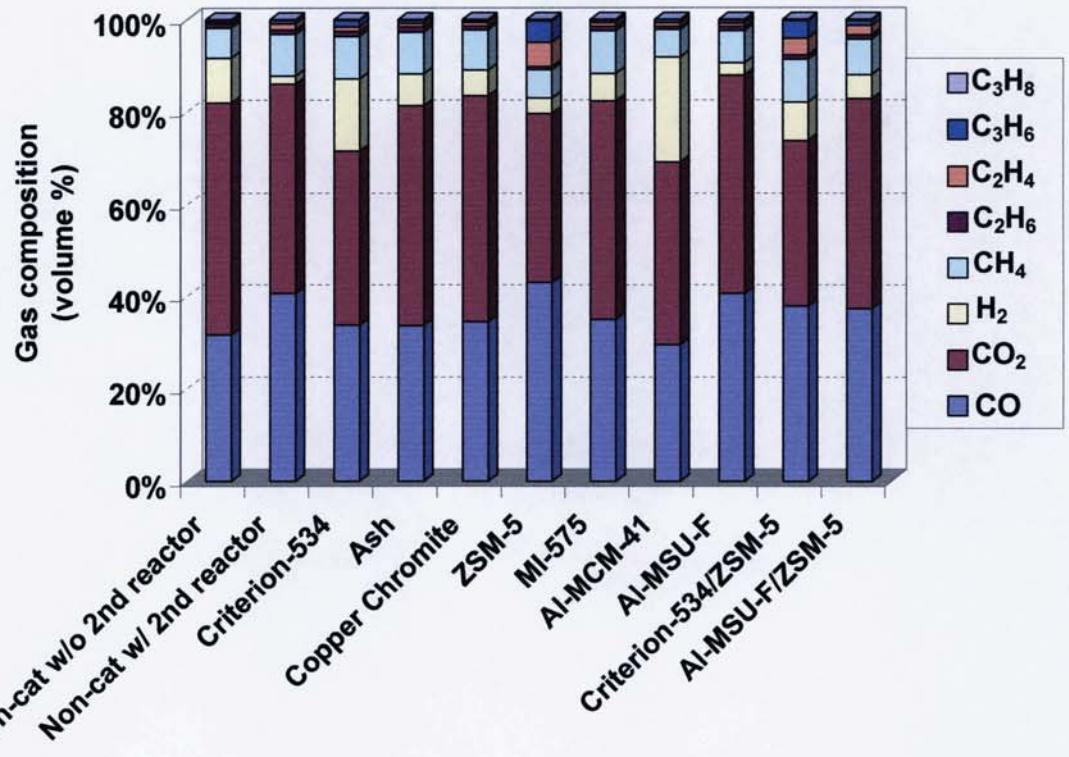

Figure 8-2 The effect of catalysts on volumetric gas composition

and hydrocarbon gases when the 2nd reactor was introduced. These results are consistent with earlier findings in section 7.2 where the thermal cracking took place by the increase of pyrolysis temperature (See Figure 7-1 and Figure 7-2). Another obvious difference in the product yields of these two non-catalytic runs is the existence of the secondary solid, which was calculated from the weight before and after the run of the 2nd reactor filled with the glass wool. In addition, the changes in the yields of reaction water and primary solid with the presence of the 2nd reactor are negligible.

To observe the effect of catalysts on pyrolysis product yields, the non-catalytic with 2nd reactor run is used as reference in stead of the one without the 2nd reactor. It can be seen from Table 8-1 that the presence of catalyst led to a significant change in product distribution. One of the most important and desired product in catalytic pyrolysis of biomass is liquid bio-oil, especially the organics fraction. The organics yield was increased with some catalysts such as copper chromite, MI-575 and Al-MSU-F, whereas the others led to the decrease in the yield. The increase in the organics yield took place at the expense of the primary solid for copper chromite and MI-575, whereas the change in organics yield with Al-MSU-F was very small. The primary solid represents all solid particles collected in the reactor unit excluding the 2nd reactor zone plus those present in the liquid bio-oil. The reduction of the primary solid due to the catalytic activity of copper chromite and MI-575 was in fact associated mainly with the decrease in the solid particles of the bio-oil (see Table 8-3). The solid in bio-oil are composed of char fines entrained from the primary reactor and the solid or high molecular weight waxy materials that could not be dissolved in ethanol at room temperature. It is expected that most of the char fines should be captured in the 2nd reactor. Therefore, the catalytic effect of copper chromite and MI-575 could be linked to the reduction of the high molecular weight compounds insoluble in ethanol. The high molecular weight material can be formed upon condensation by polymerization of the highly reactive smaller compounds present in the pyrolysis vapours [33]. Consequently, the catalysts may be involved in the transformation of the highly reactive compounds into the less reactive ones which on condensation tend not to polymerise to form high molecular weight material.

Among the catalysts that led to the reduction of organics yields, the ash, Al-MCM-4 and Al-MSU-F/ZSM-5 can be regarded as mild catalysts, whereas the Criterion-534, ZSM-5 and Criterion-534/ZSM-5 can be considered as strong catalysts based on the severity of the organics yield reduction. The decrease in the organics yield due to the catalytic effect of ash occurred simultaneously with the increases of the reaction water and gases. Therefore, the possible reactions that could be involved in the catalytic activities on the surface of the metals present in the ash (K, Na, P, Ca, Mg.Cl and Cu) were dehydration and cracking. The cracking ability of ash is also known from its effectiveness in tar decomposition during catalytic gasification [145-147]. It is important to notice that although the overall yield of gaseous products was increased by the ash, the yields of certain individual gases (see Table 8-2) such as CO, C_2H_4 and C_3H_6 decreased. This therefore leads to the different gas composition as can be seen from Figure 8-2. For the yields of solids when applying ash as catalyst, the primary solid decreased, while the secondary one increased slightly. The decrease in the primary solid yield owing to the catalytic activity of ash was similar to the case of copper chromite and MI-575 as mentioned above, which is due to the decrease in the bio-oil solids content (See Table 8-3). The slight increase of the secondary solid is due to the char deposition on the catalysts.

In the case of Al-MCM-41 catalyst, the reduction in the yields of organics and reaction water was observed together with the increase in the yields of primary and secondary solids, while the overall gas yield was barely changed. The decrease in organics and reaction water yields by Al-MCM-41 were also reported by Antonakou el al [87] when Lignocel beech wood was pyrolysed in a fixed-bed reactor. However, when miscanthus was used as feedstock, they found that the reaction water yields were increased and the organics yields were decreased. The reduction of the organics yields when CR was used as feedstock may be related mainly to the large increase (ca 5 wt%) in the yield of primary solid. Experimental data showed that the major difference in the primary solid yields between the Al-MCM-41 and the non-catalytic with 2^{nd} reactor tests was derived from the solids stuck on the wall of the electrostatic precipitator after vigorous washing with ethanol. The yields of these solids from non-catalytic with 2^{nd} reactor and Al-MCM-41 runs were 0.83 wt% and 5.63 wt% (on dry biomass fed basis), respectively. The 4.5 wt% increase is believed to be the high molecular weight material formed during the condensation of the pyrolysis vapour.

This phenomenon is opposite to the case of copper chromite and MI-575 as mentioned earlier. It is noteworthy to observe from Table 8-1 and Table 8-2 that although the gas yield was hardly changed by the use of Al-MCM-41 catalyst, the yields of some individual gases were affected by the catalyst. One of the most important changes was a dramatic increase in the yield of H_2, which occurred in conjunction with the decreases of reaction water and CO yields as well as an increase in CO_2 yield. This may be an indication of a water-gas shift reaction taking place on the Al-MCM-41 catalyst, which normally occurs over Fe-based catalysts.

Another catalytic run that resulted in a small reduction of organics yield employed a set of two catalysts, namely Al-MSU-F and ZSM-5. The main effects of this set of catalysts on product yields were a decrease of organics and a small increase of reaction water. Although the overall gas yield was decreased slightly, some gas species such as H_2 and $C_2 - C_3$ hydrocarbons were increased in concentration. However, since the mass balance closure of this run was slightly low (92.85 wt%) compared to others (94.6 – 98.50 wt%), the findings may be inconclusive.

Regarding the strong catalysts that led to drastic decreases in organics yields (Criterion-534, ZSM-5 and Criterion-534/ZSM-5), it can be noticed from the mass balance summaries (Table 8-1) that the reduction of organics yields occurred together with the increase of reaction water, secondary solid and gases. This suggests that the primary pyrolysis vapours underwent severe dehydration and cracking reactions over the catalysts that were deactivated by catalytically-formed coke and/or compounds condensed on the catalysts surface. It is obvious from the data that the extent of the dehydration reactions was similar among the three catalytic runs leading to the yields of reaction water in the range of 19.18–20.57 wt%, whereas the extent of the cracking reactions was highest in the case of two-stage catalytic process, indicating an evidence of a synergy between the two catalysts. Moreover, when using the two catalysts in series, the secondary solid yield could be decreased. The yields of primary solid differed slightly among the tests. It is important to state that the low organics yields (23-28 wt%) obtained from these strong catalysts may not look promising for pyrolysis liquid production, but if the organics are composed of products of higher value, they can be more promising than the low value high quantity products. According to Table 8-2 the yields of nearly all individual gases were increased by the

strong catalysts. In comparison with all catalytic pyrolysis runs, the Criterion-534/ZSM-5 gave highest yield of all individual gases except H_2 as the highest yield of H_2 was obtained with Al-MCM-41. Based on the volumetric gas composition (Figure 8-2), the Criterion-534 favoured the production of H_2, whereas ZSM-5 favoured the production of olefins (C_2H_4 and C_3H_6). The olefins are believed to be the intermediate products during liquid hydrocarbon synthesis with ZSM-5 zeolite. Therefore, recycling the gas stream, which contains high proportion of olefins during catalytic pyrolysis with ZSM-5 would be beneficial for liquid hydrocarbon yields. It was suggested by Diebold and Scahill [148] that the increase in the gasoline-range liquid hydrocarbons yields if the olefins were recycled is not only due to the conversion of the olefins to aromatics, but also due to the release of hydrogen in the aromatisation process which could help counter coke forming (dehydrogenation) reactions.

8.3 CHARACTERISATION OF BIO-OILS

To investigate the properties of bio-oils produced from catalytic pyrolysis runs in comparison to non-catalytic pyrolysis runs, all bio-oils were characterised using various analytical techniques in order to determine water and solids contents, basic elemental composition (C,H,N and O), heating values (HHV and LHV), molecular weight distribution, stability and chemical compounds (by GS/MS). It must be pointed out that the liquid samples subjected to the analyses were the proportionate mixtures of all fractions as previously called "Liq" (section 6.4.1.4). Therefore, the results are reported on solvent-free basis.

8.3.1 Water content

Table 8-3 summarises the water content (wt%) of the catalytic and non-catalytic bio-oils. It is important to note that the water contents in Table 8-3 are different from the reaction water yields in Table 8-1 as they have been calculated on the different basis, which includes moisture from the biomass feedstock. Although the reaction water yield of the non-catalytic with 2nd reactor run were lower than that of the non-catalytic run without 2nd reactor, the water content of the bio-oil produced from non-catalytic

pyrolysis run with 2nd reactor appeared to be higher. This is simply due to the lower organics yield of the non-catalytic with 2nd reactor.

Table 8-3 Water and solids contents (wt %) of bio-oils produced from catalytic pyrolysis of cassava rhizome

Catalyst	Water content	Solids content
Non-catalytic without 2nd reactor	31.60	3.13
Non-catalytic with 2nd reactor	33.29	3.08
Criterion-534	50.17	2.84
Ash	38.18	1.66
Copper Chromite	33.48	1.39
ZSM-5	49.87	0.90
MI-575	33.51	0.76
Al-MCM-41	32.43	4.86
Al-MSU-F	30.87	2.29
Criterion-534/ZSM-5	52.44	2.74
Al-MSU-F/ZSM-5	35.59	4.11

Water content is one of the criteria generally used for assessing the quality of bio-oils. Regardless of its complex relationship with other properties such as viscosity, flow and burning characteristics, density and pH, bio-oils of better quality should contain less water. According to Table 8-3 most of the catalysts increased the bio-oils water content, but the mesoporous alumino-silicate materials (Al-MCM-41 and Al-MSU-F) are the exceptions. The water content of the catalytic bio-oil ranged from 30.87 wt% (Al-MSU-F) to 52.44 wt% (Criterion-534/ZSM-5). The changes in the water content by the use of catalysts were rather small in most cases except that when Criterion-534, ZSM-5 and Criterion-534/ZSM-5 catalysts were employed, about half of the liquid products weight was dominated by water. The high proportion of water (>30 wt%) in bio-oil can lead to phase separation [31]. Since the liquid products collected by the 150 g/h rig were initially fractionated into 5 portions, only the fractions collected without the use of solvent (Pot 1 and Pot 2+3 oils) could be logically observed for their phase separation. The photographs of all Pot 1 oils and two selected Pot 2+3 oils are displayed in Figure 8-3. As can be seen, all of the liquid products except for the Pot 2+3 oil of the Criterion-534/ZSM-5 run were single phase. The top phase of the Pot 2+3 oil from Criterion-534/ZSM-5 run was oil-like liquid containing largely hydrocarbons, which could not be dissolved in the aqueous bottom phase. Because the water contents of the catalytic bio-oils (>31 wt%) were higher than the maximum

values allowed to meet the specifications for using bio-oils in boilers and diesel engines (27 wt%) as well as in gas turbines (25 wt%) [31], utilisation of techniques for reducing the water content is required. Some possible and promising techniques have already been discussed in section 7.3.1.

8.3.2 Solids content

The solids present in pyrolysis liquids are detrimental to their uses in various equipment, especially in injectors and turbine blades and also result in higher particulate emission [31]. The bio-oils of lower solids content can therefore be regarded as of better fuel quality if other properties do not differ significantly. The solids content of all catalytic bio-oils in comparison to those of the non-catalytic ones are listed in Table 8-3. It can be seen that the majority of the catalytic materials led to a reduction of the solids content. However, the opposite is true when the primary pyrolysis vapours were passed over the Al-MCM-41 and Al-MSU-F/ZSM-5 catalysts. According to the data in Table 8-3, ZSM-5 and MI-575 catalysts appeared to be the most promising for reducing the solids content of the bio-oils as they could lower the solids content from more than 3 wt% (without any catalyst) to less than 1 wt%. Nevertheless, the solids contents of the catalytic bio-oils are still too high to meet the specifications for using bio-oils in boilers and gas turbines (<0.05 wt%) [31]. The changes in the solids content of the bio-oils by the presence of the catalytic secondary reactor could be attributed to two reasons.

First, the catalytic bed together with the two (or three in the case of two-stage process) glass wool plugs (one at the bottom and the other on top of the catalytic bed) functioned as a filtration unit for capturing the char fines entrained from the primary reactor. The unit may not be so efficient in filtration that all char fines could be removed as it has not been designed specifically for this purpose. It is consequently suggested for future work that the catalytic secondary reactor should be designed in the way that it can efficiently filter the char fines apart from inducing the secondary reactions. This unit can be therefore called catalytic filter and serve two functions simultaneously.

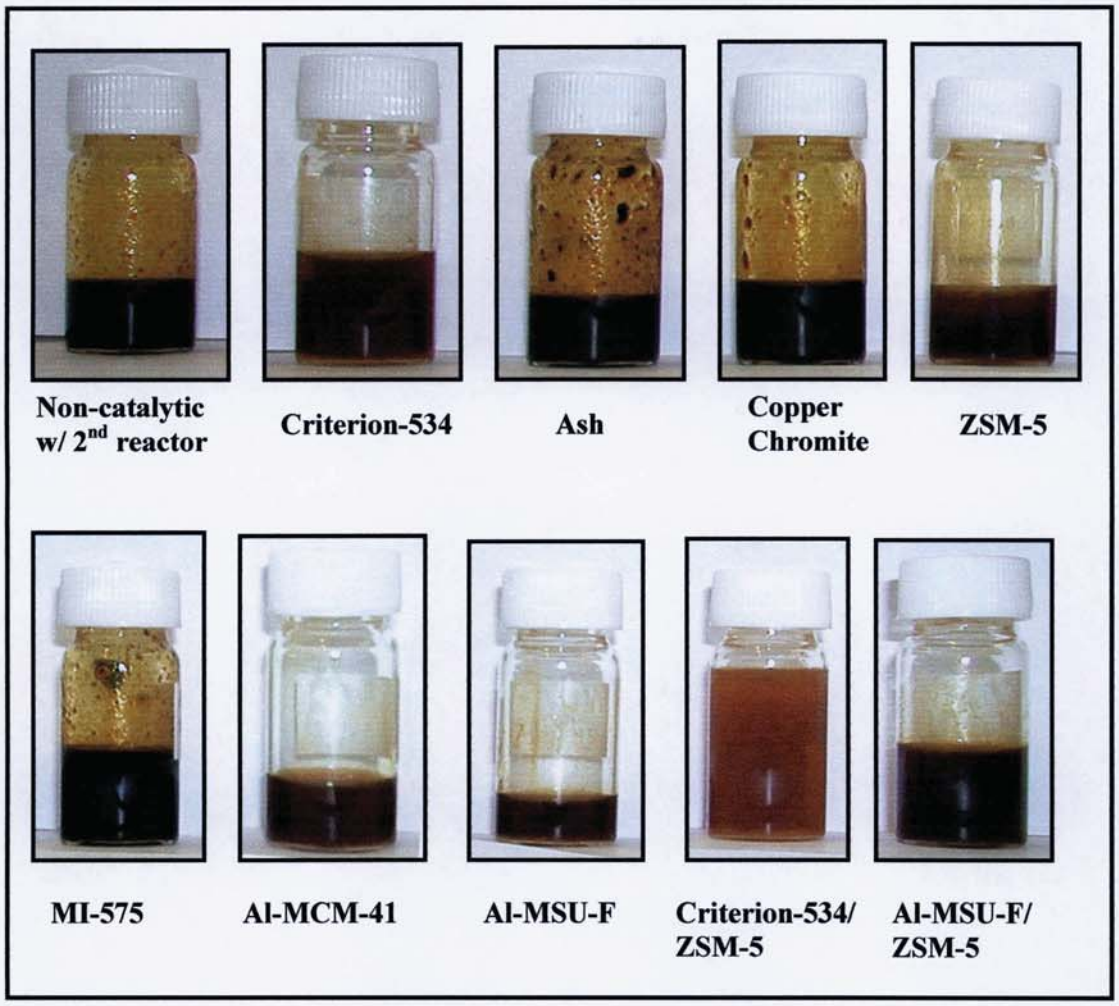

(a)

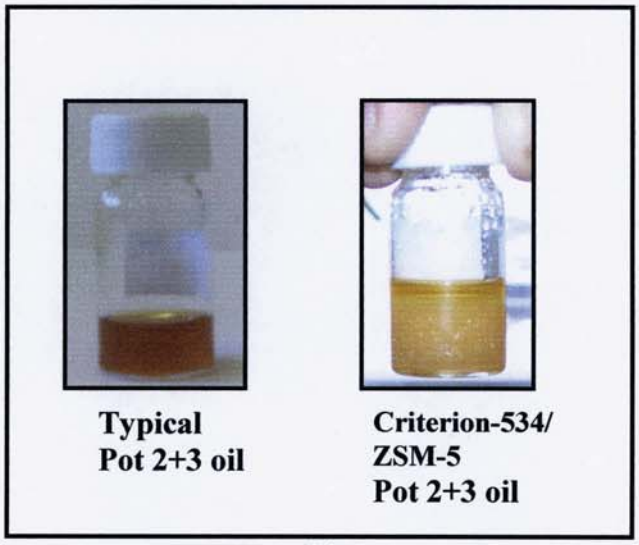

(b)

Figure 8-3 Photographs of fresh Pot 1 (a) and Pot 2+3 (b) oils produced from fast pyrolysis of cassava rhizome with different catalysts

Second, the reactions that took place on the catalyst beds could affect the reactivity toward re-polymerisation on condensation of the small species or radicals, which could lead to the formation of high molecular weight materials, which could ultimately become solid.

8.3.3 Elemental composition and heating values

Table 8-4 shows the elemental analysis of the pyrolysis liquids before and after catalysis. The main interest of this analysis lies in the oxygen content. As can be seen from the table, the presence of the secondary reactor itself caused a reduction in the oxygen content (from 38.59 wt% to 36.22 wt%). The oxygen content was reduced further to 23.30-35.38 wt% by the use of catalyst or set of catalysts. The different catalysts studied showed a wide range of the ability to deoxygenate the pyrolysis vapours. Among these, the Criterion-534 demonstrated a far higher performance in deoxygenation than the other catalysts including a well-known effective cracking and deoxygenating catalyst like ZSM-5. Based on the oxygen content of the bio-oils, the effectiveness of the catalysts in deoxygenation can be ranked as Criterion-534 >> Criterion-534/ZSM-5 > Al-MCM-41 > MI-575 > Al-MSU-F/ZSM-5, Al-MSU-F > ZSM-5 > Ash > Copper chromite. One possible reason why such a strong catalyst as ZSM-5 could not significantly reduce the oxygen content of the bio-oil compound to others is that the carbon and hydrogen were simultaneously removed in large quantities in the forms of hydrocarbon gases, carbon oxides and water, leading to a proportionate reduction of carbon, hydrogen and oxygen instead of selectively rejecting the oxygen.

Table 8-4 Elemental composition and heating values of bio-oils produced from catalytic pyrolysis of cassava rhizome

Catalyst	Elemental composition (wt %, dry basis)					HHV (MJ/kg)		LHV (MJ/kg)	
	C	H	N	O	Ash	Wet basis	Dry basis	Wet basis	Dry basis
Non-catalytic without 2nd reactor	53.09	7.27	0.81	38.59	0.23	15.80	23.10	13.94	21.51
Non-catalytic with 2nd reactor	56.14	7.14	0.44	36.22	0.23	16.18	24.26	14.3	22.70
Criterion-534	71.54	4.01	0.87	23.30	0.28	13.59	27.27	11.93	26.39
Ash	56.81	7.88	1.02	34.15	0.13	15.80	25.56	13.81	23.85
Copper Chromite	56.07	7.81	0.63	35.38	0.10	16.70	25.11	14.75	23.40
ZSM-5	56.35	9.30	0.57	33.70	0.09	13.60	27.13	11.37	25.10
MI-575	59.97	6.96	0.53	32.24	0.06	17.15	25.82	15.32	24.28
Al-MCM-41	58.01	9.16	0.79	31.67	0.36	18.75	27.75	16.61	25.76
Al-MSU-F	56.98	8.73	1.06	33.06	0.17	18.48	26.74	16.41	24.83
Criterion-534/ZSM-5	58.15	9.31	1.40	30.85	0.29	13.34	28.05	11.10	26.02
Al-MSU-F/ZSM-5	58.01	7.97	0.65	33.05	0.32	16.88	26.20	14.89	24.47

It has been reported in literature [66, 67, 71-73] that ZSM-5 catalyst was highly effective in removing oxygen from the pyrolysis oils as the oxygen content of the oils was reduced from about 33 wt% (without the catalyst) to less than 6 wt% with the catalyst [66, 67, 72] when mixed wood wastes were used as feedstock. In addition, when pyrolysing rice husk samples, the oils obtained before catalysis contained 40.2 wt% oxygen content and after catalytic upgrading with ZSM-5 at 500°C, the oxygen content of the oil was dropped to 8.1 wt% [73]. It is imperative to point out the reason why the oxygen content of the ZSM-5 catalyzed bio-oil in the current work was not as low as in the literature. This is simply because the pyrolysis liquids subjected to the elemental analysis in the present work included all liquid fractions, whereas in the literature [66, 67, 72, 73] the authors separated the aqueous and oil phases. The oxygen in the oil phase after catalysis was partly transferred into or enriched in the aqueous phase rather than entirely being removed from the liquid products. When calculating the overall oxygen content of the pyrolysis liquid (a mixture of aqueous and oil fraction) by using the yields and the oxygen content data of each fraction given in reference [66], it was found that the oxygen content was decreased from 38.85 wt% (without catalyst) to 26.51 wt% (with ZSM-5). This is still slightly better than the current study in terms of deoxygenation activity of the ZSM-5. A further explanation for the different results involved the biomass to catalyst ratio. In the

present study, approximately 100 g of biomass was fed into the system and the pyrolysis vapour evolved was passed over a fixed-bed of 100 g of ZSM-5 catalyst. This leads to a biomass/catalyst mass ratio of 1.0, whereas in the literature [66] this ratio was calculated to be around 0.5 (calculated from 200 g of catalyst used, 30 minutes experimental run time and biomass feed rate of 0.216 – 0.228 kg/h). This explains well the difference between the results obtained in the previous work [66] and the current study. The high biomass to catalyst ratios in this work (0.9 -1.0 for Criterion-534, Copper chromite, ZSM-5, MI-575 and Al-MSU-F/ZSM-5 runs, and 4.3 – 4.9 for the tests with light catalytic materials such as ash, Al-MCM-41 and Al-MSU-F) could lead to complete deactivation of the catalysts before the end of the run. As a consequence, the pyrolysis products were mixtures of genuinely catalytic and apparently non-catalytic products. It is therefore suggested for further work that the effect of biomass/catalyst ratio on yields and properties of pyrolysis products should be carried out for each catalyst.

Based on the basic elements (C, H, N and O) and ash contents, the heating values of bio-oils, both higher heating value (HHV) and lower heating value (LHV), have been calculated and the results on wet and dry bases are shown in Table 8-4. With regards to the non-catalytic pyrolysis runs, the presence of the secondary reactor slightly increased the heating values of the CR bio-oil (~1 MJ/kg on dry basis). The heating values (HHV and LHV) on dry basis were increased further by all of the catalysts studied. However, on wet or as produced basis, the heating values of bio-oils produced with Criterion-534, ZSM-5 and Criteion-534/ZSM-5 were significantly reduced, while those of ash-catalysed bio-oil decreased marginally. It is important to observe that the strong catalysts (Criterion-534, ZSM-5 and Criterion-534/ZSM-5) had relatively high HHV and LHV on dry basis (27.13 – 28.05 MJ/Kg for HHV and 25.10 – 26.39 MJ/Kg for LHV). This implies that if the bio-oils produced with these catalysts are to be used as fuel, water separation process is necessary. This process can be very simple if the bio-oils are separated into oil and aqueous phases. In fact, there is an evidence for the phase separation of bio-oils produced with Criterion-534/ZSM-5 (see Figure 8-3 (b)). On wet basis, the bio-oil produced with copper chromite, MI-575, Al-MCM-41, Al-MSU-F and Al-MSU-F/ZSM-5 had higher HHV and LHV than non-catalytic bio-oils. This indicates a clear improvement in terms of heating values by the activities of the catalysts.

By using the yields and heating values (HHV, dry basis) of the pyrolysis products in conjunction with the HHV (dry basis) of cassava rhizome, the energy yields or energy distribution of liquid, solid and gaseous products have been calculated. The results were depicted in Figure 8-4. As can be seen, the energy yield of liquid was enhanced by copper chromite MI-575, Al-MCM-41 and Al-MSU-F. The use of ash and Al-MSU-F/ZSM-5 led to a small reduction of the liquid energy yield. For strong catalysts (Criterion-534, ZSM-5 and Criterion-534/ZSM-5), considerable amount of energy in the liquid was transferred into solid and gas. It is therefore suggested for catalytic pyrolysis with these strong catalysts that the energy stored in the solid and gas should be carefully exploited.

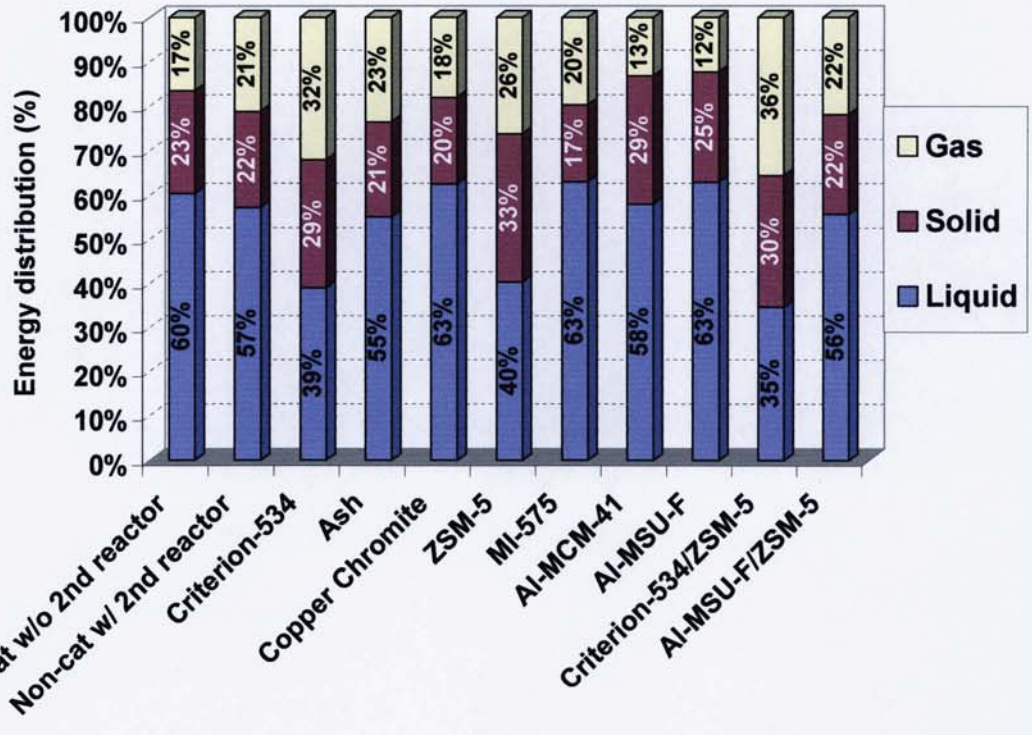

Figure 8-4 Distribution of energy from biomass feedstock to pyrolysis products

8.3.4 Molecular weight distribution and stability

One of the purposes of catalytic pyrolysis is to improve bio-oil quality in terms of viscosity. Lower viscosity renders bio-oil easier to be pumped, injected and atomised. Viscosity of bio-oil is known in literature [5, 32] to be directly related to the average molecular weight. Since viscosity measurement requires relatively large amount of samples and the liquid products obtained in this study were limited in quantity, the molecular weight analysis by GPC technique has been performed instead. It is speculated that bio-oil of lower molecular weight would have lower viscosity.

The nine catalytic bio-oils plus two non-catalytic bio-oils were subjected to GPC analysis. The results are summarised in Table 8-5. For non-catalytic oils, the presence of the 2nd reactor lowered the initial molecular weight of bio-oil (both Mw and Mn) and narrowed the molecular weight distribution as noticed from the lower polydispersity index (PD). This could be due to the secondary thermal cracking of the pyrolysis vapour, which also caused the production of gases and the reduction of organics as discussed earlier in section 8.2. The molecular weight was reduced further by catalytic reactions. Based on the extent of the Mw reduction, the catalysts can be divided into three groups. The catalysts that hardly affect the Mw of bio-oils included Criterion-534, ash and MI-575. Copper chromite and mesoporous alumino-silicate materials (Al-MCM-41 and Al-MSU-F) induced a decrease in the Mw of bio-oil, but the effect was less pronounced than when ZSM-5 was involved. In other words, the ZSM-5, Criterion-534/ZSM-5 and Al-MSU-F/ZSM-5 runs led to a significant reduction of bio-oil Mw compared to others. This confirmed the effective cracking characteristic of ZSM-5 catalyst. According to the Mw results of the fresh bio-oils, it can be concluded regardless of the water content that most of the catalysts studied have potential for improving the initial viscosity of the bio-oils.

Table 8-5 Molecular weight of fresh and stored bio-oils produced from catalytic pyrolysis of cassava rhizome

Catalyst	Fresh[a]			6 months old			Stability
	Mw[b]	Mn[c]	PD[d]	Mw[b]	Mn[c]	PD[d]	(g/mol-day)
Non-catalytic without 2nd reactor	385	252	1.53	ND[e]	ND[e]	ND[e]	N/A
Non-catalytic with 2nd reactor	377	250	1.50	468	263	1.78	0.51
Criterion-534	377	257	1.47	412	252	1.63	0.19
Ash	374	247	1.51	459	263	1.75	0.47
Copper Chromite	365	251	1.45	451	265	1.70	0.48
ZSM-5	337	213	1.58	451	265	1.70	0.63
MI-575	376	257	1.46	465	266	1.75	0.49
Al-MCM-41	362	248	1.46	458	261	1.75	0.53
Al-MSU-F	357	237	1.51	478	258	1.85	0.67
Criterion-534/ZSM-5	332	230	1.44	454	247	1.84	0.68
Al-MSU-F/ZSM-5	338	234	1.44	476	258	1.84	0.77

[a]Fresh samples were measured 1 day after production.
[b, c, d]Mw, Mn, PD refer to weight average molecular weight, number average molecular weight and polydispersity index, respectively.
[e]ND represents not determined.

The bio-oil products may not be utilised immediately after production as they may be stored and transported to the end-users. The ability of bio-oils to maintain their properties after production is consequently of great importance. This ability is known as bio-oil stability, which is normally calculated from the viscosity change after storage at a certain temperature for a certain period of time. Nevertheless, in this study, the average molecular weights of bio-oils were determined after storing bio-oils at room temperature for 6 months and the stability has been calculated according to Equation 6-3. The results are shown in Table 8-5. It can be seen that all of the weight average molecular weight (Mw) and nearly all of the number average molecular weight (Mn) increased after 6 month storage. Furthermore, the polydispersity indices of all bio-oil samples were higher after storage. In comparison to the non-catalytic bio-oil, the Mw of most of the stored catalytic bio-oils were still lower, but the Mw of the stored Al-MSU-F and Al-MSU-F/ZSM-5 bio-oil were higher. This suggests that the bio-oils produced with Al-MSU-F or Al-MSU-F/ZSM-5 catalysts should be utilised before 6 months. Regarding the calculated Mw stability, the most stable bio-oil was obtained with Critesion-534. It has very low Mw even after storage for 6 months. In addition, the bio-oils produced with ash, copper chromite and MI-575 showed a slight improvement in stability. Although the stability of the ZSM-5, Al-

MCM-41 and Criterion-534/ZSM-5 catalysed bio-oils appeared to be worse than that of the bio-oil produced without any catalyst, the catalytic bio-oils still had lower Mw than the non-catalytic one after 6 months of storage. This implies that the use of ZSM-5, Al-MCM-41 and Criterion-534/ZSM-5 did not actually deteriorate the bio-oil quality in terms of Mw and stability, but they rather ameliorate the bio-oil properties.

8.3.5 GC/MS analysis

In order to study the effect of catalysis on chemical composition of cassava rhizome bio-oils, GC/MS liquid injection analysis has been performed on nine catalytic bio-oil samples (Liq) plus one non-catalytic bio-oil produced with 2nd reactor. Based on the chromatogram obtained with these samples, up to 89 peaks have been identified and semi-quantified. The compounds corresponding to these chromatographic peaks are presented in Table 8-6 together with their synonyms, retention times (R/T, min), molecular formulae, molecular weights, origins and chemical groups. In comparison to Table 7-5 which shows the identified chemical compounds of non-catalytic CS and CR bio-oils, Table 8-6 includes some extra compounds that could not be identified during non-catalytic pyrolysis study, such as pentane (ID#3), xylenes (ID#20), trimethyl benzene (ID#31), benzofuran (ID#34), indene (ID#38), 1-methylindene (ID#46), 2,3,5-trimethyl phenol (ID#60), decane (ID#63), 2-methyl benzofuran (ID#71), trimethyl naphthalene (ID#76), antracene and phenanthrene (ID#85) and pyrene (ID#89). These compounds are called catalytically-formed compounds denoted as "CF" in the origin column of Table 8-6 since they are believed to be products of catalytic reactions. Nevertheless, this does not mean that without catalyst these compounds would not exist at all because they may be present in the non-catalytic bio-oil, but at lower concentration than the GC/MS detection limit.

Table 8-6 Identified chemical compounds present in bio-oils produced from catalytic pyrolysis of cassava rhizome

Peak ID	R/T (min)	Compound name/synomyms	Formula	MW	Origin[a]	Group
1	4.46	Acetaldehyde/Acetic aldehyde/Ethanal	C_2H_4O	44.05	C	Aldehydes
2	4.87	Furan/Furfuran/Furane/Oxacyclopentadiene	C_4H_4O	68.08	C	Furans
3	5.65	Pentane	C_5H_{12}	72.15	CF	Alkane
4	6.48	Butanal/Butyraldehyde	C_4H_8O	72.11	C	Aldehydes
5	6.69	2,3 Butanedione/Butanedione/Diacetyl	$C_4H_6O_2$	86.09	C	Ketones
6	6.77	2-Butanone/Butanone/.Methyl ethyl ketone (MEK)	C_4H_8O	72.11	C	Ketones
7	7.13	3-Pentanone/Pentan-3-one/Diethyl ketone (DEK)	$C_5H_{10}O$	86.13	C	Ketones
8	7.30	Benzene/Benzole/Coal naphtha/Phenyl hydride	C_6H_6	78.11	L	Aromatics
9	7.80	Hydroxyacetaldehyde/Glycolaldehyde	$C_2H_4O_2$	60.05	C	Misc. Oxygenates
10	8.77	2-Butenal (cis or trans)/Crotonaldehyde/Crotonal	C_4H_6O	70.09	C	Aldehydes
11	8.80	Isopropyl Alcohol/2-Propanol	C_3H_8O	60.10	C	Alcohol
12	9.24	Acetic acid/Ethanoic acid	$C_2H_4O_2$	60.05	C	Acids
13	10.37	1-Hydroxy-2-propanone/Hydroxypropanone/Acetone alcohol	$C_3H_6O_2$	74.08	C	Misc. Oxygenates
14	10.81	Toluene/Methylbenzene	C_7H_8	92.14	L	Aromatics
15	12.05	3-Hydroxy-2-butanone/2-Hydroxy-3-butanone	$C_4H_8O_2$	88.11	C	Misc. Oxygenates
16	13.45	Propanoic acid/Propionic acid/Ethanecarboxylic acid	$C_3H_6O_2$	74.08	C	Acids
17	14.62	Cyclopentanone/Ketocyclopentane/Pyran-2,4(3H)-dione, 3-acetyl-6-methyl-	C_5H_8O	84.12	C	Ketones
18	14.80	1-Hydroxy-2-butanone	$C_4H_8O_2$	88.11	C	Misc. Oxygenates
19	14.92	3-Hydroxypropanal (Isomer of 1-Hydroxy-2-propanone)	$C_3H_6O_2$	74.08	C	Misc. Oxygenates
20	15.30	Xylenes (o-; m- & p-)	C_8H_{10}	106.17	CF	Aromatics
21	15.52	2-Propenal/Acrylic aldehyde/Aqualin/2-Propen-1-one	C_3H_4O	56.06	C	Aldehydes
22	16.48	Furfural/2-Furaldehyde/2-Furanaldehyde/2-Furancarboxaldehyde	$C_5H_4O_2$	96.09	C	Furans
23	16.94	Butanedial/Succinaldehyde	$C_4H_6O_2$	86.09	C	Aldehydes
24	16.95	Styrene/Vinylbenzene	C_8H_8	104.15	L	Aromatics
25	17.85	3-Methyl-furan	C_5H_6O	82.10	C	Furans
26	19.96	5-Methyl-2(3H)-furanone/a-Angelica lactone/2,3-Dihydro-5-methyl-2-furanone	$C_5H_6O_2$	98.10	C	Furans/Lactones
27	20.16	2-Furanmethanol /2-Furfuryl alcohol	$C_5H_6O_2$	98.10	C	Furans
28	20.49	1-Acetyloxy-2-propanone/1-Acetoxypropane-2-one/2-Oxopropyl acetate	$C_5H_8O_3$	116.12	C	Misc. Oxygenates
29	20.77	2-Methyl-2-cyclopenten-1-one/2-Methyl-2-cyclopentenone	C_6H_8O	96.13	C	Ketones
30	21.54	1-(2-Furanyl)ethanone/Acetylfuran/ 2-Acetylfuran/Furyl methyl ketone	$C_6H_6O_2$	110.11	C	Furans

Table 8-6 (Continued)

Peak ID	R/T (min)	Compound name/synomyms	Formula	MW	Origin[a]	Group
31	21.77	Trimethyl benzene (1,2,3- & 1,2,4-)	C_9H_{12}	120.19	CF	Aromatics
32	22.12	2-Cyclopentene-1,4-dione	$C_5H_4O_2$	96.09	C	Ketones
33	23.03	3-Methyl-cyclopentanone &	$C_6H_{10}O$ &	98.14	C	Ketones
		Cyclohexanone &	$C_6H_{10}O$ &	98.14		
		Benzaldehyde	C_7H_6O	106.12		
34	23.37	Benzofuran/Benzofurfuran/Coumarone	C_8H_6O	118.14	CF	Furans
35	24.87	5-Methyl-2-furancarboxaldehyde/5-Methylfurfural/2-Formyl-5-methylfuran/2-Methyl-5-formylfuran	$C_6H_6O_2$	110.11	C	Furans
36	25.64	3-Methyl-2-cyclo-penten-1-one	C_6H_8O	96.13	C	Ketones
37	25.73	Butyrolactone/Dihydro-2(3H)-furanone/Butyric acid lactone	$C_4H_6O_2$	86.09	C	Furans/Lactones
38	25.40	Indene/1H-Indene	C_9H_8	116.16	CF	Aromatics
39	26.16	2(5H)-Furanone & 2(3H)-Furanone	$C_4H_4O_2$	84.07	C	Furans/Lactones
40	26.89	5-Methyl-2(5H)-furanone/β-Angelica lactone	$C_5H_6O_2$	98.10	C	Furans/Lactones
41	28.43	2-Hydroxy-3-methyl-2-Cyclopenten-1-one/Maple lactone &	$C_6H_8O_2$ &	112.00	C	Ketones
		2,5-Dimethylcyclopentanone	$C_7H_{12}O$			
42	29.20	Acetophenone/Acetylbenzene	C_8H_8O	120.15	L	Misc. Oxygenates
43	30.08	Phenol	C_6H_6O	94.11	L	Phenols
44	30.83	2-Methoxyphenol/Guaiacol/Guaicol	$C_7H_8O_2$	124.14	L	Guaiacols
45	31.14	3-Methylindene/3-Methyl-1H-indene	$C_{10}H_{10}$	130.19	L	Aromatics
46	31.28	1-Methylindene/1-Methyl-1H-indene	$C_{10}H_{10}$	130.19	CF	Aromatics
47	31.61	2-Methylfuran/Methylfuran/5-Methylfuran	C_5H_6O	82.10	C	Furans
48	32.10	Methyl 2-furoate/2-Furancarboxylic acid, methyl ester	$C_6H_6O_3$	126.11	C	Furans/Ester
49	32.38	o-Cresol/2-Methyl phenol	C_7H_8O	108.14	L	Phenols
50	32.80	Maltol/3-Hydroxy-2-methyl-4H-pyran-4-one	$C_6H_6O_3$	126.11	C	Misc. Oxygenates
51	33.40	Naphthalene/White tar	$C_{10}H_8$	128.17	L	Aromatics
52	33.78	4-Methyl-5H-furan-2-one/4-Methyl-2(5H)-furanone	$C_5H_6O_2$	98.10	C	Furans
53	34.03	p-Cresol/4-Methyl phenol	C_7H_8O	108.14	L	Phenols
54	34.12	m-Cresol/3-Methyl phenol	C_7H_8O	108.14	L	Phenols
55	34.21	2-Methoxy-3-methyl-phenol & 2-Methoxy-4-methyl-phenol/Creosol/4-Methylguaiacol/Homoguaiacol	$C_8H_{10}O_2$	138.17	L	Guaiacols
56	36.18	Xylenols/Dimethyl phenol (2,3-; 2,4- ; 2,5- & 2,6-)	$C_8H_{10}O$	122.17	L	Phenols

Table 8-6 (Continued)

Peak ID	R/T (min)	Compound name/synomyms	Formula	MW	Origin[a]	Group
57	38.03	Ethylphenol (2-; 3- & 4-)	$C_8H_{10}O$	122.17	L	Phenols
58	39.43	4-Ethyl-2-methoxyphenol/4-Ethyl guaiacol/4-Hydroxy-3-methoxy ethylbenzene/p-Ethylguaiacol	$C_9H_{12}O_2$	152.19	L	Guaiacols
59	40.79	1,4:3,6-Dianhydro-α-d-glucopyranose	$C_6H_8O_4$	144.13	C	Sugars
60	40.96	2,3,5-Trimethyl phenol	$C_9H_{12}O$	136.19	CF	Aromatics
61	41.87	2-Methoxy-4-vinylphenol/4-Vinylguaiacol/p-Vinylguaiacol/4-Hydroxy-3-methoxystyrene	$C_9H_{10}O_2$	150.18	L	Guaiacols
62	42.06	Biphenyl/Bibenzene	$C_{12}H_{10}$	154.21	L	Aromatics
63	42.43	Decane	$C_{10}H_{22}$	142.28	CF	Alkane
64	42.93	Eugenol/2-Methoxy-4-allylphenol/2-Methoxy-1-hydroxy-4-allylbenzene/Allylguaiacol	$C_{10}H_{12}O_2$	164.20	L	Guaiacols
65	43.08	4-Propyl guaiacol/2-Methoxy-4-propyl phenol	$C_{10}H_{14}O_2$	166.22	L	Guaiacols
66	43.10	Dimethyl naphthalene (1,5-; 1,6-; 2,3-; 2,6- & 2,7-)	$C_{12}H_{12}$	156.23	L	Aromatics
67	43.44	5-(Hydroxymethyl)-2-furancarboxaldehyde/5-(Hydroxymethyl)-2-furfural/HMF/5-(Hydroxymethyl)-2-furaldehyde	$C_6H_6O_3$	126.11	C	Furans
68	44.10	2,6-Dimethoxy phenol/Syringol/1,3-Dimethoxy-2-hydroxybenzene/Pyrogallol dimethylether	$C_8H_{10}O_3$	154.17	L	Syringols
69	44.80	1,4-Dimethyl naphthalene	$C_{12}H_{12}$	156.23	L	Aromatics
70	45.26	2-Methoxy-4-(1-propenyl)phenol/Isoeugenol,c&t/4-Propenylguaiacol/4-Hydroxy-3-methoxypropenylbenzene	$C_{10}H_{12}O_2$	164.20	L	Guaiacols
71	46.86	2-Methyl benzofuran	C_9H_8O	132.16	CF	Furans
72	47.34	2-Methoxy-4-(1-propenyl)phenol/Isoeugenol,c&t/4-Propenylguaiacol/4-Hydroxy-3-methoxypropenylbenzene	$C_{10}H_{12}O_2$	164.20	L	Guaiacols
73	47.84	1,2,3-Trimethoxybenzene/Methylsyringol	$C_9H_{12}O_3$	168.00	L	Syringols
74	48.18	Vanillin/2-Methoxy-4-formylphenol/4-Hydroxy-3-methoxybenzaldehyde	$C_8H_8O_3$	152.15	L	Guaiacols
75	48.36	Hydroquinone/1,4-Benzenediol/4-Hydroxyphenol/Dihydroxybenzene	$C_6H_6O_2$	110.11	L	Phenols
76	48.83	Trimethyl naphthalene (1,4,6-; 2,3,6 & 1,6,7-)	$C_{13}H_{14}$	170.25	CF	Aromatics
77	48.94	4-Hydroxybenzaldehyde/4-Formylphenol	$C_7H_6O_2$	122.12	L	Misc. Oxygenates
78	49.35	Resorcinol/1,3-Benzenediol	$C_6H_6O_2$	110.11	L	Phenols
79	51.38	1-(4-Hydroxy-3-methoxyphenyl)ethanone/Acetoguaiacone	$C_9H_{10}O_3$	166.18	L	Guaiacols

Table 8-6 (Continued)

Peak ID	R/T (min)	Compound name/synomyms	Formula	MW	Origin[a]	Group
80	53.28	1-(4-hydroxy-3-methoxyphenyl)-2-Propanone/Guaiacylacetone/Vanillyl methyl ketone/4-Hydroxy-3-methoxyphenyl acetone	$C_{10}H_{12}O_3$	180.20	L	Guaiacols
81	55.70	9-Methyl-9H-fluorene/9-Methylfluorene	$C_{14}H_{12}$	180.25	L	Aromatics
82	56.69	1,6-Anhydro-β-D-glucopyranose/Levoglucosan	$C_6H_{10}O_5$	162.14	C	Sugars
83	57.67	Methoxyeugenol/2,6-Dimethoxy-4-(2-propenyl)-phenol	$C_{11}H_{14}O_3$	194.23	L	Guaiacols
84	58.72	4-Hydroxy-3,5-dimethoxybenzaldehyde/Syringaldehyde/Syringe aldehyde/Cedar aldehyde	$C_9H_{10}O_4$	182.18	L	Syringols
85	59.10	Anthracene & Phenanthrene	$C_{14}H_{10}$	178.23	CF	Aromatics
86	61.07	1-(4-Hydroxy-3,5-dimethoxyphenyl)ethanone/Acetosyringone/3,5-Dimethoxy-4-hydroxyacetophenone/Acetosyringon	$C_{10}H_{12}O_4$	196.20	L	Syringols
87	61.30	4-(3-Hydroxy-1-propenyl)-2-methoxy phenol/Coniferol/Coniferyl alcohol	$C_{10}H_{12}O_3$	180.20	L	Guaiacols
88	62.00	1,6-Anhydro-β-D-glucofuranose	$C_6H_{10}O_5$	162.14	C	Sugars
89	70.59	Pyrene	$C_{16}H_{10}$	202.26	CF	Aromatics

[a]C, L and CF refer to carbohydrate, lignin and catalytically-formed compounds, respectively.

Regarding the compounds origin suggested in Table 8-6, it is imperative to state that due to the catalytic reactions certain compounds, for example benzene, toluene and xylenes, could be derived not only from lignin polymer, but also from carbohydrate fraction. Cellulose and hemicellulose could be thermally decomposed giving off olefinic gases, which could then be catalytically transformed to aromatic hydrocarbons by, for instance, ZSM-5 catalyst. Therefore one should be aware that the origins provided in Table 8-6 are not conclusive, but speculative based on non-catalytic pyrolysis.

After integration of the 89 peaks, the peak areas obtained have been calculated further to percentage values and the results are shown in Table 8-7. Since this table contains huge amount of multivariate data, which are composed of useful information and noise of data, the principal component analysis (PCA) technique has been applied with the aims of extracting the useful information as well as leaving the data noise behind. Several PCA models have been established using catalysts as samples and peak IDs as variables. To observe an overview of the chemical compounds distribution with different catalysts, a PCA model was set up with all catalysts studied and all compounds identified. The resultant score and loading plots of the PC1 and PC2 for this model are displayed in Figure 8-5. As can be seen from the score plot (map of catalyst samples) in Figure 8-5 (a), the catalysts that significantly changed the liquid product distribution are Criterion-534/ZSM-5, ZSM-5 and Criterion-534 as they lie far away on PC1 axis from other samples, especially the non-catalytic one. These catalysts were also found earlier to be very active according to the mass balance, water content, elemental composition, heating values and molecular weight distribution.

Table 8-7 Chromatographic peak area percentages of the compounds identified from bio-oils produced from catalytic pyrolysis of cassava rhizome

Peak ID	Non-cat w/ 2nd	Criterion	Ash	Copper Chromite	ZSM-5	MI-575	MCM	MSU	Criterion/ ZSM-5	MSU/ ZSM-5
1	1.50	2.27	1.82	1.75	1.25	2.05	0.64	1.82	2.95	1.76
2	0.00	0.00	0.52	1.08	0.31	0.00	0.36	0.65	0.40	0.00
3	0.00	0.00	0.00	0.21	0.00	0.27	0.23	0.06	0.00	0.11
4	0.09	0.10	0.14	0.08	0.00	0.13	0.07	0.05	0.00	0.05
5	1.63	1.28	1.52	2.22	1.02	2.39	1.39	1.72	1.57	1.38
6	0.54	1.69	0.70	0.00	0.40	0.00	0.21	0.24	1.26	0.48
7	0.00	0.00	0.11	0.31	2.49	0.00	0.12	0.26	0.02	0.23
8	0.08	0.64	0.00	0.00	0.55	0.06	0.00	0.00	2.88	0.09
9	1.23	1.00	0.93	1.76	1.07	1.75	1.79	1.40	0.70	1.12
10	0.68	0.56	0.55	0.74	0.00	0.71	0.52	0.58	0.44	0.55
11	0.00	0.00	0.00	0.00	0.13	0.00	0.00	0.00	0.00	0.00
12	19.16	16.32	12.90	20.70	14.96	17.50	19.30	17.54	13.96	15.25
13	11.85	7.45	9.72	13.01	6.58	11.97	13.08	11.27	6.43	10.10
14	0.00	1.31	0.00	0.00	1.26	0.00	0.00	0.00	6.27	0.64
15	0.25	0.00	0.35	0.00	0.00	0.00	0.00	0.24	0.00	0.00
16	0.20	0.23	0.18	0.19	0.21	0.05	0.12	0.28	0.13	0.09
17	0.00	0.21	0.17	0.13	0.03	0.11	0.10	0.14	0.10	0.20
18	0.27	0.28	0.30	0.24	0.21	0.27	0.35	0.42	2.11	0.22
19	5.26	5.23	3.22	5.93	4.14	6.85	7.45	4.83	2.01	1.34
20	0.00	0.33	0.00	0.00	0.89	0.00	0.00	0.00	3.37	0.16
21	0.00	0.00	0.21	0.00	0.00	0.00	0.11	0.00	0.00	0.00
22	4.50	5.34	0.35	4.74	1.57	0.39	2.34	2.99	2.83	0.21
23	0.48	0.22	0.35	0.91	1.23	0.87	1.33	0.85	0.24	0.88
24	0.00	0.00	0.00	0.00	0.97	0.00	0.00	0.00	0.54	0.00
25	0.00	0.26	4.83	0.00	0.00	4.10	0.00	0.00	0.08	0.05
26	0.41	0.30	0.37	0.41	0.07	0.47	0.43	0.40	0.30	0.39
27	0.52	0.38	0.45	0.62	0.43	0.51	0.64	0.56	0.33	0.45
28	1.27	0.93	0.87	1.37	0.82	1.35	1.39	1.41	0.90	1.10
29	0.86	1.30	0.91	0.98	0.67	0.83	1.17	1.07	0.80	0.88
30	0.27	0.14	0.12	0.29	0.07	0.21	0.26	0.14	0.00	0.15
31	0.00	0.19	0.00	0.00	0.36	0.00	0.00	0.00	0.65	0.00
32	0.45	0.33	0.33	0.46	0.14	0.41	0.53	0.49	0.29	0.34
33	2.85	3.09	1.82	3.66	1.97	3.38	5.13	3.33	1.53	3.12
34	0.00	0.08	0.00	0.00	0.00	0.00	0.00	0.00	1.03	0.00
35	0.23	0.42	0.50	0.24	0.06	0.23	0.27	0.41	0.19	0.16
36	0.27	0.82	1.45	0.91	0.08	0.28	0.72	0.16	0.40	0.68
37	0.62	0.77	0.00	0.00	0.26	0.49	0.34	0.61	0.00	0.20
38	0.00	0.00	0.00	0.00	0.20	0.00	0.00	0.00	1.21	0.00
39	1.68	1.87	1.41	2.04	1.33	1.85	2.30	1.71	1.35	1.75
40	0.48	0.25	0.29	0.34	0.15	0.39	0.41	0.56	0.43	0.42
41	3.04	3.00	2.08	2.71	2.14	2.85	4.14	1.49	2.70	2.56
42	0.00	0.00	0.00	0.00	0.00	0.00	0.00	0.03	0.00	0.00
43	0.92	4.07	0.83	0.86	2.05	0.86	0.96	0.93	3.89	0.51
44	2.38	2.34	1.99	3.13	2.13	2.44	3.75	2.99	2.82	2.53
45	0.00	0.18	0.00	0.00	0.00	0.00	0.00	0.00	0.30	0.00
46	0.00	0.00	0.00	0.00	0.06	0.00	0.00	0.00	0.00	0.00
47	0.00	0.00	0.00	0.00	0.03	0.00	0.00	0.02	0.40	0.00
48	0.00	0.00	0.00	0.00	0.00	0.00	0.03	0.03	0.00	0.00
49	0.68	1.46	0.51	0.55	1.09	0.59	0.70	0.84	1.90	0.40
50	0.00	0.00	0.00	0.00	0.00	0.00	0.00	0.00	0.00	0.06
51	0.06	0.28	0.00	0.00	1.67	0.00	0.00	0.00	1.82	0.29
52	0.67	0.60	0.45	0.75	0.38	0.65	0.70	0.68	0.45	0.55
53	0.34	0.69	0.29	0.27	0.49	0.30	0.17	0.30	0.79	0.26
54	0.47	0.00	0.00	0.39	1.18	0.36	0.18	0.24	2.37	0.38
55	3.14	3.12	2.34	3.91	2.52	3.23	4.12	3.06	2.91	2.68

Table 8-7 (Continued)

Peak ID	Non-cat w/ 2nd	Criterion	Ash	Copper Chromite	ZSM-5	MI-575	MCM	MSU	Criterion/ ZSM-5	MSU/ ZSM-5
56	0.42	1.61	0.40	0.37	0.95	0.30	0.43	0.42	2.31	0.15
57	0.17	0.34	0.00	0.20	0.00	0.00	0.04	0.10	0.50	0.06
58	0.04	1.86	1.17	1.97	0.00	1.70	1.84	1.57	0.00	1.40
59	0.66	0.47	0.60	0.64	3.13	0.57	0.68	0.60	0.57	0.57
60	0.00	0.13	0.00	0.00	0.03	0.00	0.00	0.00	0.18	0.00
61	2.66	2.58	19.63	3.00	12.05	2.62	3.50	7.79	2.54	10.66
62	0.00	0.04	0.00	0.00	0.00	0.00	0.00	0.00	0.00	0.00
63	0.00	0.29	0.00	0.00	0.00	0.00	0.00	0.00	0.09	0.00
64	0.78	0.80	0.68	0.97	0.23	0.00	1.17	0.38	0.89	0.84
65	0.00	0.23	0.24	0.32	0.00	0.34	0.49	0.37	0.21	0.33
66	0.00	0.25	0.00	0.00	0.82	0.00	0.05	0.00	1.48	0.60
67	0.63	0.48	0.31	0.70	0.40	0.59	0.62	0.56	0.43	0.40
68	1.29	1.37	0.93	1.63	0.48	1.35	1.66	1.42	1.55	0.71
69	0.00	0.09	0.00	0.00	0.47	0.00	0.00	0.00	0.09	0.00
70	0.54	0.57	0.43	0.58	0.00	0.52	0.66	0.59	1.76	0.50
71	0.00	0.24	0.00	0.00	0.23	0.00	0.00	0.20	0.22	0.13
72	2.85	3.14	2.35	3.29	2.40	2.80	3.69	3.34	1.69	2.83
73	0.73	0.76	0.56	0.88	0.63	0.76	0.90	0.94	0.77	0.68
74	0.65	0.71	0.32	0.85	6.38	0.64	0.76	1.05	0.76	0.32
75	0.21	0.39	13.40	0.42	0.00	0.24	0.32	0.17	0.37	13.02
76	0.00	0.00	0.00	0.00	0.10	0.00	0.00	0.00	0.16	0.00
77	0.12	0.07	0.00	0.11	0.08	0.20	0.23	0.10	0.16	0.06
78	0.35	0.00	0.00	0.18	0.05	0.17	0.19	0.00	0.15	0.09
79	0.46	0.55	0.32	0.54	0.52	0.46	0.49	0.43	0.81	0.33
80	0.33	0.30	0.22	0.34	0.86	0.33	0.37	0.31	0.25	0.67
81	0.00	0.06	0.00	0.00	0.00	0.00	0.00	0.00	0.04	0.00
82	13.92	8.16	0.16	0.00	7.91	11.31	0.00	9.57	0.24	8.13
83	1.24	1.23	1.01	1.56	0.98	1.33	1.61	1.44	1.40	1.23
84	0.37	0.27	0.20	0.39	0.16	0.34	0.35	0.22	0.33	0.15
85	0.00	0.05	0.00	0.00	0.05	0.00	0.00	0.00	0.14	0.00
86	0.20	0.13	0.00	0.18	0.03	0.18	0.19	0.18	0.18	0.07
87	1.84	1.49	1.21	2.79	1.44	1.90	1.89	1.38	1.62	1.31
88	0.20	0.00	0.00	0.20	0.00	0.17	0.00	0.07	0.00	0.00
89	0.00	0.00	0.00	0.00	0.00	0.00	0.00	0.00	0.02	0.00
SUM	**100.00**	**100.00**	**100.00**	**100.00**	**100.00**	**100.00**	**100.00**	**100.00**	**100.00**	**100.00**

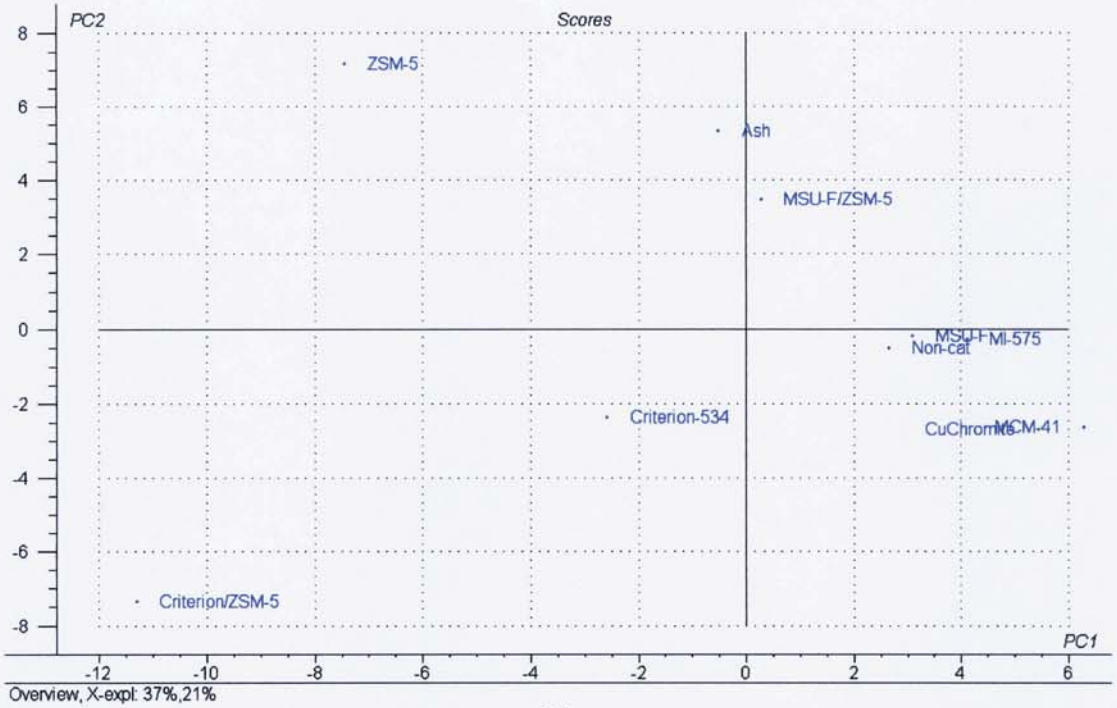

(a)

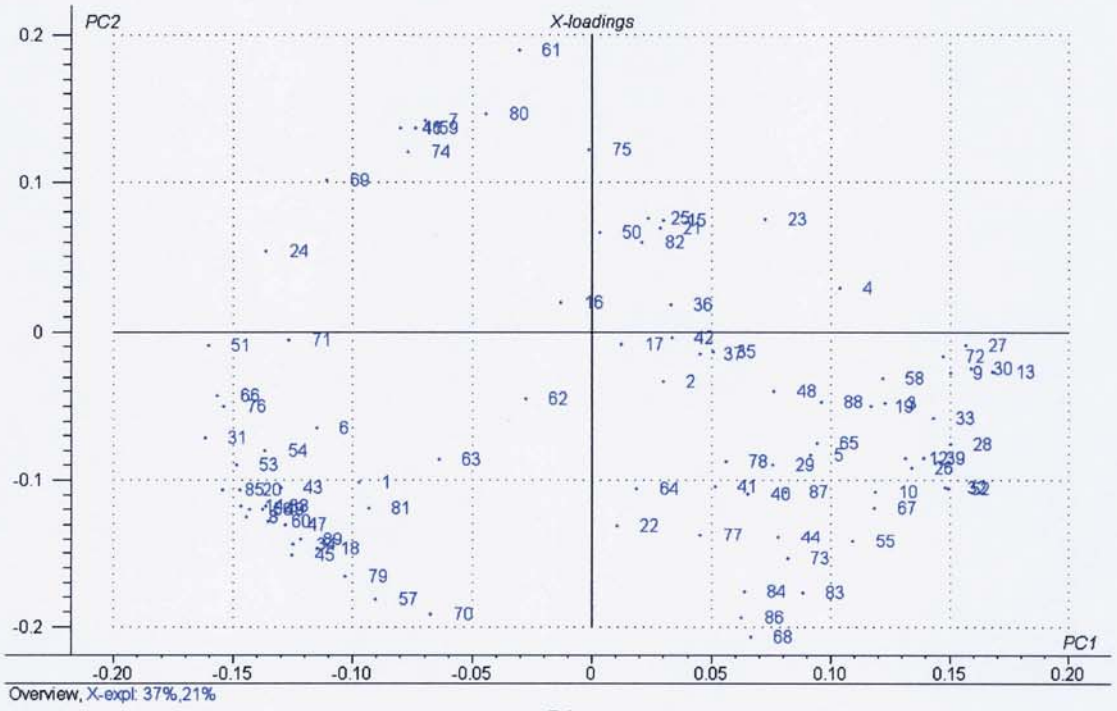

(b)

Figure 8-5 Score (a) and loading (b) plots of PC1 and PC2 for model with all catalysts and all compounds identified in catalytic CR bio-oils

To investigate further the effect of catalysts on specific groups of compounds such as hydrocarbons and phenols, two more PCA models have been created. The first one included all catalysts studied and all hydrocarbons identified in the catalytic CR bio-oils. The score and loading plots calculated from this model are presented in Figure 8-6. It can be seen from the score plot that the majority of the catalysts are clustered on the negative side of PC1 axis. This cluster includes non-catalytic, ash, copper chromite, MI-575, Al-MCM-41, Al-MSU-F and Al-MSU-F/ZSM-5 samples. Since their location in the score plot is close to the PC1 axis, these samples are not influenced by the second principal component (PC2). The only three samples that stay far away from the cluster are criterion-534/ZSM-5, ZSM-5 and Criterion-534. When observing the loading plot (Figure 8-6 (b)), it was found that all of the hydrocarbons locate on the positive PC1 except for only one compound of ID#3, which is pentane. Hence, it can be concluded based on the first two principal components which explained up to 83% of the total variance that Criterion-534/ZSM-5, ZSM-5 and Criterion-534 catalytic runs could produce hydrocarbons with statistically higher amounts than other catalytic pyrolysis runs. It is important to note that an exception should be made for pentane (ID#3) formation. According to Table 8-7, pentane was produced by the use of MI-575, copper chromite, Al-MCM-41, Al-MCM-F and Al-MCM-F/ZSM-5, while it was not detected in non-catalytic bio-oil and bio-oils produced with Criterion-534, ZSM-5, Criterion-534/ZSM-5 and ash. The hydrocarbons on the positive PC1 are mostly aromatic, except decane (ID#63). They are divided into three groups. The first group (Group I) consists of compounds that are explained mainly by the first principal component, whereas compounds in graph II and III are separated by the PC2. The hydrocarbons in group I have a strong positive relationship to the Criterion-534/ZSM-5 sample, indicating that they are largely produced by Criterion-534/ZSM-5 catalyst. Since the majority of hydrocarbon compounds are in Group I, it can be inferred that Criterion-534/ZSM-5 catalyst gave highest production of hydrocarbons compared to other catalysts studied. The chemicals in group II and III are positively related to ZSM-5 and Criterion-534 samples, respectively. In other words, the compounds of ID#46 (1-methylindene), ID#69 (1,4-dimethyl naphthalene) and ID#24 (styrene) were mainly produced by ZSM-5 catalyst, whereas biphenyl (ID#62), decane (ID#63) and 9-methyl fluorene (ID#81) were mainly produced by Criterion-534 catalyst.

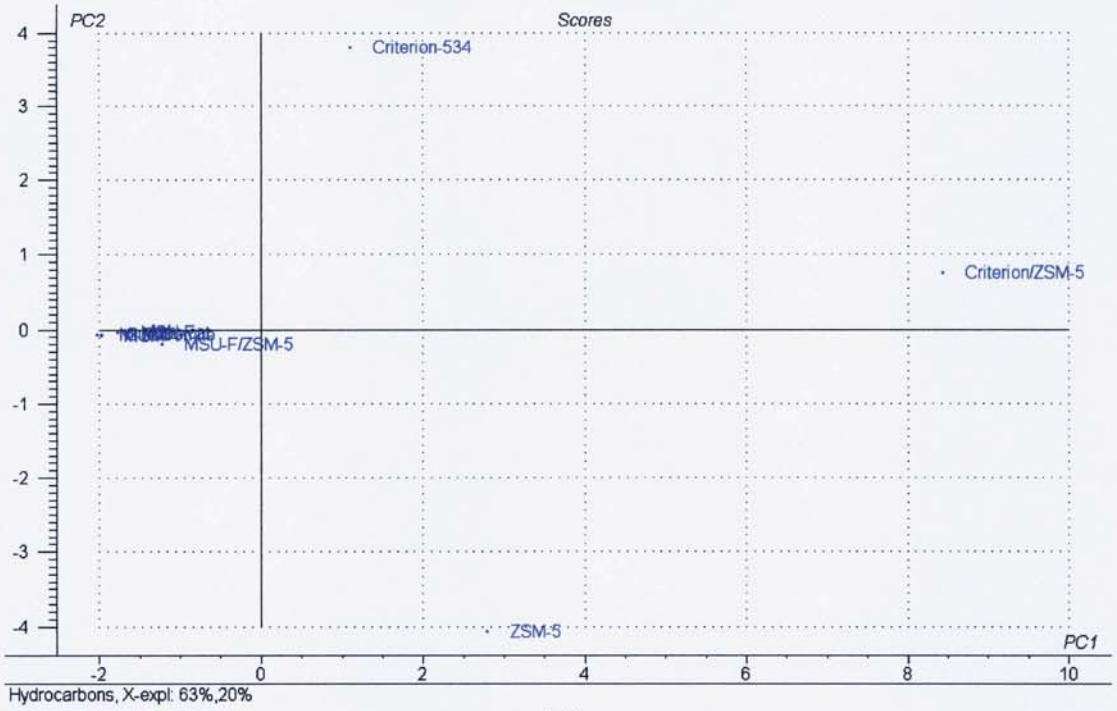

(a)

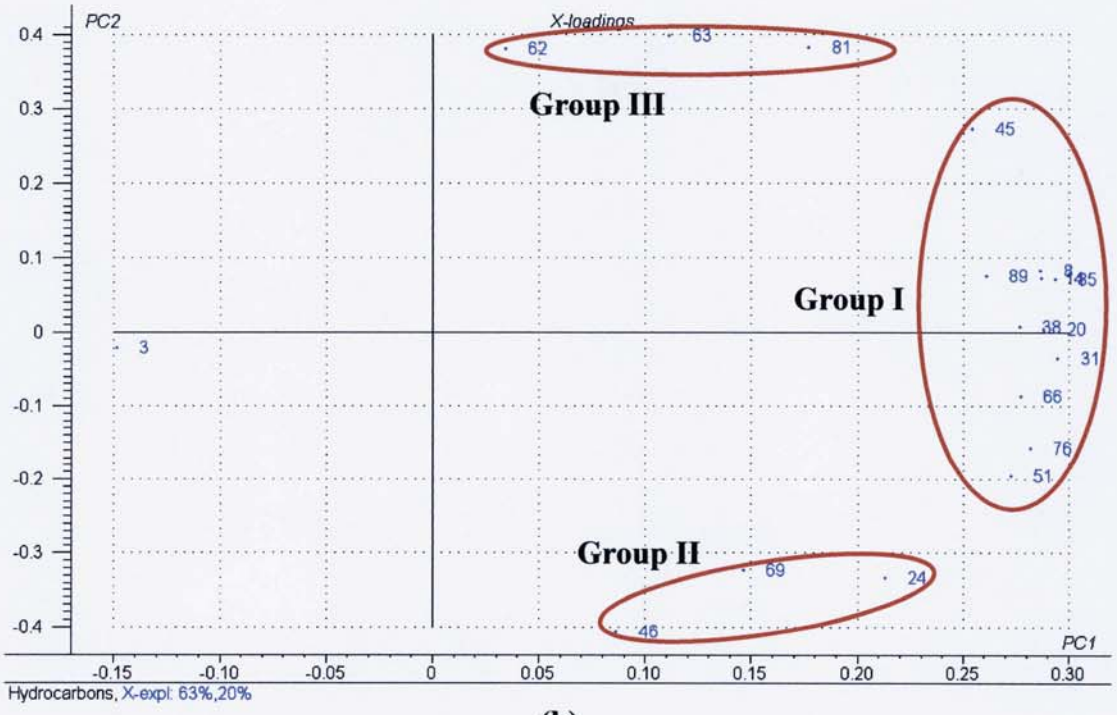

(b)

Figure 8-6 Score (a) and loading (b) plots of PC1 and PC2 for model with all catalysts and all hydrocarbons identified in catalytic CR bio-oils

It is interesting to note that most of the hydrocarbons identified are aromatic in nature and it has been known from literature [66, 67, 69-74, 76, 79, 80, 124, 148-150] that most of these compounds were produced when biomass pyrolysis vapours were passed over ZSM-5 catalysts. Some of these, especially the monocyclic aromatic hydrocarbon such as benzene (ID#8), toluene (ID#14), xylenes (ID#20), trimethyl benzene (ID#31) and styrene (ID#24) can be regarded as highly desired products since they can be used as high value chemicals or gasoline-range fuel additives. It is also of great interest to observe that with ZSM-5 or Criterion-534, these valuable hydrocarbons could be formed to a certain extent and when applying these two catalysts in series by allowing the pyrolysis vapours to pass over the Criterion-534 bed first and the catalytic vapour products underwent further catalytic reaction over ZSM-5 catalyst bed, the concentrations of these hydrocarbons were increased significantly. For example, according to Table 8-7 without catalyst the % area of benzene peak (ID#8) was 0.08%. When Criterion-534 or ZSM-5 was applied, the percentage was increased to 0.64% and 0.55%, respectively, and it was increased further to 2.88% with Criterion-534/ZSM-5 catalyst, which is nearly five times greater than when using single catalysts. Another more obvious example is the formation of toluene (ID#14). The concentrations of toluene when produced without catalysts, with Criterion-534 and with ZSM-5 were respectively 0.00%, 1.31% and 1.26%, whereas when these two catalysts were combined (Criterion-534/ZSM-5) the concentration of toluene was dramatically increased to 6.27%. Similar observations can also be made on xylenes (ID#20) and trimethy benzene (ID#31). These demonstrate a clear synergistic effect of the two catalysts. It is important to note that some of the hydrocarbons identified are polycyclic aromatic hydrocarbons (PAH) such as those of IDs#38, 45, 46, 51, 62, 66, 76, 81, 85 and 89. Some of these compounds may be carcinogenic and/or mutagenic. Therefore the direct use of these catalytic bio-oils may be harmful. However, the PAH present in the bio-oils may be further processed by, for example, hydrocracking to reform these compounds to lighter hydrocarbons.

The mechanism of the aromatics formation by zeolite ZSM-5 is believed to occur in two steps. First, the pyrolysis vapours are cracked possibly on the external surface of the zeolite, giving off olefins as intermediate products. These olefinic gases then enter the pores of the zeolite where the active acid sites locate. Within the pores, several

reactions such as oligomerisation, cyclisation, aromatisation and isomerisation take place, leading to the formation of benzene and its derivatives. When the pyrolysis vapours were passed over the Criterion-534 catalyst bed, it was found that the yields of gaseous products increased, especially the olefins (C_2H_4 and C_3H_6) (see Table 8-2). It can therefore be proposed that the reason why the aromatic hydrocarbons could be enhanced by the two-stage catalytic process is because the first catalyst bed (Criterion-534) functioned as a guard bed for cracking the primary pyrolysis vapours, generating olefins and for being deposited by condensed heavy molecules. All of these could then enhance and prolong the activation of the zeolite ZSM-5 for its capability of aromatic hydrocarbons synthesis. This concept is analogous to the application of dolomite as a guard bed for Ni-based catalyst in catalytic gasification [147]. It is also parallel to bio-oil hydrotreating processes where the first step is an initial stabilisation process at lower temperature (250–275°C), which is essential to avoid polymerisation and coking at the higher temperature (350–400°C) of a more conventional hydrotreating step [41].

Another interesting group of chemicals apart from the hydrocarbons is the phenolic fraction. Phenols can be utilised in the formulation of resins and adhesives or upgraded to methyl aryl ethers (MAE) as octane improvers [37]. The production of renewable phenolic resins by thermochemical conversion of biomass has been recently reviewed [151]. For MAE production purpose, the most favorable phenolics are phenol, cresols and xylenols because the resultant ethers have high octane numbers and their boiling points are within the range of gasoline [37]. Accordingly, phenol and its akyl-substituted derivatives identified in the catalytic CR bio-oils are monitored through a PCA model. The score and loading plots of the first two principal components (PC1 and PC2) for this model are displayed in Figure 8-7. It can be seen that up to 87% of the total variance is explained by only the PC1 and that all of the compounds lie on the positive PC1 (Figure 8-7 (b)). This means that only catalyst samples locating on the positive PC1 of the score plot (Figure 8-7 (a)) could enhance the production of these light phenolic compounds. Interestingly, they are ZSM-5, Criterion-534 and Criterion-534/ZSM-5, which have also been found earlier to yield high concentration of hydrocarbons. Among these catalysts, Criterion-534/ZSM-5 gave highest concentration of the phenols followed by Criterion-534 and ZSM-5. This shows again the synergy of combining the two strong catalysts.

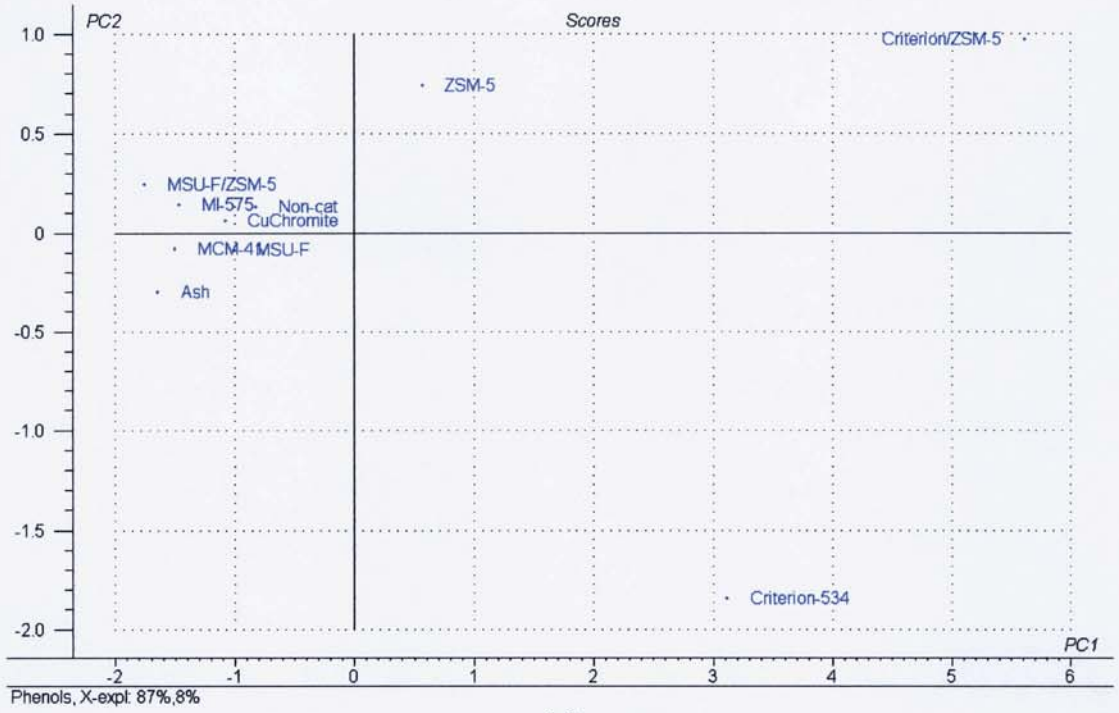

(a)

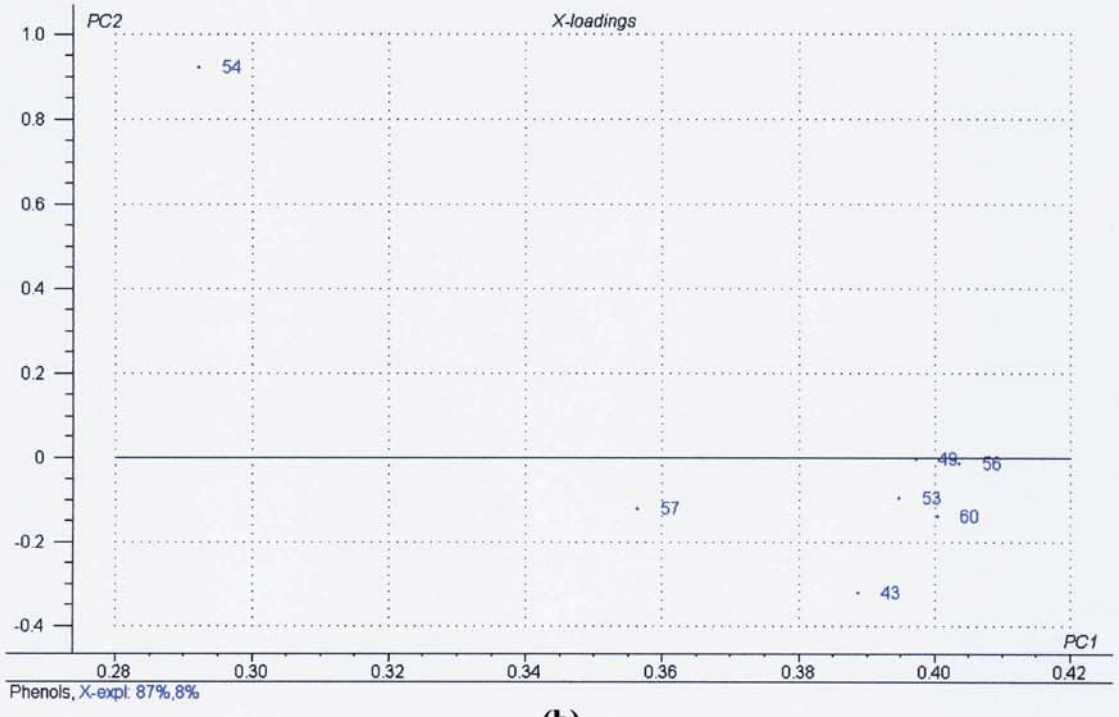

(b)

Figure 8-7 Score (a) and loading (b) plots of PC1 and PC2 for model with all catalysts and phenol and its alkylated derivatives identified in catalytic CR bio-oils

The phenol is believed to be derived from the catalytic cracking of lignin-derived compounds, especially by breaking the C-O and C-C bonds. The phenol may also be formed by hydroxylation of benzene. After the phenol is formed, alkylation reactions could occur on the highly active catalyst, which ultimately lead to the final products of alkylated phenols. In previous studies [87-89], Al-MCM-41 catalytic materials have been reported to increase the phenols concentration of the pyrolysis liquids compared to the non-catalytic runs. However, the results of the present work show that the concentration of phenol and its alkylated derivatives was hardly affected by the Al-MCM-41 when compared to the use of ZSM-5, Criterion-534 and Criterion-534/ZSM-5 catalysts.

Another PCA model has been established with all catalyst samples and all oxygenated-lignin derivatives excluding phenol and its alkylated derivatives. The resultant score and loading plots of the first two principal components are shown in Figure 8-8. It can be seen that the majority of the compounds lie on the positive PC1. When considering the score and loading plots together, it appears that ZSM-5 catalyst sample stays far away from the majority of the compounds, but it lies in the same position as compounds of ID#80, 71 and 74. Therefore, it may be concluded that ZSM-5 led to a reduction of most oxygerated lignin-derived compounds and increased the proportion of vanillin (ID#74), 2-methyl benzofuran (ID#71) and guaiacylacetone (ID#80). Similar behaviour was found with ash and Al-MSU-F/ZSM-5 samples with which 4-vinylguaiacol (ID#61), hydroquinone (ID#75) and maltol (ID#50) were increased in concentration. Since Al-MCM-41 and copper chromite samples locate on the right side of the PC1 axis of the score plot (Figure 8-8 (a)) and most of the oxygenated lignin compounds lie on the same direction of the loading plot (Figure 8-8 (b)), it may be concluded that these two catalytic pyrolysis runs produced the bio-oils with high concentration of oxygenated lignin-derived compounds. This could be due either to the lower concentration of other compounds or to the increase of the monomeric GC-detectable oxygenated lignin derivatives by cracking and/or depolymerisation of the lignin oligomers or polymers.

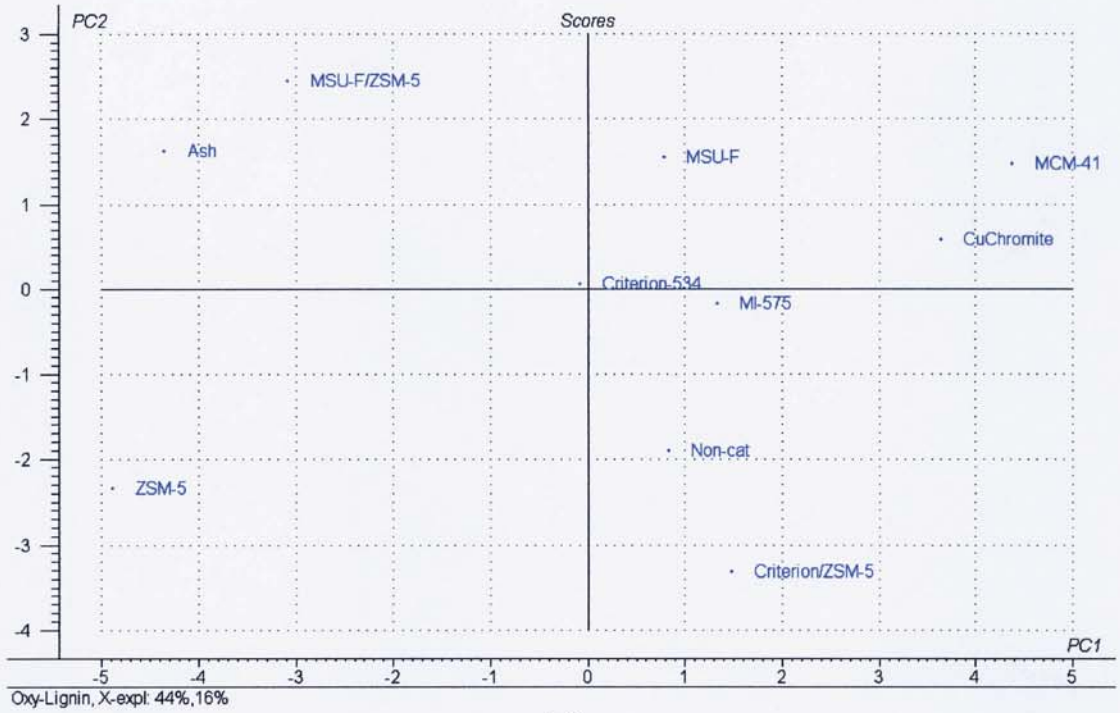

(a)

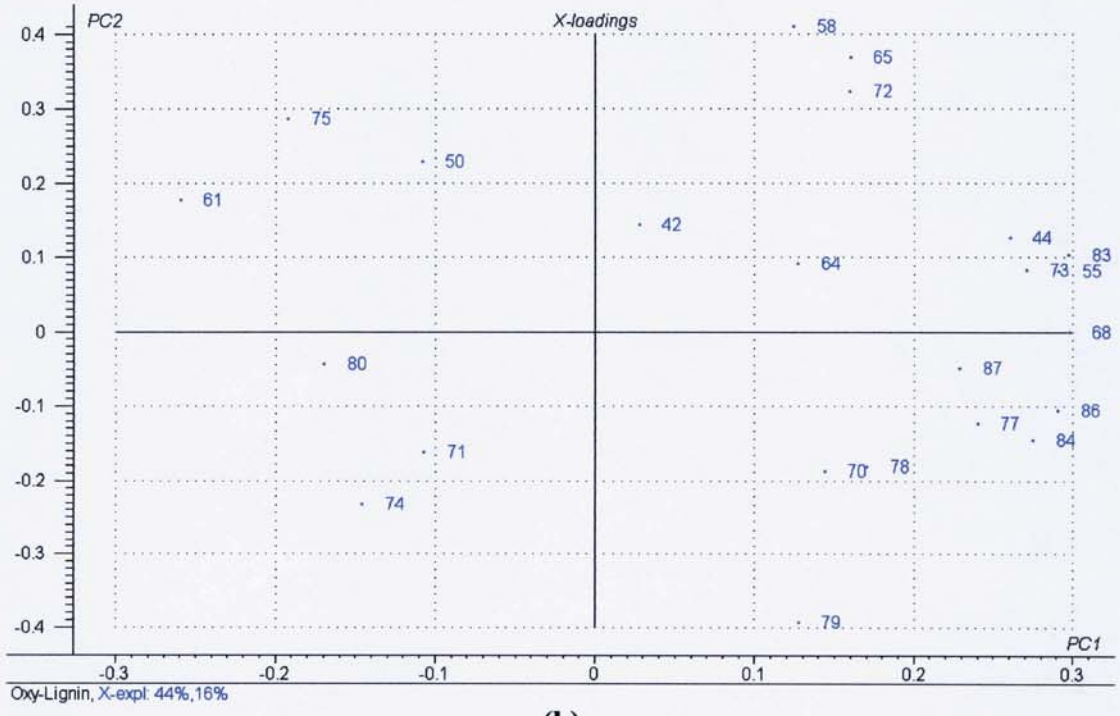

(b)

Figure 8-8 Score (a) and loading (b) plots of PC1 and PC2 for model with all catalysts and oxygenated lignin-derived compounds identified in catalytic CR bio-oils

In addition to the PCA model with lignin derivatives, the chromatographic peak area data of all carbohydrate derived compounds and all catalysts were subjected to principal component analysis. The score and loading plots of PC1 and PC2 drawn by this model are presented in Figure 8-9. It can be seen that most of the samples and variables tend to lie on the positive PC1 where the non-catalytic sample locates. Only ZSM-5, Criterion-534/ZSM-5 and ash showed different behaviour on carbohydrate-derived compounds from other samples. The ZSM-5 catalyst seems to reduce most of the compounds, but increase the proportion of isopropyl alcohol (ID#118), 1,4:3,6-dianhydro-α-d-glucopyranose (ID#59) and 3-pentanone (ID#7). With Criterion-534/ZSM-5 and ash samples, acetaldehyde (ID#1), 2-butanone (ID#6), benzofuran (ID#34), 1-hydroxy-2-batanone (ID#18) and 2-methyl furan (ID#47) appear to increase in their concentration, while most of the compounds tend to decrease. Since the ZSM-5 and Criterion-534/ZSM-5 catalysts decreased most of the oxygenated carbohydrate derived compounds and increased the hydrocarbons (Figure 8-6) and light phenols (Figure 8-7), it is likely that part of the carbohydrate derivatives were cracked and transformed into hydrocarbons and/or phenols, in addition to permanent gases.

In summary, the GC/MS analysis shows that the catalysts that considerably changed the chemical composition of the bio-oils were Criterion-534/ZSM-5, ZSM-5 and Criterion-534. These catalysts led to the statistically significant increases of valuable compounds such as hydrocarbons (benzene, toluene, xylenes, trimethyl benzene and styrene) and phenols (phenol, cresols, xylenols and ethyl phenol). Among the three catalytic bio-oils, the one produced with Criterion-534/ZSM-5 had the highest concentration of these high-value chemicals.

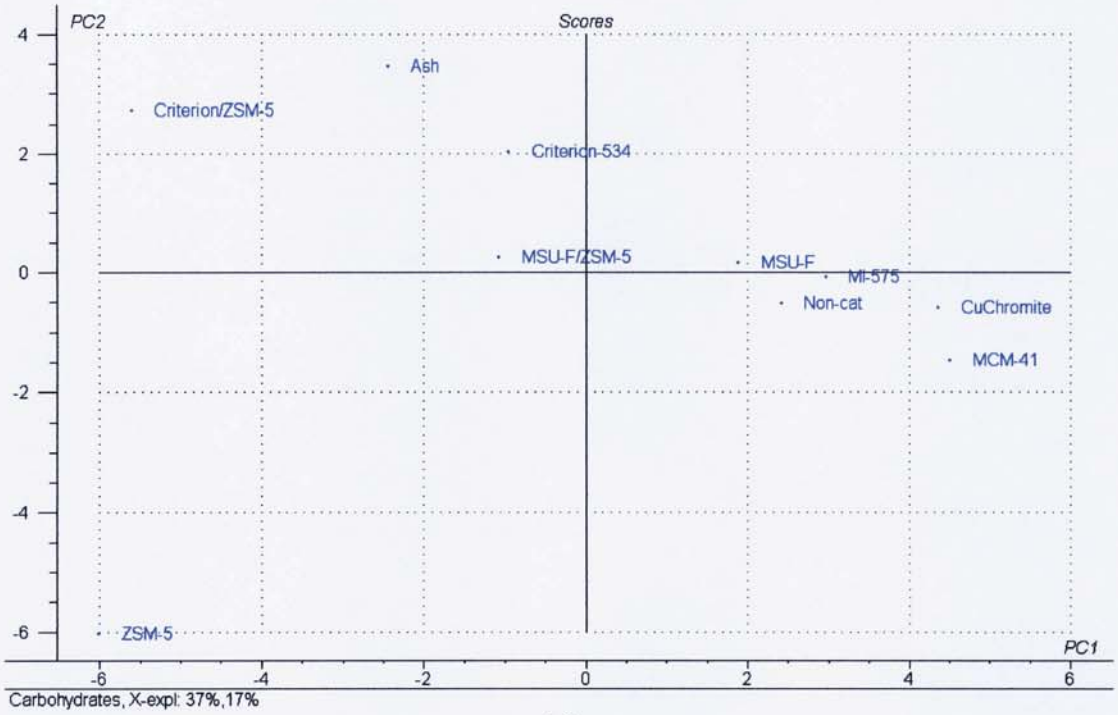

(a)

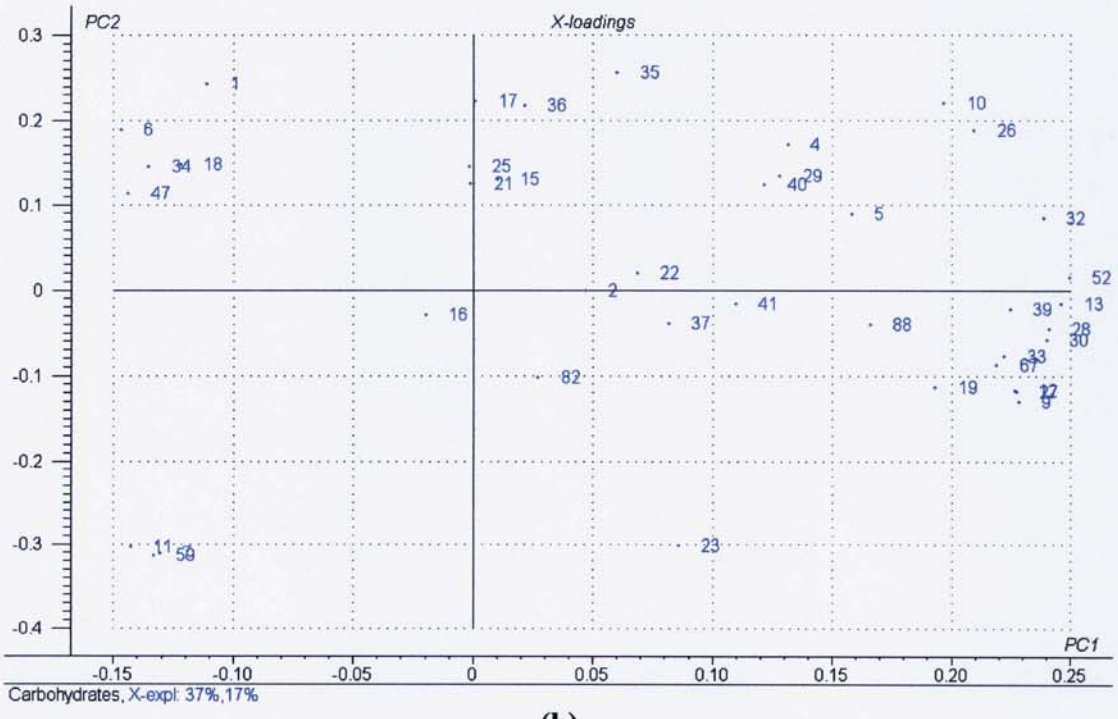

(b)

Figure 8-9 Score (a) and loading (b) plots of PC1 and PC2 for model with all catalysts and carbohydrate-derived compounds identified in catalytic CR bio-oils

8.4 CONCLUDING REMARKS

In this chapter, the results of the catalytic pyrolysis experiments using cassava rhizome as feedstock are reported and discussed. It is important to emphasise that the purpose of catalyst is to induce the reactions involving cracking, deoxygenation and product transformation so that the final catalytic bio-oils are enhanced for their utilisation. The possible applications of bio-oils produced form cassava residues in Thailand would be to replace or supplement the use of fossil fuels for power generation. At the present, the electricity production of Thailand relies mainly on the use of fossil fuels (lignite, natural gas, fuel oil and diesel fuel) in boilers, gas turbines and diesel engines. The main properties of bio-oils to meet the specifications for these applications include single-phase, water content of 25 wt% for gas turbine and 27 wt% for boiler and diesel engine and total solids content of less than 0.05 wt%. Although nearly all of the bio-oils produced from cassava residues (with and without catalyst) were single-phase, their water and solids contents measured in the laboratory scale were far too high to meet the specifications. It is therefore suggested that if the cassava residues are to be used to produce bio-oils for power production using the existing plants in Thailand, the pyrolysis plants need to have a hot vapour filtration unit to reduce the solids content to the acceptable level and need to set the condenser temperature to be high enough (suggested 50°C) to shift or remove part of the water out of the main liquid bio-oil in order to reduce its water content.

Another possible application for certain catalytic bio-oils, especially those produced with Criterion-534/ZSM-5, ZSM-5 and Criterion-534, is as raw materials for bio-refinery plants where the extraction of valuable chemicals such as BTX and phenols can be achieved at the same time as the production of energy or electricity from the rest of the bio-oil fraction. This would give greater economic promise than the use of bio-oil only as a combustion fuel. Based on the GC/MS analysis results, the use of sequential catalysis (Criterion-534 as a primary catalyst and ZSM-5 as a secondary catalyst) was found to improve the bio-oil for this application.

9 CONCLUSIONS AND RECOMMENDATIONS

9.1 CONCLUSIONS

Cassava stalk (CS) and cassava rhizome (CR) biomass samples from Thailand were used as feedstocks for bio-oil production by non-catalytic and catalytic fast pyrolysis. CS and CR were characterised for their basic composition, heating values and thermal decomposition behaviour. It was found that both feedstocks contained approximately 80% volatiles. The ash content of CS was about 2% higher than that of CR. The CS had slightly higher oxygen content and lower heating values than the CR. Based on these analyses, the CR appeared to be more promising biomass feedstock for bio-oil production than the CS. Nevertheless, when these feedstocks were analysed using TGA and DTG techniques, their thermal degradation behaviour was found to be very similar.

The CS and CR samples were used as feedstocks for the production of bio-oil in the bench-scale (150 g/h) fluidised bed reactor system. Preliminary pyrolysis runs were carried out in order to learn how to operate the rig safely and to find out possible problems that could occur with the existing equipment. It was found that both feedstocks were very difficult to feed into the reactor as the biomass particles were often blocked in the reactor feeding tube, leading to the increased pressure of the upstream entraining flow. This problem was solved in this project by designing and constructing a new feeding tube. This feeding tube had been used throughout the runs of this project and there were no blockages problems. Another problem identified during the preliminary experiments is that some of the light volatiles could escaped the product collection system of the unit, resulting in poor mass balance closure (~93% or lower). This problem was tackled by introducing a second dry-ice/acetone condenser, with which the mass balance closures were increased to 95% or higher, thus indicating a successful modification.

With the modified pyrolysis reactor system, CS and CR samples were pyrolysed at different temperatures ranging from about 440°C to 540°C. At all temperatures, the

CR gave higher liquid (organics + reaction water) yields with lower char and gas yields than the CS. Since the reaction water yields for both feedstocks were similar, the organics yields for CR were higher (~2-4%) than those for CS. The temperature that was found to be optimum for obtaining highest organics yields for the two samples was 490±15°C and at this temperature the CS and CR, respectively, yielded 46% and 50% water-free bio-oils (organics) on dry biomass fed basis.

Regarding the bio-oil properties, both feedstocks gave bio-oils of similar water content (31-33%), solids content (1.5-5.6%) and pH values (2-3). Nonetheless, the CR bio-oil had lower oxygen content and higher heating values than the CS bi-oil. In addition, although the fresh CR bio-oil appeared to have slightly higher average molecular weight (Mw) than the CS bio-oil, after ageing the CR bi-oil had much lower Mw. In other words, the stability of CR bio-oil was better than that of CS bio-oil. Therefore, based on these analyses, the CR was shown to be better feedstock for bio-oil production in comparison to the CS as the former gave higher bio-oil yield with better quality in terms of oxygen content, heating value and stability. This finding is consistent with the prediction based on the biomass characterisation as mentioned above.

In catalytic fast pyrolysis study, only CR was selected and used as feedstock. The investigation began with screening of several catalysts using a micro-scale batch reactor unit. This unit is generally known as pyrolysis-gas chromatography/mass spectrometry (Py-GC/MS). The data acquired from the screening tests were statistically evaluated applying principal component analysis (PCA) technique. It was speculated that slates, ZnO, ZrO2, CeO2, char and ash derived from char would not be effective for improving bio-oil quality, whereas ZSM-5, Criterion-534, Al-MSU-F, Al-MCM-41, copper chromite, MI-575 and ash derived from cassava rhizome were anticipated to improve the pyrolysis liquid products in terms of viscosity and deoxygenation. The latter group of catalysts was consequently chosen for larger scale (150 g/h) pyrolysis experiments.

Apart from the seven catalysts suggested from the screening tests, two catalytic pyrolysis runs were performed using a combination of two catalysts. These are Criterion-534/ZSM-5 and Al-MSU-F/ZSM-5. The effects of catalysts on pyrolysis

product yields and properties were investigated in conjunction with two non-catalytic runs (with and without 2nd reactor). It was found that all the catalysts could improve different properties of bio-oils to different extents. Based on the results, the catalysts can be divided into two groups. The first group including ash, copper chromite, MI-575, Al-MSU-F, Al-MCM-41 and Al-MSU-F/ZSM-5 is considered as mild catalysts since their organics yields were not significantly reduced. These catalysts were found to induce the cracking and deoxygenation reactions as observed from the lower initial molecular weight, lower oxygen content and higher heating values of the catalytic bi-oils in comparison with non-catalytic bio-oils. Nearly all of the catalysts (except for Al-MSU-F/ZSM-5) could also reduce the solids content of bio-oils, which is beneficial to most applications. According to the stability indices calculated from the change in the average molecular weight of the bio-oils after 6 months storage, ash, copper chromite and MI-575 were improved in stability compared to the non-catalytic bio-oil, whereas the stability of Al-MSU-F and Al-MSU-F/ZSM-5 treated bio-oils appeared to be deteriorated. In addition the stability of the Al-MCM-41 bio-oil was hardly changed compared to that of the non-catalytic oil. In general, the bio-oils upgraded with this group of catalysts may be used in the same applications as typical bio-oils produced without any catalyst.

Another group of catalysts regarded as strong catalysts includes Criterion-534, ZSM-5 and Criterion-534/ZSM-5. The organics yields obtained with these catalysts were dramatically reduced. However, the bio-oils contained significant amounts of valuable chemicals such as mono-cyclic aromatic hydrocarbons and light phenols, have low oxygen content, low solids content, very low average molecular weight and high calorific values (on dry basis), thus indicating premium grade bio-oils. Among the catalysts, Criterion-534 was found to give the lowest oxygen content and the highest stability. In addition, the concentrations of aromatic hydrocarbons, phenol and alkylated phenols appeared to be highest with the combination of the two catalysts (Criterion-534/ZSM-5). A mechanism for the synergistic increase of the aromatic hydrocarbons by the two-stage process is proposed. The first catalyst bed (Criterion-534) acted as a guard bed for cracking the primary pyrolysis vapours to produce smaller molecules including olefins and for being deposited by condensed heavy molecules, which would otherwise blocking the pores of the ZSM-5 catalyst. This could then enhance and prolong the activation of the zeolite for its capability of

aromatic hydrocarbons synthesis. Moreover, the reasons why the phenol and alkylated phenols concentrations were increased when applying this group of catalysts can be explained by two possible mechanisms. The first one involves the selective cracking of the side chain of the phenolic-based lignin derivatives such as guaiacols and syringols, leading to the production of phenol which may undergo further alkylation (such as methylation) to give alkylated phenols as the end products. The second possible mechanism is associated with the hydroxylation of benzene to give phenol as a primary product, which could undergo alkylation like the first route to produce alkylated phenols.

Based on the findings in this project, the non-catalytic CS and CR bio-oils and the bio-oils produced with the mild catalysts (ash, copper chromite, MI-575, Al-MSU-F, Al-MCM-41 and Al-MSU-F/ZSM-5) can be used as fuels in boilers, diesel engines and gas turbines for power generation provided that the pyrolysis plants have been designed to overcome the high water and solids contents. This would lead to the reduction in the use of fossil fuels, which is beneficial not only to the environment, but also to the economy of Thailand. For catalytic bio-oils produced with the strong catalysts (Criterion-534, ZSM-5 and Criterion-534/ZSM-5), which contained large proportion of valuable chemicals such as hydrocarbons and phenols, the application of these bio-oils is suggested to be as raw materials for bio-refinery plants where chemicals, fuel additives and energy can be produced simultaneously.

9.2 RECOMMENDATIONS

Following the studies reported in this thesis, recommendations for the continuation of this work are presented in this section.

The feedstocks applied in this work for bio-oil production were cassava stalk and cassava rhizome, which were processed separately. It is suggested that a mixture of these two materials with the proportion based on the residues availability should be used as feedstock for both non-catalytic and catalytic fast pyrolysis studies. In addition, since the biomass feedstocks contained about 4-6% of ash, their pre-treatment by, for example, water washing/leaching, prior to pyrolysis is recommended

in order to reduce their ash contents, which would lead to the increase of the organics yields.

Because of the limited amounts of bio-oils obtained, some important properties of bio-oils such as viscosity, density and flash point could not be measured. It is therefore recommended that fast pyrolysis of cassava residues should be also carried out in a larger-scale pyrolysis unit such as 300 g/h unit. This unit at Aston University is still under construction and commissioning. Alternatively, the 150 g/h rig may be modified in a way that higher amount of biomass can be fed. At the moment, a limitation of this rig lies in the inlet of the water condenser where accumulation of char and sticky liquid occurs, which can block the flow of pyrolysis vapour. This problem can be solved either by enlarging the inlet of the condenser using glass blowing technique or by using a bigger condenser.

For future investigation, the study of catalysts screening is recommended to include the effects of biomass/catalyst ratios and pyrolysis temperature as well as the use of mixtures of two different catalysts at different proportions. The mixtures can either be dry mixing of two catalysts or be in the form of two-stage process. If the range of mass spectrum (*m/z*) is altered to cover the detection of low molecular weight molecules such as carbon oxides and hydrocarbon gases, especially olefins, it would be beneficial to identifying suitable primary catalysts, for example, those generate significant amounts of olefins. This primary catalyst can then be used in conjunction with zeolites such as ZSM-5 for hydrocarbons synthesis. In the current study, the *m/z* was set at 28-600. This may be changed to 15-600. Since many parameters can be involved in the screening tests, the use of design of experiments (DOE) technique is recommended to minimise the total number of experiments which would reduce the cost and time and to determine which parameters are statistically significant. As some of the catalysts screened in the present work were concluded to be inactive, they should be also tested in a bench-scale pyrolysis unit in order to confirm their inactivity and to study or establish the reliability of the Py-GC/MS coupled with PCA technique.

Concerning the bench-scale (150 g/h) pyrolysis experiments, it is recommended for future work that the effects of weight hourly space velocity, biomass/catalyst ratio,

catalyst temperature, catalyst regeneration, gas stream recycling as well as the different modes of catalyst incorporation should be investigated in order to optimise the desired products (such as hydrocarbons yields). For two-stage catalytic process, the primary catalyst can be placed in the primary reactor as fluidising medium, whereas the second one can be put in the secondary reactor. With this configuration, the operating temperatures can be different. For example, if the purpose of the primary reactor is to generate olefins, the operating temperature may be set to be relatively high (depending on the types of catalyst) such as 600-700°C, while the temperature of the secondary reactor can remain at 500°C for hydrocarbons production over a catalyst bed such as zeolite ZSM-5.

10 REFERENCES

[1] McKendry P. Energy production from biomass (part 1): overview of biomass. Bioresource Technology 2002; 83:37-46.

[2] McKendry P. Energy production from biomass (part 2): conversion technologies. Bioresource Technology 2002; 83:47-54.

[3] Diebold JP, A Review of the Chemical and Physical Mechanisms of the Storage Stability of Fast Pyrolysis Bio-Oils. Colorado: National Renewable Energy Laboratory (NREL), 2000: 1-59.

[4] Czernik S, Bridgwater AV. Overview of applications of biomass fast pyrolysis oil. Energy & Fuels 2004; 18:590-598.

[5] Oasmaa A, Kuoppala E. Fast pyrolysis of forestry residue. 3. Storage stability of liquid fuel. Energy & Fuels 2003; 17:1075-1084.

[6] Scholze B, Hanser C, Meier D. Characterization of the water-insoluble fraction from fast pyrolysis liquids (pyrolytic lignin) Part II. GPC, carbonyl goups, and C-13-NMR. Journal of Analytical and Applied Pyrolysis 2001; 58:387-400.

[7] Evaluation of conditions for electricity production based on biomass. Bangkok, Thailand: EC-ASEAN COGEN Programme, 1998: 1-72.

[8] Rice. Bangkok, Thailand: Department of Alternative Energy Development and Efficiency, Ministry of Energy, 2003.

[9] Agricultural Statistics of Thailand. Office of Agricultural Economics, 2006.

[10] Malakul P, Lohsomboon P, Overview of the biomass utilization in Thailand. Meeting for LCA in ASEAN Biomass Project. International Conference Center, "EPOCHAL TSUKUBA", Japan: ASEAN Biomass Meeting 2004, 2004.

[11] Papong S, Yuvaniyama C, Lohsomboon P, Malakul P, Overview of Biomass Utilization in Thailand. Meeting for LCA in ASEAN Biomass Project. International Conference Center, "EPOCHAL TSUKUBA", Japan: ASEAN Biomass Meeting 2004, 2004.

[12] Sajjakulnukit B, Yingyuad R, Maneekhao V, Pongnarintasut V, Bhattacharya SC, Salam PA. Assessment of sustainable energy potential of non-plantation biomass resources in Thailand. Biomass and Bioenergy 2005; 29:214-224.

[13] Srisovanna P, Thailand's Biomass Energy. Electricity Supply Industry in Transition: Issues and Prospect for Asia. Bangkok, Thailand: Energy Conservation Center of Thailand, 2004: 35-42.

[14] Yokoyama S-y, Ogia T, Nalampoon A. Biomass energy potential in Thailand. Biomass and Bioenergy 2000; 18:405-410.

[15] Cassava. Bangkok, Thailand: Department of Alternative Energy Development and Efficiency, Misnistry of Energy, 2003.

[16] Cassava plant. JPEG image, 2007.

[17] Mohan D, Pittman CU, Steele PH. Pyrolysis of wood/biomass for bio-oil: A critical review. Energy & Fuels 2006; 20:848-889.

[18] Raveendran K, Ganesh A, Khilar KC. Pyrolysis characteristics of biomass and biomass components. Fuel 1996; 75:987-998.

[19] Huber GW, Dumesic JA. An overview of aqueous-phase catalytic processes for production of hydrogen and alkanes in a biorefinery. Catalysis Today 2006; 111:119-132.

[20] Huber GW, Iborra S, Corma A. Synthesis of transportation fuels from biomass: Chemistry, catalysts, and engineering. Chem Rev 2006; 106:4044-4098.

[21] Yaman S. Pyrolysis of biomass to produce fuels and chemical feedstocks. Energy Conversion and Management 2004; 45:651-671.
[22] Demirbas A. Fuel Characteristics of Olive Husk and Walnut, Hazelnut, Sunflower, and Almond Shells. Energy Sources 2002; 24:215-221.
[23] Campbell IM, Biomass, catalysts and liquid fuels. London: Holt, Rinehart and Winston, 1983.
[24] Glazer AN, Nikaido H, Microbial biotechnology : fundamentals of applied microbiology. New York ; [Oxford]: W.H. Freeman, 1995.
[25] Raveendran K, Ganesh A, Khilart KC. Influence of mineral matter on biomass pyrolysis charateristics. Fuel 1995; 74:1812-1822.
[26] Agblevor FA, Besler S. Inorganic compounds in biomass feedstocks .1. Effect on the quality of fast pyrolysis oils. Energy & Fuels 1996; 10:293-298.
[27] Bridgwater AV, Peacocke GVC. Fast pyrolysis processes for biomass. Renewable & Sustainable Energy Reviews 2000; 4:1-73.
[28] Bridgwater AV. Renewable fuels and chemicals by thermal processing of biomass. Chemical Engineering Journal 2003; 91:87-102.
[29] Piskorz J, Scott DS, Radlein D, Composition of Oils Obtained by Fast Pyrolysis of Different Woods. In: Soltes EJ, Milne TA, editors. Pyrolysis oils from biomass : producing, analyzing, and upgrading. Washington, D.C.: American Chemical Society, 1988: 167-177.
[30] Oasmaa A, Kuoppala E, Gust S, Solantausta Y. Fast pyrolysis of forestry residue. 1. Effect of extractives on phase separation of pyrolysis liquids. Energy & Fuels 2003; 17:1-12.
[31] Oasmaa A, Peacocke C, Gust S, Meier D, McLellan R. Norms and standards for pyrolysis liquids. End-user requirements and specifications. Energy & Fuels 2005; 19:2155-2163.
[32] Diebold JP, Czernik S. Additives to lower and stabilize the viscosity of pyrolysis oils during storage. Energy & Fuels 1997; 11:1081-1091.
[33] Diebold JP, Chum HL, Evans RJ, Milne TA, Reed TB, Scahill JW, Low-Pressure Upgrading of Primary Pyrolysis Oils from Biomass and Organic Wastes. In: Klass DL, editor. Energy from biomass and wastes X. London: Elsevier Applied Science, 1987: 801-830.
[34] Sipila K, Kuoppala E, Fagernas L, Oasmaa A. Characterization of biomass-based flash pyrolysis oils. Biomass & Bioenergy 1998; 14:103-113.
[35] Piskorz J, Majerski P, Radlein D, Pyrolysis of biomass - Aerosol generation: Properties, applications, and significance for process engineers. In: Overend RP, Chornet E, editors. Biomass: A Growth Opportunity in Green Energy and Value-Added Products, Vols 1 and 2. Oxford: Pergamon-Elsevier Science Ltd, 1999: 1153-1159.
[36] Fratini E, Bonini M, Oasmaa A, Solantausta Y, Teixeira J, Baglioni P. SANS analysis of the microstructural evolution during the aging of pyrolysis oils from biomass. Langmuir 2006; 22:306-312.
[37] Stoikos T, Upgrading of Biomass Pyrolysis Liquids to High-Value Chemicals and Fuel Additives. In: Bridgwater AV, Grassi G, editors. Biomass pyrolysis liquids upgrading and utilisation: Elsevier Applied Science, 1991: ix,377p.
[38] Goyal HB, Seal D, Saxena RC. Bio-fuels from thermochemical conversion of renewable resources: A review. Renewable and Sustainable Energy Reviews 2008; 12:504-517.
[39] Bridgwater AV, Fast pyrolysis. Berlin: 15th European Biomass Conference and Exhibition, 2007.

[40] Lee KH, Kang BS, Park YK, Kim JS. Influence of reaction temperature, pretreatment, and a char removal system on the production of bio-oil from rice straw by fast pyrolysis, using a fluidized bed. Energy & Fuels 2005; 19:2179-2184.
[41] Bridgwater AV. Catalysis in thermal biomass conversion. Applied Catalysis A: General 1994; 116:5-47.
[42] Nik-Azar M, Hajaligol MR, Sohrabi M, Dabir B. Mineral matter effects in rapid pyrolysis of beech wood. Fuel Processing Technology 1997; 51:7-17.
[43] Muller-Hagedorn M, Bockhorn H, Krebs L, Muller U. A comparative kinetic study on the pyrolysis of three different wood species. Journal of Analytical and Applied Pyrolysis 2003; 68-69:231-249.
[44] Das P, Ganesh A, Wangikar P. Influence of pretreatment for deashing of sugarcane bagasse on pyrolysis products. Biomass and Bioenergy 2004; 27:445-457.
[45] Fahmi R, Bridgwater AV, Darvell LI, et al. The effect of alkali metals on combustion and pyrolysis of Lolium and Festuca grasses, switchgrass and willow. Fuel 2007; 86:1560-1569.
[46] Scott DS, Paterson L, Piskorz J, Radlein D. Pretreatment of poplar wood for fast pyrolysis: rate of cation removal. Journal of Analytical and Applied Pyrolysis 2001; 57:169-176.
[47] Freda C, Barisano D, Valerio V, Nanna F, G.Braccio, Zimbardi F, Pyrolysis oils obtained from different biomasses. 14th European Biomass Conference. Paris, France, 2005: 1102-1104.
[48] Ghetti P, Ricca L, Angelini L. Thermal analysis of biomass and corresponding pyrolysis products. Fuel 1996; 75:565-573.
[49] Michael L. Boroson, Howard JB, Longwell JP, Peters WA. Product yields and kinetics from the vapor phase cracking of wood pyrolysis tars. Aiche J 1989; 35:120-128.
[50] Elliott DC, Relation of Reaction Time and Temperature to Chemical Composition of pyrolysis Oils. In: Soltes EJ, Milne TA, editors. Pyrolysis oils from biomass : producing, analyzing, and upgrading. Washington, D.C.: American Chemical Society, 1988: 55-65.
[51] Horne PA, Williams PT. Influence of temperature on the products from the flash pyrolysis of biomass. Fuel 1996; 75:1051-1059.
[52] Piskorz J, Majerski P, Radlein D, Scott DS, Bridgwater AV. Fast pyrolysis of sweet sorghum and sweet sorghum bagasse. Journal of Analytical and Applied Pyrolysis 1998; 46:15-29.
[53] Adjaye JD, Bakhshi NN. Catalytic conversion of a biomass-derived oil to fuels and chemicals I: Model compound studies and reaction pathways. Biomass and Bioenergy 1995; 8:131-149.
[54] Radlein D, Piskorz J, Majerski P, Method of Upgrading Biomass Pyrolysis Liquids for Use as Fuels and as a Source of Chemicals by Reaction with Alcohols. Canadian Patents Database. U.K. , 1996.
[55] Boucher ME, Chaala A, Pakdel H, Roy C. Bio-oils obtained by vacuum pyrolysis of softwood bark as a liquid fuel for gas turbines. Part II: Stability and ageing of bio-oil and its blends with methanol and a pyrolytic aqueous phase. Biomass and Bioenergy 2000; 19:351-361.
[56] Boucher ME, Chaala A, Roy C. Bio-oils obtained by vacuum pyrolysis of softwood bark as a liquid fuel for gas turbines. Part I: Properties of bio-oil and its blends with methanol and a pyrolytic aqueous phase. Biomass and Bioenergy 2000; 19:337-350.

[57] Oasmaa A, Kuoppala E, Selin JF, Gust S, Solantausta Y. Fast pyrolysis of forestry residue and pine. 4. Improvement of the product quality by solvent addition. Energy & Fuels 2004; 18:1578-1583.
[58] Oasmaa A, Sipila K, Solantausta Y, Kuoppala E. Quality improvement of pyrolysis liquid: Effect of light volatiles on the stability of pyrolysis liquids. Energy & Fuels 2005; 19:2556-2561.
[59] Bridgwater AV, Cottam ML. Opportunities for biomass pyrolysis liquids production and upgrading. Energy & Fuels 1992; 6:113-120.
[60] Ferdous D, Dalai AK, Bej SK, Thring RW. Pyrolysis of lignins: Experimental and kinetics studies. Energy & Fuels 2002; 16:1405-1412.
[61] Salter EH, Catalytic pyrolysis of biomass for improved liquid fuel quality. Birmingham: University of Aston in Birmingham, 2001.
[62] Hagen J, Industrial catalysis : a practical approach, 2nd ed. ed. Weinheim: Wiley-VCH, 2006.
[63] Adjaye JD, Bakhshi NN. Production of hydrocarbons by catalytic upgrading of a fast pyrolysis bio-oil. Part II: Comparative catalyst performance and reaction pathways. Fuel Processing Technology 1995; 45:185-202.
[64] Adjaye JD, Bakhshi NN. Production of hydrocarbons by catalytic upgrading of a fast pyrolysis bio-oil. Part I: Conversion over various catalysts. Fuel Processing Technology 1995; 45:161-183.
[65] Katikaneni SPR, Idem RO, Bakhshi NN, Catalytic conversion of a biomass-derived oil using various catalysts. In: Kaltschmitt M, Bridgwater AV, editors. Biomass Gasification and Pyrolysis: State of the Art and Future Prospects. Newbury: Cpl Press, 1997: 411-421.
[66] Williams PT, Horne PA. The Influence of Catalyst Regeneration on the Composition of Zeolite-Upgraded Biomass Pyrolysis Oils. Fuel 1995; 74:1839-1851.
[67] Williams PT, Horne PA. The influence of catalyst type on the composition of upgraded biomass pyrolysis oils. Journal of Analytical and Applied Pyrolysis 1995; 31:39-61.
[68] Horne PA, Williams PT. Premium Quality Fuels and Chemicals from the Fluidized-Bed Pyrolysis of Biomass with Zeolite Catalyst Upgrading. Renewable Energy 1994; 5:810-812.
[69] Horne PA, Williams PT. The effect of zeolite ZSM-5 catalyst deactivation during the upgrading of biomass-derived pyrolysis vapours. Journal of Analytical and Applied Pyrolysis 1995; 34:65-85.
[70] Horne PA, Williams PT. Upgrading of biomass-derived pyrolytic vapours over zeolite ZSM-5 catalyst: Effect of catalyst dilution on product yields. Fuel 1996; 75:1043-1050.
[71] Williams PT, Horne PA. Characterization of Oils from the Fluidized-Bed Pyrolysis of Biomass with Zeolite Catalyst Upgrading. Biomass & Bioenergy 1994; 7:223-236.
[72] Williams PT, Horne PA. Analysis of Aromatic-Hydrocarbons in Pyrolytic Oil Derived from Biomass. Journal of Analytical and Applied Pyrolysis 1995; 31:15-37.
[73] Williams PT, Nugranad N. Comparison of products from the pyrolysis and catalytic pyrolysis of rice husks. Energy 2000; 25:493-513.
[74] Williams PT, Nugranad N, Horne PA, Influence of steam on the formation of polycyclic aromatic hydrocarbons in the zeolite catalytic upgrading of biomass pyrolysis oils. In: Kaltschmitt M, Bridgwater AV, editors. Biomass Gasification and Pyrolysis: State of the Art and Future Prospects. Newbury: Cpl Press, 1997: 422-430.

[75] Chen NY, Walsh DE, Koenig LR, Fluidized-Bed Upgrading of Wood Pyrolysis Liquids and Related Compounds. In: Soltes EJ, Milne TA, editors. Pyrolysis oils from biomass : producing, analyzing, and upgrading. Washington, D.C.: American Chemical Society, 1988: 277-289.
[76] Olazar M, Aguado R, Bilbao J, Barona A. Pyrolysis of sawdust in a conical spouted-bed reactor with a HZSM-5 catalyst. Aiche J 2000; 46:1025-1033.
[77] Atutxa A, Aguado R, Gayubo AG, Olazar M, Bilbao J. Kinetic description of the catalytic pyrolysis of biomass in a conical spouted bed reactor. Energy & Fuels 2005; 19:765-774.
[78] Lappas AA, Samolada MC, Iatridis DK, Voutetakis SS, Vasalos IA. Biomass pyrolysis in a circulating fluid bed reactor for the production of fuels and chemicals. Fuel 2002; 81:2087-2095.
[79] Horne PA, Nugranad N, Williams PT. Catalytic coprocessing of biomass-derived pyrolysis vapours and methanol. Journal of Analytical and Applied Pyrolysis 1995; 34:87-108.
[80] Evans RJ, Milne T, Molecular-Beam, Mass-Spectrometric Studies of Wood Vapor and Model Compounds over an HZSM-5 Catalyst. In: Soltes EJ, Milne TA, editors. Pyrolysis oils from biomass : producing, analyzing, and upgrading. Washington, D.C.: American Chemical Society, 1988: 311-327.
[81] Gayubo AG, Aguayo AT, Atutxa A, Prieto R, Bilbao J. Deactivation of a HZSM-5 zeolite catalyst in the transformation of the aqueous fraction of biomass pyrolysis oil into hydrocarbons. Energy & Fuels 2004; 18:1640-1647.
[82] Gayubo AG, Aguayo AT, Atutxa A, Aguado R, Bilbao J. Transformation of oxygenate components of biomass pyrolysis oil on a HZSM-5 zeolite. I. Alcohols and phenols. Industrial & Engineering Chemistry Research 2004; 43:2610-2618.
[83] Gayubo AG, Aguayo AT, Atutxa A, Valle B, Bilbao J. Undesired components in the transformation of biomass pyrolysis oil into hydrocarbons on an HZSM-5 zeolite catalyst. Journal of Chemical Technology and Biotechnology 2005; 80:1244-1251.
[84] Baerlocher C, Meier WMAozst, Meier WM, Olson D, Atlas of zeolite framework types, 5th rev. ed. / Ch. Baerlocher, W.M. Meier, D.H. Olson. ed. Amsterdam ; London: Elsevier, 2001.
[85] Adam J, Blazso M, Meszaros E, et al. Pyrolysis of biomass in the presence of Al-MCM-41 type catalysts. Fuel 2005; 84:1494-1502.
[86] Adam J, Antonakou E, Lappas A, et al. In situ catalytic upgrading of biomass derived fast pyrolysis vapours in a fixed bed reactor using mesoporous materials. Microporous and Mesoporous Materials 2006; 96:93-101.
[87] Antonakou E, Lappas A, Nilsen MH, Bouzga A, Stocker M. Evaluation of various types of Al-MCM-41 materials as catalysts in biomass pyrolysis for the production of bio-fuels and chemicals. Fuel 2006; 85:2202-2212.
[88] Iliopoulou EF, Antonakou EV, Karakoulia SA, Vasalos IA, Lappas AA, Triantafyllidis KS. Catalytic conversion of biomass pyrolysis products by mesoporous materials: Effect of steam stability and acidity of Al-MCM-41 catalysts. Chemical Engineering Journal 2007; 134:51-57.
[89] Nilsen MH, Antonakou E, Bouzga A, Lappas A, Mathisen K, Stocker M. Investigation of the effect of metal sites in Me-Al-MCM-41 (Me = Fe, Cu or Zn) on the catalytic behavior during the pyrolysis of wooden based biomass. Microporous and Mesoporous Materials 2007; 105:189-203.

[90] Adam J, Blazsó M, Mészáros E, et al., Vapour phase upgrading of biomass pyrolysis products with mesoporous SBA-15 and FCC catalysts. 14th European Biomass Conference. Paris, France, 2005: 857-861.
[91] Triantafyllidis KS, Iliopoulou EF, Antonakou EV, Lappas AA, Wang H, Pinnavaia TJ. Hydrothermally stable mesoporous aluminosilicates (MSU-S) assembled from zeolite seeds as catalysts for biomass pyrolysis. Microporous and Mesoporous Materials 2007; 99:132-139.
[92] Melo RAA, Giotto MV, Rocha J, Urquieta-Gonzılez EA. MCM-41 ordered mesoporous molecular sieves synthesis and characterization. Materials Research 1999; 2:173-179.
[93] Nokkosmaki MI, Kuoppala ET, Leppamaki EA, Krause AOI. Catalytic conversion of biomass pyrolysis vapours with zinc oxide. Journal of Analytical and Applied Pyrolysis 2000; 55:119-131.
[94] Ates F, Putun AE, Putun E. Fixed bed pyrolysis of Euphorbia rigida with different catalysts. Energy Conversion and Management 2005; 46:421-432.
[95] Ates F, Putun AE, Putun E. Catalytic pyrolysis of perennial shrub, Euphorbia rigida in the water vapour atmosphere. Journal of Analytical and Applied Pyrolysis 2005; 73:299-304.
[96] Ates F, Putun AE, Putun E. Pyrolysis of two different biomass samples in a fixed-bed reactor combined with two different catalysts. Fuel 2006; 85:1851-1859.
[97] Scholze B, Long-term Stability, Catalytic Upgrading, and Application of Pyrolysis Oils - Improving the Properties of a Potential Substitue for Fossil Fuels. Hamburg: University of Hamburg, 2002.
[98] Radlein DSAG, Mason SL, Piskorz J, Scott DS. Hydrocarbons from the catalytic pyrolysis of biomass. Energy Fuels 1991; 5:760-763.
[99] Juutilainen SJ, Simell PA, Krause AOI. Zirconia: Selective oxidation catalyst for removal of tar and ammonia from biomass gasification gas. Applied Catalysis B: Environmental 2006; 62:86-92.
[100] Thomas CL, Catalytic processes and proven catalysts. London: Academic Press, 1970.
[101] Bridgeman TG, Darvell LI, Jones JM, et al. Influence of particle size on the analytical and chemical properties of two energy crops. Fuel 2007; 86:60-72.
[102] Ona T, Sonoda T, Shibata M, Fukazawa K. Small-scale method to determine the content of wood components from multiple eucalypt samples. Tappi Journal 1995; 78:121-126.
[103] Phyllis, database for biomass and waste. Energy research Centre of the Netherlands (ECN), 2005.
[104] Parikh J, Channiwala SA, Ghosal GK. A correlation for calculating HHV from proximate analysis of solid fuels. Fuel 2005; 84:487-494.
[105] Channiwala SA, Parikh J. A unified correlation for estimating HHV of solid, liquid and gaseous fuels. Fuel 2002; 81:1051-1063.
[106] Sheng C, Azevedo JLT. Estimating the higher heating value of biomass fuels from basic analysis data. Biomass and Bioenergy 2005; 28:499-507.
[107] Demirbas A. Calculation of higher heating values of biomass fuels. Fuel 1997; 76:431-434.
[108] Tia S, Prukamornpan P, Jitvootthikai P, Lao SS, Chayawattana T. Combustion of biomass in a fluidised-bed furnace. Journal of Research and Development KMUTT 1999; 2:47-63.

[109] Duangduen J, Supatimatsarow D, Polsane T, Gas production from cassava rhizome as an alternative to petroleum fuels used for MSW (municipal solid wastes) disposal. Energy Conservation Promotion Fund. Bangkok, 2002: 12-15.
[110] Tsai WT, Lee MK, Chang YM. Fast pyrolysis of rice husk: Product yields and compositions. Bioresource Technology 2007; 98:22-28.
[111] Orfao JJM, Antunes FJA, Figueiredo JL. Pyrolysis kinetics of lignocellulosic materials-three independent reactions model. Fuel 1999; 78:349-358.
[112] Rao TR, Sharma A. Pyrolysis Rates of Biomass Materials. Energy 1998; 23:973-978.
[113] Varhegyi G, Antal MJ, Jakab E, Szabo P. Kinetic modeling of biomass pyrolysis. Journal of Analytical and Applied Pyrolysis 1997; 42:73-87.
[114] Svenson J, Pettersson JBC, Davidsson KO. Fast Pyrolysis of the Main Components of Birch Wood. Combust Sci andTech 2004; 176:977-990.
[115] Demirbas A, Demirbas MF. Biomass and Wastes: Upgrading Alternative Fuels. Energy Sources 2003; 25:317-329.
[116] Meier D, Fortmann I, Odermatt J, Faix O. Discrimination of genetically modified poplar clones by analytical pyrolysis-gas chromatography and principal component analysis. Journal of Analytical and Applied Pyrolysis 2005; 74:129-137.
[117] Schwarzinger C. Identification of fungi with analytical pyrolysis and thermally assisted hydrolysis and methylation. Journal of Analytical and Applied Pyrolysis 2005; 74:26-32.
[118] Sellers KW, Towns CM, Mubarak CR, Kloppenburg L, Bunz UHF, Morgan SL. Characterization of high molecular weight poly(p-phenylenethynylene)s by pyrolysis gas chromatography/mass spectrometry with multivariate data analysis. Journal of Analytical and Applied Pyrolysis 2002; 64:313-326.
[119] Statheropoulos M, Mikedi K, Tzamtzis N, Pappa A. Application of factor analysis for resolving thermogravimetric-mass spectrometric analysis spectra. Analytica Chimica Acta 2002; 461:215-227.
[120] Esbensen KH, Guyot D, Westad F, Houmøller LP, Multivariate data analysis : in practice : an introduction to multivariate data analysis and experimental design, 5th ed. / Kim H. Esbensen / with contributions from Dominique Guyot, Frank Westad, Lars P. Houmøller. ed. Oslo: Camo Process AS, 2002.
[121] Scholze B, Meier D. Characterization of the water-insoluble fraction from pyrolysis oil (pyrolytic lignin). Part I. PY-GC/MS, FTIR, and functional groups. Journal of Analytical and Applied Pyrolysis 2001; 60:41-54.
[122] Rodriguez J, HernandezCoronado MJ, Hernandez M, Bocchini P, Galletti GC, Arias ME. Chemical characterization by pyrolysis gas chromatography mass spectrometry of acid-precipitable polymeric lignin (APPL) from wheat straw transformed by selected streptomyces strains. Analytica Chimica Acta 1997; 345:121-129.
[123] Nonier MF, Vivas N, de Gaulejac N, Absalon C, Soulie P, Fouquet E. Pyrolysis-gas chromatography/mass spectrometry of Quercus sp wood application to structural elucidation of macromolecules and aromatic profiles of different species. Journal of Analytical and Applied Pyrolysis 2006; 75:181-193.
[124] Nokkosmaki MI, Kuoppala ET, Leppamaki EA, Krause AOI. A novel test method for cracking catalysts. Journal of Analytical and Applied Pyrolysis 1998; 44:193-204.
[125] Kuroda K, Nakagawa-Izumi A, Mazumder BB, Ohtani Y, Sameshima K. Evaluation of chemical composition of the core and bast lignins of variety Chinpi-3

kenaf (Hibiscus cannabinus L.) by pyrolysis-gas chromatography/mass spectrometry and cupric oxide oxidation. Industrial Crops and Products 2005; 22:223-232.
[126] Hernandez M, Hernandez-Coronado MJ, Montiel MD, et al. Pyrolysis/gas chromatography/mass spectrometry as a useful technique to evaluate the ligninolytic action of streptomycetes on wheat straw. Journal of Analytical and Applied Pyrolysis 2001; 58:539-551.
[127] Faix O, Meier D, Fortmann I. Thermal-Degradation Products of Wood - Gas-Chromatographic Separation and Mass-Spectrometric Characterization of Monomeric Lignin Derived Products. Holz Als Roh-Und Werkstoff 1990; 48:281-285.
[128] Faix O, Meier D, Fortmann I. Thermal-Degradation Products of Wood - a Collection of Electron-Impact (Ei) Mass-Spectra of Monomeric Lignin Derived Products. Holz Als Roh-Und Werkstoff 1990; 48:351-354.
[129] Faix O, Fortmann I, Bremer J, Meier D. Thermal-Degradation Products of Wood - Gas-Chromatographic Separation and Mass-Spectrometric Characterization of Polysaccharide Derived Products. Holz Als Roh-Und Werkstoff 1991; 49:213-219.
[130] Faix O, Fortmann I, Bremer J, Meier D. Thermal-Degradation Products of Wood - a Collection of Electron-Impact (Ei) Mass-Spectra of Polysaccharide Derived Products. Holz Als Roh-Und Werkstoff 1991; 49:299-304.
[131] Interpretation of PCA Results: Through the scores and loadings in interesting projections. Combinatorial Sciences and Material Informatics Collaboratory (CoSMIC), 2007.
[132] Liu P, Improvement of bio-oil stability in wood pyrolysis process. Birmingham: Aston University, 2003.
[133] Peacocke GVC, Ablative pyrolysis of biomass. University of Aston in Birmingham, 1994.
[134] Oasmaa A, Peacocke C, A guide to physical property characterisation of biomass-derived fast pyrolysis liquids. Espoo: Technical Research Centre of Finland, 2001.
[135] A user guide of PL DataStream high resolution data acquisition system for Cirrus^{TM}. Polymer Laboratories, 2007.
[136] Beis SH, Onay O, Kockar OM. Fixed-bed pyrolysis of safflower seed: influence of pyrolysis parameters on product yields and compositions. Renewable Energy 2002; 26:21-32.
[137] Asadullah M, Anisur Rahman M, Mohsin Ali M, et al. Jute stick pyrolysis for bio-oil production in fluidized bed reactor. Bioresource Technology 2007; 99:44-50.
[138] Sensoz S, Demiral I, Ferdi Gercel H. Olive bagasse (Olea europea L.) pyrolysis. Bioresource Technology 2006; 97:429-436.
[139] Asadullah M, Rahman MA, Ali MM, et al. Production of bio-oil from fixed bed pyrolysis of bagasse. Fuel 2007; 87:2514-2520.
[140] Sensoz S, Can M. Pyrolysis of Pine (Pinus Brutia Ten.) Chips: 1. Effect of Pyrolysis Temperature and Heating Rate on the Product Yields. Energy Sources 2002; 23:347-355.
[141] Luo Z, Wang S, Liao Y, Zhou J, Gu Y, Cen K. Research on biomass fast pyrolysis for liquid fuel. Biomass and Bioenergy 2004; 26:455-462.
[142] Zhang Q, Chang J, Wang TJ, Xu Y. Upgrading bio-oil over different solid catalysts. Energy & Fuels 2006; 20:2717-2720.
[143] Bridgwater AV, Meier D, Radlein D. An overview of fast pyrolysis of biomass. Organic Geochemistry 1999; 30:1479-1493.
[144] Oasmaa A, Meier D, Characterisation, analysis, norms and standards. In: Bridgwater AV, editor. Fast pyrolysis of biomass: a handbook volume 3, 2005.

[145] Han J, Kim H. The reduction and control technology of tar during biomass gasification/pyrolysis: An overview. Renewable and Sustainable Energy Reviews 2008; 12:397-416.
[146] Abu El-Rub Z, Bramer EA, Brem G. Review of catalysts for tar elimination in Biomass gasification processes. Industrial & Engineering Chemistry Research 2004; 43:6911-6919.
[147] Sutton D, Kelleher B, Ross JRH. Review of literature on catalysts for biomass gasification. Fuel Processing Technology 2001; 73:155-173.
[148] Diebold J, Scahill J, Biomass to Gasoline Upgrading Pyrolysis Vapors to Aromatic Gasoline with Zeolite Catalysis at Atmospheric Pressure. In: Soltes EJ, Milne TA, editors. Pyrolysis oils from biomass : producing, analyzing, and upgrading. Washington, D.C.: American Chemical Society, 1988: 264-275.
[149] Samolada MC, Papafotica A, Vasalos IA. Catalyst evaluation for catalytic biomass pyrolysis. Energy & Fuels 2000; 14:1161-1167.
[150] Horne PA, Williams PT. Reaction of oxygenated biomass pyrolysis model compounds over a ZSM-5 catalyst. Renewable Energy 1996; 7:131-144.
[151] Effendi A, Gerhauser H, Bridgwater AV. Production of renewable phenolic resins by thermochemical conversion of biomass: A review. Renewable and Sustainable Energy Reviews 2007; In Press, Corrected Proof.

APPENDIX-A : PUBLICATIONS

The following is a list of publications that were produced during the course of this work.

Pattiya A, Titiloye JO, Bridgwater AV. Fast pyrolysis of agricultural residues from cassava plantation for bio-oil production, The 2nd Joint International Conference on "Sustainable Energy and Environment (SEE 2006)". Bangkok, Thailand, 2006: C-007.

Pattiya A, Titiloye JO, Bridgwater AV. Catalytic pyrolysis of cassava rhizome, The 2nd Joint International Conference on "Sustainable Energy and Environment (SEE 2006)". Bangkok, Thailand, 2006: B-020.

Pattiya A, Titiloye JO, Bridgwater AV. Catalytic effect of char and ash in fast pyrolysis of cassava rhizome, 15th European Biomass Conference and Exhibition. Berlin, Germany, 2007: 1374-1377.

Pattiya A, Titiloye JO, Bridgwater AV. Fast pyrolysis of cassava rhizome in the presence of catalysts. Journal of Analytical and Applied Pyrolysis, 2008; 81:72-79.

Pattiya A, Titiloye JO, Bridgwater AV. Evaluation of catalytic pyrolysis of cassava rhizome by principal component analysis. Submitted to Fuel, 2007

APPENDIX-B : MASS BALANCE SPREADSHEETS

The calculation of mass balance for fast pyrolysis experiments with 150 g/h unit was performed using an Excel file containing 4 spreadsheets, namely "Data", "Data during run", "GC" and "Summary". These blank spreadsheets are shown in this section.

"Data" spreadsheet

Test

Name	
Number	
Rig	
Date	

Fluidising medium

Name		
Particle size		μm

Feedstock

Name		
Particle size		μm
Moisture and ash contents		

	Weight (g)		
Container no.	1	2	3
Container			
Moist feedstock			
Container+dry feedstock			
Container + ash			

Pyrolysis system

Components	Weight before run (g)		Weight after run (g)
	Without anti-seize/vacuum grease	**With** anti-seize/vacuum grease	
Reactor			
Reactor+blocking wire+transfer line			
Reactor+blocking wire+transfer line + flidising medium			
Charpot			
Complete reactor assembly			
Secondary Reactor			
Reactor without bottom part			
Reactor bottom part			
Transfer line			
Glass wool			
Catalyst			
Reactor (without bottom part)+Glass wool+Catalyst			
Glassware			
Transition pipe			
Water condenser			
Electrostatic precipitator (EP)			
Flask 1			
Dry ice/acetone condersers			
Flask 2+3			
Cotton wool filter			
Feeder			
Bare feeder			
Entrain tube			
Feedstock			
Complete feeder system			

"Data" spreadsheet (continued)

Ethanol washing

Component			Weight (g)	
			Water condenser	EP
Ethanol used				
Liquid (tarry oil+ethanol)				
Weight BEFORE evaporating ethanol				
Weight AFTER evaporating ethanol				

Char and water contents of liquids by vacuum filtration and Karl Fischer titration, respectively

Component	No.	Weight (g)			Water content (wt %)
		Filter paper + container	Liquid + char	Char + filter paper + container	
Ethanol washing liquid from water condenser	1				
	2				
	3				
Ethanol washing liquid from EP	1				
	2				
	3				
Pot 1 oil	1				
	2				
	3				
Pot 2+3 oil	1				
	2				
	3				

Catalyst

Name		
Particle size		µm
Particle density		g/cm3

"Data during run" spreadsheet

Test Name
Time at the beginning

Time (mins)	System exit gas meter reading (m^3)	Temperature (°C)													Gas at the outlet of cotton wool filter
		Reactor			Temperature control 1		Temperature control 2		Secondary Reactor		Furnace 1		Furnace 2		
		In bed	Near feed tube	Freeboard	Reading	Set point	Reading	Set point	Bed	Exit	Reading	Set point	Reading	Set point	
NOTE>>		T1	T2	T3	T4				T5	T6					

Time at the end

"Data during run" spreadsheet (Continued)

Test Name | AP

Time (mins)	Nitrogen flow rate			Pressure				Electrostatic Precipitator		Notes
	Fluidising (l/min)	Feeder top (cm^3/min)	Entrain (l/min)	Feeder (inch water)	Reactor (inch water)	Gas outlet (cm water)	Inlet nitrogen (bar)	Voltage (kV)	Current (mA)	
NOTE>>										

"GC" spreadsheet

Injection	Time	% by volume									Total
		H_2	N_2	CH_4	CO	CO_2	C_2H_4	C_2H_6	C_3H_6	C_3H_8	
Average											
Stdev											-
MW		2.02	28.01	16.04	28.01	44.01	28.05	30.07	42.08	44.10	-
Mass (g)											
wt %			-								

"Summary" spreadsheet

			Unit	
Test name				
Fluidising medium				
	particle size		µm	
Feedstock				
	particle size		µm	
Moisture content			wt%	
Ash content			wt%, dry basis	
Reactor temperature			°C	
Vapour residence time			seconds	
Feed rate			g/h, dry basis	
Product yields			%, dry basis	
	Char			
	Liquids			
		Organics		
		Reaction water		
	Gas			
		H_2		
		CH_4		
		CO		
		CO_2		
		C_2H_4		
		C_2H_6		
		C_3H_6		
		C_3H_8		
Closure			%, dry basis	